Trophic interactions of a chitin-degrading microbiome of an aerated agricultural soil

Dissertation

To obtain the Academic Degree

Doctor rerum naturalium

(Dr. rer. nat.)

Submitted to the Faculty of Biology, Chemistry and Earth Sciences

of the University of Bayreuth

by

Adam Simon Wieczorek

Bayreuth, August 2017

This doctoral thesis was prepared at the Department of Ecological Microbiology at the University of Bayreuth from April 2011 until August 2017 and was supervised by PD Dr. Steffen Kolb.

This is a full reprint of the dissertation submitted to obtain the academic degree of Doctor of Natural Sciences (Dr. rer. nat.) and approved by the Faculty of Biology, Chemistry and Geosciences of the University of Bayreuth.

Date of submission: 29.08.2017
Date of defence: 28.06.2018

Acting dean: Prof. Dr. Stefan Peiffer

Doctoral committee:
PD Dr. Steffen Kolb (1st reviewer)
Prof. Dr. Dirk Schüler (2nd reviewer)
Dr. habil. Marie Spohn (chair)
Prof. Dr. Heike Feldhaar

Content

Tables

Supplemental tables

Figures

Supplemental figures

Equations

Abbreviations

α	bunsen solubility coefficient
^{12}C	most common isotope on earth
^{13}C	heavy isotope of the element carbon
°C	degree centigrade
A_{260}, A_{280}	adsorption at 260nm, and 280 nm
ad	fill up to
APS	ammonium persulfate
ATP	adenosine triphosphate
ATPase	adenosine triphosphatase
BLAST	Basic Local Alignment Search Tool
bp	base pairs
C	1. carbon 2. coverage
cDNA	copy deoxyribonucleic acid
conc.	concentration
CsTFA	caesium trifluoroacetate
CTAB	cetyl trimethylammonium bromide
ddH_20	deionized double-distilled water
DEPC-H_2O	diethylpyrocarbonate-treated water
DNA	deoxyribonucleic acid
DNAse	deoxyribonuclease
dNTP	deoxyribonucleotide
dsDNA	double-stranded DNA
DW	dry weight
e.g.	exempli grata (Latin);´for example´
EC	enzyme commission number
EDTA	ethylenediaminetetraacetate
et al.	*et alii* (Latin), ´and others´
F	forward primer
FID	flame ionization detector
FW	fresh weight
g	gravitational acceleration
GC	gas chromatography
HEPES	2-[4-(2-hydroxyethyl)piperazin-1-yl]ethanesulfonic acid; buffer
HPLC	high performance liquid chromatography
i.e.	*id est* (Latin);´that is´
IPTG	isopropyl-β-D-1-thiogalactopyranoside
IRD	infra-red dye
kb	kilobase
LB	Lurani-Bertani; culture medium
lg	decadic logarithm
Lt_2	clay loam (German soil classification)
MW	molecular weight
N	1. nitrogen 2. total number of analyzed sequences
n	1. amount of substance 2. number of replicates/considered values
N_A	Avogadro constant
NCBI	National Center for Biotechnology Information
n_{gas}	amount of gas in the gaseous phase
n_{dis}	amount of physically dissolved gas
n_{tot}	total amount of gas

no.	number
OD_{660}	optical density at 660 nm
OTU	operational taxonomic unit
PAGE	polyacrylamide gel
p_{act}	actual air pressure
PCR	polymerase chain reaction
PCR-H_2O	particle-free autoclaved water
PEG	polyethylene glycol
pH	the negative decimal logarithm of the proton concentration in a solution
p_a	atmospheric pressure
p_i	partial pressure of gases
p_o	overpressure in flasks
pk_a	acid dissociation constant
PLFA	phospholipid fatty acids
PMO	polysaccharide monooxygenase
pmoA	gene encoding the particulate methane monooxygenase
ppm	parts per million
PUL	polysaccharide utilization loci
p_o	overpressure in incubation flasks
qPCR	quantitative polymerase chain reaction
R	reverse primer
R	universal gas constant
RDP	Ribosomal Database Project
RID	refractive index detector
RNA	ribonucleic acid
RNAse	ribonuclease
rpm	rounds per minute
rRNA	ribosomal nucleic acid
RT-PCR	reverse transcription PCR
S	standard deviation
Seq.	sequence
SIP	stable isotope probing
SOC	super optimal broth; medium
sp.	species
t	1. ton 2. value that implies statistical significance
TAE	tris-acetate-EDTA; buffer
T_{act}	actual temperature
Taq	thermostable DNA polymerase isolated from *Thermus aquaticus*
TBE	tris-borat-EDTA; buffer
TCD	thermal conductivity detector
TEMED	N,N,N,N-tetramethylethylendiamine
temp.	temperature
T_m	basic melting temperature
TRF	terminal restriction fragment
TRFLP	terminal restriction fragment length polymorphism
Tris	tris(hydroxymethyl)-aminomethane
U	unit
UFZ	Helmholtz-Center for Environmental Research
UV	ultraviolet
V	volume
v/v	volume per volume
V_l	volume of the liquid phase
V_g	volume of the gas phase
VWD	variable wavelength detector
w	weight

w/v	weight per volume
W_g	gravimetric water content

1. Introduction

1.1. The global carbon cycle

Production and decomposition of organic carbon (carbon cycling) in aquatic and terrestrial ecosystems was close-to-balance for a long time (Schlesinger & Andrews 2000). Anthropogenic activities perturbed the fine equilibration of production and decomposition, and continue to change the dynamics of the global carbon budget. Burning of fossil fuels and intensive land use elevated the atmospheric carbon dioxide (+ 4.5 Gt carbon per year in a period from 2006-2015) and methane concentrations causing the greenhouse effect (Fig. 1; Le Quéré *et al.*, 2016). 1.0 Gt of carbon per year were released from land-use-change activities (e.g. deforestation for agriculture) which were initially the main cause for the increase above pre-industrial levels (Fig. 1). 9.3 Gt of carbon per year were released from fossil fuels and industry which became the dominant source of anthropogenic emissions after the industrial revolution (Fig. 1).

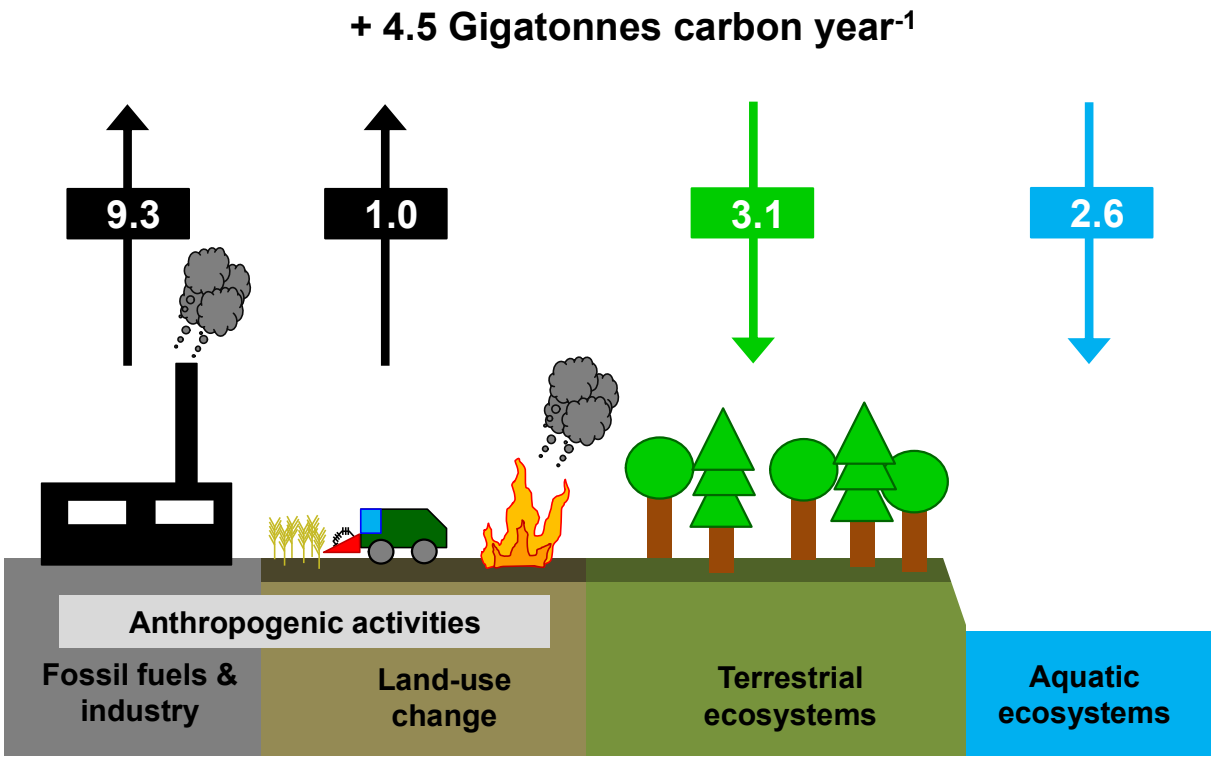

Figure 1. Schematic depiction of global sources and sinks of carbon dioxide. Global sinks and sources and the exchange with the atmosphere are displayed. Numbers represent estimated amounts of carbon in Gt year^{-1}. Note that terrestrial and aquatic systems are also sources of carbon dioxide and that values were omitted for simplicity of the scheme. Arrows pointing downwards indicate the consumption of carbon by the ecosystem type. Arrows pointing upwards indicate the amount of carbon that is released to the atmosphere. Scheme was modified according to Schellenberger 2011 based on values according to Le Quéré *et al.*, 2016.

Aquatic and terrestrial ecosystems are both net sinks for atmospheric carbon dioxide (Fig. 1), impairing anthropogenic activities on the atmospheric carbon balance. The amount of carbon taken up by aquatic and terrestrial ecosystem is 3.1 and 2.6 Gt of carbon per year, respectively (Le Quéré *et al*., 2016). However, the turnover in terrestrial ecosystems is higher. About 122.8 Gt of carbon per year are fixed by autotrophic plants (Dumonceaux 2005, Lal 2008a,b). Approximately 60 Gt carbon per year are released in the form of carbon dioxide to the atmosphere by plant respiration and other events like, e.g., wild fires (Falkowski *et al*., 2000; Lal 2008a,b). Microbial decomposition of organic matter accounts for another 60 Gt carbon per year that is released to the atmosphere as carbon dioxide (Lal 2008a,b). The carbon and energy stored in plant organic matter (for example in structural biopolymers like cellulose and lignin) and root exudates released by plants is driving the soil (microbial) food web (bacteria, fungi, protists), which is responsible for the decomposition of organic matter (Scheu 2002; Singh & Gupta 1977; Stockmann *et al*., 2013). However, not only plant organic matter is subject to decomposition. Also, dead biomass of eukaryotic consumers (e.g. herbivores and predators) and the soil microbiome itself is subject to decomposition (Gougoulias *et al*., 2014). Therefore, different organic compounds with contrasting levels of degradability are subject to microbial degradation at the same time. Readily degradable compounds are for example catabolic precursors of cell material (proteins, nucleic acids, lipids and polysaccharides) located in cytoplasm of prokaryotic and eukaryotic cells that are released after cell death (Lewis 2000; Sharon *et al*., 2009). More recalcitrant organic compounds are polysaccharides like cellulose, xylan and starch that are major constituents of plant organic matter, or chitin, chitosan, and glucans that are structural constituents of bacterial and fungal cell walls (Braun & Hantke 1974; Bowman & Free 2006; Cabeen & Jacobs-Wagner 2005; Fernandez *et al*., 2016). Another group of biopolymers are lignins that are constituents of woody and non-woody plant biomass (Lewis & Yamamoto 1990) in which they function as structural elements. Because of their aromatic structures, they are degraded slower than polysaccharides and accumulate to a higher extent than other biopolymers (Kirk & Farrell 1987; Thevenot *et al*., 2010). Selective preservation due to recalcitrance of organic matter is considered to be one of the major mechanisms for stabilization of organic matter in soils, i.e. it is not degraded by the soil microbiome and persists (Dungait *et al*., 2012; Marschner *et al*., 2008; Schmidt *et al*., 2011; Six *et al*., 2002; Sollins *et al*., 1996; von Lützow *et al*., 2006, 2008). Furthermore, organic matter can be stabilized by spatial inaccessibility against microbial degraders (e.g. due to occlusion, intercalation, hydrophobicity and encapsulation) or interaction with mineral surfaces (Fe-, Al-, Mn-oxides, phyllosilicates) and metal ions (von Lützow *et al*., 2006, 2008). Other factors that influence the degradation of organic matter and the community compositions and activity of the associated degraders are prevailing physicochemical factors like pH, water content and

temperature (Kirschbaum 1995; von Lützow & Kögel-Knabner 2009; Wardle 1992). Land use changes such as the conversion of natural forests, grasslands, and wetlands to agricultural ecosystems have a dramatic effect on the physiochemical conditions and the structure and diversity of soil microbiomes. A consequence is a decreased storage capacity of organic carbon in soils and an increased release of carbon dioxide into the atmosphere (Schimel 1995; Schlesinger & Andrews 2000).

1.2. Chitin – a major polysaccharide in soils

Chitin is after cellulose the second most abundant polysaccharide on earth and is subject to rapid microbial turnover in the environment (Gooday 1990a). It consists of alternating β-1-4-linked *N*-acetylglucosamine (GlcNAc) residues and is structurally highly similar to cellulose that consists of β-1-4-linked glucose residues (Fig. 2).

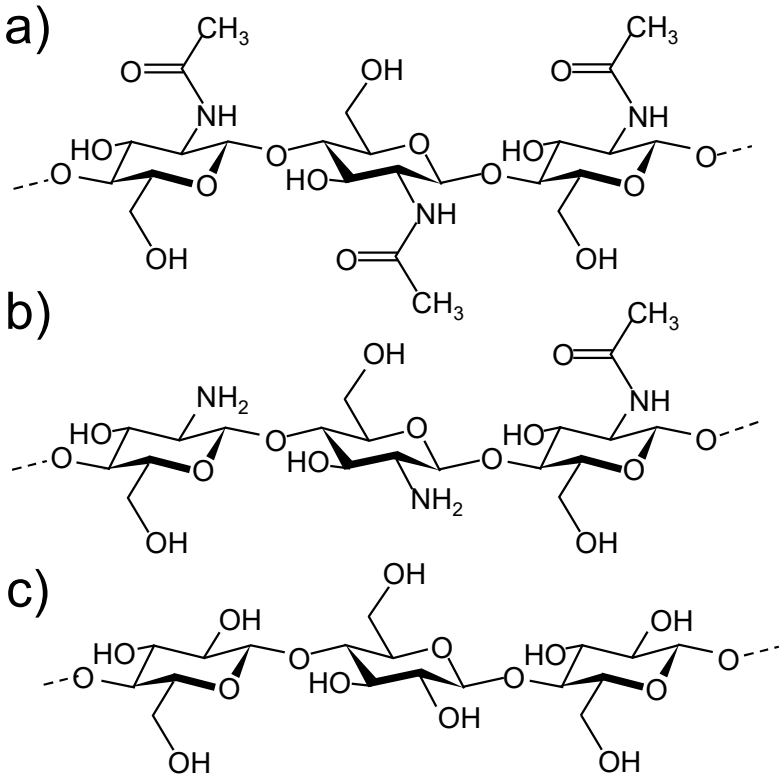

Figure 2. Molecular structures of chitin (a), chitosan (b) and cellulose (c).

Three forms of chitin are known. The most widely distributed form chitin is helical α-chitin and is typically found in arthropods (Gooday 1990a). The helical form of α-chitin results from two chains with antiparallel arrangement, i.e. the chains run in opposite directions. The core

structure of the chains are *N,N`*-diacetylchitobiose units. β-chitin is a less common form of chitin often found in mollusks and diatoms. Its chains are arranged in parallel direction which allows more flexibility than the α-chitin (Gooday 1990a). A third form of chitin is γ-chitin, in which the poly-*N*-acetylglucosamine chains are orientated in parallel and antiparallel directions. Chitin is always cross-linked with other structural components, e.g. with the glucans in fungal cell walls, bonded either directly or by peptide bridges. The degree of acetylation is varying in fungi and invertebrates from a fully acetylated (chitin) to fully deacetylated (chitosan) (Gooday 1990a). However, set values for the degree of acetylation for the definition of chitin and chitosan do not exist. Typically, the degree of acetylation in chitin and chitosan is 0.90 and less than 0.35, respectively (Pillai *et al*., 2009; Wu & Zivanovic 2008; Zargar *et al*., 2015).

1.2.1. Occurrence of chitin

Chitin can almost exclusively be found in *Eukaryota*. The only possible exception known for *Prokaryota* is that it might be a structural component of the spore walls of *Streptomyces* (Gooday 1990a). Within *Eukaryota*, chitin is absent in vertebrates and probably also in plants (Gooday 1990b). However, polymers rich in β-1,4-linked *N*-acetylglucosamine have been reported for plants (Benhamou & Asselin 1989; Gooday 1990b). Among *Protista*, chitin occurs in some amoebae, ciliates and chrysophyte algae (Gooday 1990a,b). Chitin is widely distributed as a structural component in invertebrates, e.g. hydrozoa, nematodes, mollusks, brachiopods and arthropods. In fungi, chitin seems to be ubiquitous with only few exceptions (Gooday 1990a,b). Fungal cell walls may contain up to 25% chitin (Blumenthal & Roseman 1957) and since fungi can reach up to 60-90% of the microbial biomass in agricultural soils, they are thus the main source of chitin in such soils (Fernandez & Koide 2012).

1.2.1.1. Non-chitin associated occurrence of *N*-acetylglucosamine

Bacterial cell walls are next to chitin another major source of *N*-acetylglucosamine. There, it is a component of peptidoglycan that is a polymer of the two amino sugars *N*-acetylglucosamine (GlcNAc) and *N*-acetylmuramic acid (MurNAc), connected by a β-1,4 glycosidic bond and a cross-linking peptide chain of three to five amino acids attached to MurNAc (Cabeen & Jacobs-Wagner 2005; Martin 1966; Osborn 1969; Schleifer & Kandler 1972; Silhavy *et al*., 2010). GlcNAc is also a component of hyaluronic acid, which is a major component of the extracellular matrix and is widely distributed throughout connective, epithelial and neural tissues of animals (Ashry & Aly 2007; Chen *et al*., 2010). In addition, GlcNAc and sulfated GlcNAc can be detected in heparin or keratin sulfate (Bhavanandan & Meyer 1966; Chen *et al*., 2010; Danishefsky *et al*., 1969). Thus, *N*-acetylglucosamine is a very abundant amino sugar in various environments and organisms.

1.2.2. Annual production of chitin

It is difficult to quantify the annual production of chitin. Numbers are in the range of 10^{10} to 10^{11} tons per year (Gooday 1990a,b; Beier & Bertilsson 2013). However these values are estimates, often based on the numbers of commercial fisheries of Antarctic krill (Gooday 1990a,b). For comparison, it is estimated that cellulose is produced on earth at least at a rate of 10^{9} to 10^{10} tons per year (Coughlan 1985; Henrissat 1994).

1.2.3. Degradation of chitin

A process in which chitin is degraded is defined as chitinoclastic (Beier & Bertilsson 2013). However, the degradation of chitin involves different pathways and enzymatic tools. Major routes for the degradation of chitin are the direct route, i.e. enzymatic breakdown of chitin to *N*-acetylglucosamine oligomers, or the indirect, i.e. chitin is deacetylated prior enzymatic hydrolysis (Fig. 3; Beier & Bertilsson 2013; Gooday 1990b). Deacetylation of chitin to chitosan before further breakdown might be important in estuarine sediments (Hillman *et al*.,1989a,b). Nonetheless, for aquatic and terrestrial ecosystems it has not been evaluated which chitin hydrolysis route prevails (Beier & Bertilsson 2013).

1.2.3.1. Enzymatic hydrolysis of chitin

Glycoside hydrolases (EC 3.2.1.-) is a super family of enzymes hydrolyzing the glycosidic bond between two or more carbohydrates or between a carbohydrate and a non-carbohydrate moiety. Glycoside hydrolases (GH) that hydrolyze the glycosidic bonds in chitin are referred to as chitinases (EC 3.2.1.14). However, chitinases can be found within different families of glycoside hydrolases, namely within family 18, 19, 23, and 48 (Adrangi & Faramarzi 2013; Arimori *et al*., 2013; Cohen-Kupiec & Chet, 1998; Fujita *et al*., 2006; Karlsson & Stenlid 2009). Most known chitinases belong to GH families 18 or 19, whereby the latter is mainly restricted to plants. GH 18 is dominated by chitinase genes of chitinolytic *Bacteria* (Cohen-Kupiec & Chet 1998; Karlsson & Stenlid 2009). GH 18 and 19 chitinases differ in the reaction mechanism what is reflected by their low degree of similarity to each others families on amino acid level and different three-dimensional structures (Iseli *et al*., 1996). Few chitinases belong to GH families 23 and 48 (Adrangi & Faramarzi 2013; Arimori *et al*., 2013; Fujita *et al*., 2006). In addition, it has been suggested that members of the GH 20 family, typically cleaving of GlcNAc from the non-reducing ends of soluble chitin oligomers, can directly cleave GlcNAc from chitin and hence act as chitinases (Beier & Bertilsson 2013; LeCleir *et al*., 2007).

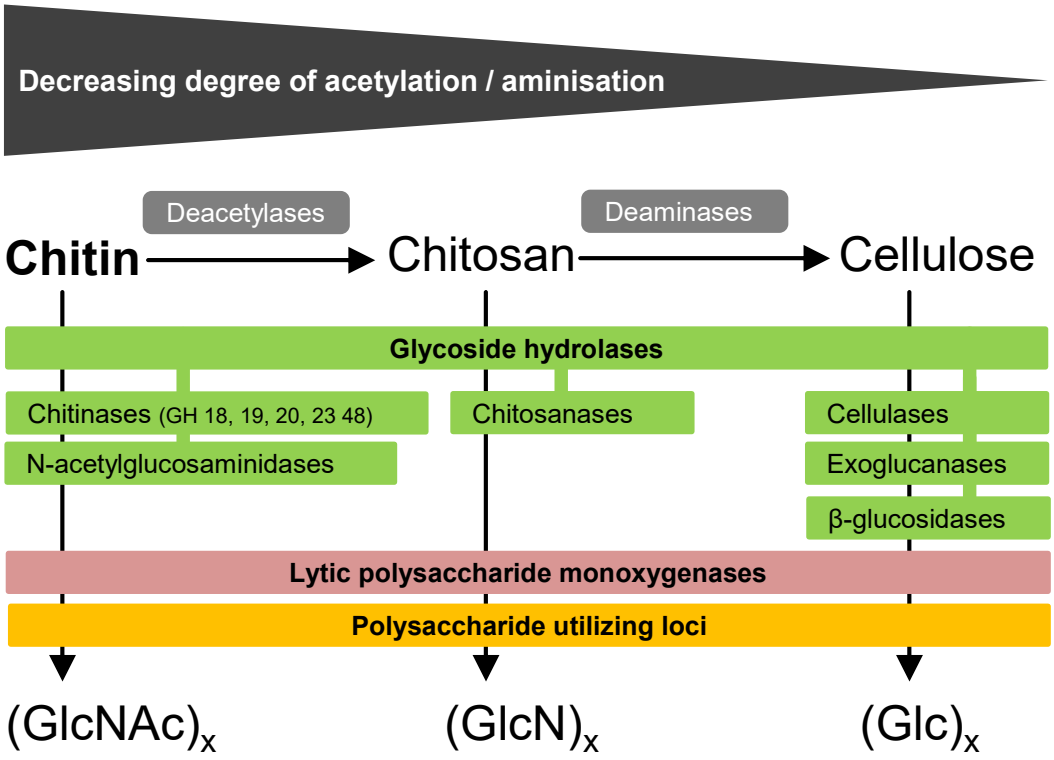

Figure 3. Pathways and enzymes involved in the degradation of chitin.

Depending on the active site and the mode of action chitinases can display exo- and endo-activity (Beier & Bertilsson 2013; Karlsson & Stenlid 2009; van Scheltinga *et al*., 1994; van Aalten *et al*., 2000). Processive exochitinases cleave $[GlcNAc]_2$ dimers from the reducing and non-reducing end of the chain while sliding along the chitin polymer (Fig. 4; Horn *et al*., 2006; Hult *et al*., 2005; Sikorski *et al*., 2006). Endochitinases are non-processive and cleave the chitin polymer randomly at more amorphous sites of the polymer (Fig. 4; Horn *et al*., 2006; Sikorski *et al*., 2006; Vaaje-Kolstad *et al*., 2013). The combination of exo- and endochitinases leads to increased efficiency of chitin hydrolysis, implying that each form of chitinase has a differential function in the process of chitin degradation (Suzuki *et al*., 2002). Typical hydrolysis products are $[GlcNAc]_2$ dimers and longer oligomers of chitin. Single GlcNAc molecules are only produced to a low extend (Beier & Bertilsson 2013). Finally, β-*N*-acetylglucosaminidases (EC 3.2.1.30) located in the cytoplasm or periplasmic space cleave $[GlcNAc]_2$ into GlcNAc or GlcNAc from the non-reducing end of soluble chitin oligomers (Beier & Bertilsson 2013; Gooday 1990b).

1.2.3.2. Complexed enzyme systems

Cellulosomes are large, cell bound multienzyme complexes, with numerous subunits tightly linked facilitating the degradation of cellulose and hemicellulose (Bayer *et al*., 2004; Fontes & Gilbert 2010). These complexed enzyme systems are commonly found in anaerobic microorganism bacteria (and fungi), particularly in *Clostridia* and other microorganisms often found in rumen. A possible explanation for the evolution of such elaborate enzymatic machineries is, that cellulosomes are highly efficient in the deconstruction of plant wall material and minimize the distance over which hydrolysis products have to be transported by diffusion, which is necessitated due to the energetic constraints of anoxic environments (Bayer *et al*., 1994; Fontes & Gilbert 2010; Lynd *et al*., 2002; Schwarz 2001). Functional analogs to cellulosomes for the degradation of chitin, which can be referred as chitinosomes, have not been described so far and the question arises, if such a system for chitin degradation exists (Bayer *et al*., 1998; Brurberg *et al*., 2001). In this respect, the detection of an endochitinase in the cellulosome of the cellulolytic bacterium *Clostridium thermocellum* is noteworthy (Doi & Kosugi 2004; Zverlov *et al*., 2002) and implies that cellulosomes might be somehow involved in the degradation of chitin. Unfortunately, the information on this topic is limited and it would be promising to study the potential of known cellulosomes to break down chitin.

1.2.3.3. Degradation of chitin by polysaccharide monooxygenases

In recent years, a new group of enzymes, called polysaccharide monooxygenases (PMOs), has been discovered, which facilitates the degradation of chitin by oxidative cleavage, i.e. molecular oxygen is used to oxidize the C–H bond at either C1 and/or C4 carbon atoms to C–OH (Fig. 4; Dimarogona *et al*., 2013; Span & Marletta 2015; Vaaje-Kolstad *et al*., 2010, 2013; Walton & Davies 2016). The oxidative cleavage mechanism has first been demonstrated for the protein CBP21 of *Serratia marcescens.* CBP21 was originally described as a chitin-binding protein belonging to family 33 of enzymes classified as carbohydrate-binding modules (Vaaje-Kolstad *et al*., 2010). Actually, PMOs were ‘known’ for almost a decade but were wrongly annotated as family 61 glycoside hydrolases (GH61s) or family 33 carbohydrate-binding modules (CBM33s) until their catalytic function was revealed (Beeson *et al*., 2015). They were reclassified in CAZy database from GH61 and CBM33 to AA9 and AA10, respectively (Levasseur *et al*., 2013). The AA9 family mostly comprises fungal PMOs predominantly active on cellulose (Beeson *et al*., 2015; Busk & Lange 2015; Floudas *et al*., 2012; Hemsworth *et al*., 2016). Family AA10 largely contains bacterial and viral PMOs active on chitin and cellulose (Busk & Lange 2015; Forsberg *et al*., 2011, 2014a,b; Hemsworth *et al*., 2016; Vaaje-Kolstad *et al*., 2010). In recent years, two novel families, AA11 and AA13, fungal PMOs with activities on chitin and starch have been added (Hemsworth *et al*., 2014;

Lo Leggio *et al*., 2015; Vu *et al*., 2014). Nonetheless, little is known about the distribution of chitin- and cellulose-active PMOs in *Bacteria* (Beeson *et al*., 2015). As PMOs require oxygen, their catalytic activity seems to be absent in strictly anaerobic chitinolytic bacteria as suggested by comparative genome analysis (Bai *et al*., 2016). Genomic studies revealed *Actinobacteria*, *Firmicutes* and *Proteobacteria* to be PMO-containing taxa (Book *et al*., 2014; Bai *et al*., 2016). However, a relatively small amount of terrestrial genomes was considered in the analysis. Thus, the occurrence and distribution of PMOs in the bacterial (and archaeal) kingdom remains elusive. Nevertheless, the discovery of new families of PMOs with activity on cellulose, hemicellulose, and starch suggests that oxidative cleavage is a widely spread mechanism for the degradation of a variety of polysaccharides (Agger *et al*., 2014; Forsberg *et al*., 2011; Horn *et al*., 2012; Lo Leggio *et al*., 2015; Vu *et al*., 2014).

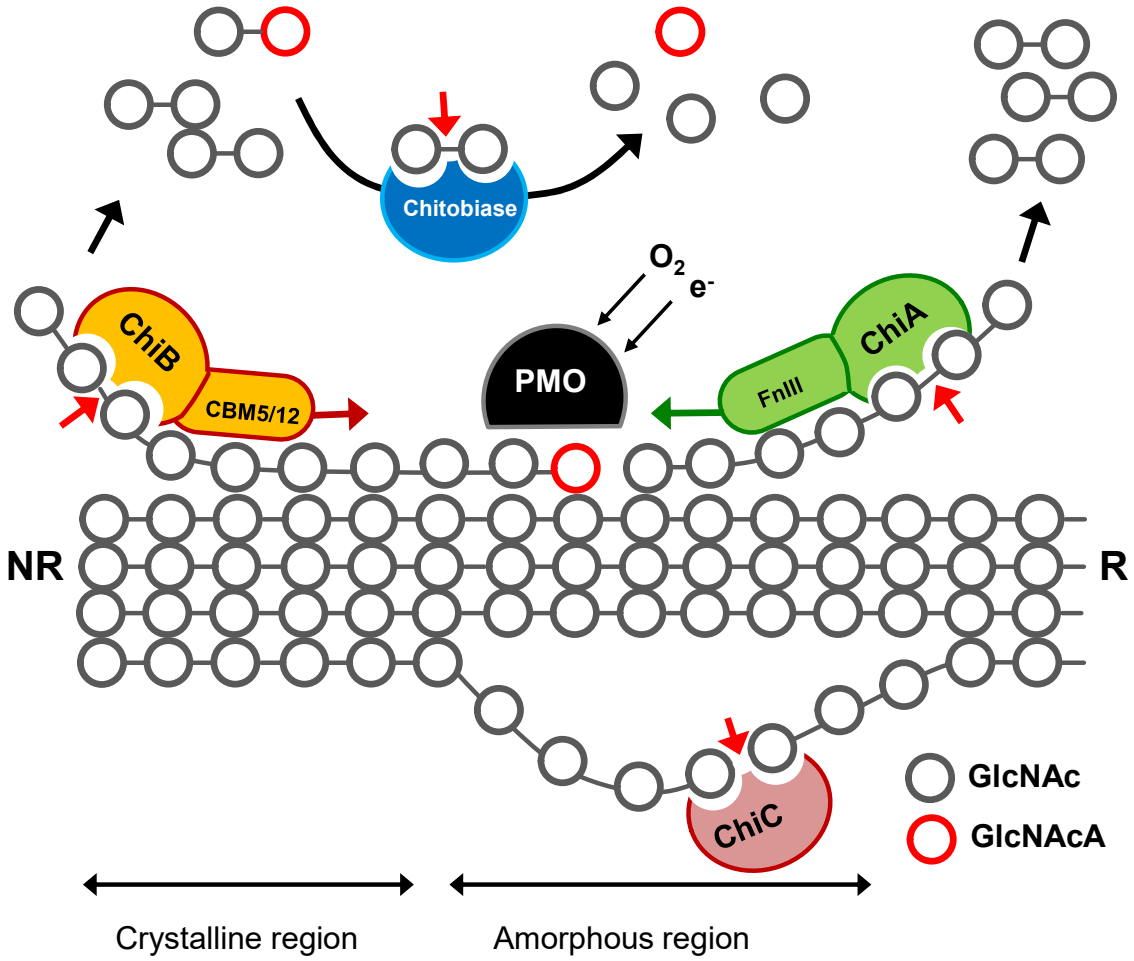

Figure 4. Hypothetical model of chitin degradation by the chitinolytic machinery of *Serratia marcescens*. Chitobiose dimers are cleaved from the non-reducing (NR) and reducing ends (R) of densely packed chitin-fibers by the processive exochitinases ChiB and ChiA respectively. The endochitinase ChiC randomly introduces cuts in the more amorphous regions of the chitin fibers opening these regions for the activity of ChiA and ChiB. Red arrows indicate the location of cleavage. In contrast to the hydrolysis mechanism of chitinases, polysaccharide monooxygenase (PMO) introduces breaks in the chitin fibers by oxidative cleavage yielding aldonic acids (GlcNAcA; red circles). The ultrastructure and reaction mechanism of the PMO enables activity in the crystalline regions. Thereby, PMO creates new chain ends for processive exochitinases. The chitobiase converts chitobiose and short chito-oligosaccharides to monomers. The model was modified from Vaaje-Kolstad *et al*., 2013.

1.2.3.4. Polysaccharide utilizing loci: potential involvement in chitin degradation

Beside the known form of organization of polysaccharide degrading enzymes, i.e. free excreted enzymes (non-complexed) and the complexed organization in cellulosomes (1.2.3.2), a third form was proposed in recent years. Cell-wall associated multiprotein systems were discovered in *Bacteroidetes* and are currently referred to as '*polysaccharide utilizing loci*' (PULs) (Martens *et al*., 2009). PULs are chromosomally organized in gene clusters encoding lipoproteins with polysaccharide recognition motives and glycoside hydrolases that are embedded in the outer membrane. The oligosaccharides retrieved by

cleavage of chitin are transported into the periplasm via membrane-spanning β-barrel proteins of the TonB-dependent receptor family that transport solutes and macromolecules via energy derived from the proton motive force (Martens *et al*., 2009). The oligosaccharides are then cleaved to dimers and monomers by glycoside hydrolases in the periplasm. PULs were first described as *starch utilization systems* (SUS) in gut derived *Bacteroidetes*. However, genomic analyses soon indicated that PULs might have a broad target spectrum including cellulose, hemicellulose, chitin, agarose and alginate (Allouch *et al*., 2004; Bauer *et al*., 2006; Salyers *et al*., 1977; Martens *et al*., 2009; Xie *et al*., 2007). Recently, convincing evidence for the hypothesis of PUL based cellulose degradation by *Bacteroidetes* has been documented (Naas *et al*., 2014). Notably, chitinases organized in a PUL-manner were discovered in the genome of the chitin degrading bacterium *Flavobacterium johnsoniae* (McBride *et al*., 2003). Nonetheless, it remains unclear to which extent cell-wall embedded multiprotein systems contribute the degradation of chitin by terrestrial microbiomes.

1.3. Biological degradation of chitin by the soil microbiome

Chitin is a major polysaccharide in soils, as it is an essential constituent of fungal and insects cell walls. Since chitin can make up 25% of fungal cell walls and fungi can reach up to 60-90% of the microbial biomass in agricultural soils, they are the main source of chitin in such soils (Fernandez & Koide 2012). Chitin can be degraded under oxic and anoxic conditions (Beier & Bertilsson 2013; Gooday 1990b). Small soluble saccharides (e.g. dimers and monomers) derived from the enzymatic breakdown of chitin (1.2.3.1.) can be taken up by chitinolytic and saccharolytic microorganisms. After transport into the cytoplasm the soluble saccharides can be metabolized as a source of energy, carbon, and/or nitrogen (Geisseler *et al*., 2010; Gooday 1990b; Kellner & Vandenbol 2010; Keyhani & Roseman 1999).

Agricultural, grassland and forests soils are considered to be well aerated, therefore soluble hydrolysis products are primarily mineralized to carbon dioxide by aerobic respiration (Fig. 5; Beier & Bertilsson 2013; Gooday 1990b). Chitin degradation in aerated soils has been subject to investigation in several studies (Kielak *et al*., 2013; Makarios-Laham & Lee 1995; Metcalfe *et al*., 2002; Okafor 1966,1967; Veldkamp 1955).

Nonetheless, even in largely oxic soils the oxygen distribution is heterogenous and spatially and temporarily dynamic depending on aggregate size, soil texture, water content, and other biogeochemical factors (Or *et al*., 2007). These biogeochemical factors and microbial aerobic respiration lead to the development of oxygen-limited or oxygen-free (anoxic) microzones (Küsel & Drake 1995; Picek *et al*., 2000; Pett-Ridge & Firestone 2005; Wagner *et al*., 1996).

Anaerobic degradation of chitin is best studied in the water column and in the sediments of aquatic ecosystems (Boyer 1986, 1994; Hillmann *et* al., 1989a; Köllner *et al*., 2012).

Sediments are largely anoxic ecosystems where organic matter is mineralized by anaerobic and facultative aerobic prokaryotes to methane and carbon dioxide via an intermediary ecosystem metabolism by the microbiome (Boyer 1986; Drake *et al*., 2009; Wüst *et al*., 2009). After enzymatic hydrolysis of polysaccharides, such as chitin, cellulose, or hemicellulose, the soluble hydrolysis products are fermented by primary fermenters to acids, alcohols, molecular hydrogen, and carbon dioxide. Secondary fermenters, acetogens, and methanogens metabolize these substrates to the terminal products, methane and carbon dioxide (Drake *et al*., 2009; McInerney *et al*., 2008; Schink & Stams 2006; Wüst *et al*., 2009). Almost no information is available on the anaerobic degradation of chitin in aerated soils (Manucharova *et al*., 2006; Reguera & Leschine 2001). Also, in the field of cellulose degradation, surprisingly few studies addressed the anaerobic degradation of cellulose in the anoxic microzones of aerated soils (Leschine 1995; Lynd *et al*., 2002; Schellenberger *et al*., 2010). As the degradation of chitin fibers by glycoside hydrolases is independent of oxygen, the chitinoclastic process under anoxic conditions will mainly differ in the metabolization of the soluble saccharides. Thus, a crucial factor for the anaerobic degradation of chitin in aerated soils is the type and quantity of alternative electron acceptors available. Alternative electron acceptors relevant in such soils are ferric iron, manganese, and nitrate (Tiedje *et al*., 1984; Weber *et al*., 2006). The Gibbs free energy of anaerobic respiration with e.g. nitrate or ferric iron is higher than Gibbs free energy of fermentation processes (Lengeler *et al*., 1999; Madigan & Martinko 2006; Thauer *et al*., 1977; Zehnder & Stumm 1988). Therefore, if alternative electron acceptors are available, they are first respired by microorganisms when an environment becomes anoxic (Achtnich *et al*., 1995; Lueders & Friedrich 2000; Peters & Conrad 1996; Zehnder & Stumm 1988). When the concentration of alternative electron acceptors is below the threshold that allows energy conservation, production of fermentation products by fermentative taxa excels the substrate consumption by heterotrophic respiring taxa and thus, fermentation products accumulate (Weber *et al*., 2006; Westermann 1993). This is in agreement with observations made by Schellenberger *et al*. (2010), who showed that under anoxic conditions cellulose degradation had initially been associated with iron and nitrate respiration, which was followed by fermentation of the cellulose hydrolysis products. Based on this knowledge, possible microbial interactions and associated metabolic processes during the anaerobic degradation of chitin are proposed in Figure 5b.

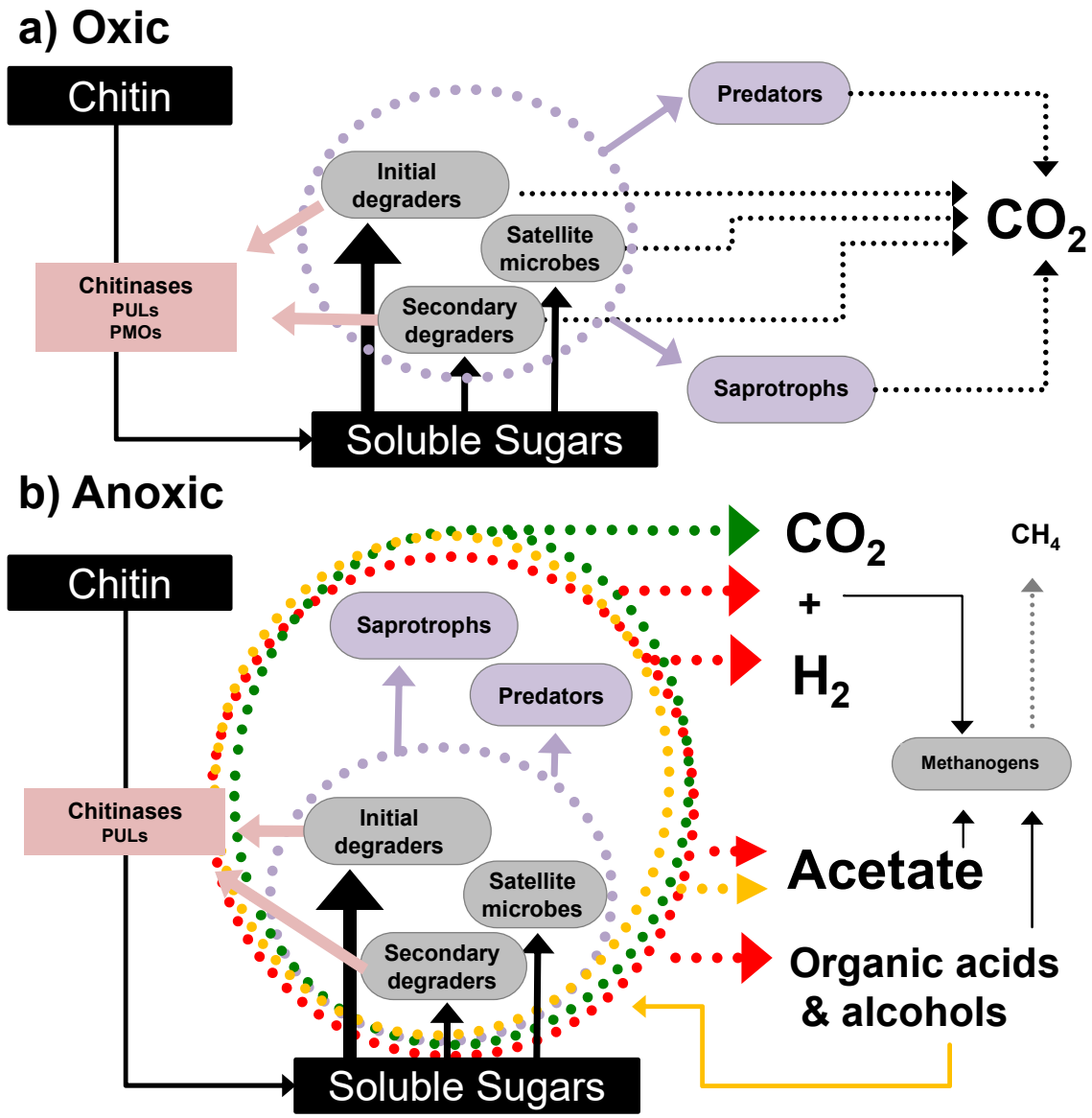

Figure 5. Model of possible microbial interactions during chitin degradation in an aerated soil under oxic (a) and anoxic (b) conditions. Initial degraders colonize chitin fibers and degrade chitin with endo- and exo-chitinases, polysaccharide monooxygenases (PMO) or polysaccharide utilizing loci (PUL). Satellite microbes consume the excess chitin hydrolysis products without producing own chitin degrading enzymes. Secondary degraders that are better adapted to low substrate availability replace the initial degraders. Chitin degraders and satellite microbes are potential prey (indicated by the purple dotted circles) for predators or degraded by saprotrophic bacteria after their death. Under oxic conditions microbes conserve energy by the respiration of oxygen (black dotted lines). Under anoxic conditions microbes conserve energy by respiration of nitrate, ferrous iron, or sulfate (green dotted lines), by fermentation (red dotted lines), by acetogenesis (orange dotted lines), or by methanogenesis (grey dotted lines). Methane is a minor product (indicated by the smaller font size) under most *in situ* conditions.

1.4. Diversity of chitin-degrading microorganisms

Nutritional chitinolysis, i.e. degradation of chitin to obtain carbon and energy, can be found within in the domains *Bacteria* and *Archaea* of the domain *Prokaryota* and within the fungi of the domain *Eukaryota* (Beier & Bertilsson 2013; Gooday 1990a,b). Only few studies exist that demonstrate or indicate a chitinolytic lifestyle of *Archaea* (Beier & Bertilsson 2013).

1.4.1. *Eukaryota*

The most important taxonomic group within the *Eukaryota* with regard to chitinolysis are fungi (Beier & Bertilsson 2013; Gooday 1990a,b). Important fungal taxa are *Mucorales*, *Deuteromycetes,* and *Ascomycetes* (Gooday 1990b). Chitinolytic fungi often have inducible enzymatic systems for chitin degradation and the number of chitinases in their genomes ranges from 10 to 25 (Seidl 2008; Sivan & Chet 1989). Some authors suggest that fungi are the most important chitin degraders in forest soils, probably due to their potential of rapid filamentous growth enabling them to colonize particulate chitin (Gray & Baxby 1968; Gray & Bell 1963; Gooday 1990a).

As a reflection of the ubiquity and quantity of chitin in nature, the ability to degrade chitin can also be found in plants, animals (Gooday 1990a), rotifers (Štrojsová & Vrba 2005), and some algae (Vrba *et al*., 1996). However, the function assigned to plant chitinases is to be a defense mechanism against fungal plant pathogens (Gooday 1990b; Mauch *et al*., 1988). So far, nutritional chitinolysis is only known in insectivorous plants (Gooday 1990a). Animal-associated chitin degradation has been best studied for fish. The supposed role of fish chitinases is thereby to digest shell shrimps (Gooday 1990a).

1.4.2. *Archaea*

Currently, only few chitinolytic *Archaea* have been described. *Thermococcus chitonophagus*, a hyperthermophilic, anaerobic archaeum, was isolated from a hydrothermal vent site of the Mexican west coast (Huber *et al*., 1995). *Thermococcus kodakaraensis* (previously classified into the genus *Pyrococcus*) is a hyperthermophilic archaeon isolated from a solfatara (102 °C, pH 5.8) (Tanaka *et al*., 1999; Atomi *et al*., 2004). *Pyrococcus furiosus* is a heterotrophic anaerobic archaeon with an optimum growth temperature of 98 to 100°C and was isolated from hot sediments of the beach of Porto di Levante, Vulcano Island, Italy (Fiala & Stetter 1986; Gao *et al*., 2003). So far, all three described chitinolytic archaeal strains are hyperthermophiles isolated from sediments. Therefore, the question arises if also mesophilic chitinolytic *Archaea* exist that contribute to overall chitin degradation in aerated soils.

1.4.3. *Bacteria*

Bacteria are the most important degraders of chitin in many ecosystems including soils. However, fungi can also be of significant relevance under certain conditions (Beier & Bertilsson 2013). Most knowledge about chitinolytic bacteria was obtained by studying pure cultures after targeted isolation and cultivation approaches (Gooday 1990b). Cultured chitinolytic bacteria can be found in the phyla or classes of members of *Acidobacteria*, *Actinobacteria*, *Bacteroidetes* (*Cytophaga*), *Betaproteobacteria*, *Gammaproteobacteria*, and *Firmicutes* (Foesel *et al*., 2013; Gooday 1990b; Someya *et al*., 2011; Yang *et al*., 2005). Among cultivated chitinolytic bacteria, *Actinomycetales* (*Actinobacteria*) are frequently and readily isolated from soil samples (Gooday 1990a; Gray & Baxby 1968; Manucharova *et al*., 2011; Metcalfe *et al*., 2002; Okafor 1966, 1967; Skinner & Dravis 1937; Veldkamp 1955). *Streptomyces* (*Actinomycetales*) are abundant in terrestrial soil ecosystems and very important for the initial decomposition of organic matter (Schrempf 2007). They encode a broad spectrum of extracellular enzymes with different substrate targets, e.g. chitin, cellulose, lignocellulose, or xylan (Chater *et al*., 2010; Schrempf 2007). Remarkably, *Streptomyces coelicolor* A3(2), the most widely used *Streptomycetes* laboratory strain, encodes 11 chitinases, eight cellulases, three amylases and two pectate lyases (Chater *et al*., 2010; Hopwood 2007; Saito *et al*., 2003). In addition to *Actinomycetales*, members of *Bacteroidetes*, *Firmicutes,* and *Beta-* and *Gammaproteobacteria* are frequently and readily isolated from terrestrial soils and considered as important chitin degraders in those ecosystems (Beier & Bertilsson 2013; Das *et al*., 2010; Someya *et al*., 2011; Yasir *et al*., 2009). The predominance of *Actinobacteria*, *Proteobacteria,* and *Firmicutes* was reinforced by several cultivation-independent studies analyzing the 16S rRNA or *chiA* (chitinase; GH18 family, subfamily A) genes (Cretoiu *et al*., 2012, 2013, 2014; Hjort *et al*., 2010; Ikeda *et al*., 2007; Kielak *et al*., 2013; Metcalfe *et al*., 2002). *Acidobacteria* are abundant in soils, but difficult to cultivate (Janssen 2006). Thus, many aspects of their ecophysiology are not completely understood. For a long time, a chitinolytic lifestyle was not known for *Acidobacteria*. However, the recent isolation and description of *Blastocatella fastidiosa* together with evidence from genome studies suggest that this physiological trait is typical for *Acidobacteria* (Foesel *et al*., 2013; Ward *et al*., 2013). The majority of the prokaryotic species still is uncultured (Rappé & Giovannoni 2003). It is therefore very likely that many taxa exist that are directly or indirectly involved in the *in situ* degradation of chitin, but have yet to be described as such or still await isolation.

Table 1. List of bacterial and archaeal phyla including cultured aerobic and obligate anaerobic chitinolytic species.

	Representative species	Reference
Aerobes		
Bacteria		
Armatimonadetes	*Chthonomonas calidirosea*	Lee *et al*., 2011
Acidobacteria	*Blastocatella fastidiosa*	Foesel *et al*., 2013
Actinobacteria	Streptomyces coelicolor	Chater *et al*., 2010
Bacteroidetes	*Flavobacterium johnsoniae*	Sangkhobol & Skerman 1981
Betaproteobacteria	*Silvimonas terrae*	Yang *et al*., 2005
Gammaproteobacteria	*Serratia marcescens*	Vaaje-Kolstad *et al*., 2013
Deltaproteobacteria	*Sorangium cellulosum*	Garcia & Müller 2014
Firmicutes	*Paenibacillus chitinolyticus*[a]	Kuroshima *et al*., 1996
Obligate Anaerobes		
Bacteria		
Firmicutes	*Ruminiclostridium cellulolyticum*	Reguera & Leschine 2001
Archaea		
Euryarcheota	*Thermococcus chitonophagus*	Huber *et al*., 1995

[a]facultative aerobic

1.5. Detection of chitin-degrading microorganisms

The first chitinolytic bacteria were discovered in 1937 (Skinner & Dravis 1937). Since then, most of the knowledge about their physiology, diversity, and ecological niches was derived from (pure) culture-dependent studies (Gooday 1990b). In the late 80´s of the 20th century molecular tools found their way into microbiology and microbial ecology research. The ribosomal approach to study the microbial diversity soon made it obvious that a major part of the prokaryotic diversity is unknown (Rappé & Giovannoni 2003). Up to date, microbiomes of various ecosystems are studied by the analysis of 16S rRNA genes (Hirsch *et al*., 2010; Rappe & Giovannoni 2003; Schimel 2016; Schloss *et al*., 2016; Sinclair *et al*., 2015; Van Elsas & Boersma 2011). However, in recent years 'omic' technologies (e.g. transcriptomics, metabolomics, metagenomics, and/or proteomics) have increasingly been applied to study activity, metabolic networks, food webs, and community structure of microbiomes (Jansson *et al*., 2012; Prosser *et al*., 2015; Schimel 2016; Van Elsas & Boersma 2011; Vilchez-Vargas *et al*., 2010; von Bergen *et al*., 2013). In addition to 16S rRNA gene analysis, genes encoding key enzymes of metabolic pathways (so called functional gene markers) can be used to study functional groups (e.g. methane oxidizers or sulfate reducers)(Kolb *et al*. 2003; Meyer & Kuever 2007; Murrell & Radajewski 2000; Muyzer & Stams 2008; Wagner *et al*., 1998). The key metabolic enzymes for chitin degradation are chitinases (Beier & Bertilsson 2013; Gooday 1990b). Most bacterial chitinases are known to belong to the GH 18 family (Cohen-Kupiec & Chet 1998; Karlsson & Stenlid 2009), which is further divided into the subfamilies A, B, and C (Cantarel *et al*., 2009; Henrissat & Bairoch 1993; Karlsson & Stenlid 2009; Suzuki *et al*., 1999, 2002). Primer systems to study chitinases in the environment have been developed for subfamily A (Hobel *et al*., 2005; LeCleir *et al*., 2004; Metcalfe *et al*., 2002; Williamson *et al*., 2000; Xiao *et al*., 2005) and have been widely used to study chitinolytic bacteria biodiversity in various environments (Beier *et al*., 2011; Beier & Bertilsson 2013; Cottrell *et al*., 1999; Cretoiu *et al*., 2012; Hjort *et al*., 2010; Hobel *et al*., 2005; Kielak *et al*., 2013; Köllner *et al*., 2012; LeCleir *et al*., 2004, 2007; Metcalfe *et al*., 2002; Peter *et al*., 2011; Ramaiah *et al*., 2000; Williamson *et al*., 2000; Xiao *et al*., 2005). However, an apparent problem studying the chitinolytic subpopulations in microbial communities is that *chiA* as a functional gene marker likely does not cover all chitinolytic microorganisms. Not all bacteria necessarily possess this type of chitinase and might just rely on other chitinase variants and/or mechanisms (e.g. polysaccharide monooxygenases or polysaccharide utilizing loci; 1.2.3.) for chitin cleavage and degradation (Hemsworth *et al*., 2016). The research on microbial chitin degradation is so far not as extensive as on microbial cellulose degradation. The research on cellulases, the key enzymes of cellulolytic organisms, has shown that their high genetic and structural heterogeneity does not allow designing appropriate primer systems (Bayer *et al*. 2006; Lynd *et al*., 2002). Therefore, a more

comprehensive approach is to analyze the shift in the 16S rRNA gene community structure after supplementation of exogenous chitin. However, such results have to be interpreted with caution as a possible stimulation of certain taxa might be due to cross-feeding or microbial 'cheating', i.e. consuming chitin hydrolysis products without producing own chitin degradation enzymes (Beier & Bertilsson 2013). Therefore, a combined approach, i.e. studying *chiA* and 16S rRNA genes simultaneously, as it was done in several recent studies, seems to be the best solution so far (Cretoiu *et al*., 2012, 2013, 2014), although the uncertainty to distinguish between chitinolytic and saccharolytic taxa cannot be avoided.

Stable isotope probing (SIP) is a method that relies on the incorporation of a substrate that is highly enriched in a stable isotope. In combination with 16/18S rRNA gene or functional gene marker analysis, SIP allows to identify microorganisms that utilize a particular growth substrate (Dumont & Murrell 2005; Radajewski *et al*., 2000, 2003; Manefield *et al*., 2002a,b). In the beginning of SIP as analytical tool in environmental microbiology, only simple substrates like methane or glucose were available, but soon more complex substrates like phenolic compounds or polysaccharides were used (Bastias *et al*., 2009; Bernard *et al*., 2007; Dallinger & Horn 2014; Eichorst & Kuske 2012; Haichar *et al*., 2007; Schellenberger *et al*., 2010; Winderl *et al*., 2010). A further development of the SIP approach is the analysis of labeled proteins allowing to couple phylogenetic with functional information of the phenotype (Jehmlich *et al*., 2008; Seifert *et al*., 2012). So far, no study exists in which [^{13}C]-labeled chitin has been used to study the microbial taxa involved in chitin degradation.

1.6. Environmental influences on microbial chitin degradation

Chitinolytic and saccharolytic microorganisms catalyze the degradation of chitin (1.2.3.), thereby holding a key role in the turnover of carbon and nitrogen of ecosystems. They are part of a complex microbial community (i.e., microbiome) responsible for the degradation of the (often recalcitrant) biopolymers (e.g. polysaccharides, lipids, or lignin) produced by prokaryotes and eukaryotes. The microbiome of agricultural soils of arable land is subject to rapidly changing environmental conditions. Environmental factors that influence microbiome's members degrading chitin are for example the soil type, water content, temperature, substrate availability, and soil pH (Kielak *et al*., 2013; Manucharova *et al*., 2006, 2011; Terahara *et al*., 2009; Yaroslavtsev *et al*., 2009). Oxygen availability is another important factor that affects soil microbiomes and is directly associated with the water content, aggregate size, and properties of biogeochemical interfaces (Six *et al*., 2004; Or *et al*., 2007; Totsche *et al*., 2010). While agricultural soils are largely aerated, microbially induced, and spatially heterogeneously distributed, anoxic microzones can coexist within oxic microzones (Küsel & Drake 1995; Pett-Ridge & Firestone 2005; Picek *et al*., 2000; Wagner *et al*.,1996).

1.6.1. Oxygen availability determines microbial processes in soils

Oxygen availability is directly associated with the soil water content as the (microbial) consumption may exceed the diffusion of oxygen at the interface of gas-filled and water saturated pores (Brune *et al*., 2000; Dassonville *et al*., 2004; Greenwood 1961). This leads to the formation of anoxic microzones, which sustain even in largely aerated soils (Küsel & Drake 1995; Pett-Ridge & Firestone 2005; Picek *et al*., 2000; Wagner *et al*., 1996). Facultative aerobes and obligate anaerobes are capable of utilizing other electron acceptors than oxygen or ferment under anoxic conditions in order to conserve energy. Thus, they can be metabolically active under anoxic conditions (Böck 2000; Nealson & Saffarini 1994; Muyzer & Stams 2008; Tiedje 1988). Increased water saturation, e.g. after a rain event, increases spatially and temporally the formation of anoxic microzones, thus favoring the activity of facultative aerobic and anaerobic microorganisms. In anoxic microzones, alternative electron acceptors are sequentially utilized based on their standard redox potentials and concentrations according to the thermodynamic theory (Peters & Conrad 1996; Zehnder & Stumm 1988).

1.7. Hypotheses and objectives

Chitin is the second most abundant polysaccharide after cellulose and is subject to microbial turnover in the environment. Microbial degradation of chitin in soil substantially contributes to carbon turnover and release of terrestrial ecosystem (Beier & Bertilsson 2013; Gooday 1990a,b). In aerated soils, chitin can be found in protists, arthropods, and fungi as a structural component (Gooday 1990a,b; Martínez *et al*., 2009). Thereby, fungi represent the main source of chitin in such soils as fungi have cell walls with up to 25% chitin and account for up to 60-90% of the microbial biomass in aerated soils (Blumenthal & Roseman 1957; Fernandez & Koide 2012). Chitin degradation can theoretically occur via to two major degradation pathways. It can be deacetylated to chitosan or can be hydrolyzed to *N*,*N´*-diacetylchitobiose and oligomers of *N*-acetylglucosamine by aerobic and anaerobic microorganisms (1.2.3.1; Beier & Bertilsson 2013; Gooday 1990a,b). Which pathway of chitin hydrolysis is preferred by soil microbial communities is unknown. In addition, chitin is a major resource of carbon and energy for soil microbiomes and it is therefore a driver of soil microbial food webs. The interactions and dynamics of members of a soil microbiome degrading chitin and the influence of oxygen on the carbon flow from chitin degradation are largely not resolved in aerated soils. Thus, the following hypotheses were addressed in the doctoral project:

Hypothesis 1: Chitin in aerated soil is not degraded via prior deacetylation to chitosan.

Hypothesis 2: During the degradation of chitin, different subsets of members of the soil microbiome are activated depending on differences in the oxygen availability, which is a consequence of the heterogeneity of aggregate structures in an aerated soil.

Hypothesis 3: Oxygen limitation changes the path of chitin-derived carbon in the bacterial and micro-eukaryotic food web.

The objective to adress hypothesis 1, was to determine the microbial processes associated with chitin and chitosan hydrolysis and degradation and to assess metabolic responses and identities of chitinolytic microorganisms by analyzing the chitinases marker gene *chiA*. To assess hypotheses 2 and 3, the objective was to resolve the carbon flow path through the microbiome and the trophic interactions between its members in an agricultural soil sample under oxic and anoxic conditions using a stable-isotope labeling approach. 16S rRNA- and protein-based stable isotope probing (SIP) together with chemical analytics was used to resolve the microbial conversion of supplemental [^{13}C]-chitin and microorganisms in soil slurries from a wheat-planted field in south Germany.

2. Materials and methods

2.1. Gases, chemicals and media

Gases were obtained from Rießner-Gase GmbH (Lichtenfels, Germany). Unless otherwise stated chemicals and laboratory equipment were supplied from AppliChem (Darmstadt, Germany), Sigma-Adrich (Steinheim, Germany), BioRad (Richmond, USA), Carl Roth (Karlsruhe, Germany), Eppendorf (Hamburg, Germany), Fluka (Buchs, Switzerland), and Merck (Darmstadt, Germany). The ultrapure water purification system Seralpur Pro 90 CN (Seral Erich Alhäuser, Ransbach-Baumbach, Germany) was used to produce deionized-double distilled water (ddH_20). For molecular work, if necessary, RNAse/DNAse-free water (Gibco® Invitrogen, Germany) was used. For transformation of competent cells and cultivation of clones (2.5.11.) different culture media were utilized (2.1.2.; 2.1.3.).

2.1.1. LB agar plates

All components were mixed and filled up to 980ml with ddH_20. The pH was adjusted to 7 and the volume finally was filled up to 1L. The medium was autoclaved and poured into sterile plastic dishes that were stored at 4°C after solidification.

Table 2. LB medium (Lurani-Bertani medium) agar plates.

Component	Amount	Final Concentration
Tryptone	10 g	1.0 %
Yeast extract	5 g	0.5 %
NaCl	5 g	0.5 %
Agar	15 g	1.5 %
ddH_20	ad 1,000 ml	
pH 7		

2.1.2. LB agar plates with ampicillin

The medium for agar plates with ampicillin was prepared as described (2.1.1.). In addition, 1 ml of sterile-filtered ampicillin (100 $mg \cdot ml^{-1}$) was added to the autoclaved medium after it cooled down to approximately 60°C.

2.1.3. SOC medium

Table 3. SOC medium (Super-Optimal-Broth medium).

Component	Amount	Final Concentration
Tryptone	2.0 g	2.0 %
Yeast extract	0.5 g	0.5 %
NaCl solution (1 M)	1.0 ml	10.0 mM
KCl solution (1 M)	0.25 ml	2.5 mM
$MgCl_2$ solution (2 M)	1.0 ml	20.0 mM
Glucose solution (1 M)	1.0 ml	20.0 mM
ddH_20	ad 100 ml	
pH 7		

All components except the $MgCl_2$ and glucose solutions were combined and filled up to approximately 95 ml and then autoclaved. Afterwards, sterile filtered (Ø 0.2 µm) $MgCl_2$ and glucose solutions were added. The pH was adjusted using sterile filtered solutions and the medium was finally filled up with ddH_20 to 100 ml. The medium was again sterile filtered and stored at -20°C.

2.1.4. Trace element solution

Table 4. Trace element solution.

Component	Amount	Final Concentration
Nitrilotriacetic acid	1.5 g	7.85 mM
$MnSO_4 \cdot H_2O$	0.5 g	2.96 mM
$FeSO_4 \cdot 7H_2O$	0.1 g	0.36 mM
$CoCl_2 \cdot 6H_2O$	0.1 g	0.42 mM
$CaCl_2 \cdot 2H_2O$	0.1 g	0.68 mM
$ZnSO_4 \cdot H_2O$	0.1 g	0.35 mM
$CuSO_4 \cdot H_2O$	0.01 g	0.04 mM
$AlK(SO_4)_2 \cdot 12H_2O$	0.02 g	0.04 mM
H_3BO_3	0.01 g	0.16 mM
$Na_2MoO_4 \cdot 2H_2O$	0.01 g	0.04 mM
ddH_2O	ad 1000 ml	

[a]Modified after Balch *et al*., 1979.

2.2. Sampling site and soil characteristics

The sampling site is located on the research farm 'Klostergut Scheyern' near Munich, Germany (48°30.0´N, 11°20.7´E). The upper 20 cm-layer of the aerated agricultural soil (Table 5) was sampled in April 2011 and 2012, stored under dark and moist conditions at 2°C and processed within a week.

Table 5. Soil characteristics[a].

	Klostergut Scheyern, Germany
Coordinates	48°30.0´N, 11°20.7´E
Soil type[b]	Dystric Cambisol
Texture (clay:silt:sand)[c]	28 : 33 : 40 ≙ clay loam (Lt2)
W_g (%)	17.7 ± 0.8[d]; 21.9 ± 1.0[e]
Total C (%)[c]	1.2 ± 0.0
Total N (%)[c]	0.2 ± 0.0
C/N ratio[c]	6.9 ± 0.1
pH	6.6 ± 0.1
Inorganic ions	**µmol $g_{soil\ DW}^{-1}$**
NH_4^+	0.06 ± 0.15[d]; 0.00 ± 0.00[e]
NO_3^-	3.54 ± 0.14[d]; 2.2 ± 0.2[e]
Total Fe	40.0 ± 15.8[d]; 103.4 ± 37.5[e]
Total Mn	5.3 ± 3.1[d]; 10.0 ± 6.7[e]
SO_4^{2-}	0.03 ± 0.14[d]; 1.2 ± 0.1[e]

[a]values are means of 3-36 replicates
[b]Fuka *et al*., 2008
[c]Eckelmann 2005
[d]year 2011
[e]year 2012
[f]Institute for Central Analytics, University of Bayreuth, Germany.
Wg, gravimetric water content.
DW, dry weight.

2.3. Soil microcosms

Microcosms were prepared as soil slurries by mixing soil with sterile oxic or anoxic water (ratio 1:2.5) in a total volume of one liter in sterile rubber-stoppered 2-liter-flasks. Soil from April 2011 was used in experiments with GlcNAc and GlcN, and soil sampled in April 2012 was used in experiments with chitin, chitosan, and $[GlcNAc]_2$. Slurries were placed on ice and flushed with sterile argon or sterile air for one hour. In unsupplemented controls no substrate was added to determine indigenous processes and carbon turnover for each experiment. Incubations were performed at 20°C in the dark.

2.3.1. Treatments for stable isotope probing

A stable isotope probing experiment was set up in order to resolve the microbial food web and to identify taxa involved in the degradation of chitin. Soil slurries were prepared by mixing fresh sampled soil with sterile oxic or anoxic water (ratio 1:2.5) in a total volume of one liter in sterile rubber-stoppered 2-liter flasks. Soil sampled in April 2012 was used. The 'master' slurries were flushed with sterile argon (100%) or sterile air for one hour and homogenized on an end-over-end shaker over night at 5°C. The slurries were then separated into 110-ml aliquots in butyl rubber-stoppered 500-ml flasks (Müller & Krempel, Bülach, Switzerland) with argon or air as the atmosphere. Microcosms were set up in duplicate. 0.125 g of [U-^{13}C]-chitin (U=Uniform, >98% ^{13}C) or [U-^{12}C]-chitin (1.1% ^{13}C) derived from *Aspergillus niger* (Iso*Life*, Wageningen, Netherlands) was added at the onset of incubation; this amount equals 5 mmol of carbon. From here on, uniformly labeled [U-^{13}C]-chitin or [U-^{12}C]-chitin will be referred as [^{13}C]-chitin and [^{12}C]-chitin. To minimize 'cross-labeling' by either the autotrophic or heterotrophic fixation of the [^{13}C]-carbon dioxide formed during the degradation of the primary labeled substrate, chitin-supplemented treatments were periodically flushed for 15 minutes with sterile dinitrogen or air. Oxic and anoxic control incubations were not supplemented with chitin. Supplemented and control slurries were incubated in the dark at 20°C on an end-over-end shaker (60 rounds per minute).

2.3.2. Treatments to determine the route of chitin degradation

To determine whether chitin is degraded 'directly' or via prior deacetylation to chitosan (1.2.3.1.; Fig. 3) soil slurries supplemented with chitin or chitosan were set up. Slurries were prepared by mixing soil with sterile oxic or anoxic water (ratio 1:2.5) in a total volume of one liter in sterile rubber-stoppered 2-liter-flasks. Soil sampled in April 2012 was used. For chitin- and chitosan-supplemented slurries, 0.2 g of ground chitin or chitosan (acetylation degree 95% and 15–25%, respectively) (Sigma-Aldrich® GmbH, Germany) was added at the onset of incubation. The 'master' slurries were homogenized on an end-over-end shaker for 1.5 h

at 5°C and were then divided in 80mL aliquots in rubber-stoppered 0.5 L flasks (Müller & Krempel, Bülach, Switzerland) with sterile argon or air as atmosphere. Treatments were conducted in triplicates. The flasks were incubated in the dark on an end-over end shaker (60 rounds per minute) at 20°C.

2.3.3. Treatments with chitin hydrolysis products

Soil slurries were prepared by mixing soil with sterile oxic or anoxic water (ratio 1:2.5) in a total volume of one liter in sterile rubber-stoppered 2-liter-flasks. Soil from April 2011 was used in experiments with GlcNAc and GlcN, and soil sampled in April 2012 was used in treatments with $[GlcNAc]_2$. Soluble N-sugars were supplemented with a final concentration of 250 µM GlcNAc, GlcN (AppliChem GmbH, Darmstadt, Germany) and 125 µM $[GlcNAc]_2$ (Megazyme, Bray, Ireland) were added at the onset of incubation. The 'master' slurries were homogenized on an end-over-end shaker for 1.5 h at 5°C and were then divided in 80 ml aliquots in rubber-stoppered 0.5 L flasks (Müller & Krempel, Bülach, Switzerland) with sterile argon or air as atmosphere. Treatments were conducted in triplicates. The flasks were incubated in the dark on an end-over end shaker (60 rounds per minute) at 20°C.

2.4. Analytical methods

2.4.1. pH measurements

The pH was measured with a pH meter (U457-S7/110 combination pH electrode; Ingold, Germany) and a digital pH meter (WTW pH 330, Wissenschaftlich-Technische Werkstätten, Weilheim, Germany).

2.4.2. Dry weight and soil moisture

Dry weight and moisture contents of soils were determined by weighing four samples of fresh soil followed by drying at 60°C for several days and subsequent weighing (Schachtschabel *et al.*, 1992).

2.4.2. Gases

Carbon dioxide, hydrogen gas, and methane were measured with a gas chromatograph (Multigas Analyzer SRI 8610C, SRI Instruments, Torrance, CA) equipped with a thermal conductivity detector (TCD) and a helium ionization detector (HID). 1 ml gas sample were injected on a 'sample loop' that separately loaded 50 µl of gas sample on the two columns.

Table 6. Gas chromatograph parameters.

	CO_2, CH_4	H_2
Detector	Thermal Conductivity Detector (TCD)	Helium Ionization Detector (HID)
Column	HayeSep-D column 2m x 1/8'' SRI Instruments Torrance, CA, USA	molecular sieve column 13X 2m x 1/8'' Restek, Bellefonte, PA, USA
Carrier Gas	Helium	Helium
Flow rate	40 ml min^{-1}	20 ml min^{-1}
Oven temperature	60°C	60°C
Detector temperature	175°C	150°C
Column injection volume	50 µl	50 µl
Special settings	TCD amplifier high	HID current on, 250°C
Retention time	CO_2: 2.68 min; CH_4 1.46 min	0.72 min

Chromatograms were integrated and analyzed with PeakSimple (SRI Instruments, Torrance, CA, USA) and the use of external standards with known gas concentrations. Actual room temperature, actual air pressure, and volume of gas and liquid phase were considered for the calculation of the gas concentrations (Equation 1 - Equation 5).

Equation 1. Total amount of gases.

$$n_t = n_g + n_{lp} + (n_{lc})$$

n_g (mmol) was calculated using the ideal gas law (Equation 2).

Equation 2. Ideal gas law.

$$n_g = \frac{p_i \times V_g}{R \times T}$$

p_i, the partial pressure of the gas (in mbar); V_g, the volume of the gas phase (in ml); R, the universal gas constant (83.145 mbar·ml·K^{-1}·$mmol^{-1}$); T, the actual temperature in K.

p_i was calculated from the measured gas concentration C (in %), the current atmospheric pressure p_a (in mbar), and the overpressure measured in the flasks p_o (in mbar) according to Equation 3.

Equation 3. Partial pressure of gases.

$$p_i = \frac{C \times (p_a + p_o)}{100}$$

n_{lp} is dependent on the gas specific solubility coefficient (α) listed in Table 7 and was calculated according to Equation 4.

Equation 4. Physically dissolved gases in the liquid phase.

$$n_{lp} = \frac{n_g \times V_l \times \alpha}{V_g}$$

V_l , volume of the liquid phase (in ml).

n_{lc} has to be included in the calculation of total amounts of a gas if it reacts chemically with the solvent. Thus, n_{lc} was calculated for CO_2, which reacts with water predominately to bicarbonate in the pH range of the experiments in this dissertation (Equation 5).

Equation 5. Chemically dissolved CO_2 (bicarbonate).

$$n_{lc} = n_{lp} \times 10^{pH\ -pK}$$

pKa, the logarithmic acid dissociation constant for bicarbonate is 6.37.

Table 7. Bunsen solubility coefficients[a].

Gas	Bunsen solubility coefficients α (in water)			
	5°C	15°C	20°C	25°C
CO_2	1.38	0.99	0.85	0.74
H_2	0.020	0.018	0.018	0.017
CH_4	0.046	0.036	0.032	0.029

[a]Blachnik 1998

2.4.2.1. [^{12}C]- and [^{13}C]-carbon dioxide

For the analysis of $^{12}CO_2$ and $^{13}CO_2$ in the gas samples, GC-MS analysis was performed by Henrike Höke and Sara Ferdi at the Department of Molecular Systems Biology (Helmholtz Centre for Environmental Research-UFZ, Leipzig, Germany). A Perkin–Elmer GC Clarus 600 system with a Rtx®-1 capillary column (60 m x 320 µM) was used. For GC-MS detection, an electron ionization system was operated with an ionization energy of 70 eV. Mass spectra

were taken from 14 to 70 Da. Helium was used as carrier gas at a constant flow with 300 kPa, and an injection volume of 10 µl (split ratio 10:1) was employed manually by use of gastight syringes. Each sample was measured five times. The total amount of $^{12}CO_2$ and $^{13}CO_2$ was analyzed by extraction of the masses 44 and 45 followed by peak integration. The peak areas were corrected with $^{12}CO_2$ and $^{13}CO_2$ indoor air values and finally the ratio of the masses 45/44 was calculated.

2.4.3. Soluble organic compounds

Organic acids and sugars were determined by high-performance liquid chromatography (HPLC; Hewlett Packard 1090 Series II) with an Aminex ion exclusion column (HPX-87H,300 x 7.8 mm, BioRad, Richmond, CA, USA) using 4mM phosphoric acid as eluent. The compounds were detected with an UV detector (G1314B, Series 1200, Agilent Technologies, Böblingen, Germany) and a refractive index detector (G1362A, Series 1200, Agilent Technologies). Liquid samples were centrifuged at 13,000 g (Himac CT15E, Hitachi Koki Co.,Ltd., Tokyo, Japan) for 15 min and the supernatant was filtrated (HPLC nylon filter, pore volume 0.2 µm, Infochroma, Zug, Switzerland) into flange bottles with aluminum caps (VWR International, Darmstadt, Germany). The flow rate of the mobile phase was 0.8 ml·min^{-1} and the oven temperature was 60°C. Compounds were identified and quantified with external standards with known concentrations and the 2D ChemStation software (Agilent, Böblingen, Germany).

2.4.4. Inorganic compounds

2.4.4.1. Ferrous iron (Fe^{2+})

Ferrous iron concentrations were determined photometrically. 80 µl of the soil slurry samples were mixed with 3.92 ml HCl (0.5 N) to solubilize the ferrous iron bound to the soil matrix. After incubation for 1 hour at room temperature the sample was filtrated (HPLC nylon filter, pore size 0.2 µm, Infochroma, Zug, Switzerland) to remove soil particles. 50 µl acetate buffer (200 g CH_3COONH_4, 250 ml CH_3COOH, ad 500 ml ddH_2O) and 50 µl of a phenanthroline solution (1 g 1,10-Phenanthrolinium-chloridemonohydrate, ad 200 ml ddH_2O) were added to 450 µl of the filtrated sample, leading to the development of a red-colored Fe-phenanthroline-complex. 160 µl of the mixture were immediately transferred to microtiter plates (Orange Scientific, Braine-l'Alleud, Belgium) and extinction was measured at 512 nm by a µQuant microplate spectrophotometer (BioTek, Bad Friedrichshall, Germany). External standards with known concentrations were used for quantification.

2.4.4.2. Nitrate (NO_3^-), ammonium (NH_4^+), sulfate (SO_4^{2-}) and total amounts of iron and manganese

Compounds were analyzed by standardized colorimetric methods by the Institute of Central Analytics, University of Bayreuth. External standards with known concentrations were used for quantification.

2.5. Nucleic acids and proteins analytics

2.5.1. Extraction of nucleic acids

DNA and RNA from soil slurry samples was extracted by modified protocol of Griffiths *et al*. (2000). 2 ml soil slurry were transferred to 2 ml micro-centrifuge tubes (Eppendorf, Hamburg, Germany) centrifuged at 13,000 g (Himac CT15E, Hitachi Koki Co., Ltd., Tokyo, Japan) for 15 min. The supernatant was discarded. 0.4 g of the soil pellet were transferred to 2 ml screw-capped tubes (VWR International, Darmstadt, Germany) that were filled with 1 g of baked (12 h, 200°C) zirconium beads (0.5 g Ø 0.1 mm, 0.5 g Ø 0.5 mm; CarlRoth, Karlsruhe, Germany). 0.5 ml preheated (60°C) extraction buffer (5% CTAB, 350 mM NaCl, 120 mM potassium phosphate buffer [containing KH_2PO_4 and K_2HPO_4], pH 8), 0.5 ml phenol/chloroform/isoamyl alcohol (25:24:1) were added and samples were bead beaten two times at 5.5. m/s in a Bead Beater (FastPrep FP 120, Thermo Savant, USA) for 30 seconds and samples were handled on ice from thereon. Samples were centrifuged 10 min at 13,000 x g, 4°C, 1-15K Sartorius microcentrifuge) and the liquid phase containing the nucleic acids was transferred in a new 1.5 ml microcentrifuge tube (from here all steps were performed in certified RNase-and DNase-free tubes). 500 µl chloroform/isoamylalcohol (24:1) were added, samples were mixed, and centrifuged (10 min at 13,000 x g, 4°C) to separate the nucleic acids from residual proteins and phenol. Supernatant was transferred to sterile 2 ml tubes and two volumes precipitation buffer (0.1 M Hepes pH 7 - 30% PEG; Fluka, Neu-Ulm, Germany) until the solution was clear to precipitate the nucleic acids. The samples were incubated for two hours at room temperature and centrifuged (10 min at 13,000 × g, 4°C) to pelletize the precipitated nucleic acids and the supernatant was discarded. 0.5 ml ice cold ethanol (70%) was added, centrifuged, and the supernatant was discarded to remove salts. Nucleic acids were dried at room temperature and dissolved in 52 µl DNase/RNase-free ddH_2O. Nucleic acid extraction was checked spectrophotometrically (2.5.4.1.) and extracts were stored at -80°C.

2.5.2. Separation of DNA and RNA

DNA was removed by enzymatic digestion with DNase I (1 $U \cdot \mu l^{-1}$, Fermentas) for 45 min at 37°C under constant shaking (300 rpm) in a thermomixer (Thermomixer comfort, Eppendorf, Hamburg, Germany) to obtain RNA only. RNA was removed from coextracts by enzymatic digestion with RNase A (10 $\mu g \cdot \mu l^{-1}$, Fermentas, St. Leon-Roth, Germany) for 30 min at room temperature to obtain DNA only. Enzymatic digestions were stopped by isopropanol precipitation of nucleic acids (2.5.3.).

2.5.3. Purification and precipitation of nucleic acids

2.5.3.1. Isopropanol precipitation

One volume of nucleic acid extracts treated with DNase I or RNase A (2.5.1.) were precipitated with 0.7 volume of ice cold isopropanol and 0.1 volume of sodium chloride (5 M) (Green & Sambrook 2012). Nucleic acids were incubated for 12 h in a freezer (-20°C) and pelleted by centrifugation (1 h at 18,000 × g, 4°C). Pellets were washed by adding 0.5 ml ice cold ethanol (70%) and subsequent centrifugation. Supernatant was removed and pellets dried at room temperature and dissolved in 20 µl DNase/RNase-free ddH_2O.

2.5.3.2. Gel extraction

PCR products amplified for TRFLP analyses (2.5.8.5.; 2.5.10.) and PCR products for the construction of gene libraries (2.5.8.5.; 2.5.11.) were purified by agarose gel extraction (Montage gel extraction kit, Millipore, Bedford, USA) according to the manufacturer's protocol to separate and purify the products of the desired size from unspecific byproducts. Agarose gel electrophoresis was performed for 1 hour at 70 mV as described elsewhere (2.5.5.). Ethidium bromide stained DNA was visualized by UV light (302 nm, Transilluminator UVT-20M, Herolab GmbH, Wiesloch, Germany). DNA-bands of the desired size were excised from the gel with a sterile knife and transferred to the Montage gel extraction columns. Finally, gel extracts were purified by isopropanol precipitation (2.5.3.1.).

2.5.3.3. Filter plates

PCR products that were subjected to mung bean endonuclease digestion (2.5.10.1.) and PCR products representing clone insert sequences or re-amplified *chiA* genes thereof (2.5.8.5) were purified with Millipore PCR96 Cleanup Plates (Millipore Cooperation, Bedford, USA) according to the manufacturer’s protocol. Samples were loaded onto the filters and plates were evacuated for 12 minutes with a suction pump (KNF Neuberger, Balterswil, Switzerland). PCR products were dissolved in 25 µl tris buffer (10 mM, pH 8.5) and transferred into sterile 0.5 ml tubes (LoBind tubes, Eppendorf, Hamburg, Germany).

2.5.4. Quantification of nucleic acids

2.5.4.1. NanoDrop-based quantification

Purity and concentrations of nucleic acids and were determined spectrophotometrically with a ND1000 (PEQLAB Biotechnology GmbH, Erlangen, Germany) and supplied software. Absorption (A) at 230, 260, and 280 nm wavelength were measured. Ratios of A260/A280 between 1.6 and 2.0 and A260/A230 of above 1.0 indicated that nucleic acid extracts were pure with little protein/phenol and humic acid contaminations, respectively (Tsutsuki & Kuwatsuka 1979; Lottspeich & Engels 2006; Green & Sambrook 2012). In addition, the absorption spectrum should be low at 230 nm, because humic acids strongly absorb at this wavelength (Tsutsuki & Kuwatsuka 1979).

2.5.4.2. Pico- and Ribogreen-based quantification

For the accurate quantification of DNA or RNA (≤ 10 ng·µl^{-1}) a fluorescence-based method, which is less sensitive to interferences by contaminants than NanoDrop (2.5.3.1), was used. Quantification of DNA and RNA was performed in microtiter plates with the Quant-iT-PicoGreen dsDNA reagent Kit and the Quant-iT-RiboGreen Quantitation Reagent Kit (both Invitrogen, Karlsruhe, Germany), respectively according to the manufacturer's protocol. Fluorescence was measured with a FLx800 microplate fluorometer (BioTek, Bad Friedrichshall, Germany) and the signals were recorded with the software Gen5 (BioTek, Bad Friedrichshall, Germany). Concentrations were evaluated with external DNA/RNA standards delivered by the manufacturer.

2.5.5. Agarose gel electrophoresis

Nucleic acid extracts (2.5.1.) and PCR products (2.5.8.) were analyzed by horizontal agarose gel electrophoresis, a method that separates nucleic acids in an electrical field dependent on their size (Aaij & Borst 1972; Green & Sambrook 2012). Gels were prepared with 1% w/v low EEO standard agarose (AppliChem GmbH, Darmstadt, Germany) and 1 × TAE buffer (40 mM Tris-HCl, 20 mM acetate, 1 mM EDTA, pH 8). The mixture was heated in a microwave until the agarose completely melted. After cool down to approximately 60°C ethidium bromide (3,8-diamino-5-ethyl-6-phenyl-phenenthridium bromide, BioRad) at a final concentration of 0.08 mg·ml^{-1} was added. Liquid gels were poured into a gel rack and transferred into migration chambers (BioRad Mini- or Maxi- Sub cell, BioRad) after solidification. Migration chambers were filled 1 × TAE buffer. 5 µl sample was mixed with 1 µl 6 × Blue Orange loading dye (Promega, Madison, WI, USA) or self-prepared 6 x loading dye (0.05% bromophenol blue, 0.05% xylene cyanol, 55% glycerol) and transferred into the gel slots. 2 µl molecular weight marker (MWM 1, Bilatec, Viernheim, Germany) were used to determine the length of products. Electrophoresis was performed for 20-60 min at 80-120 V

(Power-Pak 3000, BioRad). DNA-bands containing nucleic acids were visualized by UV light (302 nm, Transilluminator UVT-20M, Herolab GmbH, Wiesloch, Germany). The UV-illuminated gel was photographed with a Canon PowerShot G5 camera (Canon, Krefeld, Germany).

2.5.6. Stable isotope probing (SIP)

Stable isotope probing (SIP) is a method that relies on the incorporation of a substrate that is highly enriched in a stable isotope. Organisms that feed on substrates marked with heavy stable isotopes (e.g., [^{13}C]-carbon labeled [^{13}C]-cellulose) incorporate the heavy isotopes into biopolymers (e.g., RNA or DNA) and can be identified by the analysis of 16/18S rRNA gene or functional gene markers (Dumont & Murrell 2005; Manefield *et al.*, 2002a,b; Radajewski *et al.*, 2000, 2003; Schellenberger *et al.*, 2010).

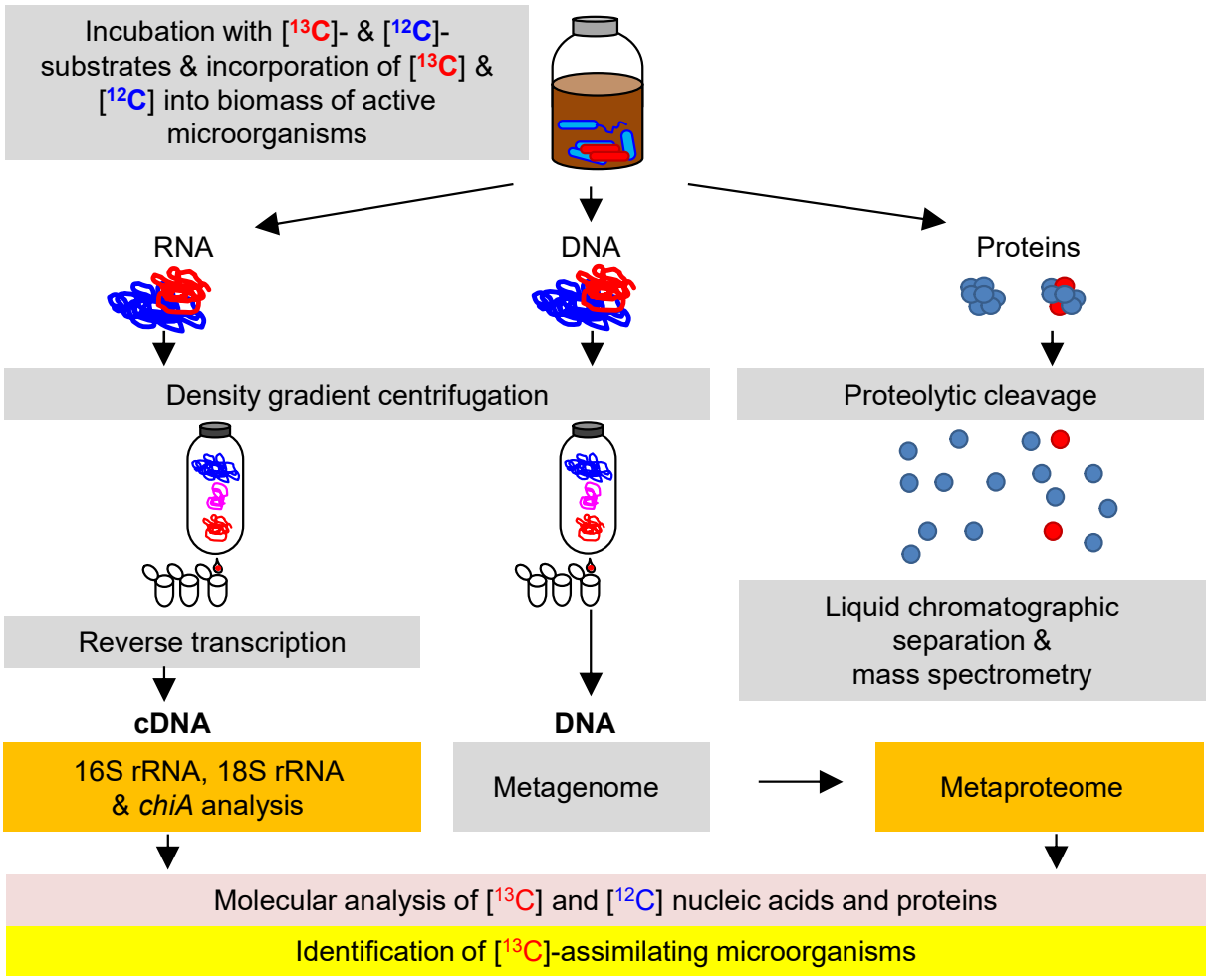

Figure 6. Schematic protocol of stable isotope probing (SIP). See text for details.

2.5.6.1. RNA based stable isotope probing (RNA SIP)

To separate [^{13}C]-labeled 'heavy' RNA from the 'light' [^{12}C]-RNA the slightly modified protocol of Whiteley *et al*. (2007) was applied. Nucleic acids were extracted from samples of oxic and anoxic soil slurries (2.3.1.) before and after the incubation with [^{13}C]- and [^{12}C]-substrates. DNA was digested to obtain RNA (2.5.2.). A gradient solution with a buoyant density of 1.790 ± 0.006 g ml^{-1} was prepared. Therefore, 83.3% cesium trifluoroacetate (CsTFA; buoyant density 2.0 g·ml^{-1}, GE Healthcare, Buckinghamshire, UK), 13.5% gradient buffer (100 mM Tris; 100 mM potassium chloride; 1mM EDTA; pH 8) and 3.2% deionized formamide were mixed. The density was measured (2.5.6.4.) and the desired buoyant density was adjusted by adding gradient buffer were added until the gradient solution had a buoyant density of 1.790 ± 0.006 g ml^{-1}. 500 ng of RNA were mixed with 1 ml of gradient solution and transferred into a 4.9 ml centrifugation tube (OptiSeal Polyallomer Tube, 13 x 48 mm; Beckmann, Palo Alto, USA). The tubes were filled with gradient solution, balanced until a maximal difference of 0.05 g was achieved, closed with a plug and placed in an ultra-vertical VTi 65.2 Rotor (Beckman). Aluminum spacers were placed on the tubes and screws were closed with a torque wrench adapter (200 inch-pounds, Beckham Coulter, Fullerton, USA) to a bolting torque of 60 inch pounds. 'Heavy', potentially [^{13}C]-labeled RNA was separated from 'lighter' non-labeled [^{12}C]-RNA by isopycnic centrifugation (130,000 × g or 37,800 rpm at 20°C for 67 h) in a LE-70 ultra-centrifuge (Beckman). The rotor ran out non-braked. Oxic and anoxic samples were centrifuged in two separate runs with 8 gradients each, yielding a total of 16 gradients. For each run the same gradient buffer solution was used to exclude gradient heterogeneity. In addition, control tubes ('blanks') containing gradient solution but no RNA were entrained in each centrifugation run and the resulting gradient was used to determine the buoyant density of the fractions (2.5.6.4.).

2.5.6.2. DNA based stable isotope probing (DNA SIP)

To separate [^{13}C]-labeled 'heavy' DNA from the 'light' [^{12}C]-DNA a slightly modified protocol of Neufeld *et al*. (2007b) was applied. DNA from oxic and anoxic samples from the sampling time points day 28 and 42 was extracted (2.5.1.; 2.5.2.), pooled equimolarly and a total of 4000 ng was added to the gradient solution. The gradient solution was produced by mixing 80.8% cesium chloride (CsCl; buoyant density 1.881 g·ml^{-1}, Sigma-Aldrich, Munich, Germany) and 19.5% gradient buffer (100 mM Tris-HCl; 100 mM potassium chloride; 1 mM EDTA; pH 8). The desired buoyant density was adjusted by adding gradient buffer until the gradient solution had a buoyant density of 1.725 ± 0.005 g ml^{-1}. Filling of the centrifugation tubes, balancing and rotor handling was done as described elsewhere (2.5.6.1.). The isopycnic centrifugation was done at 177,000 × g or 44,100 rpm at 20°C for 40 h. The rotor ran out non-braked.

2.5.6.3. Fractionation

After the centrifugation (2.5.6.1.; 2.5.6.2.), gradients were fractionated manually (Manefield *et al*., 2002a). The centrifugation tubes were fixed vertically in a rag. A peristaltic pump (Econo Pump 1, Biorad, Hercules, USA) was connected with a silicon tube (1.6 mm inner diameter) to a sterile needle (23G × 1''). The needle was inserted into the tube underneath the plug. A second needle was used to drill a hole into the bottom of the tube. Brilliant blue colored ddH_2O was pumped onto the gradient solution at a flow rate of 0.45 $ml \cdot min^{-1}$. Fractions (450 µl each) were collected in 60-second-intervals from every gradient in 1.5 ml microcentrifuge tubes. The eleventh fraction was contaminated with colored water and therefore discarded.

2.5.6.4. Determination of the buoyant density of fractions

The buoyant density of fractions (2.5.6.3.) was determined in the 'blank' (i.e., gradients) without nucleic acids. The fractions were tempered (DNA-SIP 20°C, RNA-SIP 25°C) in a water bath (Manefield *et al*., 2002b; Neufeld *et al*., 2007b). The fractions were mixed thoroughly, 100 µl were transferred by pipetting them into a sterile 1.5 ml microcentrifuge tube and the weight was determined on an analytical balance (Analytic AC 120 S, Sartorius, Garching, Germany). Densities were decreasing linearly with ascending fraction numbers (Fig. 7) and showed comparable linear regressions indicating that the establishment of the CsTFA (RNA) and CsCL (DNA) gradients by isopycnic centrifugation was successful and reproducible.

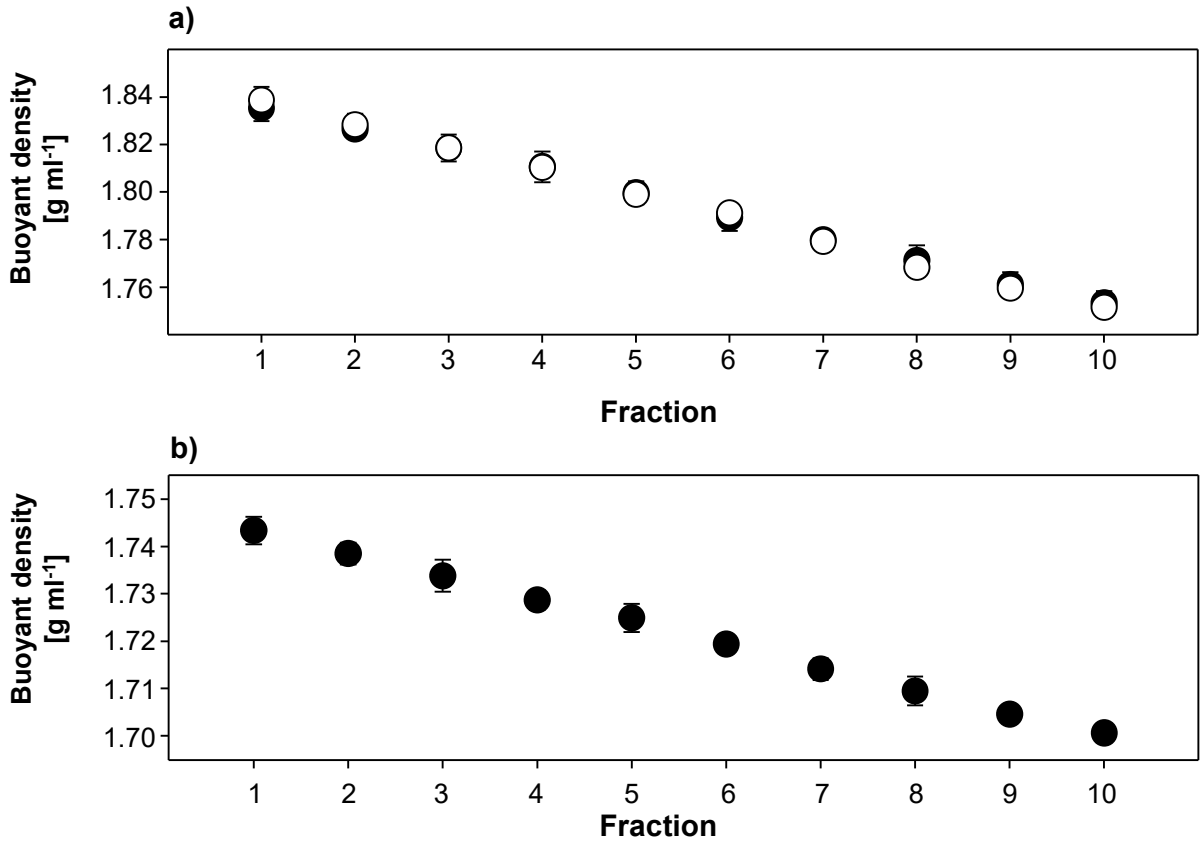

Figure 7. Buoyant densities of gradient solutions. a) RNA-SIP. Buoyant density of gradient solution in fractions was measured at 25°C. White circles, oxic samples. Black circles, anoxic samples. The density of each fraction was measured at 25°C (Manefield *et al*., 2002b). b) DNA-SIP. Buoyant density of gradient solution in fractions was measured at 20°C. The density of each fraction was measured at 20°C (Neufeld *et al*., 2007b).

2.5.6.5. Precipitation of nucleic acids after isopycnic centrifugation

RNA precipitation was performed as described by Degelmann *et al*. (2009). 150 µl of each fraction were mixed with 97.5 µl sodium acetate solution (3 M, pH 5.2), 10.2 µl glycogen solution (10·mg ml^{-1}), and 750 µl ice cold ethanol (96%). Precipitation was done overnight at -20°C and afterwards the RNA was pelletized by centrifugation (13,000 × g, 20 min, at 4°C). The supernatant was discarded and the pellet was washed with 500 µl ice cold ethanol (70% in RNAse-free ddH_2O, -20°C). Pellets were dried at room temperature and resuspended with 20 µl RNase-free ddH_2O. RNA was quantified by fluorescence-based methods (2.5.4.2.) and finally transcribed into complementary DNA (cDNA, 2.5.7.).

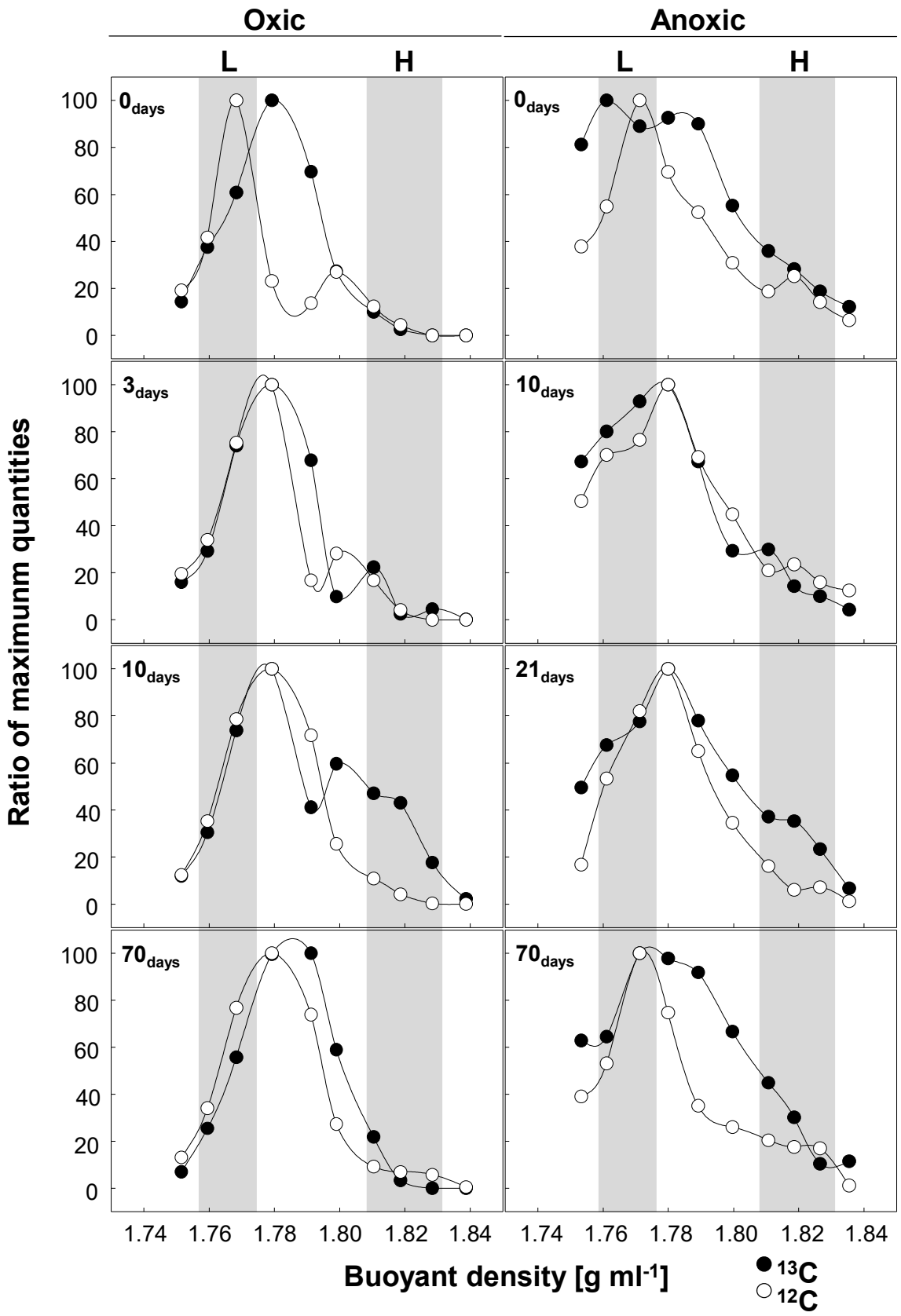

Figure 8. RNA distribution in the fractions 1-10. RNA in each fraction of a gradient was quantified with the Quant-iT RiboGreen RNA Assay Kit (Invitrogen, Germany). Grey transparent boxes mark the 'light' fractions (L) and 'heavy' fractions (H) presumably representing unlabeled and labeled RNA respectively.

DNA precipitation was performed as described by Neufeld *et al.* (2007b). 400 µl of PEG solution (0.1 M HEPES pH 7.0 − 30% PEG 6000 solution; Sigma-Aldrich, Germany) and 13.6 µl glycogen solution (10·mg ml^{-1}) were added to 200 µl fraction in a sterile 1.5m centrifugation tube. Tubes were mixed well by in inversion and the DNA precipitated for two hours at room temperature. DNA was pelletized by centrifugation (13,000 × g, 20 min, at 4°C). The supernatant was discarded and the pellet was washed with 500 µl ice cold ethanol (70% in RNAse-free ddH_2O, -20°C). Pellets were dried at room temperature and resuspended with 30 µl DNase-free TE-buffer (10 mM Tris–HCl, 1 mM EDTA, pH 8.0).

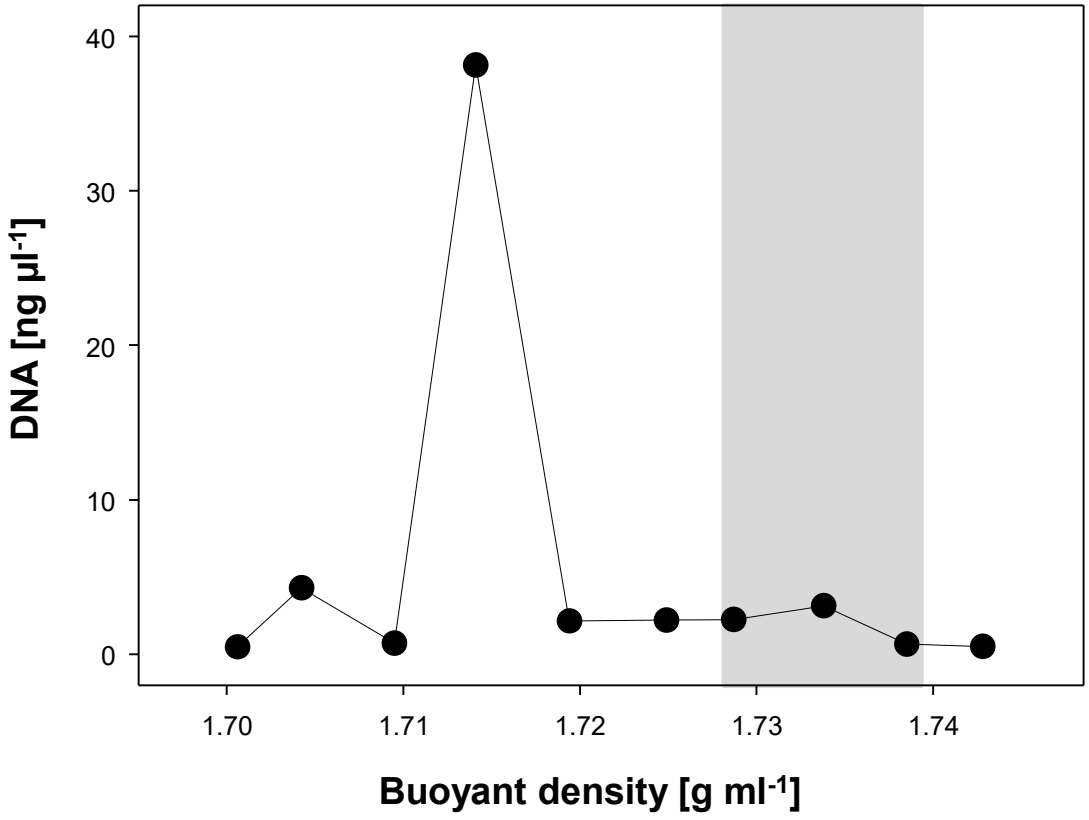

Figure 9. DNA distribution in the fractions 1-10. DNA was quantified with the Quant-iT PicoGreen DNA Assay Kit (Invitrogen, Germany). The grey box marks the 'heavy' fractions presumably representing labeled DNA that was used for the construction of the metagenome.

2.5.7. Reverse transcription of RNA into cDNA

The RNA samples did not yield PCR products, demonstrating that the RNA solutions were DNA-free. Reverse transcription of RNA was performed with random hexamer primers (SuperScript III First-Strand Synthesis Supermix, Invitrogen, Karlsruhe, Germany) according to the manufacturer's protocol. RNA (10 ng to 1 µg) was mixed with 1 µl random hexamer primers (50 ng·µl^{-1}), 1 µl d NTPs (10mM) and RNase-free ddH_2O (ad 13 µl). The mixture was incubated at 65°C for 5 min and placed on ice immediately. T4 GP32 protein (EURx Ltd., Gdansk, Poland) was added at this point to a final concentration of 10 µg ml^{-1}. Reverse transcription was performed after the addition of 4 µl 5 × First-Strand Buffer, 1 µl 0.1 M DTT, 1 µl RNAseOUT and 1 µl SuperScript III RT enzyme (200 U·µl^{-1}) at 25°C for 10 min followed by 2 h at 50°C. The reaction was terminated by a 5 min incubation at 85°C.

2.5.8. Polymerase chain reaction (PCR)

Polymerase chain reaction is a method to generate multiple copies of a particular DNA fragment. Enzymatic amplification can be divided into three steps: denaturation of template DNA, annealing of primers and elongation of the complementary strand by a thermally stable DNA-polymerase. PCR reactions were pipetted on ice according tables 9-10, 13-17 in either single 0.2 ml PCR tubes or 96 well plates. Primers and nucleotides were purchased from Microsynth (Balgach, Switzerland) and Eppendorf (Hamburg, Germany), respectively. Amplification reactions were performed in a SensoQuest labcycler (SensoQuest GmbH, Göttingen, Germany) using the thermoprotocols listed in table tables 9-10, 13-17. Lids and heating blocks of thermocyclers were preheated to 95°C before PCR was started by placing the PCR tubes or plates into the cycler.

Table 8. List of primers used in this study. Primer sets for the phylogenetic analysis of 16S rRNA genes of *Bacteria* and *Archaea* by next generation technologies were chosen as suggested by Klindworth *et al*., 2013.

Target Gene	Primer	Sequence 5′-3′	Reference
16S rRNA *Bacteria*	Bakt_341F	CCT ACG GGN GGC WGC AG	Muyzer *et al*., 1998
	Bakt_805R	GAC TAC HVG GGT ATC TAA TCC	Herlemann *et al*., 2011
16S rRNA *Archaea*	A519F	CAG CMG CCG CGG TAA	Wang & Qian 2009
	Arch1017R	GGC CAT GCA CCW CCT CTC	Yoshida *et al*., 2005
18S rRNA *Eukaryota*	TAReuk454FWD1	CCA GCA SCY GCG GTA ATT CC	Stoeck *et al*., 2010
	TAReukREV3	ACT TTC GTT CTT GAT YRA	Stoeck *et al*., 2010
chiA	ChiA_F2	CGT GGA CAT CGA CTG GGA RTW YCC	Hobel *et al*., 2005
	ChiA_R2	CCC AGG CGC CGT AGA RRT CRT ARS WCA	Hobel *et al*., 2005
pJET vector plasmid	pJET1.2 Forward	CGA CTC ACT ATA GGG AGA GCG GC	Thermo Fisher Scientific Inc.
	pJET1.2 Reverse	AAG AAC ATC GAT TTT CCA TGG CAG	Thermo Fisher Scientific Inc.

2.5.8.1. Amplification of clone inserts.

DNA fragments ligated into vector plasmids of clones were amplified following PCR conditions in Table 9. Length of DNA fragments was determined by agarose gel electrophoresis (2.5.5.) and PCR-products of the desired length were sequenced (2.6.1.).

Table 9. PCR reaction mix and thermoprotocol for the pJET1.2-PCR.

PCR reaction mix		Thermoprotocol			
Chemical[a] (conc. of stock)	**Volume (final conc.)**	**Step**	**Temp.**	**Time[b]**	
10x PCR buffer	5 µl	Initial denaturation	95°C	5′	
$MgCl_2$ (25 mM)	5 µl (2.5 mM)				
Nucleotides (2 mM each)	5 µl (0.2 mM)	Denaturation	95°C	60″	35x
pJET1.2 Forward[c] (10 µM)	2.5 µl (0.5 µM)	Annealing	54°C	45″	
pJET1.2 Reverse[c] (10 µM)	2.5 µl (0.5 µM)	Elongation	72°C	90″	
Taq polymerase (5 $U \cdot \mu l^{-1}$)	0.1 µl (0.02 $U \cdot \mu l^{-1}$)				
PCR-H_2O	13.9 µl	Final elongation	72°C	5′	
Template[d]	2 µl	Storage	8°C	∞	

[a]CRYSTAL Taq-DNA-Polymerase kit (biolab products GmbH, Gödenstorf, Germany) containing the Taq polymerase, the PCR buffer, and the $MgCl_2$ solution was used for pJET1.2-PCR.
[b]Minutes: ′; seconds: ″.
[c]See Table 8.
[d]Cell material from colonies of clones were resuspended in 50 µl of PCR-H_2O and 2 µl of the resulting cell suspension were used as template for pJET1.2-PCR.

2.5.8.2. Amplification of bacterial 16S rRNA transcripts.

Bacterial 16S rRNA transcripts were amplified from cDNA following a two-step amplification protocol to minimize potential primer biases (Berry *et al.*, 2011). In addition, 6-nucleotides (MID) instead of the commonly used 10-nucleotide barcodes were used (Table 12). The first amplification round with untagged primers (25 cycles; see Table 10 for details) was followed by a second amplification round using primers carrying adaptors, key and MID (10 cycles; see Fig. 10 and Table 13 for details). Amplicons were gel-purified (2.5.3.2.), quantified (2.5.4.) and pyrosequenced (2.6.2.).

Table 10. PCR reaction mix and thermoprotocol for the bacterial 16S rRNA PCR.

PCR reaction mix		Thermoprotocol			
Chemical[a] (conc. of stock)	**Volume (final conc.)**	**Step**	**Temp.**	**Time[b]**	
10x PCR buffer	2.5 µl	Initial denaturation	95°C	3′	
$MgCl_2$ (25 mM)	2.5 µl (2.5 mM)				
Nucleotides (2 mM each)	2.5 µl (0.2 mM)	Denaturation	95°C	40″	25x
Bakt_341F[c] (10 µM)	1.25 µl (0.5 µM)	Annealing	55°C	2′	
Bakt_805R[c] (10 µM)	1.25 µl (0.5 µM)	Elongation	72°C	1′	
Taq polymerase (5 $U \cdot \mu l^{-1}$)	0.1 µl (0.02 $U \cdot \mu l^{-1}$)				
PCR-H_2O	2.5 µl	Final elongation	72°C	7′	
Template	12.4 µl	Storage	4°C	∞	

[a]CRYSTAL Taq-DNA-Polymerase kit (biolab products GmbH, Gödenstorf, Germany) containing the Taq polymerase, the PCR buffer, and the $MgCl_2$ solution was used for bacterial 16S rRNA PCR.
[b]Minutes: ′; seconds: ″.
[c]See Table 8.

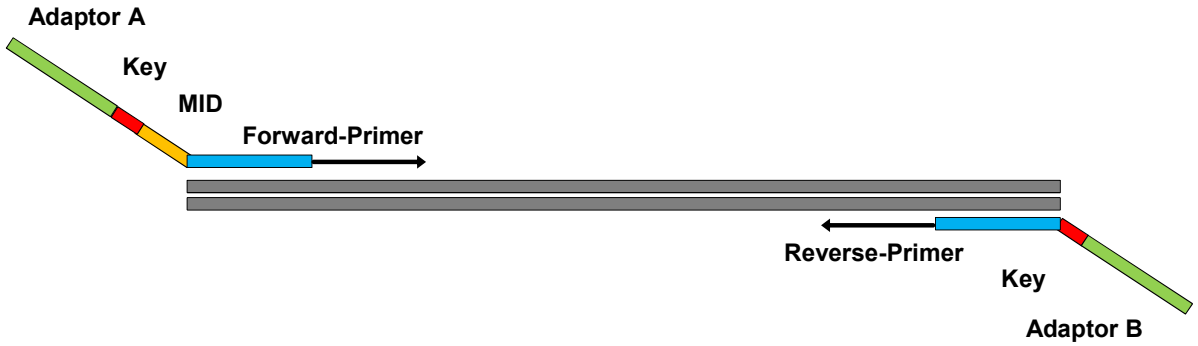

Figure 10. Primer design for pyrosequencing of bacterial 16S rRNA transcripts.

Table 11. Primer sequences and primer design for pyrosequencing of bacterial 16S rRNA transcripts.

	Pyrosequencing primer design			
	Adaptor	Key	MID[b]	Template specific[a]
Forward	5′-CCATCTCATCCCTGCGTGTCTCCGAC	TCAG	NNNNNN	(Bakt_341F)-3′
Reverse	5′-CCTATCCCCTGTGTGCCTTGGCAGTC	TCAG	-	(Bakt_805R)-3′

[a]See Table 8 for primer sequences.
[b]See Table 12 for MID sequences.

Table 12. MID sequences used for 16S rRNA gene pyrosequencing primers.

		Oxic			Anoxic	
		Heavy	Light		Heavy	Light
[^{13}C]-chitin	**t_0**	5′-**ACGAGC**-3′	5′-**ACTATC**-3′	**t_0**	5′-**TAGCAC**-3′	5′-**TAGTGC**-3′
	t_1	5′-**ACTCGC**-3′	5′-**AGCGTC**-3′	**t_3**	5′-**TATCGC**-3′	5′-**TCACGC**-3′
	t_3	5′-**AGCTAC**-3′	5′-**AGTCAC**-3′	**t_5**	5′-**TCTAGC**-3′	5′-**TCTCAC**-3′
	t_{12}	5′-**ATACTC**-3′	5′-**ATATAC**-3′	**t_{12}**	5′-**TGACAC**-3′	5′-**TGCATC**-3′
[^{12}C]-chitin	**t_0**	5′-**ATCATC**-3′	5′-**ATCTGC**-3′	**t_0**	5′-**TGTCTC**-3′	5′-**TGTGAC**-3′
	t_1	5′-**ACACTG**-3′	5′-**AGCACG**-3′	**t_3**	5′-**TACACG**-3′	5′-**TACGTG**-3′
	t_3	5′-**AGTATG**-3′	5′-**ATAGTG**-3′	**t_5**	5′-**TACTAG**-3′	5′-**TAGCTG**-3′
	t_{12}	5′-**TACAGC**-3′	5′-**TAGATC**-3′	**t_{12}**	5′-**TATATG**-3′	5′-**TATCAG**-3′

Table 13. PCR reaction mix and thermoprotocol for the bacterial 16S rRNA transcript PCR with barcoded primers for pyrosequencing.

PCR reaction mix		**Thermoprotocol**			
Chemical[a] (conc. of stock)	**Volume (final conc.)**	**Step**	**Temp.**	**Time[b]**	
10x PCR buffer	5 µl	Initial denaturation	95°C	3′	
$MgCl_2$ (25 mM)	5 µl (2.5 mM)				
Nucleotides (2 mM each)	5 µl (0.2 mM)	Denaturation	95°C	40″	10x
Forward[c] (5 µM)	5 µl (0.5 µM)	Annealing	55°C	2′	
Reverse[c] (10 µM)	2.5 µl (0.5 µM)	Elongation	72°C	1′	
Taq polymerase (5 U·µl^{-1})	0.2 µl (0.02 U·µl^{-1})				
PCR-H_2O	22.3 µl	Final elongation	72°C	7′	
Template	5 µl	Storage	4°C	∞	

[a]CRYSTAL Taq-DNA-Polymerase kit (biolab products GmbH, Gödenstorf, Germany) containing the Taq polymerase, the PCR buffer, and the $MgCl_2$ solution was used for the 16S rRNA PCR with barcoded primers for pyrosequencing.
[b]Minutes: ′; seconds: ″.
[c]See Table 11.

2.5.8.3. Amplification of archaeal 16S rRNA transcripts.

Archaeal 16S rRNA fragments were amplified from cDNA following PCR conditions in Table 14.

Table 14. PCR reaction mix and thermoprotocol for the archaeal 16S rRNA PCR.

PCR reaction mix		Thermoprotocol			
Chemical[a] (conc. of stock)	**Volume (final conc.)**	**Step**	**Temp.**	**Time[b]**	
10x PCR buffer	2.5 µl	Initial denaturation	95°C	5′	
$MgCl_2$ (25 mM)	2.5 µl (2.5 mM)				
Nucleotides (2 mM each)	2.5 µl (0.2 mM)	Denaturation	95°C	1′	30x
A519F[c] (10 µM)	1.25 µl (0.5 µM)	Annealing	58°C	1′	
Arch1017R[c] (10 µM)	1.25 µl (0.5 µM)	Elongation	72°C	1′	
Taq polymerase (5 $U \cdot \mu l^{-1}$)	0.1 µl (0.02 $U \cdot \mu l^{-1}$)				
PCR-H_2O	12.4 µl	Final elongation	72°C	5′	
Template	2.5 µl	Storage	4°C	∞	

[a]CRYSTAL Taq-DNA-Polymerase kit (biolab products GmbH, Gödenstorf, Germany) containing the Taq polymerase, the PCR buffer, and the $MgCl_2$ solution was used for the archaeal 16S rRNA PCR.
[b]Minutes: ′; seconds: ″.
[c]See Table 8.

2.5.8.4. Amplification of eukaroytic 18S rRNA transcripts.

Eukaryotic 18S rRNA fragments were amplified from cDNA following PCR conditions in Table 15.

Table 15. PCR reaction mix and thermoprotocol for the eukaryotic 18S rRNA PCR.

PCR reaction mix		Thermoprotocol			
Chemical[a] (conc. of stock)	**Volume (final conc.)**	**Step**	**Temp.**	**Time[b]**	
10x PCR buffer	2.5 µl	Initial denaturation	95°C	5′	
$MgCl_2$ (25 mM)	2.5 µl (2.5 mM)				
Nucleotides (2 mM each)	2.5 µl (0.2 mM)	Denaturation	95°C	1′	30x
TAReuk454FWD1[c] (10 µM)	1.25 µl (0.5 µM)	Annealing	58°C	1′	
TAReukREV3[c] (10 µM)	1.25 µl (0.5 µM)	Elongation	72°C	1′	
Taq polymerase (5 $U \cdot \mu l^{-1}$)	0.1 µl (0.02 $U \cdot \mu l^{-1}$)				
PCR-H_2O	9.9 µl	Final elongation	72°C	5′	
Template	5 µl	Storage	4°C	∞	

[a]CRYSTAL Taq-DNA-Polymerase kit (biolab products GmbH, Gödenstorf, Germany) containing the Taq polymerase, the PCR buffer, and the $MgCl_2$ solution was used for the eukaryotic 18S rRNA PCR.
[b]Minutes: ′; seconds: ″.
[c]See Table 8.

2.5.8.5. Amplification of *chiA* gene fragments and transcripts.

ChiA transcripts for Illumina sequencing were amplified from cDNA following PCR conditions in Table 16. *ChiA* gene fragments for TRFLP analysis (2.5.10.) and cloning (2.5.11.) were amplified following PCR conditions in Table 17.

Table 16. PCR reaction mix and thermoprotocol for the *chiA* PCR.

PCR reaction mix		Thermoprotocol[a]			
Chemical[b] (conc. of stock)	**Volume (final conc.)**	**Step**	**Temp.**	**Time[c]**	
10x PCR buffer	2.5 µl	Initial denaturation	95°C	3′	
$MgCl_2$ (25 mM)	2.5 µl (2.5 mM)				
Nucleotides (2 mM each)	2.5 µl (0.2 mM)	Denaturation	95°C	45″	30x
ChiA_F2[d] (100 µM)	0.25 µl (1 µM)	Annealing	42°C	45″	
ChiA_R2[d] (100 µM)	0.25 µl (1 µM)	Elongation	72°C	90″	
Taq polymerase (5 $U \cdot \mu l^{-1}$)	0.1 µl (0.02 $U \cdot \mu l^{-1}$)				
PCR-H_2O	11.9 µl	Final elongation	72°C	5′	
Template	5 µl	Storage	4°C	∞	

[a]according Hobel *et al*., 2004
[b]CRYSTAL Taq-DNA-Polymerase kit (biolab products GmbH, Gödenstorf, Germany) containing the Taq polymerase, the PCR buffer, and the $MgCl_2$ solution was used for the *chiA* PCR.
[c]Minutes: ′; seconds: ″.
[d]See Table 8.

Table 17. PCR reaction mix and thermoprotocol for the c*hiA* PCR for cloning and TRFLP analysis.

PCR reaction mix		Thermoprotocol[a]			
Chemical[b] (conc. of stock)	**Volume (final conc.)**	**Step**	**Temp.**	**Time[c]**	
5 Prime Master Mix	20 µl	Initial denaturation	95°C	3′	
$MgCl_2$ (25 mM)	2 µl (2.5 mM)				
BSA (5 $mg \cdot ml^{-1}$)	1 µl (100 $ng \cdot \mu l^{-1}$)	Denaturation	95°C	45″	35x
ChiA_F2[d,e](100 µM)	0.5 µl (1 µM)	Annealing	42°C	45″	
ChiA_R2[d] (100 µM)	0.5 µl (1 µM)	Elongation	72°C	90″	
PCR-H_2O	24 µl				
Template	2 µl	Final elongation	72°C	5′	
		Storage	4°C	∞	

[a] according Hobel *et al*., 2004
[b]5Prime Master Mix kit (5 PRIME GmbH, Hamburg, Germany) containing the Taq polymerase, the PCR buffer including nucleotides, and the $MgCl_2$ solution was used for *chiA* PCR.
[c]Minutes: ′; seconds: ″.
[d]See Table 8.
[e]Primer was labeled with the infrared dye “Dyomics 681” (Microsynth AG, Balgach, Switzerland) at the 5’ end for TRFLP analysis.

2.5.9. DNA-SIP-retrieved metagenome

The efficiency of peptide identification in a protein-SIP experiment can be increased by the use of a high coverage metagenome as reference database (e.g. Delmotte *et al*., 2009). In order to increase the likelihood of identifying [^{13}C]-labeled peptides and to reduce the sequencing effort, the metagenome was created from the 'heavy' fractions of a DNA-SIP. Therefore, nucleic acids were extracted from 0.4 g soil slurry samples (Griffith *et al*., 2000) from both replicates of the [^{13}C]-chitin treatment day 28 and day 42 of oxic and anoxic conditions, respectively. DNA was quantified with the Quanti-iT PicoGreen Assay Kit (Invitrogen, Karlsruhe, Germany), pooled equimolar, added to a gradient solution, subjected to isopycnic centrifugation and further processed as described (Hunger *et al*., 2011). 'Heavy' fractions 2, 3 and 4 (Fig. 9) were pooled and the DNA concentration was increased by 'Multiple Displacement Amplification' using the REPLI-g Mini Kit (Qiagen, Hilden, Germany) according to the manufacturer´s instructions. The metagenome was sequenced by LGC Genomics GmbH with the Illumina MiSeq V2 technology (2.6.2.) and reagents generating 31 million raw reads. Raw sequences were trimmed and assembled into 33.039 contigs with an average size of 1,114b using 'CLCbio' (CLCbio, Aarhus, Denmark) by Dr. Huub Op den Camp (Radboud University Nijmegen, The Netherlands). The assembled metagenome was automatically annotated with MG-RAST (Meyer *et al*., 2008).

2.5.10. Terminal Restriction Fragment Length Polymorphism (TRFLP) analysis

TRFLP is a PCR-based fingerprinting method, i.e. it allows to rapidly study microbial communities in various environments and/or the impact of various factors on them. The method is based on the amplification of variants of a single gene with fluorescence labeled primers and subsequent restriction of the PCR products with one or more restriction endonucleases (Liu *et al*. 1997; Thies 2007). This yields terminal-labeled restriction fragments (TRFs) which are length separated on a polyacrylamide gel (PAGE) (Liu *et al*., 1997). Differences in microbial communities finally result in different TRF profiles (Marsh 2005). TRFs can be affiliated with microbial taxa by *in silico* digestion of known representatives of the gene of interest. In this doctoral project, TRFLP targeting *chiA* (1.2.3.1.) was used to study the response of microbial communities to chitin, chitosan, and potential hydrolysis products thereof (1.7.; 2.3.2.). Therefore, *chiA* genes were PCR amplified using fluorescence labeled forward primers (2.5.8.5.).

2.5.10.1. Mung bean endonuclease digestion

Single stranded regions of an amplicon, generated by premature termination of the elongation step during PCR, promote the formation of 'pseudo-TRFs' that significantly bias the TRFLP analysis (Egert & Friedrich 2003). Pseudo-TRFs result from non-restriction digestion as the restriction enzyme requires double strand DNA to cut or by false restriction digestion at non-terminal restriction sites due to formation palindromic secondary structures that allow restriction enzymes to cut single stranded DNA (Egert & Friedrich 2003). Thus, single stranded extensions at the terminal ends were removed with the mung bean endonuclease (New England Biolabs, Ipswich, USA). Purified PCR product (50 µl, 2.5.3.3.) were mixed with 5.5 µl reaction buffer NEB2 (10x) and 2 µl mung bean endonuclease (0.5 U μl^{-1}). Incubation was performed at 30°C for 1 h. The reaction was stopped by purifying the samples with Millipore PCR96 Cleanup Plates (Millipore Cooperation, Bedford, USA; 2.5.3.3.).

2.5.10.2. Digestion with restriction enzymes

In silico digestion testing of various endonucleases with a *chiA* data set retrieved from samples of the conducted slurry incubations (2.5.11.) revealed highest phylotype resolution *in silico* (with MEGA version 5 and the REPK Web Tool; Collins & Rocap 2007; Tamura *et al*., 2011) for the endonuclease *AluI* (5' → 3'restriction site: AG^CT). 7 µl purified PCR product were mixed with 1 µl reaction buffer NEB4 (10x), 1 µl BSA (10x), and 1 µl restriction enzyme (2 U μl^{-1}; New England Biolabs GmbH, Frankfurt am Main, Germany). Restriction digestion was performed at 37°C for 4 hours. Reaction was stopped by heat inactivation of the enzyme for 20 minutes at 80°C. Remaining DNA was quantified with the Quant-iT-PicoGreen dsDNA reagent Kit (Invitrogen, Karlsruhe, Germany) (2.5.4.2.) and diluted with PCR-H_2O to a concentration of 0.5 ng μl^{-1}.

2.5.10.3. Denaturing polyacrylamide gel electrophoresis (PAGE)

Denaturing polyacrylamide gel electrophoresis (PAGE) was performed on a NEN model 4300 DNA analyzer (Licor, Lincoln, USA) as described elsewhere (Hamberger *et al*., 2008). Gel plates (Borofloat glass plates 25 mm x 25 mm x 5 mm, LICOR, Lincoln, USA) were thoroughly cleaned sequentially with ddH_2O, ethanol (70%), and isopropanol (80%). 50 µl bind-silane solution (1:1 bind silane [plusOne; GE Healthcare, Piscataway, USA] and 10% CH_3COOH) was applied to the plates as a thin film at the area at which the comb has to be inserted to stabilize the gel pockets. The plates were separated by spacers (0.2 mm thick), fixed with assembly rails and casting plate, and placed in the gel casting stand. For the polyacrylamide gel, 15 g urea (Roche Pharma, Reinach, Switzerland), 3.75 ml of 40% acrylamide-bis solution (37.5:1; 2.6% C; Bio-RAD, Hercules, USA), 6 ml 5 x TBE buffer (450 mM Tris, 450 mM H_3BO_3, 10 mM EDTA, pH 8 [Sambrook & Russell 2001]), and 9.25 ml

ddH_2O were gently mixed. The solution was filtered (Ø 0.2 µm) was to remove excess undissolved salts. 175 µl ammonium persulfate (440 mM) and 17 µl ultra-pure N,N,N,N-tetramethylethylendiamine (TEMED, ultra-pure; Invitrogen, Karlsruhe, Germany) were added to the gel solution to start the polymerization reaction. The gel was immediately poured between the two gel plates. A plastic rectangular tooth comb (48 lanes) was inserted, and the polymerization was carried out for approximately 45 minutes at room temperature. The assembled glass plates were placed into the DNA analyzer, the buffer tanks were fixed, and filled with 1 x TBE buffer. The comb was pulled and residual urea in the gel pockets was removed by flushing them with buffer. A pre-run was performed for 25 min at 1,200 V and 45 °C. 2 µl of sample and a size standard (µ-STEP-24a, 50 - 700 bp; Microzone, Haywards Heath, UK) were mixed with 2 µl Stop-Solution (Licor, Lincoln, NE, USA), denatured for 3 min at 95 °C on a Gradient thermo cycler (Biometra, Göttingen, Germany), and placed on ice. 0.8 µl sample and 0.5 µl size standard were loaded onto the gel. The gel electrophoresis was performed for 4 h at 1,200 V and 45 °C.

2.5.11. Construction of clone libraries

Cloning was performed to separate single *chiA* fragments from PCR products derived from DNA samples of soil slurries (2.5.8.5.) with the CloneJET PCR Cloning Kit (Thermo Fisher Scientific, Erlangen, Germany). Therefore, the *chiA* genes were ligated into vector plasmids (2.5.11.1.) that were subsequently transformed into competent cells of *Escherichia coli* (2.5.11.2.). Plasmids containing the DNA fragments (positive clones) were reproduced during growth of the transformed cells on agar plates. Cell material of positive clones was used to amplify inserted DNA fragments via PCR (Table 9; 2.5.8.). Resulting PCR products were used for Sanger sequencing (2.6.1.).

2.5.11.1. Ligation

PCR-derived DNA fragments were ligated into the linearized pJET1.2/blunt cloning vector. The 5'-ends of the vector contain phosphoryl groups, therefore, phosphorylation of the PCR primers is not required. As PCR-products were generated with a Taq DNA polymerase (2.5.8.1.) they contained 3'-dA overhang. Thus, PCR -products were blunted prior to ligation (Table 18) with a proprietary thermostable DNA blunting enzyme (included in the kit) because the cloning vector requires blunt ends. Ligation reaction was performed at a molar insert to vector ratio of 3:1. The amount of insert DNA that had to be added to the ligation reaction to achieve this ratio was calculated according to Equation 6 and corresponded to 15 ng.

Equation 6. Molar insert to vector ratio.

$$insert\ (ng) = \frac{vector\ (ng) \times insert\ size\ (bp)}{vector\ size\ (bp)} \times molar\ insert\ to\ vector\ ratio$$

$insert\ (ng)$, amount of insert; $vector\ (ng)$, amount of vector used for ligation reaction (50 ng for 20 µl reaction); $insert\ size\ (bp)$, size of the insert; $vector\ size\ (bp)$, size of the pJET1.2/blunt cloning vector (2974 bp).

Table 18. Composition of the blunting reaction[a].

Component	Volume
2X Reaction Buffer	10 µl
Gel purified PCR product	1-7 µl
ddH_2O	ad 17 µl
DNA Blunting Enzyme	1 µl
	18 µl

[a]The reaction was mixed thoroughly for 3-5 s and then incubated at 70°C for 5 min. Afterwards the mixture was chilled on ice.

Table 19. Composition of the ligation reaction[a].

Component	Volume
Blunting reaction	18 µl
pJET1.2/blunt Cloning Vector (50 ng/µl)	1 µl
T4 DNA Ligase	1 µl
	20 µl

[a]The reaction was mixed briefly, centrifuged for 3-5 s to collect drops and incubated at room temperature for 5 min.

2.5.11.2. Transformation and screening

Glycerol cultures of competent *Escherichia coli* JM 109 cells (Promega) that were stored at 80°C were thawed on ice. 50 µl competent cells were gently mixed with 2 µl of circularized vector plasmids and incubated for 30 min on ice. Heat shock transformation was performed at exactly 42°C for 50 s in a water bath. Cells were placed back on ice for two minutes immediately after the heat shock. 950 µl soc medium (2.1.3.) was added to the cells and incubated at 37°C for 90 min on a thermomixer (Eppendorf, Hamburg, Germany) under constant slow shaking (300 rpm). Finally, about 400 µl of transformed cells were plated on LB/Ampicillin-plates (2.1.2.) and incubated overnight at 37°C. The vector contains a lethal restriction enzyme gene that is disrupted by ligation of a DNA insert into the cloning site. Thus, only cells with insert containing plasmids (recombinant plasmids) are able to form colonies.

2.6. Sequencing

2.6.1. Sanger sequencing

Purified pJET1.2-PCR products of *chiA* DNA gene insert sequences (2.5.8.1.) of chitin, chitosan, and chitobiose treatments (2.3.2.; 2.3.3.) were sent to Macrogen (Amsterdam, The Netherlands) for sequencing by chain-termination (also known as Sanger sequencing; Mardis 2013; Sanger & Coulson 1975; Sanger *et al*., 1977). Sequences of *chiA* genes of *N*-acetylglucosamine and glucosamine (2.3.3.) were obtained by commercial cloning and sequencing of vector inserts by LGC Genomics (Berlin, Germany).

2.6.2. High-throughput sequencing

For pyrosequencing of 16S rRNA transcript PCR, amplicons carrying pyrosequencing adapters and barcodes (Fig. 10; 2.5.8.2.) were produced by a two-step amplification protocol to minimize a potential ligation or primer biases (2.5.8.2.; Berry *et al*., 2011). Sequencing was performed at the Göttingen Genomics Laboratory (Göttingen, Germany) employing the Roche GS-FLX 454 pyrosequencer and GS FLX Titanium series reagents (Roche, Mannheim, Germany) according to the manufacturer's instructions (Dallinger *et al*., 2014). PCR amplicons of 16S archaeal rRNA transcripts, 18S eukaryotic rRNA transcripts and *chiA* transcripts were sequenced using the Illumina technology by the LGC Genomics GmbH (Berlin, Germany) with a MiSeq sequencer and V3 reagents. The DNA-SIP retrieved metagenome (2.5.9.) was sequenced with a MiSeq sequencer and V2 reagents by the LGC Genomics GmbH.

2.7. Sequence analysis

2.7.1. Analysis of pyrosequencing-derived data

Sequences were provided by LGC Genomics in the *.sff data format from 4 separate sequencing runs. Data files were converted into the *.fastq data format with NextGen Sequence Workbench (http://www.dnabaser.com/download/nextgen-fastq-editor). Raw fastq files were merged into two fastq files, one for the oxic and anoxic treatment respectively. The key sequence was removed and sequences were trimmed to 446bp. Sequences were trimmed and quality filtered using 'ACACIA', such that erroneous homopolymers were corrected and low-quality reads were discarded from the dataset (Bragg *et al*., 2012). Prior to clustering, potential chimeras were filtered out using the 'UCHIME' algorithm implemented in 'USEARCH' with the latest RDP Gold database for high-quality 16S rRNA gene reference sequences (Edgar *et al*., 2011). Information on the sequence numbers after each step is given in Table 20. Sequences with a minimum length of 400 bp were analyzed using Jaguc2 (Nebel *et al*., 2011). In brief, Jaguc2 operates with average linkage clustering and pairwise

alignments for calling operational taxonomic units (OTUs). Thus, this method is rather insensitive to sequencing errors such as insertions and deletions. Family-level OTUs were called with an average sequence similarity threshold of 87.5% (Yarza *et al*., 2010).

Table 20. Sequence number after each step of sequence preparation prior clustering into family level OTUs. Raw reads of the oxic and anoxic libraries were converted into the fastq format and pooled into one fastq file respectively.

	Number of sequences	
	Oxic	**Anoxic**
Pooled raw fastQ files	126740	106712
Key removed	126740	106712
Trimmed to 446bp	126721	106709
Quality checked[a]	122305	103029
Chimeras removed[b]	99456	87060

[a] with 'ACACIA', i.e. erroneous homopolymers were corrected and low quality reads were discarded from the dataset (Bragg *et al*., 2012)

[b]Potential chimeras were filtered out using the 'UCHIME' algorithm implemented in 'USEARCH' with the latest RDP Gold database for high quality 16S rRNA gene reference sequences (Edgar *et al*., 2011). See material and methods for further details.

2.7.2. Analysis of Illumina sequencing-derived data

Sequences (1 million read pairs, 300 bp paired-end read) were provided by LGC Genomics GmbH (Berlin, Germany) in the *.fastq data format. Paired-end forward and reverse reads were combined using BBMerge 34.48 (http://bbmap.sourceforge.net/) by the LGC Genomics GmbH and used for further analysis. Random subsamples (4000 sequences each) were taken using USEARCH as the computing time of Jaguc2 for the clustering increases exponentially (Nebel *et al*., 2011). Prior clustering barcodes as used in the pyrosequencing analysis were added to the fastq files *in silico*. After the addition of barcode sequences, sample files were merged into two fastq files, one file for the oxic and anoxic samples respectively. Sequences were trimmed to 446bp. Sequences with a minimum length of 400 bp were analyzed using Jaguc2. Two separate clustering runs were performed for oxic and anoxic treatments. Family-level OTUs were called with an average sequence similarity threshold of 87.5% for archaeal 16S rRNA transcript and eukaryotic 18S rRNA transcript sequences (Yarza *et al*., 2010) and 80% for *chiA* gene transcripts.

2.7.3. Analysis of Sanger sequencing-derived data

The retrieved data set of partial *chiA* gene fragments (206 sequences) was quality-checked, i.e. chimeras were manually removed and the *chiA* identity of the sequences was verified by BLAST Search (Altschul et al., 1990) in the nucleotide database of Genbank. The sequences were edited, translated into amino acid sequences, and aligned using CLUSTALW and MUSCLE algorithms in MEGA version 5 (Tamura *et al*., 2011). Translated *chiA* sequences

were clustered into OTUs based on a similarity cutoff of 50% using the software DOTUR (Schloss & Handelsman 2005).

2.7.4. Identification of labeled taxa

Mean differences (± standard deviation) of the relative abundances per OTU in amplicon libraries derived from 'heavy' fractions of [^{13}C]- and [^{12}C]-treatments at the start of incubation (t_0) were 0.04 ± 0.19% and 0.05 ± 0.39% for the oxic and anoxic treatments, respectively. Thus, technical variations were minimal. Differences in relative abundances that exceeded the mean difference delineated from amplicon libraries at the start of the incubation (see above) plus threefold standard deviation were considered significant. The significance threshold was 0.61% and 1.21% for the oxic and anoxic treatments, respectively, suggesting a correct detection rate of differences in 99.73% of the cases (Westgard *et al*., 1981). Family-level OTUs that met two of the criteria i-iii and criteria iv were scored 'labeled' at a certain timepoint t_x: (i) $R_a - R_b > T$ (R_a and R_b are the relative abundances of an OTU in the 'heavy' fractions of the [^{13}C]- and [^{12}C]-treatment at t_x, respectively); (ii) $R_a - R_c > T$ (R_c is the relative abundance of an OTU in the 'light' fractions of the [^{13}C]-treatment at t_x); (iii) $R_a - R_d > T$ (R_d is the relative abundance of an OTU in the 'heavy' fractions of the [^{13}C]-treatment at t_0); (iv) $R_{cs} > T$ ($R_{cs} = [3 \times R_a - R_b - R_c - R_d] / 3$, i.e. the average relative CAP-SIP abundance [hereafter referred to as Rcs score]). Raw relative abundances and average relative CAP-SIP abundances of labeled OTUs are listed in Tables S1 and S2.

2.7.5. Rarefaction analyses and coverage

Rarefaction curves and 95%-confidence intervals were calculated using the aRarefact-Win software (http://strata.uga.edu/software/) according to the Hurlbert-rarefaction concept (Heck *et al*., 1975; Hurlbert 1971). The analysis allows comparing the richness in samples that have not been sampled equally. Flattening and plateauing curves indicate that sampling effort was sufficient and that most of the expected diversity was covered. Not sufficient sampling is reflected in steeply increasing curves.

The coverage indicates the ratio of detected to expected OTUs (Good 1953) and was calculated according to Equation 7.

Equation 7. Coverage.

$$C = \left(1 - \frac{N_X}{n}\right) \times 100$$

C, coverage (%); N_X , numbers of OTUs that occur once; n, total number of sequences

2.7.6. Phylogenetic trees

ChiA transcript libraries were prepared by Illumina-Amplicon sequencing of PCR products from cDNA (2.8.8.5.; 2.6.2.; 2.7.2.) and *chiA* gene libraries by Sanger sequencing of PCR products (2.5.11.; 2.6.1.; 2.7.3.). The *chiA* trees were calculated using translated amino acid sequences by applying the neighbor-joining algorithm implemented in MEGA 5 (Fig. 19; Tamura *et al*., 2011) and MEGA 6 (Fig. 29, 30; Tamura *et al*., 2013). Partial deletion with a site coverage cut-off value of 80% was chosen for gaps and missing data treatment. The topology of the neighbor-joining tree was confirmed with MEGA implemented maximum likelihood and maximum parsimony algorithms, using the same data set. 1,000 bootstraps for each algorithm were calculated. Average values are shown for nodes that were congruent with all three algorithms. Tree branches in which reference sequences grouped together with sequences of a single OTU were condensed in figure 19.

Bacterial 16S rRNA cDNA sequence libraries were prepared by pyrosequencing (2.6.2.; 2.7.1.). Phylogenetic trees (Fig. 25a, 26a, 35 and 36) were calculated from OTU representative sequences of taxa labeled by assimilation of [^{13}C]-chitin derived carbon (2.7.4.) and from reference sequences. The consensus trees were calculated with the maximum likelihood method and 1000 bootstraps. Dots at nodes indicate confirmation of topology by neighbor joining (white circles) and maximum parsimony (grey circles) algorithms. Black circles indicate confirmation by both algorithms.

2.7.7. Nucleotide sequence accession numbers

Partial *chiA* gene sequences derived by Sanger sequencing (2.6.1.; 3.1.6.) were deposited in the European Nucleotide Archive (ENA) of the European Bioinformatics Institute with accession numbers HG315747 to HG315952. Representative 16S rRNA transcript sequences of labeled OTUs (3.2.2.1., 3.2.2.2.) and representative transcript sequences of *chiA* OTUs (3.2.3.) were deposited in the ENA archive with accession numbers LT907870 to LT907902 and LT907849 to LT907862, respectively. Raw high-throughput sequencing datasets obtained in the study (2.6.2.) can be found under sample accession numbers ERS1346811-ERS1346814 (18S rRNA reads of *Eukaryota*; 3.2.5.), ERS1262549-ERS1262552 (16S rRNA reads of *Archaea*; 3.2.4.), ERS1257899-ERS1258026 (16S rRNA reads of *Bacteria*; 3.2.2.1, 3.2.2.2.), and ERS1346815-ERS1346846 (*chiA* reads; 3.2.3.) in the ENA archive.

2.8. Metaproteomics

Detection and identification of proteins was done by Dr. Nico Jehmlich and coworkers at the Department of Molecular Systems Biology (Helmholtz Centre for Environmental Research-UFZ, Leipzig, Germany), the Institute of Biochemistry (Faculty of Biosciences, Pharmacy and

Psychology, University of Leipzig, Germany) and the Department of Isotope Biogeochemistry (Helmholtz Centre for Environmental Research-UFZ, Leipzig, Germany).

2.8.1. Protein extraction

Protein extraction from soil slurry samples was performed using a modified phenol extraction protocol as described previously (Taubert *et al*., 2012), with minor modifications. In total, 5 ml of extraction buffer (0.1 M Tris-HCl, pH 6.8, 1.25% SDS, 20 mM DTT) were added to 5 g of soil slurry and incubated on a shaker for 1 h. After centrifugation (4°C, 7,000 x g, 30 min), the supernatant was mixed with 3 mL phenol (1 g ml^{-1}) followed by shaking for 15 min and repeated centrifugation. The phenol phase was transferred to a new vial and the remaining aquatic phase was again extracted with 3 ml of phenol. Both phenol phases were combined and washed twice with 3 mL of ddH_2O. Proteins were precipitated by addition of fivefold volume of 100 mM ammonium acetate in methanol during incubation over night at 20°C. Protein pellets were harvested by centrifugation (4°C, 7,000 x g and 30 min). The pellet was washed twice with acetone and dried by vacuum centrifugation.

2.8.2. Proteolytic cleavage using trypsin

Protein pellets were dissolved in 30 µl SDS sample buffer (2% SDS, 2 mM beta-mercaptoethanol, 4% glycerol, 40 mM Tris-HCl pH 6.8, 0.01% bromophenolblue), heated to 90°C for 5 min and separated on a 1-D SDS polyacrylamide gel (12.5%, 1.0 mm thickness, running condition: 10 mA for 10 min followed by 20 mA for 20 min). The gel lanes were cut into three gel pieces, destained using acetonitrile for 2 times 15 min and subsequently proteolytically cleaved using trypsin (Sigma, Munich, Germany), overnight at 37°C. Peptide mixtures were desalted using C18 purification (Shevchenko *et al*., 2007) prior to mass spectrometric analysis.

2.8.3. Liquid chromatographic separation and mass spectrometry

Mass spectrometry was performed on a Orbitrap Fusion MS (Thermo Fisher Scientific, Waltham, MA, USA) coupled to a TriVersa NanoMate (Advion, Ltd., Harlow, UK). 5 µL of the protein lysates were separated with a Dionex Ultimate 3000 nano-LC system (Dionex/Thermo Fisher Scientific, Idstein, Germany) using two mobile phases: mobile phase A was 0.1% formic acid, mobile phase B contained 80% acetonitrile and 0.08% formic acid. Peptides were loaded for 5 min on the precolumn (µ-precolumn, cartridge column, 3 µm particle size, 75 µm inner diameter, 2 cm, C18, Thermo Fisher Scientific) at 4% mobile phase B and eluted from the analytical column (PepMap Acclaim C18 LC Column, 15 cm, 3 µm particle size, Thermo Scientific) over a 60 min gradient of mobile phase B (4-55% B). The MS instrument was set to ‘top speed’ modus with a cycle time of 3 s, using the Orbitrap analyzer for MS and MS/MS scans with higher energy collision dissociation (HCD)

fragmentation at normalized collision energy of 28%. MS scans were measured at a resolution of 120,000 in the scan range of 400-1500 m/z. MS ion count target was set to 4 x 105 at a maximum injection time of 120 ms. Ions for MS/MS scans were isolated in the quadrupole with an isolation window of 2 Da and were measured with a resolution of 15,000. Automatic gain control target was set to 5 x 104 with a maximum injection time of 200 ms.

2.8.4. Proteomic data analysis

The 'PROteomics results Pruning & Homology group ANotation Engine' (PROPHANE, Schneider *et al*., 2011, www.prophane.de) was used to assign proteins to their phylogenetic origin and evaluate the microbial composition of the community. PROPHANE relied on protein abundances calculated on the basis of the normalized spectral-abundance-factor (NSAF) (Zybailov *et al*., 2006). The OpenMS platform (Sturm *et al*., 2008) was used for the analysis of ^{13}C incorporation. The acquired *.raw files were converted to *.mzML files using MSConvert (Chambers et al., 2012). The files were then searched by Open Mass Spectrometry Search Algorithm (OMSSA) (Geer *et al*., 2004) against a database containing the six-frame translation of the DNA SIP based metagenome combined with common contaminants (keratin, trypsin) (containing 106,128 protein-coding sequence entries). Peptide sequences were considered as identified with a FDR <1% calculated using a decoy database. The MetaProSIP node was used to detect labeled peptides matching to previously identified peptides whereby the precursor mass tolerance was set to 5 ppm, and the minimum correlation threshold was 0.7. By extracting all peaks related to the labeled peptides, the distribution of isotope incorporation rates was quantitatively reconstructed (Sachsenberg *et al*., 2014) (http://openms.de/metaprosip). The labeled features were further manually reviewed to ensure valid peptide matches. In order to obtain phylogenetic information the Unipept-database (http://unipept.ugent.be/) was used (Mesuere *et al*., 2012). This web tool retrieves given peptide sequences in UniProtKB accession numbers and assigns the lowest common phylogenetic ancestor.

2.9. Calculations and statistical analyses

2.9.1. Carbon and electron recoveries

2.9.1.1. Carbon and electron recoveries in slurries supplemented with chitin

The quantification of chitin and chitosan in aerated soil is difficult and often inaccurate (Montgomery 1990). To estimate the level of degradation estimated recoveries were calculated based on the assumption that the supplemented chitin has been completely degraded. Approximately 44 mM carbon and 176 mM reductant were supplemented by the addition of chitin in the stable isotope experiment (2.3.1.).

2.9.1.2. Total recovery

Equation 8. Total recovery.

$$R_y = \frac{\sum(n_x \times y_x)}{n_y} \times 100$$

R_y, total carbon or electron recovery in %. n_x, net molar amount of a compound X (CO_2, H_2, acetate, (iso-)butyrate, or propionate) that was formed during the incubation. y_x, number of carbon atoms per molecule of compound X or number of electrons per molecule of compound X that can be transferred if the compound is completely oxidized. n_y, total amount of carbon or reductant supplemented.

2.9.2. Average and standard deviation

Averages and standard deviations were calculated based on the concentrations of compounds detected in the different replicates according to Equation 9 and Equation 10 (Precht *et al*., 2005; Sachs 1999) using Microsoft Excel 2007 (Redmond, USA).

Equation 9. Average.

$$\overline{x} = \frac{1}{n} \times \sum_{i=1}^{n} x_i$$

$\overline{x}$, average; n, number of replicates; i, continuous index that runs from 1 to n; x_i, concentration of a compound measured for a certain replicate.

Equation 10. Standard deviation.

$$S = \sqrt{\frac{1}{n-1} \times \sum_{i=1}^{n} (x_i - \overline{x})^2}$$

S, standard deviation.

Error propagation ($S_{\overline{y}}$) was calculated with Equation 11 by addition of means. Error propagation occurs when means of distinct measurements are combined (Fenner 1931; Precht *et al*., 2005; Sachs 1999).

Equation 11. Error propagation.

$$S_{\overline{y}} = \sqrt{\left(S_{\overline{x_1}}\right)^2 + \left(S_{\overline{x_2}}\right)^2}$$

$S_{\overline{y}}$, error propagation by addition of means.

2.9.3. Statistics

For statistical analysis the PAST software package was used (Hammer *et al*., 2001). The data were tested for normal distribution with the Shapiro-Wilk Test (Royston 1992). The assumed null hypothesis, that normal distribution is given, was rejected, when the p value was smaller than 0.05.

2.9.3.1. Test of significance of difference

Kruskal-Wallis and Mann-Whitney pairwise comparison tests were used to analyze samples for significant differences (Kruskal & Wallis 1952; Zar 1996). The Kruskal-Wallis test does not assume normal distribution (Bärlocher 2008) but does assume equal shaped distribution for all groups. For both tests the null hypothesis, that the samples are similar, is accepted when the p value is higher than 0.05.

2.9.3.2. Canonical correspondence analysis

Canonical correspondence analysis (CCA) is correspondence analysis of a site/species matrix (Legendre & Legendre 1998; Ter Braak 1986). Values for environmental variables (e.g. pH, temperature, or water content) are given for each site. It is a direct ordination technique whereby the ordination axes represent linear combination of the environmental variables. CCA allows to statistically analyze different treatments with not normally distributed data (Schütte *et al*., 2008). CCA analysis was conducted with the PAST software package (Hammer *et al*., 2001).

For the analysis of TRFLP data, relative abundances of TRFs were used as variables and correlated with TRF patterns of each treatment replicate using the same data as presented (3.1.5.). Presentation option ‘scaling 2’ was chosen to emphasize the relationships between single TRFs and TRF patterns. Selected TRFs were subsequently tested for significant increase from t_0 to t_{END} with Mann–Whitney U test (Table 21). For the analysis of pyrosequencing-derived data relatives abundancies of OTUs were used as variables. In addition, CCA was used to identify taxa and environmental factors that were linked with major differences between the various datasets in the [^{13}C]-chitin labeling experiment (3.2.2.3.).

2.10. Contribution of other workers to this dissertation

Experimental design, measurements, data analyses, and interpretation of data were conducted by me unless otherwise noted below. Data presented in chapter 3.1. and 3.2. were published in peer-reviewed journals (Wieczorek et al., 2014, 2019). Therefore, the presentation and discussion of the data in this dissertation is similar how the data were presented in the journal publications. Soil samples were provided by Prof. Dr. Michael Schloter (Research Unit Environmental Genomics, Helmholtz Centre Munich, Germany).

2.10.1. Experiments presented in chapter 3.1.

Most of the analytical measurements (2.4.) presented and the extraction of DNA were conducted by Florian Just within the framework of his Bachelor thesis (University of Bayreuth). Analytical raw data were reanalyzed by me and presented in an appropriate manner.

2.10.2. Experiments presented in chapter 3.2.

GC-MS analysis was performed by Henrike Höke and Sara Ferdi at the Department of Molecular Systems Biology (Helmholtz Centre for Environmental Research-UFZ, Leipzig, Germany). Metaproteome analysis (2.8.) was performed by Vanessa Lünsmann, Dr. Nico Jehmlich, PD Dr. Lorenz Adrian, and Prof. Dr. Martin von Bergen at the Department of Molecular Systems Biology and the Department of Isotope Biogeochemistry (Helmholtz Centre for Environmental Research-UFZ, Leipzig, Germany). Dr. Huub J.M. Op den Camp conducted the assembly for the metagenome (2.5.9.) that was used for metaproteome analysis (2.8.). Dr. Antonis Chatzinotas (Department of Environmental Microbiology, Helmholtz Centre for Environmental Research-UFZ, Leipzig, Germany) suggested the primers used for the analysis of the eukaryotic community (2.5.8.4.) and contributed to the interpretation of eukaryotic data.

3. Results

3.1. Route of chitin degradation in an aerated soil

Chitin degradation through a microbiome can occur via to two major degradation pathways, either ‘directly’, i.e. enzymatic breakdown of chitin to *N*-Acetylglucosamine oligomers, or ‘indirectly’, i.e. chitin is deacetylated prior enzymatic hydrolysis (1.2.3.1.). However, is it not known which pathway of chitin degradation is preferred by soil microbiomes. To answer hypothesis 1 of the doctoral thesis (1.7.) microbial processes associated with chitin and chitosan hydrolysis and degradation were determined and associated chitinolytic microorganisms identified by analyzing the chitinases marker gene *chiA*. The data presented in this chapter (3.1.) were published in a peer-reviewed journal (Wieczorek *et al*., 2014).

3.1.1. Chitin and chitosan degradation under oxic conditions

In chitin-supplemented soil slurries, carbon dioxide production was stimulated indicating that chitin was degraded (Fig. 11). In chitosan-supplemented soil slurries, carbon dioxide production was not stimulated within 41 days. However, after 156 days the carbon dioxide concentration was threefold higher in chitosan-supplemented soil slurries (Fig. 12), indicating that microorganisms in the sampled soil were not adapted to this substrate. Concentration of ammonium increased in chitin-supplemented treatments, while it decreased below the detection limit in the control treatments (Fig. 11), indicating that ammonium was released from chitin by ammonification. Ammonium concentrations of the chitosan-supplemented treatments were similar to those of the control treatments. The increased ammonium availability in chitin-supplemented treatments likely stimulated nitrification as the increase of nitrate concentration was higher in the chitin-supplemented treatments. The pH was not affected by chitin supplementation in contrast to chitosan supplementation which was associated with a pH shift from 5.2 to 6.3.

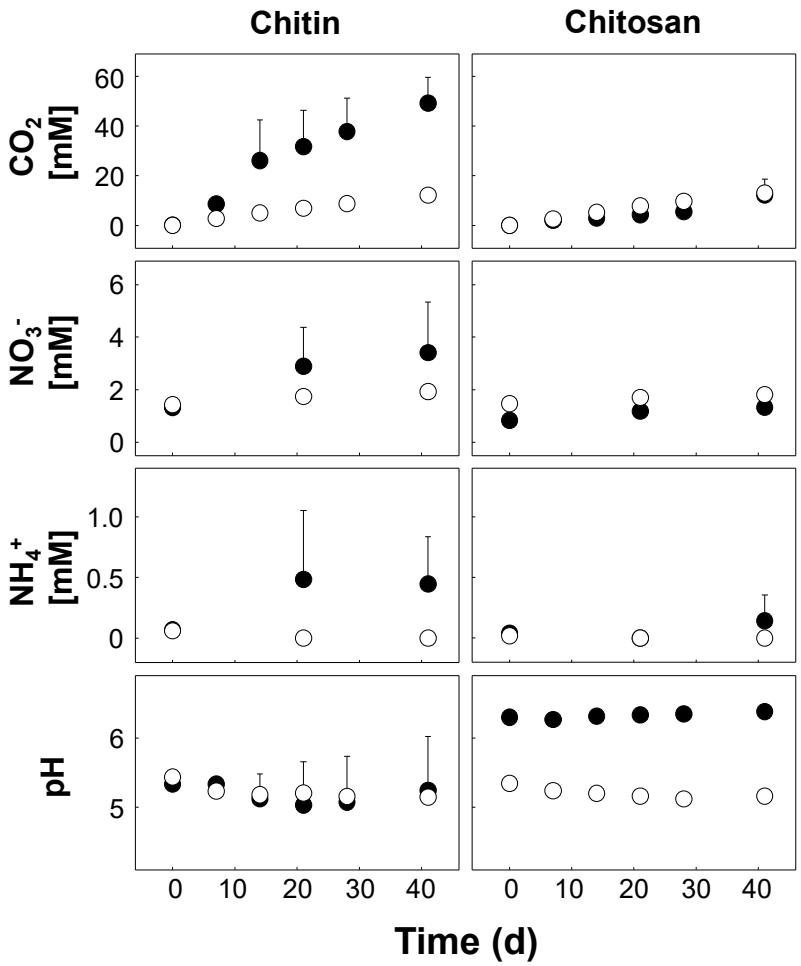

Figure 11. Compound spectrum of chitin- and chitosan-supplemented soil slurries and unsupplemented controls under oxic conditions. Blacked filled circles, substrate supplemented. White filled circles, unsupplemented controls. Values are the means of triplicate microcosms.

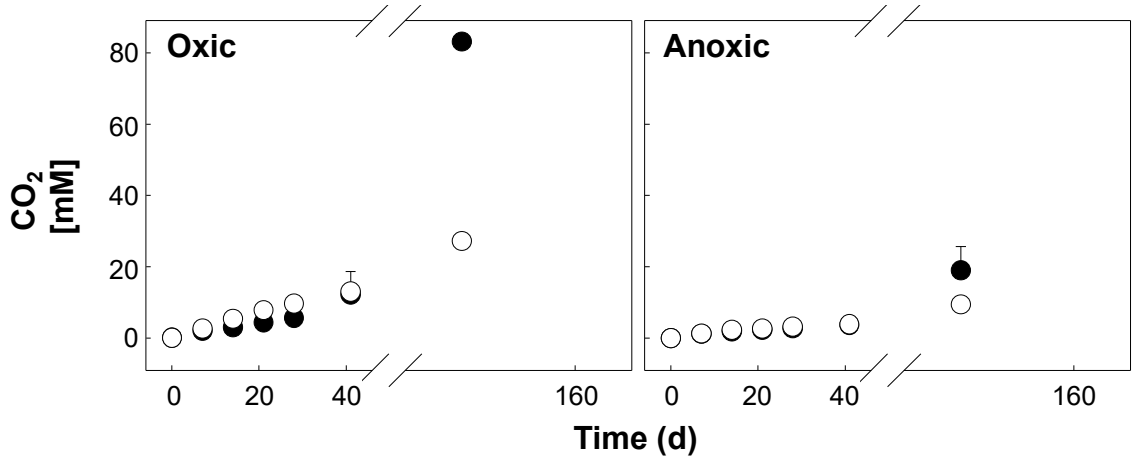

Figure 12. Carbon dioxide concentration in soil slurries supplemented with chitosan and controls under oxic and anoxic conditions after 156 days. Blacked filled circles, substrate supplemented. White filled circles, unsupplemented controls. Values are the means of triplicate microcosms.

3.1.2. Chitin and chitosan degradation under anoxic conditions

As under oxic conditions, chitosan supplementation did not impact on the concentrations of measured compounds within 41 days of measurement. Carbon dioxide concentrations were similar to the values in unsupplemented controls (Fig. 12). Thus, chitosan was likely not degraded by the soil microorganisms. Supplemented chitin was degraded. However, degradation was slower compared to the oxic conditions. Measured products were acetate (5.06 mM), propionate (0.08 mM), butyrate (0.14 mM), molecular hydrogen (0.75 mM), and carbon dioxide (1.7 mM), suggesting that various fermentation metabolisms were active (Fig. 13). Potential products of chitin hydrolysis ($[GlcNAc]_2$ and GlcNAc) were below the detection limit, i.e. they did not exceed concentrations of 30 µM. pH increased from 5.4 to 6.4 (chitin) and 6.1 to 6.8 (chitosan). No methane was measured and measurements after 41 days revealed that high amounts of ferrous iron (9.7 ± 0.5 mM) were formed.

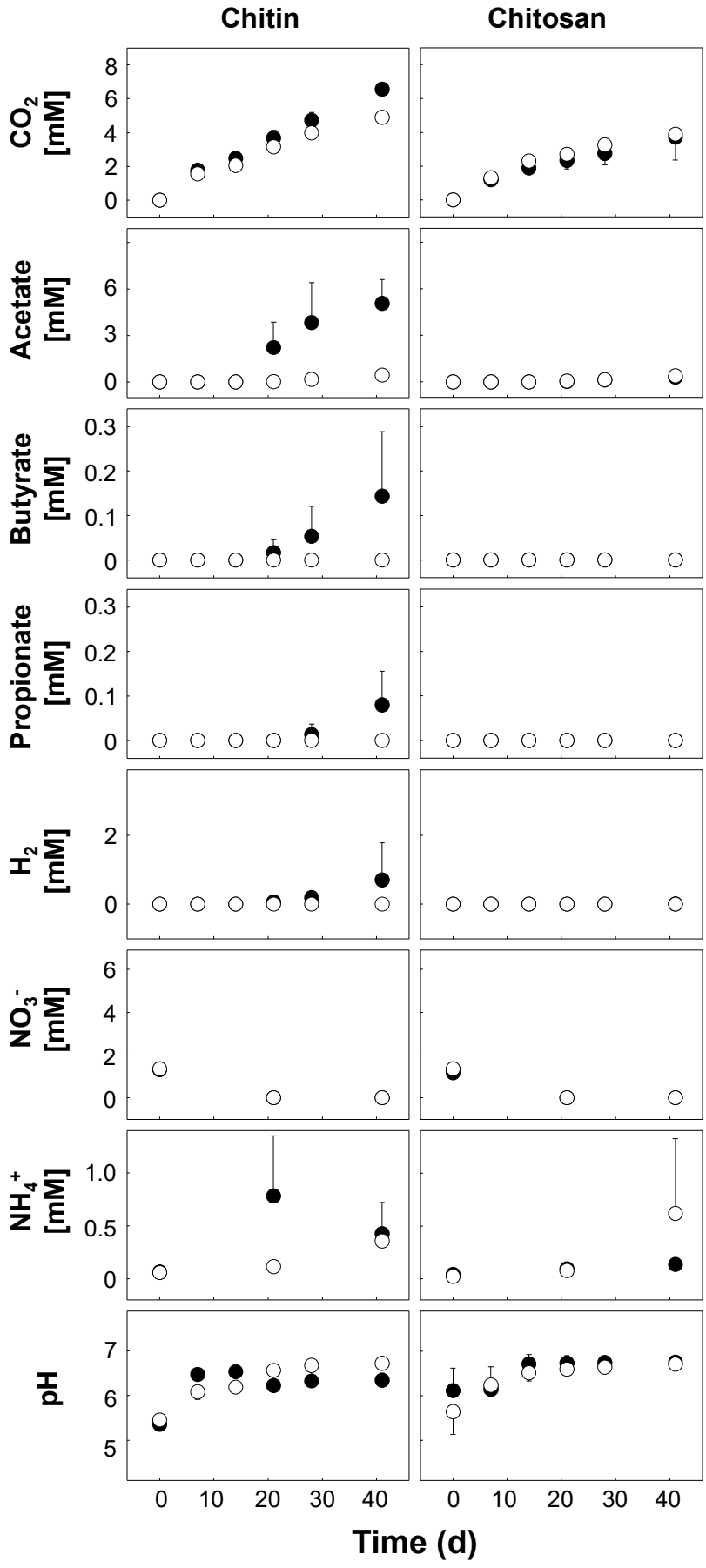

Figure 13. Compound spectrum of chitin- and chitosan-supplemented soil slurries and unsupplemented controls under anoxic conditions. Blacked filled circles, substrate supplemented. White filled circles, unsupplemented controls. Values are the means of triplicate microcosms.

3.1.3. Degradation of potential chitin and chitosan hydrolysis products under oxic conditions

The capability of the soil microbial community to metabolize typical chitin and chitosan hydrolysis products was tested by supplementation of $[GlcNAc]_2$, GlcNAc, and GlcN to soil slurries. Concentration of supplemented $[GlcNAc]_2$ and GlcNAc decreased over time (GlcN was not measurable with the HPLC settings used) going along with increased carbon dioxide production in supplemented treatments, indicating that added compounds were mineralized by the soil microorganisms. GlcNAc transiently accumulated in $[GlcNAc]_2$-supplemented slurries indicating that most of the $[GlcNAc]_2$ was extracellularly hydrolyzed, since GlcNAc was detectable in the liquid phase of the slurries (Fig. 14). Substantial release of ammonium was not observed and detectable nitrate concentrations stayed constant. pH was stable at values around 5.1 (chitobiose) and 6.1 (*N*-acetylglucosamine, glucosamine).

3.1.4. Degradation of potential chitin and chitosan hydrolysis products under anoxic conditions

The decrease of $[GlcNAc]_2$ and GlcNAc concentrations was slower in anoxic incubations suggesting slower uptake and metabolization rates under anoxic conditions. GlcNAc accumulated in $[GlcNAc]_2$-supplemented slurries and started to decrease at the end of the experiment. $[GlcNAc]_2$, GlcNAc, and GlcN stimulated the carbon dioxide production and acetate was formed in GlcNAc- and GlcN-supplemented slurries. As for the oxic conditions, a substantial release of ammonium was not observed. Concentrations of nitrate decreased over time. However, nitrate respiration was not stimulated by the supplemented sugars. The pH increased from 5.1 to 5.5 (chitobiose) and from 6.1 to 6.4 (GlcNAc, GlcN).

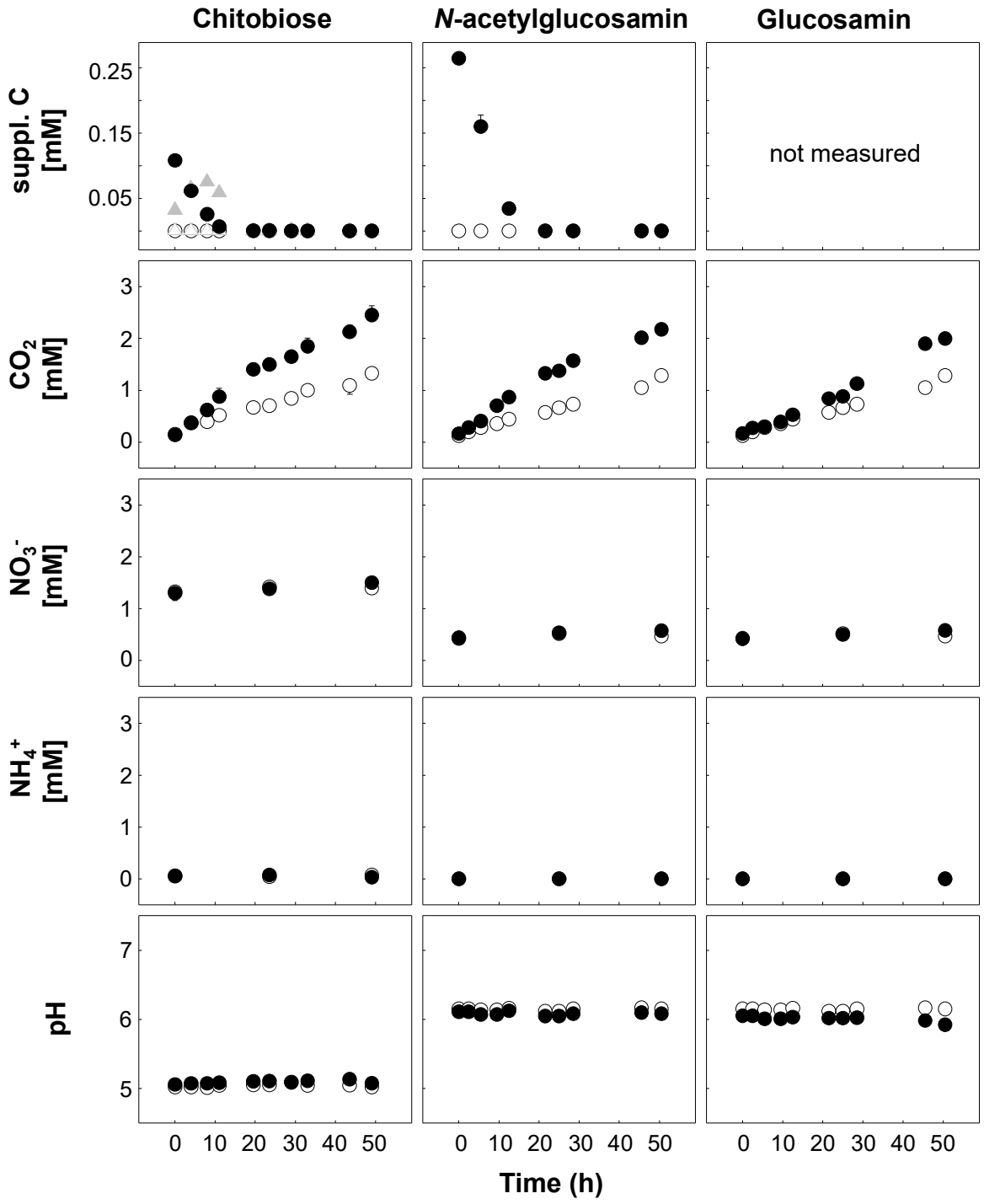

Figure 14. Compound spectrum of chitobiose-, *N*-acetylglucosamine- and glucosamine-supplemented soil slurries and unsupplemented controls under oxic conditions. Blacked filled circles, substrate supplemented. White filled circles, unsupplemented controls. Grey filled triangles, *N*-acetylglucosamine in chitobiose-supplemented soil slurries. White filled triangles, *N*-acetylglucosamine in unsupplemented controls. Values are the means of triplicate microcosms.

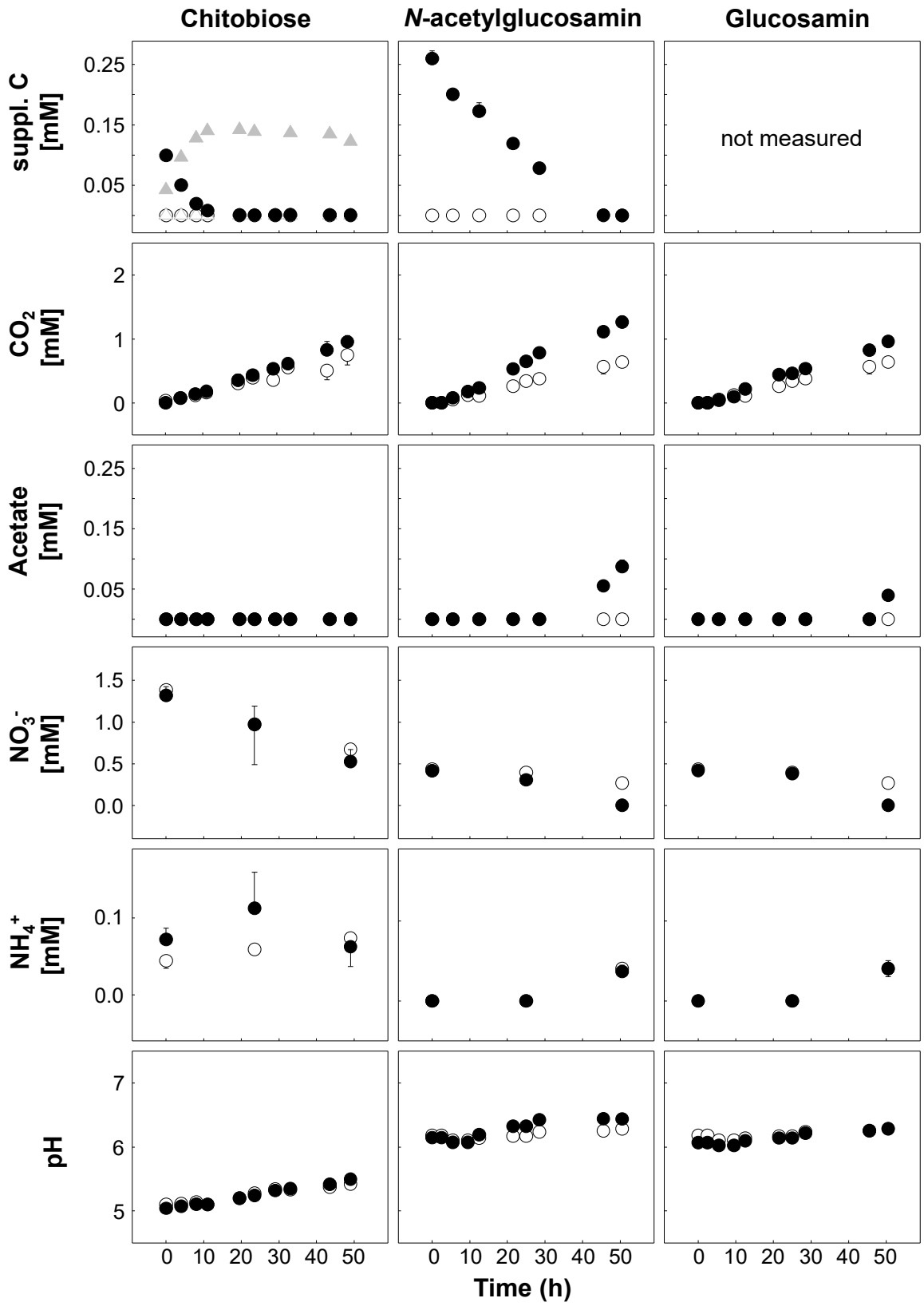

Figure 15. Compound spectrum of chitobiose-, *N*-acetylglucosamine- and glucosamine-supplemented soil slurries and unsupplemented controls under anoxic conditions. Blacked filled circles, substrate supplemented. White filled circles, unsupplemented controls. Grey filled triangles, *N*-acetylglucosamine in chitobiose-supplemented soil slurries. White filled triangles, *N*-acetylglucosamine in unsupplemented controls. Values are the means of triplicate microcosms.

3.1.5. TRFLP analysis

The microbiome's response to supplementation of chitin, chitosan, and their potential hydrolysis products $[GlcNAc]_2$, GlcNAc, and GlcN was analyzed by TRFLP analysis of *chiA* gene fragments (Fig. 16; Fig. 17). Therefore, DNA extracts from each replicate of a treatment were analyzed to assess the variability of phylotype diversity in the soil slurries. TRFLP results were analyzed by CCA (Fig. 18) and Mann-Whitney U test allowing to identify statistically significantly changed TRFs.

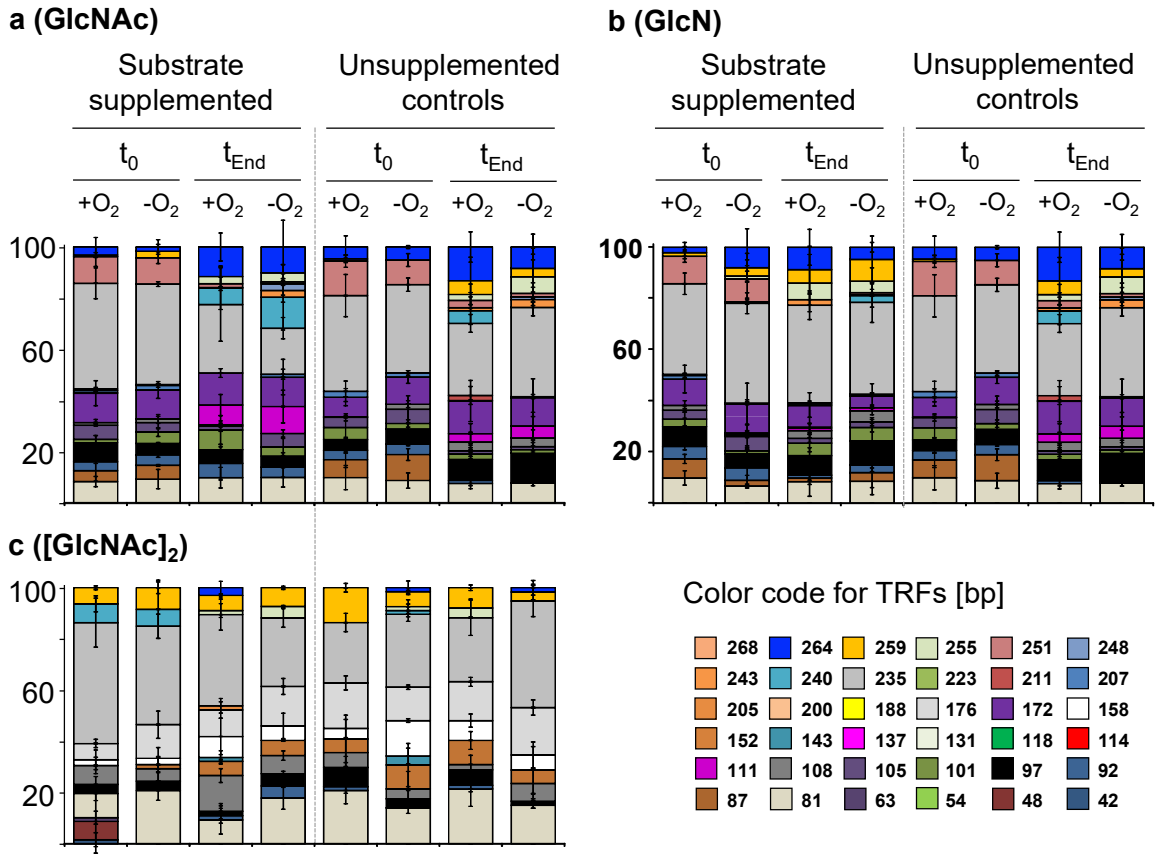

Figure 16. *chiA* TRFLP patterns of GlcNAc-, GlcN- and $[GlcNAc]_2$-supplemented soil slurries. The corresponding process data are presented in Figs. 14, 15. In each panel the first four bars represent samples from slurries with substrate and the next four bars represent samples from a control experiment without substrate supplementation. Within, the order is as follows: t_0 oxic, t_0 anoxic, t_{END} oxic and t_{END} anoxic (a, b, and c). Per time point three experimental replicates were analyzed, i.e., each value of a TRF is based on three DNA extracts (n = 3). Error bars, standard deviation.

An effect of substrate supplementation and/or oxygen availability on *chiA* TRF patterns was not evident for $[GlcNAc]_2$-, GlcNAc-, and GlcN-supplemented slurries (Fig. 16). Likely, the incubation time of 2 days was too short to allow substantial growth. Thus, there were no significant changes in the TRF patterns (Fig. 18).

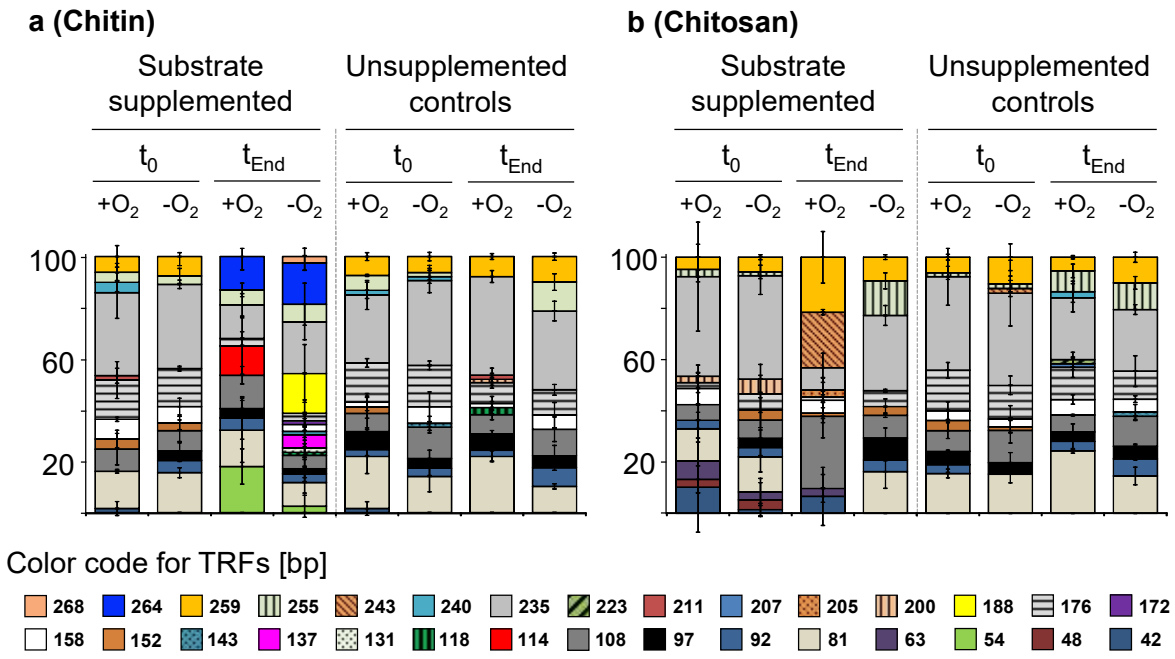

Figure 17. *chiA* TRFLP patterns of chitin- and chitosan-supplemented soil slurries. The corresponding process data are presented in Figs. 11, 13. In each panel the first four bars represent samples from slurries with substrate and the next four bars represent samples from a control experiment without substrate supplementation. Within, the order is as follows: t_0 oxic, t_0 anoxic, t_{END} oxic, and t_{END} anoxic. t_{END} was at 41 days. Experimental replicates were analyzed, i.e., each value of a TRF is based on three DNA extracts (n = 3). Error bars, standard deviation.

In the chitosan supplemented slurries, TRF patterns of *chiA* fragments at t_{END} under oxic conditions were separated according to CCA plots from t_0 TRF patterns and the t_{END} unsupplemented controls (Fig. 18). Since no potential degradation products could be detected at that time point (Fig. 13), a change due to the degradation of chitosan seems unlikely.

Supplementation of chitin clearly impacted on the *chiA* TRF patterns under oxic and anoxic conditions (Figs. 17, 18). Several TRFs that were either absent or less abundant at t_0 responded positively towards chitin supplementation and led to a shift in the TRF patterns (Figs. 17, 18). t_{END} TRF patterns of chitin-supplemented slurries were different from t_0 patterns and the corresponding unsupplemented controls at t_{END} under both oxic and anoxic conditions (Figs. 17, 18). Thereby, the TRF patterns under anoxic condition exhibited a larger variability. Under oxic conditions, TRFs 114bp and 54bp positively responded and correlated with the shift of TRF patterns (Fig. 18), whereby TRF 54bp had the stronger influence. Under anoxic conditions TRFs 137bp and 188bp responded positively and were responsible for the shift (Fig. 18). TRF 264bp was detected under oxic and anoxic conditions (Figs. 17; 18) and correlated with the shift of the patterns under oxic and anoxic conditions. TRFs 54bp, 114bp, 188bp, and 264bp significantly increased their relative abundance (Table 21).

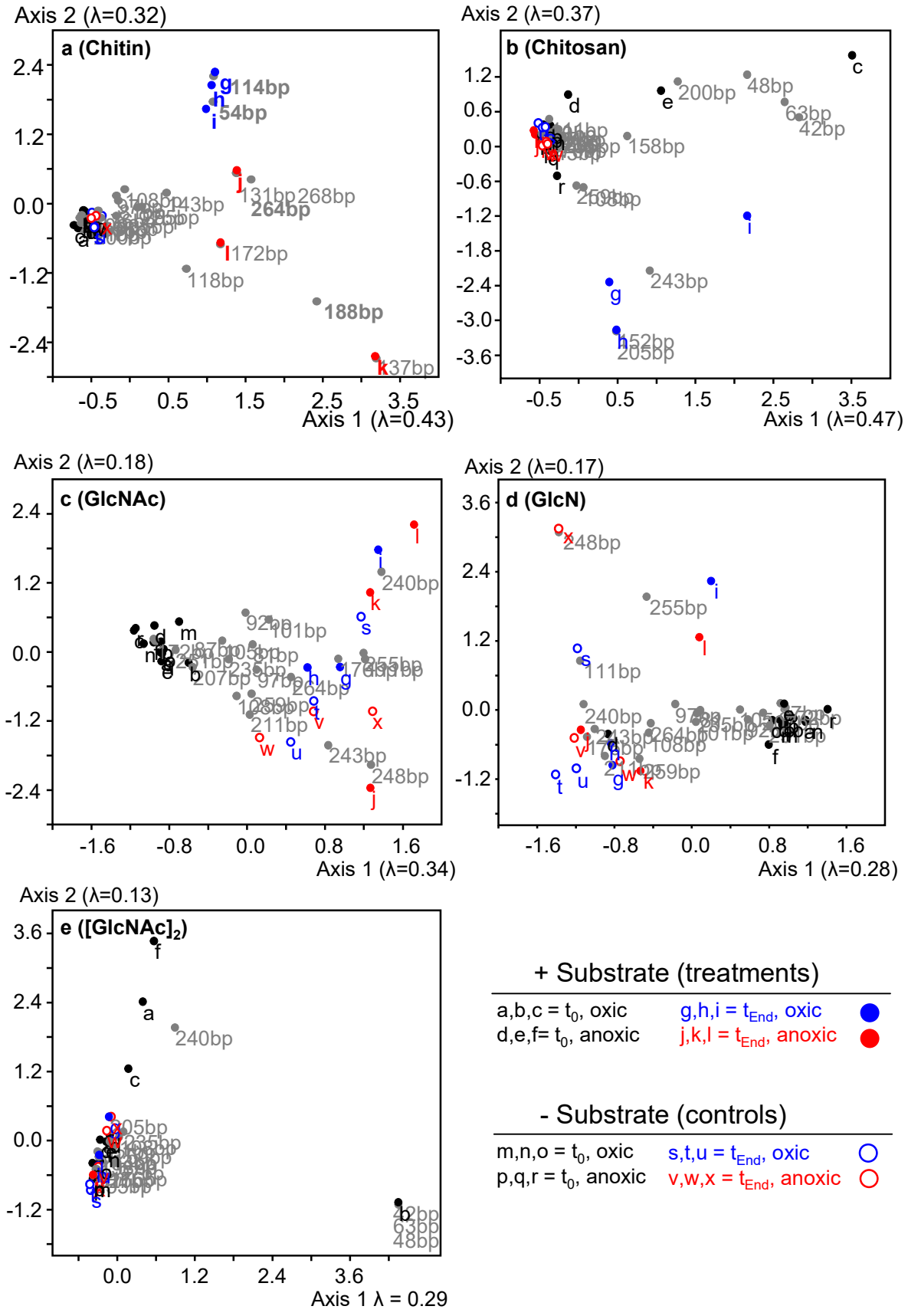

Figure 18. Effect of supplementation of chitin, chitosan, $[GlcNAc]_2$, GlcNAc, and GlcN on *chiA* TRF patterns as revealed by Canonical Correspondence Analysis (CCA). Single replicates of datasets presented in Figs. 16, 17 were used for the analysis.

The response of TRF 114bp was less significant ($p \leq 0.20$) and was found in only two of three replicates (relative abundance 10.7 ± 10.2%). TRF 137bp influenced the pattern for one replicate (replicate k, Fig. 4a) under anoxic conditions due to its high relative abundance (14.6%) but the increase of its relative abundance was not significant ($p \leq 0.51$, Fig. 17a and Table 21).

Table 21. Mann-Whitney U test of significance with TRFs identified by CCA plots that correlated with chitin supplementation under oxic and anoxic conditions. * = significant on a 10% level.

		Mann-Whitney U test		
condition	**TRF**	**U[a]**	**t[b]**	**P[c]**
oxic	54bp	0	-1.86	**0.06***
	114bp	1.5	-1.29	0.20
	264bp	0	-1.86	**0.06***
anoxic	118bp	3	-0.67	0.51
	131bp	3	-0.67	0.51
	137bp	3	-0.67	0.51
	143bp	3	-0.67	0.51
	172bp	3	-0.67	0.51
	188bp	0	-1.86	**0.06***
	264bp	0	-1.86	**0.06***
	268bp	3	-0.67	0.51

[a]test statistic
[b]t-value
[c]p-value

3.1.6. Diversity of *chiA*-like phylotypes

Rarefaction analysis revealed sufficient sampling depth based on the cut-off value (similarity ≥50%). However, a plateau indicative of a complete coverage of phylotype diversity was not fully reached (Fig. 20). 206 *chiA*-like phylotypes were detected and grouped into 42 OTUs (Fig. 19). The high number of detected OTUs suggested a large *chiA* phylotype richness in the microbial community of the investigated agricultural soil. 22 OTUs affiliated with *chiA*-phylotypes of cultivated species (similarity ≥60%), and were assigned to *Beta*- and *Gammaproteobacteria* (OTU 2, 12, 19), *Actinobacteria* (OTU 7 and 20), *Acidobacteria* (OTU 4 and 26), *Bacteroidetes* (OTU 9, 14, and 28), *Firmicutes* (OTU 10 and 15), *Planctomycetes* (OTU 1), *Chloroflexi* (OTU 11), and micro-eukaryotes (OTU 17, 21, 24, 25, 41, 27, and 37) (Fig. 19).

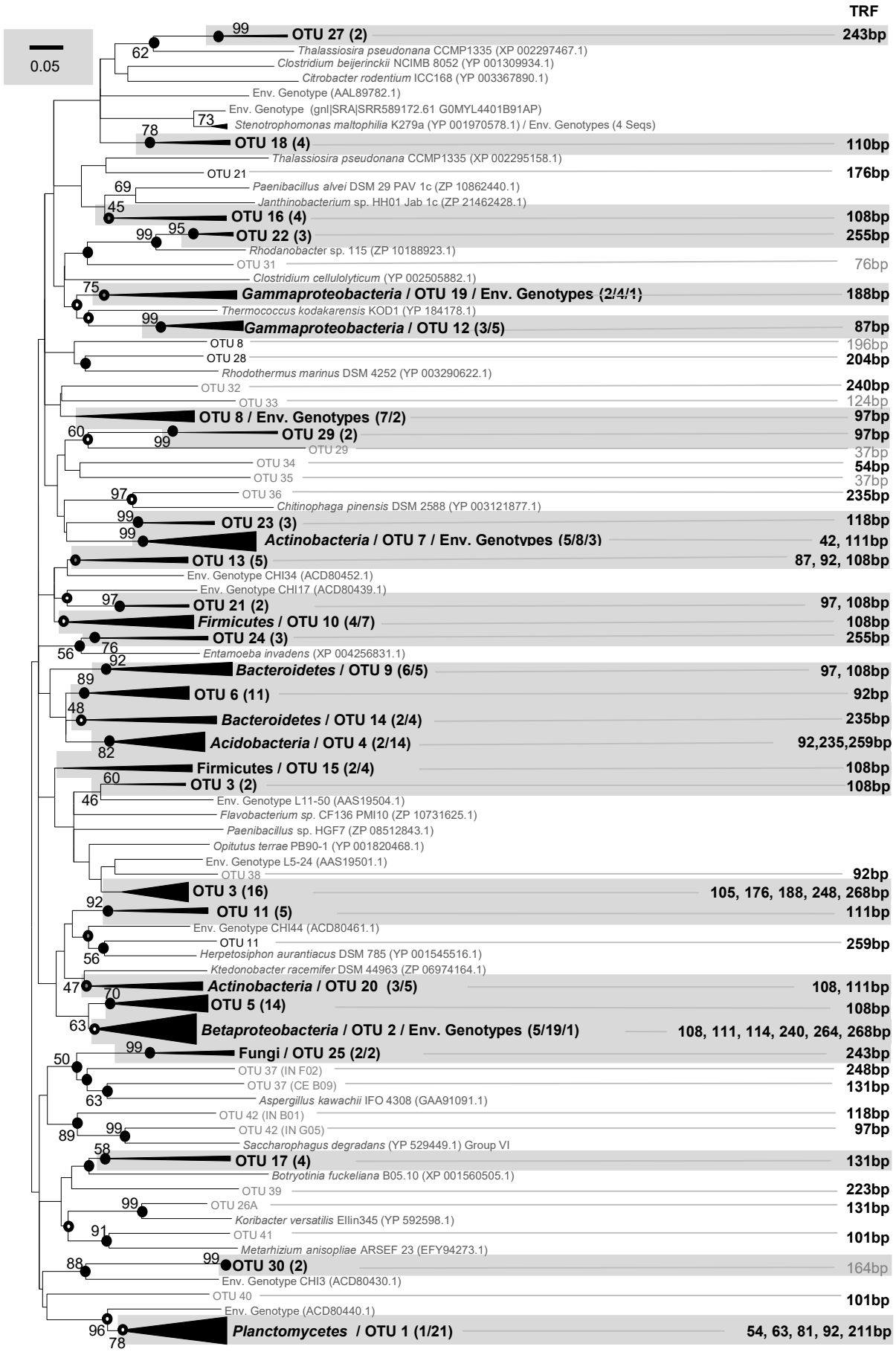
TRF
0.05
OTU 27 (2) 243bp
Thalassiosira pseudonana CCMP1335 (XP 002297467.1)
Clostridium beijerinckii NCIMB 8052 (YP 001309934.1)
Citrobacter rodentium ICC168 (YP 003367890.1)
Env. Genotype (AAL89782.1)
Env. Genotype (gnl|SRA|SRR589172.61 G0MYL4401B91AP)
Stenotrophomonas maltophilia K279a (YP 001970578.1) / Env. Genotypes (4 Seqs)
OTU 18 (4) 110bp
Thalassiosira pseudonana CCMP1335 (XP 002295158.1)
OTU 21 176bp
Paenibacillus alvei DSM 29 PAV 1c (ZP 10862440.1)
Janthinobacterium sp. HH01 Jab 1c (ZP 21462428.1)
OTU 16 (4) 108bp
OTU 22 (3) 255bp
Rhodanobacter sp. 115 (ZP 10188923.1)
OTU 31 76bp
Clostridium cellulolyticum (YP 002505882.1)
Gammaproteobacteria / OTU 19 / Env. Genotypes (2/4/1) 188bp
Thermococcus kodakarensis KOD1 (YP 184178.1)
Gammaproteobacteria / OTU 12 (3/5) 87bp
OTU 8 196bp
OTU 28 204bp
Rhodothermus marinus DSM 4252 (YP 003290622.1)
OTU 32 240bp
OTU 33 124bp
OTU 8 / Env. Genotypes (7/2) 97bp
OTU 29 (2) 97bp
OTU 29 37bp
OTU 34 54bp
OTU 35 37bp
OTU 36 235bp
Chitinophaga pinensis DSM 2588 (YP 003121877.1)
OTU 23 (3) 118bp
Actinobacteria / OTU 7 / Env. Genotypes (5/8/3) 42, 111bp
OTU 13 (5) 87, 92, 108bp
Env. Genotype CHI34 (ACD80452.1)
Env. Genotype CHI17 (ACD80439.1)
OTU 21 (2) 97, 108bp
Firmicutes / OTU 10 (4/7) 108bp
OTU 24 (3) 255bp
Entamoeba invadens (XP 004256831.1)
Bacteroidetes / OTU 9 (6/5) 97, 108bp
OTU 6 (11) 92bp
Bacteroidetes / OTU 14 (2/4) 235bp
Acidobacteria / OTU 4 (2/14) 92,235,259bp
Firmicutes / OTU 15 (2/4) 108bp
OTU 3 (2) 108bp
Env. Genotype L11-50 (AAS19504.1)
Flavobacterium sp. CF136 PMI10 (ZP 10731625.1)
Paenibacillus sp. HGF7 (ZP 08512843.1)
Opitutus terrae PB90-1 (YP 001820468.1)
Env. Genotype L5-24 (AAS19501.1)
OTU 38 92bp
OTU 3 (16) 105, 176, 188, 248, 268bp
OTU 11 (5) 111bp
Env. Genotype CHI44 (ACD80461.1)
OTU 11 259bp
Herpetosiphon aurantiacus DSM 785 (YP 001545516.1)
Ktedonobacter racemifer DSM 44963 (ZP 06974164.1)
Actinobacteria / OTU 20 (3/5) 108, 111bp
OTU 5 (14) 108bp
Betaproteobacteria / OTU 2 / Env. Genotypes (5/19/1) 108, 111, 114, 240, 264, 268bp
Fungi / OTU 25 (2/2) 243bp
OTU 37 (IN F02) 248bp
OTU 37 (CE B09) 131bp
Aspergillus kawachii IFO 4308 (GAA91091.1)
OTU 42 (IN B01) 118bp
OTU 42 (IN G05) 97bp
Saccharophagus degradans (YP 529449.1) Group VI
OTU 17 (4) 131bp
Botryotinia fuckeliana B05.10 (XP 001560505.1)
OTU 39 223bp
OTU 26A 131bp
Koribacter versatilis Ellin345 (YP 592598.1)
OTU 41 101bp
Metarhizium anisopliae ARSEF 23 (EFY94273.1)
OTU 30 (2) 164bp
Env. Genotype CHI3 (ACD80430.1)
OTU 40 101bp
Env. Genotype (ACD80440.1)
Planctomycetes / OTU 1 (1/21) 54, 63, 81, 92, 211bp

Figure 19. Phylogenetic tree of *chiA* OTUs (206 sequences) and references (78 sequences). *ChiA* gene libraries were prepared from pooled DNA extracts of each substrate treatment and data were combined for the figure. Gray numbers in parentheses, accession numbers of reference sequences. For condensed branches, OTUs and taxonomic affiliation of reference sequences are indicated in bold letters and the numbers of reference sequences, OTU sequences and environmental sequences are given in parentheses. Accession numbers for reference sequences of the condensed branches can be found in Fig. S2. Numbers on the right side, TRFs corresponding to phylotypes identified by *in silico* analysis. The tree was calculated using translated amino acid sequences with neighbor-joining algorithm (MEGA 5; Tamura et al., 2011) including bootstrapping (1,000 replicates; percentage values at nodes). Open circles and gray filled circles at nodes, these nodes were confirmed by maximum likelihood and maximum parsimony algorithms, respectively, using the same data set. Black circles, confirmation by both algorithms. Scale bar, 5% sequence divergence.

In contrast, OTUs 3, 5, 6, 8, 13, 16, 18, 22, 23, 29–36, and 38–42 represented novel *chiA* phylotypes based on their high dissimilarity to known *chiA* phylotypes (dissimilarity > 40%) and their separate branching (Fig. 19; S2). Eukaryote-like *chiA* sequences accounted for a minor fraction of detected *chiA* OTUs and were closest related to those of either fungi (*Basidiomycota*; OTU 17, 25 and 41), *Amoebozoa* (OTU 24), or diatoms (*Heterokontophyta*, OTUs 21 and 27) (Figs. 17, 19). *Basidomycota* are known to be comprised of chitinolytic species (Gooday 1990a,b; Tracey 1955). Bacteria might have outcompeted chitinolytic *Basidiomycota* in soil slurries based on data of the current study (Figs. 17, 19). Nonetheless, it should be noted that used primers were developed for targeting bacterial *chiA* sequences, and thus conclusions with regard to eukaryotic phylotypes are limited.

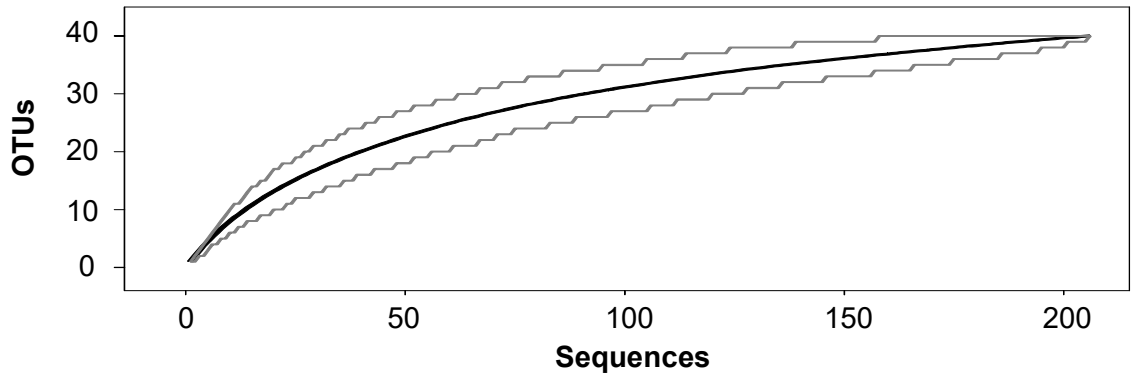

Figure 20. Rarefaction analyses of the ChiA amino acid sequences obtained from *in silico* translation of gene sequences. OTUs were defined with a cut off value of 50% amino acid dissimilarity. The enclosed area indicates 95% confidence interval.

3.2. Aerobic and anaerobic degradation of chitin-derived carbon and associated prokaryotes

3.2.1. Degradation of chitin by an agricultural soil microbiome

Microbiomes in agricultural soils are driven by carbon and energy input from plant-derived organic residues, including root exudates. This input is partially transformed into the fungal and arthropod biomass (Gooday 1990a,b; Martínez *et al*., 2009), which, together with plant residues, contributes substantially to the pool of substrates being mineralized by the soil microbiome (Singh & Gupta 1997; Scheu 2002). Structural polymers form a major part of this pool of substrates, notably cellulose, chitin, hemicelluloses, and lignin. Chitin is globally the second most abundant biopolymer after cellulose. However, unlike cellulose its degradation in aerated soils and associated taxa are not well understood. Thus, RNA- and protein-based stable isotope probing (SIP) together with chemical analytics was used to resolve the microbial conversion of supplemental [^{13}C]-chitin and microorganisms in soil slurries from a wheat-planted field in south Germany. The data presented in this chapter (3.2.) were published in a peer-reviewed journal (Wieczorek *et al*., 2019).

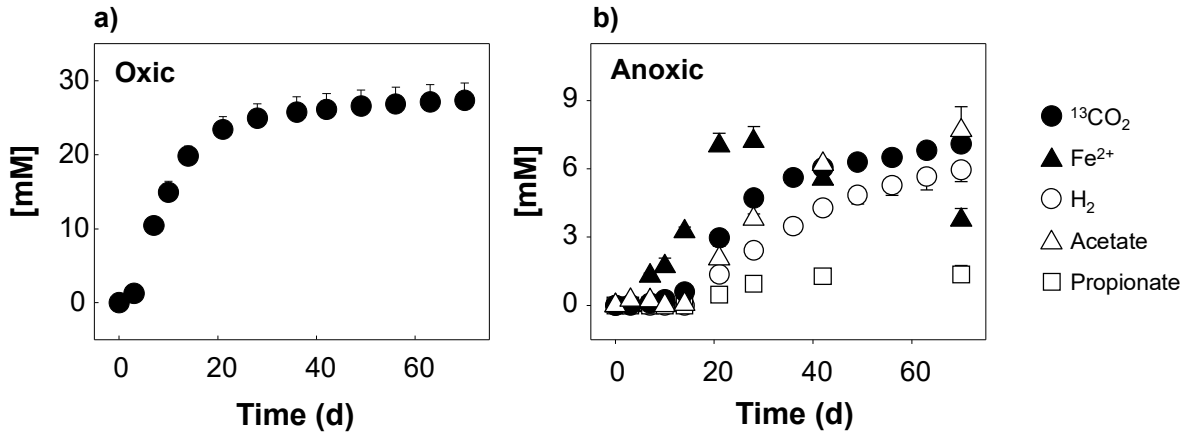

Figure 21. Aerobic and anaerobic chitin degradation. Only main products detected (> 1 mM) are displayed. Values are the means of duplicate microcosms. Error bars indicate the standard deviations. All products except carbon dioxide are net values, i.e. values of unsupplemented controls have been subtracted from [^{13}C]-treatments. Displayed carbon dioxide values were calculated from the percentage of [^{13}C]-carbon dioxide measured in the [^{13}C]-chitin treatment. Values of the [^{12}C]-chitin treatments were alike and can be found together with the gross values of all treatments in the supplemental information (Figs. 22, 23).

3.2.1.1. Aerobic chitin degradation

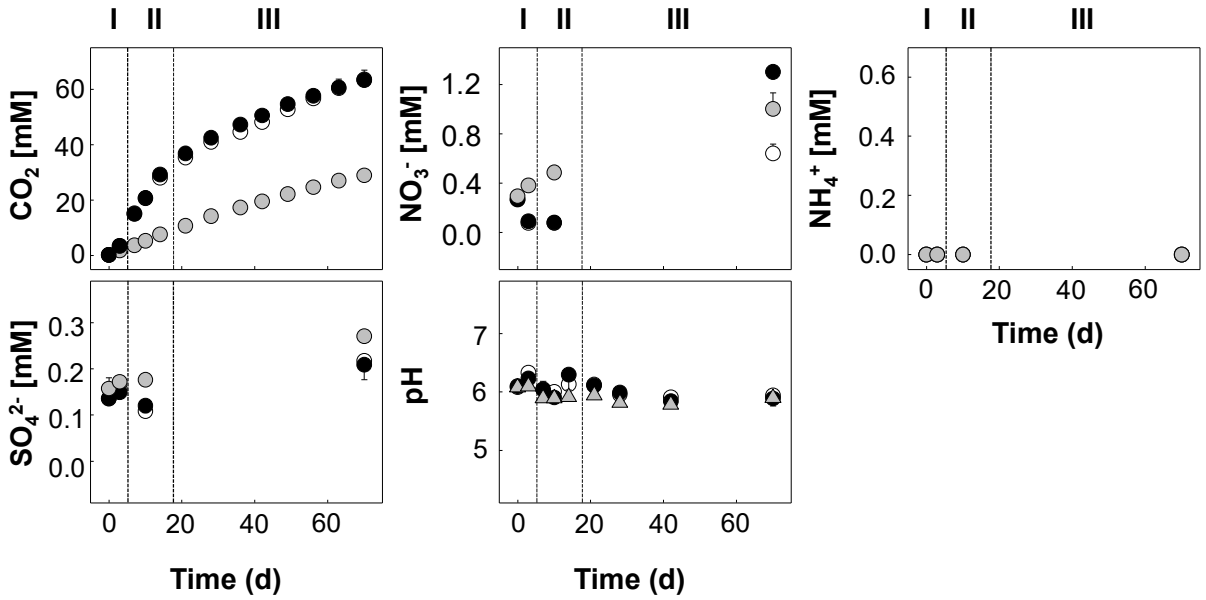

Figure 22. Measured compounds in oxic soil slurries. Black circles, supplemented with [^{13}C]-chitin. White circles, supplemented with [^{12}C]-chitin. Grey circles, unsupplemented controls. Error bars, standard deviations. Numerals indicate the different phases during chitin degradation. After a short lag phase (I), the rate of ^{13}C formation from chitin increased (II) and then slowed substantially after 21 days (III). Values are the means of duplicate microcosms.

Under oxic conditions, supplemental chitin stimulated carbon dioxide production after a lag phase of three days (Fig. 22). [^{13}C]-carbon dioxide accumulation leveled off after 20 days (Fig. 21), suggesting that the supplemented [^{13}C]-chitin was consumed. At the end of the incubation, 63% of the chitin carbon was recovered as carbon dioxide (Table 22). The unrecovered fraction of chitin-derived carbon was likely incorporated into the newly formed microbial biomass and microbial residues (Gooday 1990b). Chitin-derived ammonium, which can be released during aerobic chitin degradation (3.1.1.; Wieczorek *et al*., 2014), did not accumulate and was also not converted to nitrate (Fig. 22). In addition, nitrate concentrations decreased in chitin-supplemented slurries in the beginning of incubation while they slowly increased in the controls (Fig. 22).

Table 22. Carbon and electron recoveries based on the assumption of the complete degradation of the supplemented [^{13}C]-chitin.

	Oxic			Anoxic	
Day	**Carbon recovery (%)**	**Electron recovery (%)**	**Day**	**Carbon recovery (%)**	**Electron recovery (%)**
3	3.0	n.d.	**3**	1.1	1.1
10	33.9	n.d.	**10**	0.7	1.2
21	54.0	n.d.	**21**	19.8	19.5
70	62.9	n.d.	**70**	57.9	54.1

n.d., could not be determined.

3.2.1.2. Anaerobic chitin degradation

The anaerobic degradation of chitin was slower compared to the aerobic degradation and could be separated into three distinct phases on the process level. Carbon dioxide was only slightly stimulated compared to the unsupplemented controls (Fig. 23) by chitin supplementation during the first 20 days, and only small amounts of [^{13}C]-carbon dioxide accumulated (Fig. 21). In this initial phase, nitrate and ferric iron were reduced (Fig. 23). In addition, also sulfate concentrations started to decrease. Thus, this phase is characterized by the reduction of alternative electron acceptors. Fermentation was likely ongoing as small amounts of acetate were produced in [^{13}C]-chitin-supplemented slurries. However, acetate was apparently consumed and thus, fermentation played a minor role in this initial phase. The second phase (between days 20 and 41) was characterized by the accumulation of molecular hydrogen, acetate, propionate, and small amounts of butyrate and isobutyrate (Fig. 23). These typical fermentation products indicate that fermentation was stimulated by the chitin supplementation (Fig. 23). In addition, also the iron reduction was stimulated and ongoing (Fig. 23). In the final phase, fermentation product accumulation slowed down, and iron reduction stopped, whereas methane started to accumulate (Fig. 23). Up to 58% of the carbon and 54% of the electrons of the supplemented chitin were recovered in the fermentation products of the anoxic treatments (Table 22). Ammonium accumulation was stimulated, however in low amounts, indicating that most of the chitin-derived ammonium was consumed, likely via assimilatory pathways.

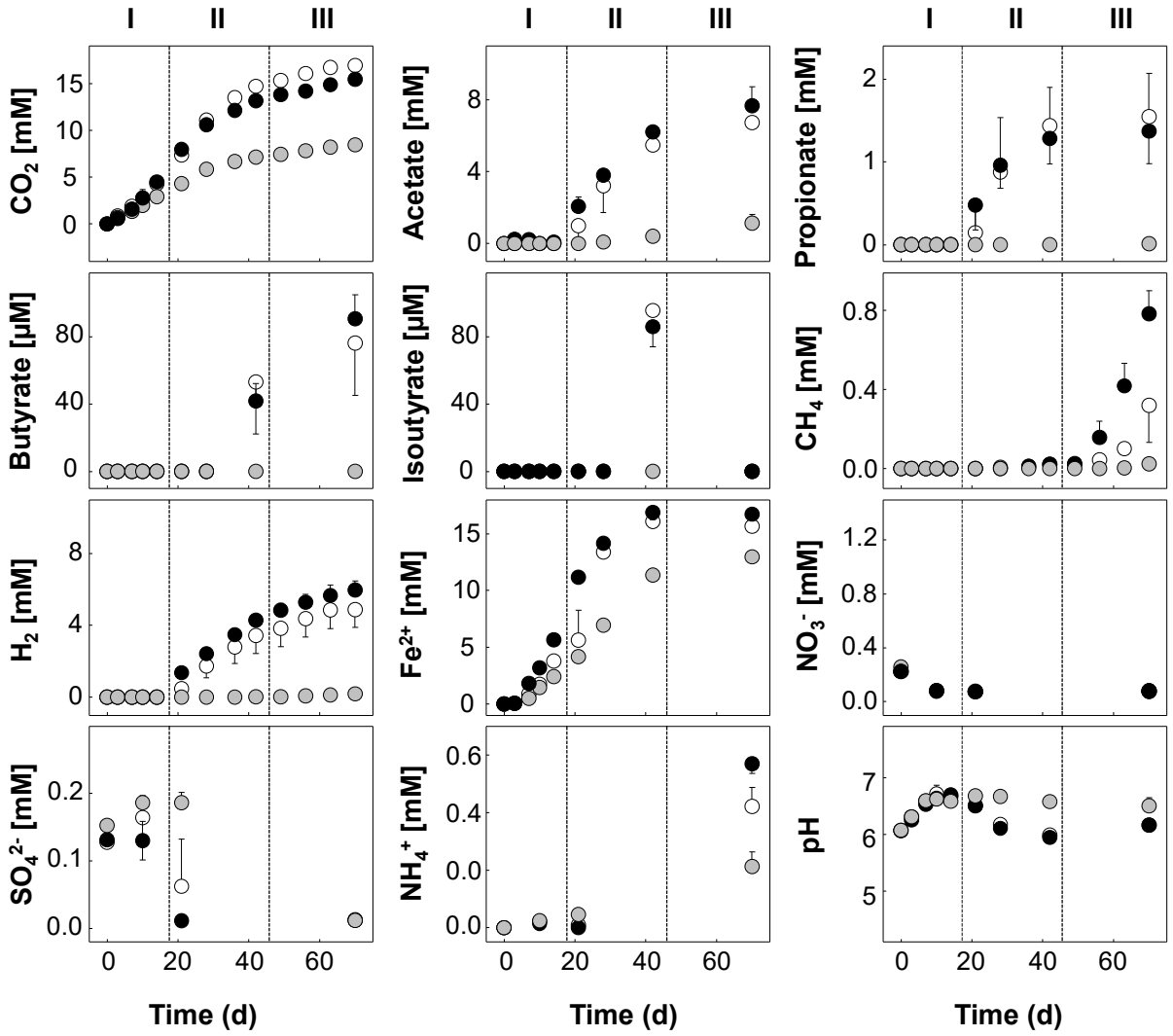

Figure 23. Measured compounds in anoxic soil slurries. Black circles, supplemented with [^{13}C]-chitin. White circles, supplemented with [^{12}C]-chitin. Grey circles, unsupplemented controls. Error bars, standard deviations. Numerals indicate the different phases during chitin degradation. In the first twenty days, the degradation of chitin was slow (I). Then, the apparent degradation rate increased, and ferric iron reduction and fermentation were highly stimulated by chitin supplementation (II). The last phase (III) was characterized by decreases in the apparent degradation rate and methane production. Values are the means of duplicate microcosms.

3.2.2. Active *Bacteria* assimilating [^{13}C]-chitin-derived carbon

Active bacterial taxa involved in the degradation of chitin were identified by 16S rRNA gene pyrosequencing amplicon libraries derived from cDNA of heavy and light fractions according to a modified CAP-SIP approach (Dallinger *et al.*, 2014; 2.7.4.).

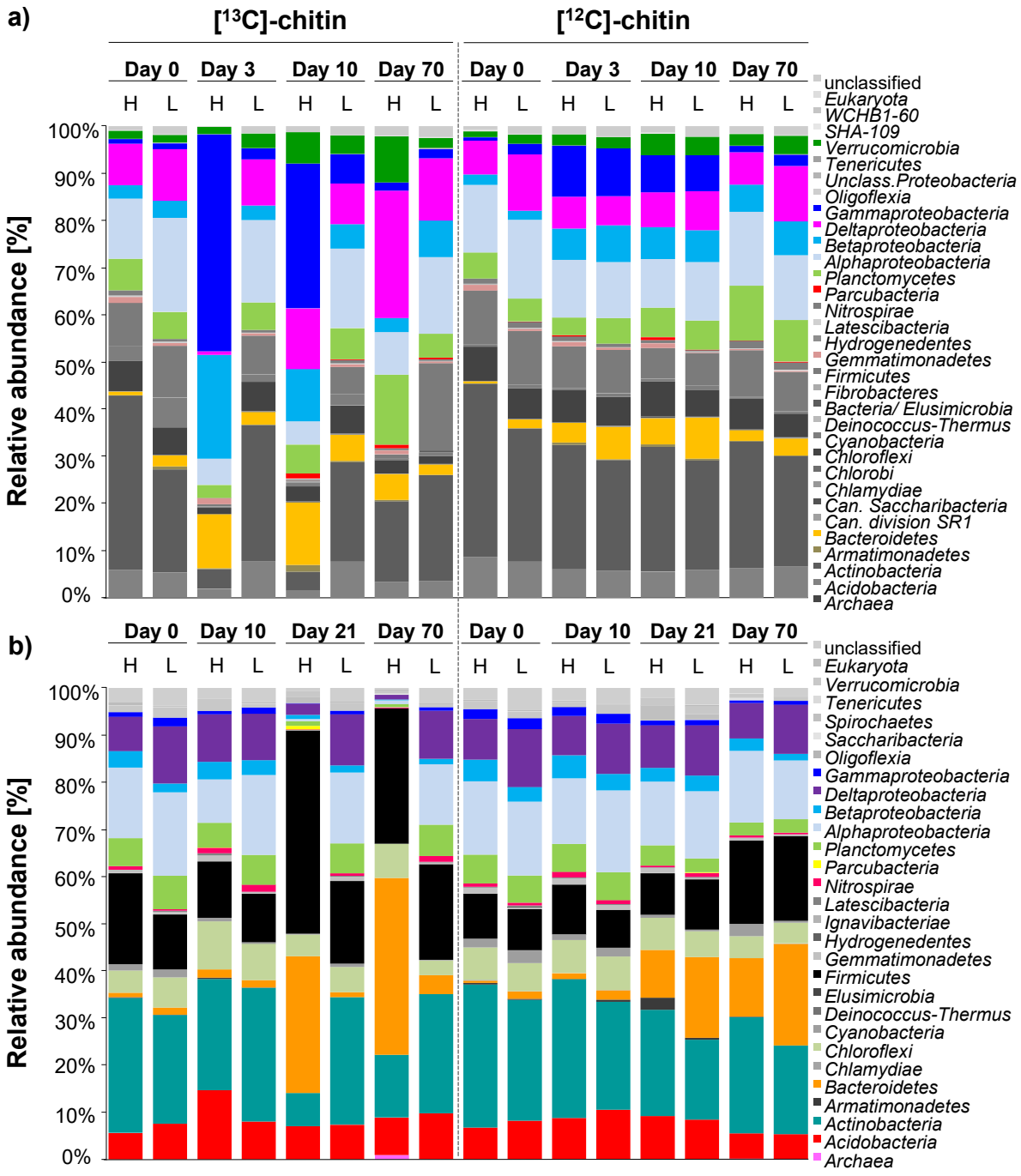

Figure 24. Shift of microbial community composition due to incorporation of [^{13}C]-carbon. Microbial community compositions are based on 16S rRNA transcript libraries derived from cDNA of heavy and light fractions after isopycnic centrifugation of RNA from [^{13}C]- and [^{12}C]-chitin soil slurry incubations under oxic (a) and anoxic (b) conditions. H, heavy fractions. L, light fractions. Jaguc2 (Nebel *et al.*, 2011) was used to cluster pyrosequencing derived sequences into family level OTUs with sequence similarity threshold of 87.5% (Yarza *et al.*, 2010). OTUs were phylogenetically affiliated by local nucleotide BLAST using Jaguc2 against the latest SILVA SSU database release. See section 2.7.4. for more information.

3.2.2.1. Active *Bacteria* labeled by ^{13}C under oxic conditions

22 family level OTUs affiliated with *Bacteroidetes*, *Gemmatimonadetes*, *Planctomycetes*, *Proteobacteria,* and *Verrucomicrobia* were labeled in a distinct temporal sequence under oxic conditions (Fig. 25; Table S1).

The labeling ratio (i.e., the percentage of labeled taxa) was highest for the first time point analyzed (day 3) with 73.3% and decreased over time (Fig. 25b). *Bacteroidetes*, *Beta*-, and *Gammaproteobacteria* were the most intensely labeled phyla after three days with 9%, 18.2%, and 42.3% R_{CS} score (see 2.7.4. for definition), respectively (Fig. 25b). Within *Beta*- and *Gammaproteobacteria,* the labeled family level OTUs affiliated with *Oxalobacteraceae* and *Pseudomonadaceae*. The labeled *Oxalobacteracea* phylotype was related most closely to *Massilia* species (Fig. 25a). The most closely related described species of the labeled *Pseudomonadaceae* phylotype were *Cellvibrio* species (Fig. 25a). Within *Bacteroidetes, Cytophagaceae*, *Flavobacteriaceae*, *Sphingobacteriaceae,* and *Chitinophagaceae* were labeled. In addition, *Gemmatimonadaceae* (*Gemmatimonadetes),* and *Caulobacteriaceae* (*Alphaproteobacteria)* were labeled. However, their R_{CS} score, i.e. 0.9% and 2.9% respectively, of the labeled taxa was minor.

The labeling ratio decreased towards day 10 to 53.4% and *Oxalobacteraceae* and *Pseudomonadaceae* were still the most intensely labeled families. Nevertheless, the proportions of the both families decreased as additional phylotypes of different phyla also were labeled, including *Deltaproteobacteria*, *Planctomycetes*, and *Verrucomicrobia* (Fig. 25). The labeled *Deltaproteobacteria* OTUs were affiliated with *Bacteriovoracaea*, *Bdellovibrionaceae,* and uncultured *Myxococcales* and had a R_{CS} score of 1.6%, 2.4%, and 4.3%, respectively (Table S1). Within *Planctomycetes, Phycisphaerae* with a R_{CS} score of 1.7 % were labeled. Within *Verrucomicrobia,* family level OTUs affiliated with *Verrucomicrobiaceae* (1.0% R_{CS}) and *Optitutaceae* (0.8% R_{CS}) were labeled.

Towards the end of the incubation period, the labeling ratio of *Pseudomonadaceae* further decreased and a label of *Oxalobacteraceae* was no longer detectable whereas the percentage of *Deltaproteobacteria*, *Planctomycetes,* and *Verrucomicrobia* further increased, indicating a substantial shift in the taxa that assimilated ^{13}C (Fig. 25). The labeling of OTUs affiliating with *Opitutacea*e and *Verrucomicrobiaceae* was no longer detectable, however, an additional OTU affiliating with an uncultured family within *Chthoniobacterales* was labeled. The proportion of labeled *Planctomycetes* increased and additional OTUs affiliated with *Gemmataceae* and *Tepidisphaeraceae* with a R_{CS} score of 2.7% and 0.9% were labeled, respectively. Within the *Deltaproteobacteria,* OTU 779 affiliated with *Bdellovibrionaceae* was no longer detectable, however the labeling ratio of the other OTUs further increased (Table S1).

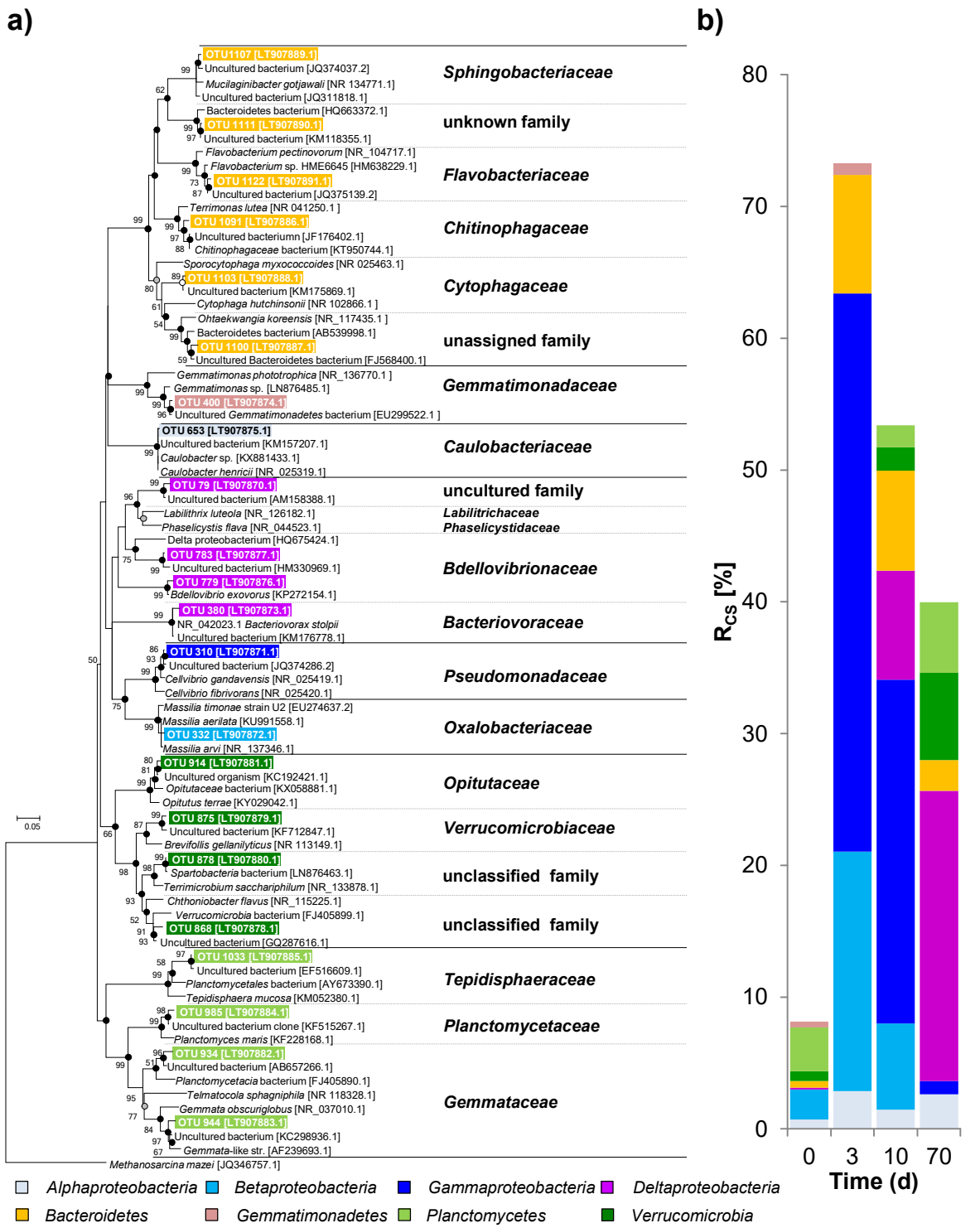

Figure 25. Phylogenetic tree of 16S rRNA cDNA sequences (a) and R_{CS} scores (b) from phylotypes labeled by assimilation of [^{13}C]-chitin-derived carbon in soil slurries under oxic conditions. a), the consensus tree was calculated with the maximum likelihood method and 1,000 bootstraps. Dots at nodes indicate confirmation of topology by neighbor-joining (white circles) and maximum parsimony (grey circles) algorithms. Black circles indicate confirmation by both algorithms. Accession numbers are given in brackets. Scale bar, 5% evolutionary distance. *Methanosarcina mazei* [JQ346757.1] was used as the out group. **b)**, R_{CS} scores are net relative abundances of labeled taxa, i.e. respective values from [^{12}C]-chitin incubations were subtracted in a comparative approach. At t_0, relative abundance values are presented. See material and methods for details on criteria for labeling and calculation of R_{CS} scores (2.7.4.).

3.2.2.2. Active *Bacteria* labeled by ^{13}C under anoxic conditions

Under anoxic conditions, 11 family level OTUs were labeled. The first time point for the analysis of label incorporation for the anoxic treatments was after 10 days when the carbon recovery (a measure for the progress in chitin degradation) was in the same range as that of the oxic treatments after 3 days (Table 22). In the first phase of the anoxic chitin degradation, the total labeling ratio was low, at 15.9% (Fig. 26b). *Acidobacteria* incorporated the largest fraction of ^{13}C (6.6% R_{CS}), followed by *Firmicutes* (3.7% R_{CS}), *Deltaproteobacteria* (3.0% R_{CS}), *Chloroflexi* (1.8% R_{CS}), and *Verrucomicrobia* (1.4% R_{CS}) (Fig. 26b; Table S2). OTU 410 was grouped into *Acidobacteriaceae* with Candidatus *Koribacter versatilis* as the closest described relative (Fig. 26a). OTU 203 was affiliated most closely with the genus *Paenibacillus* (*Paenibacillaceae, Firmicutes*). The next cultivated species affiliated with OTU 120 was *Geobacter psychrophilus* (*Geobacteriaceae).* OTU 548 was grouped into *Anaerolineaceae* (*Chloroflexi*) and OTU 2 was affiliated with an unclassified family within the *Verrucomicrobiales* (*Verrucomicrobia*).

At day 21, in the second phase of anaerobic chitin degradation, the labeling ratio increased up to 66.4% (Fig. 26b) indicating that labeled taxa incorporated higher amounts of ^{13}C. Uncultured *Bacteroidetes* and *Firmicutes* were labeled and harbored the largest fraction of the total label, while the label fractions in *Acidobacteria* and *Chloroflexi* had decreased (Fig. 26b; Table S2). Within the *Firmicutes*, the R_{CS} scores of *Paenibacillaceae* increased from 3.7 to 11.6% and additionally OTU 423 (11.6% R_{CS}) and OTU 416 (15.2% R_{CS}) affiliating with *Lachnospiraceae* and *Ruminococcaceae* were labeled. Within the *Bacteroidetes,* one OTU (754) affiliated with an uncultured family was labeled. The labeling of unclassified *Verrucomicrobia* and *Geobacteraceae* was no longer detectable (Fig. 26b).

At the end of incubation, the total labeling ratio was 64.2%. Uncultured *Bacteroidetes* became the most abundantly labeled phylum (32.2% R_{CS}) followed by *Firmicute*s (22% R_{CS}), *Acidobacteria* (4.8% R_{CS}), and *Chloroflexi* (3.6% R_{CS}) (Fig. 26b; Table S2). Within the *Firmicutes*, OTU 440 affiliated with uncultured *Firmicutes* was labeled and the label for OTU 416 (*Ruminococcaceae*) vanished (Table S2).

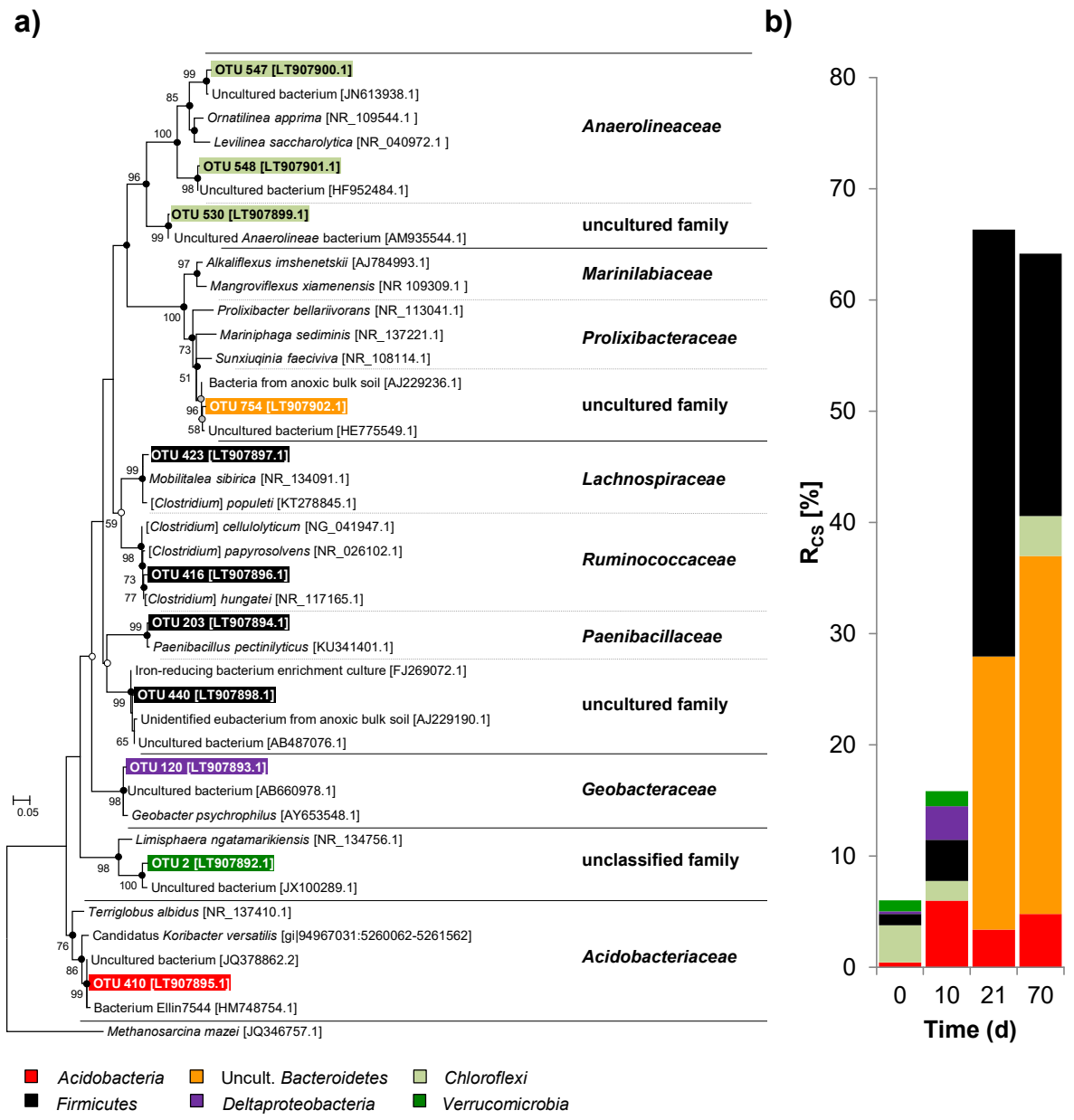

Figure 26. Phylogenetic tree of 16S rRNA cDNA sequences (a) and R_{CS} scores (b) from phylotypes labeled by assimilation of [^{13}C]-chitin derived carbon in soil slurries under anoxic conditions. a), the consensus tree was calculated with the maximum likelihood method and 1,000 bootstraps. Dots at nodes indicate confirmation of topology by neighbor-joining (white circles) and maximum parsimony (grey circles) algorithms. Black circles indicate confirmation by both algorithms. Accession numbers are given in brackets. Scale bar, 5% evolutionary distance. *Methanosarcina mazei* [JQ346757.1] was used as the out group. **b)**, R_{CS} scores are net relative abundances of labeled taxa, i.e. respective values from [^{12}C]-chitin incubations were subtracted in a comparative approach. At t_0, relative abundance values are presented. See material and methods for details on criteria for labeling and calculation of R_{CS} scores (2.7.4.).

3.2.2.3. Canonical correspondence analysis

The canonical correspondence analysis (CCA) is a multivariate direct ordination technique and the axes represent linear combinations of environmental parameters (Ramette 2007). It was used to extract major gradients among combinations of explanatory variables in a dataset, i.e. it was used to identify taxa and environmental factors that were linked with major differences between the different datasets tested. Therefore, the relative abundances of phyla were treated as environmental parameters as well and used to compile CCA plots within the PAST software (2.9.3.2.).

3.2.2.3.1. Impact of oxygen on the microbiome's composition

To study the effect of oxygen on the bacterial community structure, only relative abundances of [^{12}C]-treatments were analyzed by CCA (Fig. 27). The analysis revealed that the community structure shifted differentially depending on the presence and absence of oxygen. The heavy and light fractions of oxic (day 3, 10 and 72) and anoxic (day 21 and 72) treatments grouped distinctly separated from each other and from the day 0 samples. Heavy and light fractions of t_0 samples of oxic and anoxic treatments grouped together suggesting that the community structure was very similar at the start of incubation (Fig. 27). In addition, day 0 and day 10 samples of the anoxic treatment grouped together (Fig. 27).

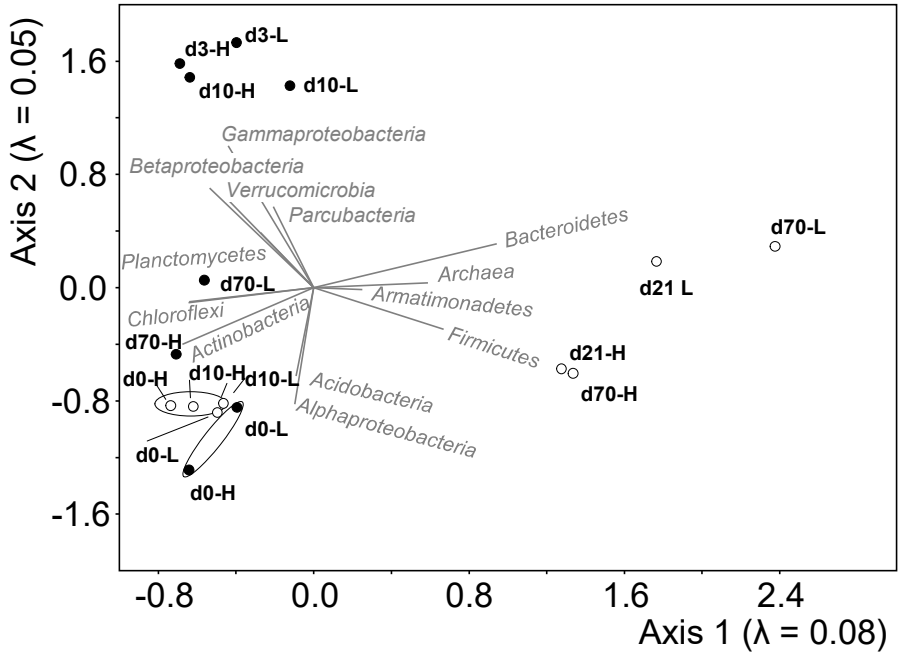

Figure 27. Canonical correspondence analysis (CCA) of the community composition in cDNA of heavy and light fractions of RNA SIP gradients from [^{12}C]-chitin-treated soil slurries under oxic and anoxic conditions. White-filled circles, anoxic conditions. Black-filled circles, oxic conditions. d, day. H, heavy fractions. L, light fractions.

3.2.2.3.2. Impact of [^{13}C]-chitin on the bacterial community structure

The community structures of [^{13}C] and [^{12}C] heavy and light fractions were compared via CCA. Under oxic conditions [^{13}C] heavy fractions were separated from each other and from [^{12}C] heavy and light fractions and [^{13}C] day 0 samples. The shift for of the community structure of day 3 heavy fractions was mainly caused by the phyla *Beta-* and *Gammaproteobacteria*, and *Bacteroidetes* (Fig. 28a). *Armatimonadetes* and *Bacteroidetes* were the main cause for the differential placement of the community structure of day 10 heavy fractions of the [^{13}C]-treatment (Fig. 28a). The differential placement of heavy fractions of day 70 was caused by *Deltaproteobacteria*, *Planctomycetes,* and *Verrucomicrobia* (Fig. 28a).

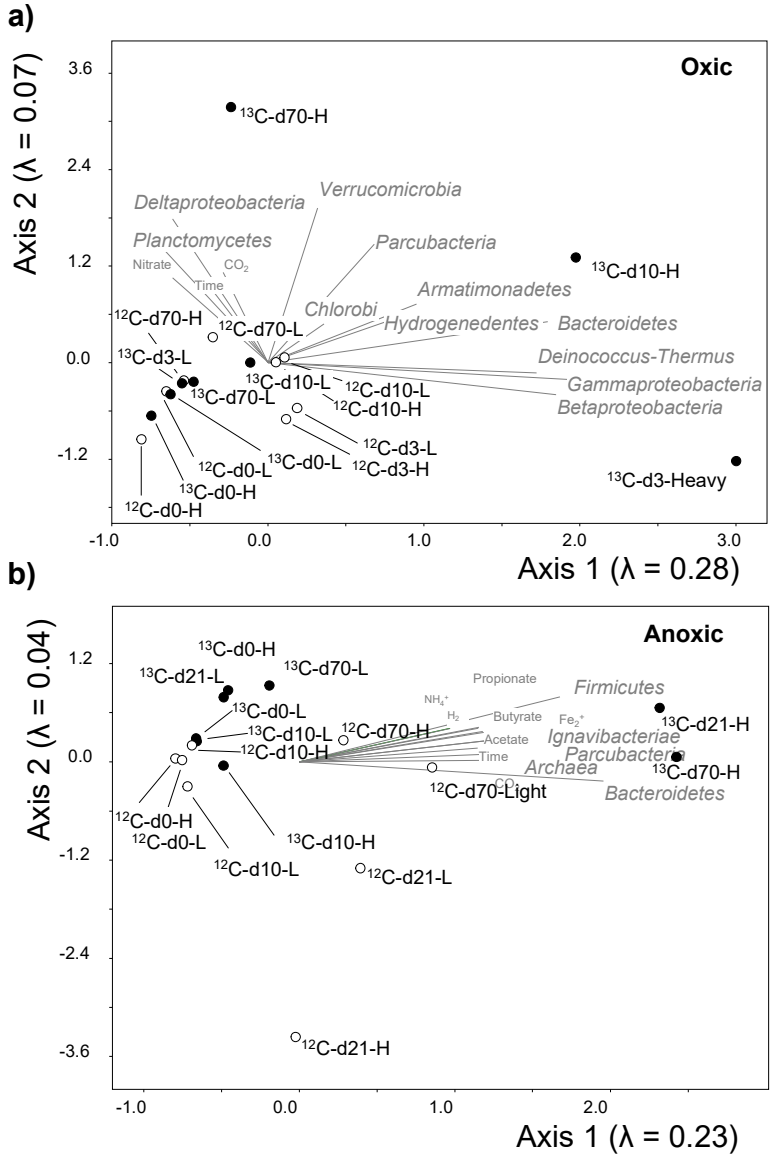

Figure 28. Canonical correspondence analysis (CCA) of the community composition in the cDNA retrieved from the heavy and light fractions of RNA SIP gradients from [^{13}C]- and [^{12}C]-chitin treated soil slurries under oxic and anoxic conditions. Black-filled circles, [^{13}C]-chitin treatment. White-filled circles, [^{12}C]-chitin treatment.

Under anoxic conditions, day 21 and day 70 community structures of heavy fractions of the [^{13}C]-treatment grouped distinctly from other community structures. The shifts were caused by *Archaea*, *Bacteroidetes*, *Firmicutes*, *Ignavibacteriae,* and *Parcubacteria* (Fig. 28b).

3.2.3. [^{13}C]-label in *chiA* transcripts

The detection of *chiA* transcripts was used as a specific marker for chitinolytic microorganisms as they encode mainly for bacterial GH18 chitinases (1.2.3.1.). *ChiA* transcripts were obtained from the SIP gradients for both experimental treatments. The most abundant phylotype in heavy and light fractions under both oxic and anoxic conditions was OTU 0, which is affiliated with *Betaproteobacteria* (Fig. 29). Transcripts affiliating with actinobacterial chitinases were mainly detected in the light fractions under oxic conditions at all time points. However, under anoxic conditions, transcripts of actinobacterial chitinases were only detected in the first time points (Fig. 30). A finding of note is the detection of *Planctomycetes*-like *chiA* transcripts under both conditions at the beginning, but their absence at later time points under anoxic conditions. The *Oxalobacteraceae*-affiliated phylotype OTU 4 likely became labeled under oxic conditions (at day 3), i.e. the relative abundance in the heavy fractions of the [^{13}C]-treatment was clearly higher than in the light fractions and compared to the corresponding [^{12}C]-treatment. However, it was not possible to calculate R_{CS} scores because of too high significance thresholds. Similar to that, OTU 6 likely became labeled (at day 21) under anoxic conditions and was most closely related to a *Treponema bryantii* (*Spirochaetes*) hypothetical protein. However, as *Spirochaetes* were not labeled on 16S rRNA level (3.2.2.2.), and all of next related sequences were affiliated with *Firmicutes*, OTU 6 was classified as a *Firmicutes*-like *chiA.*

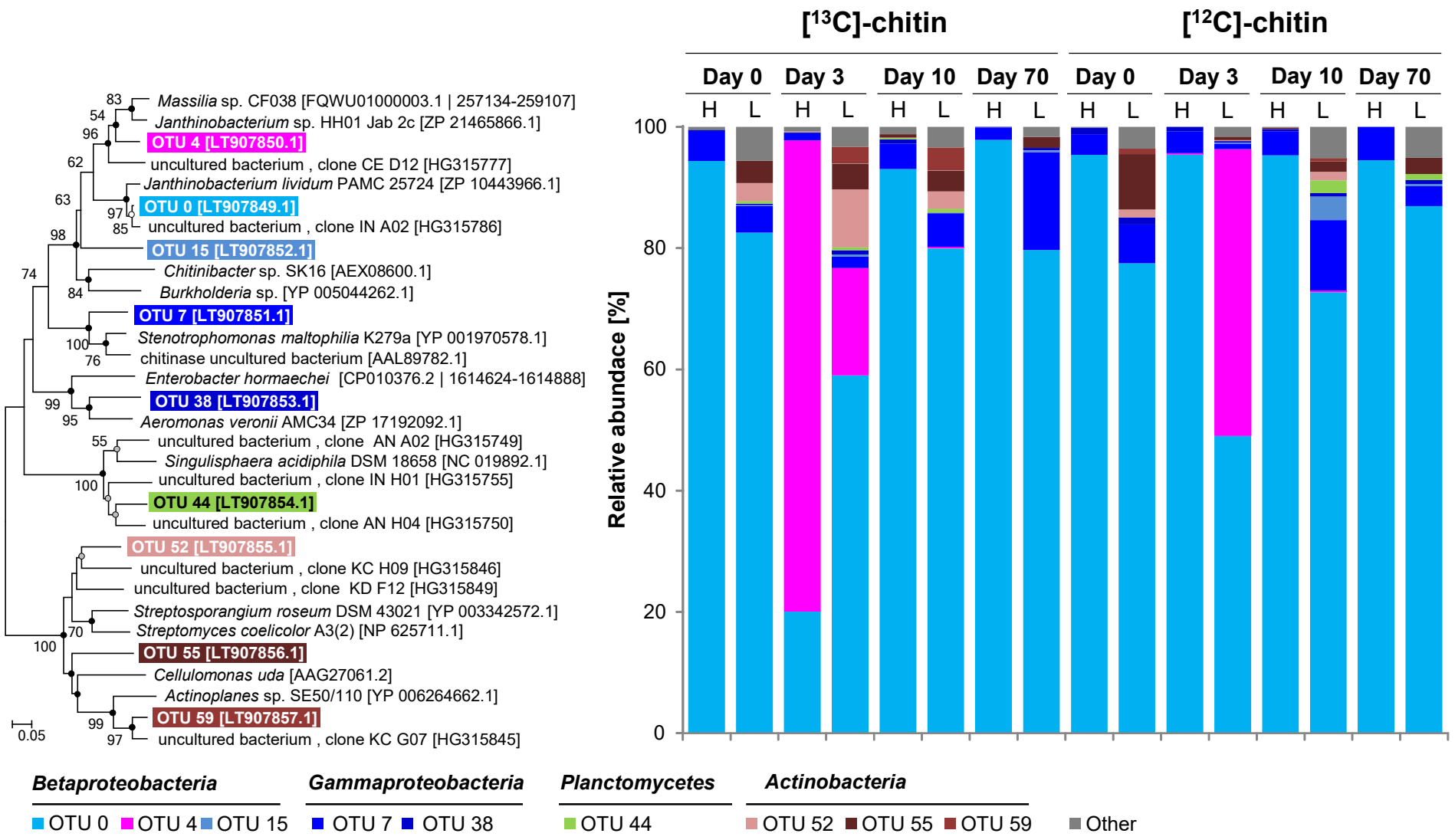

Figure 29. Phylogenetic tree and relative abundances of *chiA* OTUs in the heavy and light RNA of [^{13}C]- and [^{12}C]-chitin treatments under oxic conditions. *ChiA* gene libraries were prepared by Illumina-Amplicon sequencing of PCR-products from cDNA. Accession numbers are given in brackets. The tree was calculated using translated amino acid sequences with neighbor-joining algorithm (MEGA 6; Tamura *et al.*, 2013) including bootstrapping (1,000 replicates; percentage values at nodes). Open circles and gray filled circles at nodes, these nodes were confirmed by maximum likelihood and maximum parsimony algorithms, respectively, using the same data set. Black circles, confirmation by both algorithms. Scale bar, 5% sequence divergence.

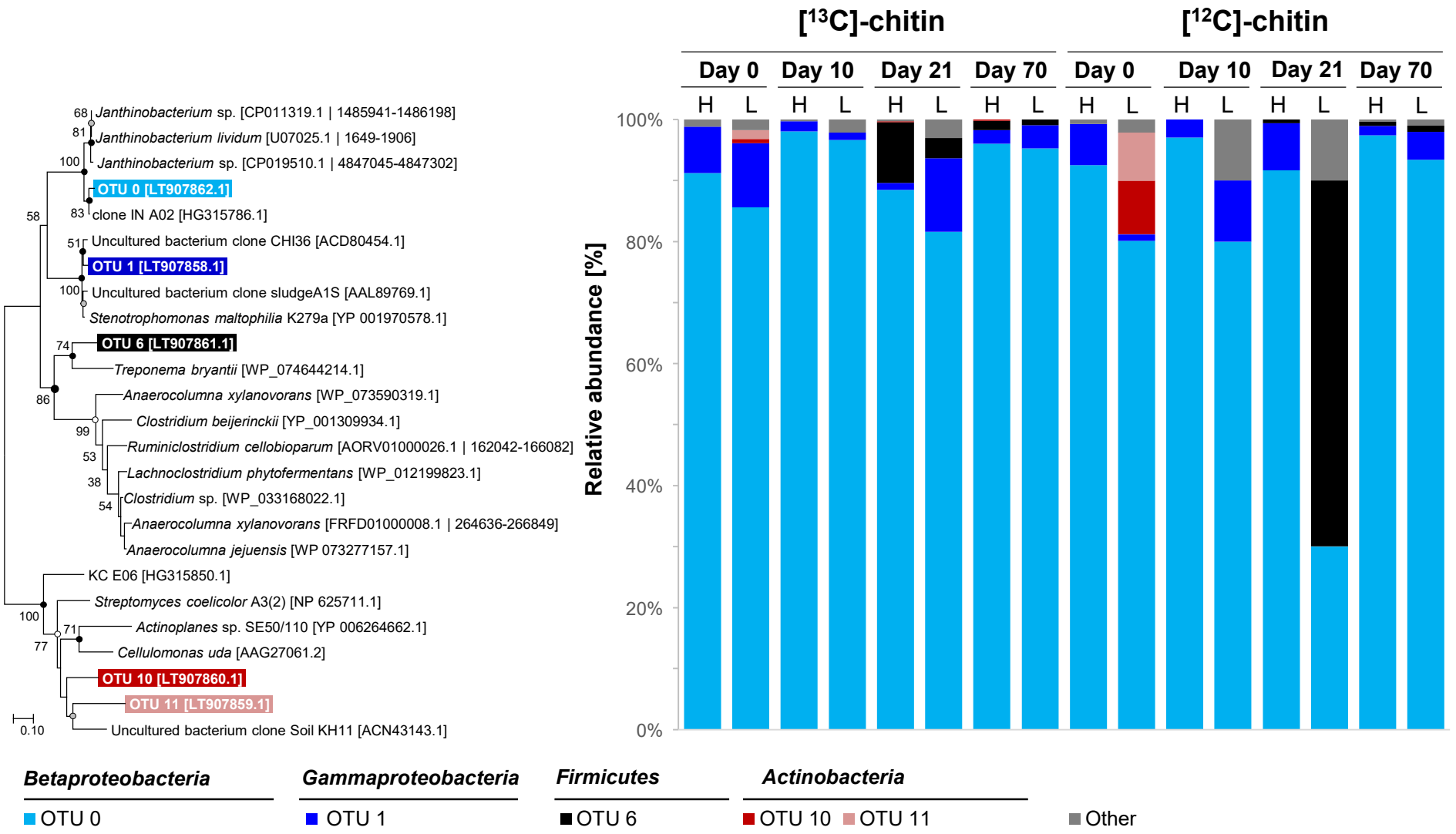

Figure 30. Phylogenetic tree and relative abundances of *chiA* OTUs in the heavy and light RNA of [^{13}C]- and [^{12}C]-chitin treatments under anoxic conditions. *ChiA* gene libraries were prepared by Illumina-Amplicon sequencing of PCR-products from cDNA. Accession numbers are given in brackets. The tree was calculated using translated amino acid sequences with neighbor-joining algorithm (MEGA 6; Tamura *et al*., 2013) including bootstrapping (1,000 replicates; percentage values at nodes). Open circles and gray filled circles at nodes, these nodes were confirmed by maximum likelihood and maximum parsimony algorithms, respectively, using the same data set. Black circles, confirmation by both algorithms. Scale bar, 10% sequence divergence.

3.2.4. Archaeal members of the soil microbiome

A [^{13}C]-labeling of *Archaea* was not detected, i.e., no PCR products were obtained from the cDNA of heavy fractions with taxon-specific primers. However, equimolarly pooled archaeal 16S rRNA transcript PCR products obtained from cDNA of light fractions from [^{13}C]-chitin [^{12}C]-chitin treatments were Illumina-sequenced (2.5.8.3., 2.7.2.). The archaeal community composition of the oxic and anoxic incubations was alike at the beginning of the incubation and did not significantly change over time. The taxon diversity was low on the phylum level, i.e., only *Thaumarchaeota* and *Crenarchaeota* were detected. Nonetheless, *Euryarchaeota* (methanogens) were slightly stimulated under anoxic conditions (Fig. 31).

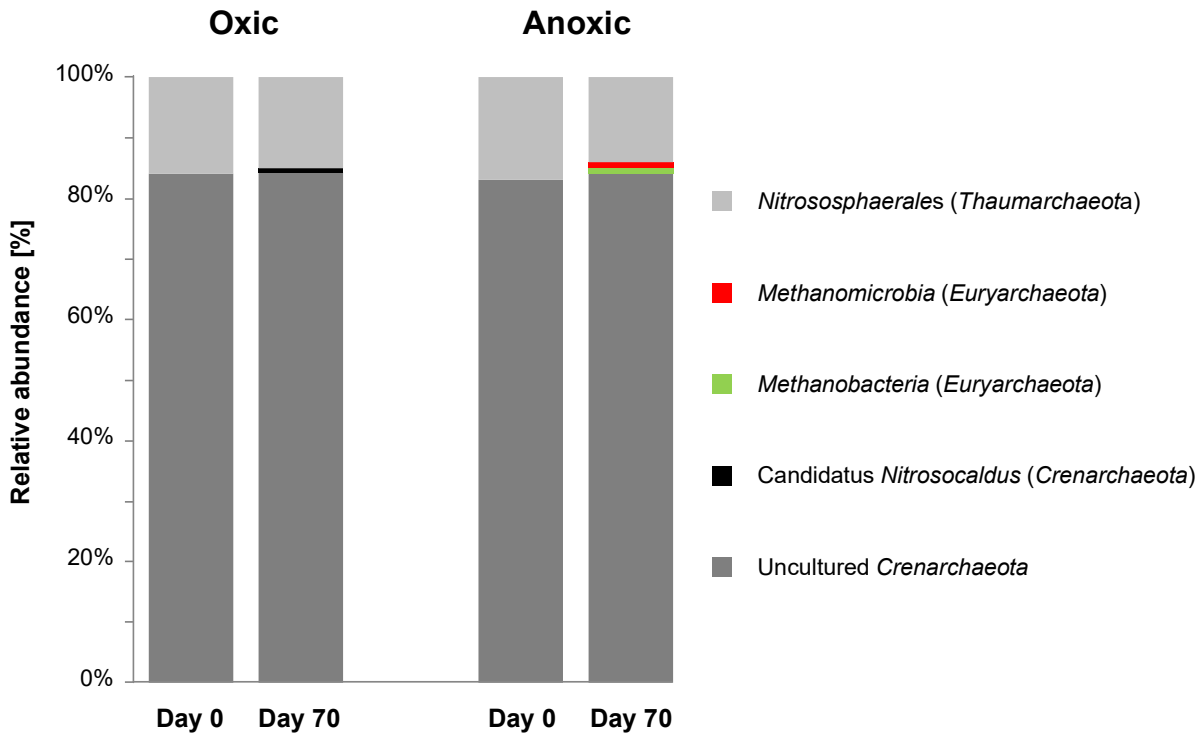

Figure 31. Detectable *Archaea* at day 0 and after 70 days of incubation under oxic and anoxic conditions. Libraries were prepared from pooled PCR products derived from light fractions of [^{13}C]- and [^{12}C]-chitin treatments.

3.2.5. *Eukaryota* of the soil microbiome

A [^{13}C]-labeling of *Eukaryota* was not detected, i.e., no PCR products were obtained from the cDNA of heavy fractions with taxon-specific primers. However, equimolarly pooled 18S rRNA transcript PCR products obtained from cDNA of light fractions from [^{13}C]-chitin [^{12}C]-chitin treatments were Illumina-sequenced (2.5.8.4., 2.7.2.). *Eukaryota* substantially responded in the experiment. While the percentages of *Fungi*, *Amoebozoa* and *Rhizaria* slightly decreased under oxic conditions over time, the percentage of *Alveolata* increased and was predominant after 70 days (65%) (Fig. 32). However, in the absence of oxygen, the fraction of *Alveolata* decreased from 36% to 18%, while those of *Rhizaria* and *Stramenopiles* increased from 5% to 14% and from 4% to 7%, respectively.

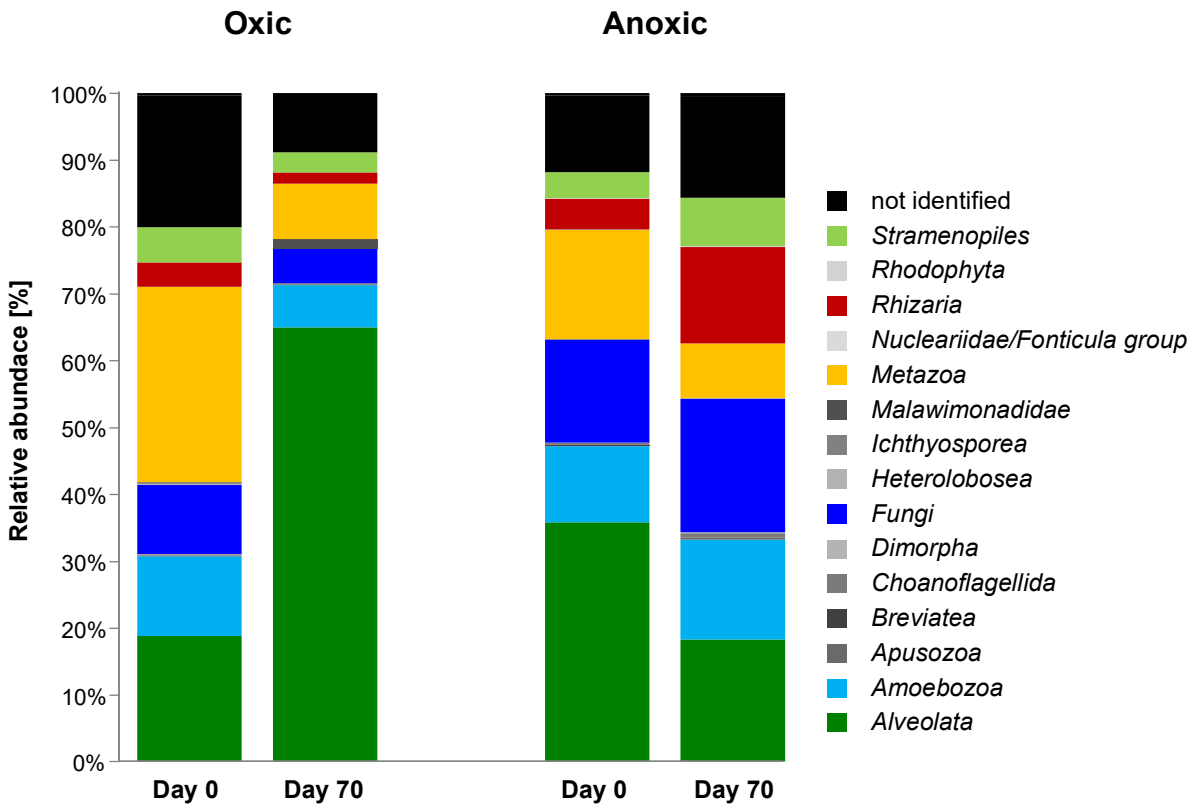

Figure 32. Detectable *Eukarya* at day 0 and after 70 days of incubation under oxic and anoxic conditions. Libraries were prepared from pooled PCR products derived from light fractions of [^{13}C]- and [^{12}C]-chitin treatments.

3.2.6. [^{13}C]-label in proteins

In total, 1,407 peptides affiliated with 557 protein groups were identified in the dataset. Of these, only a minor fraction (23 peptides) was [^{13}C]-labeled (Table 23). In both the oxic and anoxic treatment conditions, the peptides were highly labeled at the beginning of the incubations (days 10 and 14 anoxic; day 10 oxic) with a relative isotope abundance (RIA) of ^{13}C of approximately 95%. Most of the labeled peptides belonged to chaperone proteins for which the phylogenetic origin could not be resolved (Table 23). In the oxic treatments, the RIA values of all peptides at day 10 were high, with approximately 96 ± 2% abundance. At the end of the incubation (after 70 days), the RIA value decreased 20 ± 2%. Under oxic conditions, the peptides of the two chaperones affiliated with *Proteobacteria* were labeled to similar degrees after ten days. Under anoxic conditions, a RNA-binding protein that affiliated with *Optitutaceae* (*Verrucomicrobia*) was labeled after 10 days.

Table 23. List of identified [^{13}C]-labeled peptides. The functional classifications (descriptions) and the highest phylogenetic assignments are given. RIA = relative isotope abundance. Lr = labeling ratio.

						Phylogeny
	Peptide	Day	RIA	Lr	Function	highest taxonimic rank
Oxic	ARVEDALHATR	10	95.3	0.55567	60kDa Chaperonin	heterogenous kingdom
	DLLPILEQVAK	10	96.8	0.60367	60kDa Chaperonin	*Proteobacteria*
	EGVITVEDGK	10	96.1	0.79255	60kDa Chaperonin	heterogenous kingdom
	GYRPQFYFR	10	96.7	0.87281	Elongation factor	heterogenous kingdom
	LPANLIQAQR	10	96.3	0.77596	6PGD*	heterogenous kingdom
	TSDNAGDGTTTATVLAQAIVR	10	95.5	0.94325	60kDa Chaperonin	*Betaproteobacteria*
	TTCTGVEMFR	10	89.3	0.83213	elongation factor	heterogenous kingdom
	VEDALHATR	10	95.9	0.50387	60kDa Chaperonin	heterogenous kingdom
	VGAATEVEMKEK	10	96.9	0.76434	60kDa Chaperonin	heterogenous kingdom
	VGAATEVEMK	10	96.4	0.75088	60kDa Chaperonin	heterogenous kingdom
	AAVEEGIVPGGGVALIR	70	18.0	0.41726	60kDa Chaperonin	heterogenous kingdom
	ARVEDALHATR	70	22.4	0.40690	60 kDa chaperonin	heterogenous kingdom
	VEDALHATR	70	21.0	0.39212	60kDa Chaperonin	heterogenous kingdom
Anoxic	AAVEEGIVPGGGVALIR	10	97.4	0.06799	60kDa Chaperonin	heterogenous kingdom
	AGDNVGLLLR	10	94.8	0.22761	Elongation Factor	heterogenous kingdom
	ALTVNEARPK	10	97.1	0.89650	RNA-binding protein	*Opitutaceae (Bacteria)*
	ARVEDALHATR	10	94.8	0.50719	60 kDa chaperonin	heterogenous kingdom
	ARVEDALHATR	10	95.3	0.55567	60 kDa chaperonin	heterogenous kingdom
	VEDALHATR	10	96.2	0.46335	60 kDa chaperonin	heterogenous kingdom
	VGAATEVEMK	10	96.2	0.66830	60 kDa chaperonin	heterogenous kingdom
	AQIEETTSDYDREK	14	90.9	0.47418	60 kDa chaperonin	*Bacteria*
	TSLTAAITK	14	87.8	0.71561	Elongation Factor	heterogenous kingdom
	VGKDGVITVEESK	14	91.8	0.15427	60kDa Chaperonin	*Bacteria*

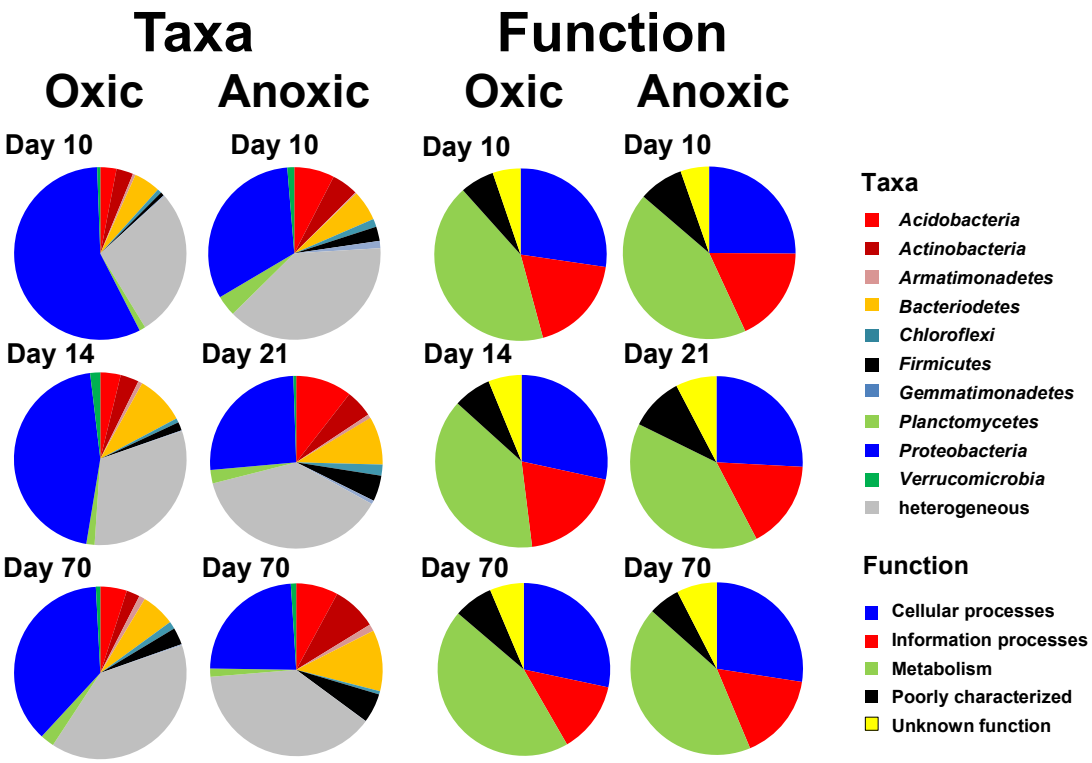

Figure 33. Phylogenetic and functional analysis of metaproteomes derived from chitin-degrading soil slurries. Proteins were assigned to their phylogenetic origin with PROPHANE (Schneider *et al*., 2011). Per metaproteome, an average of 557 peptides was analyzed.

Oxygen availability and time did not substantially alter the compositional patterns of the functional categories of the identified peptides (Fig. 33). However, differences in the phylogenetic affiliation of the identified peptides occurred (Fig. 33). At day 10, the fraction of peptides that were affiliated with *Proteobacteria* was 57% in the oxic but only 32% in the anoxic treatment, whereas the percentage of peptides with uncertain affiliation was higher under anoxic conditions. Moreover, the fraction of peptides affiliated with *Acidobacteria* and *Firmicutes* slightly increased over the incubation period in the anoxic treatment. The proportion of peptides of Proteobacteria decreased over time under both conditions. However, this effect was more pronounced in the oxic treatments. It is noteworthy that the fraction of peptides affiliated with *Acidobacteria*, *Bacteroidetes*, and *Firmicutes* increased over time in the treatment without oxygen.

3.3. Comparison of taxa labeled with [^{13}C]-chitin and [^{13}C]-cellulose

In a previous study, bacterial taxa were identified by means of RNA-SIP that assimilated carbon from [^{13}C]-cellulose in the same soil as used in this study (Schellenberger *et al.*, 2010). Therefore, bacterial taxa labeled in this study by [^{13}C]-chitin derived carbon were compared with taxa labeled by [^{13}C]-cellulose (Fig. 34). Bacterial taxa that were labeled with carbon from both substrates were within the same family or genus (Fig. 35, 36).

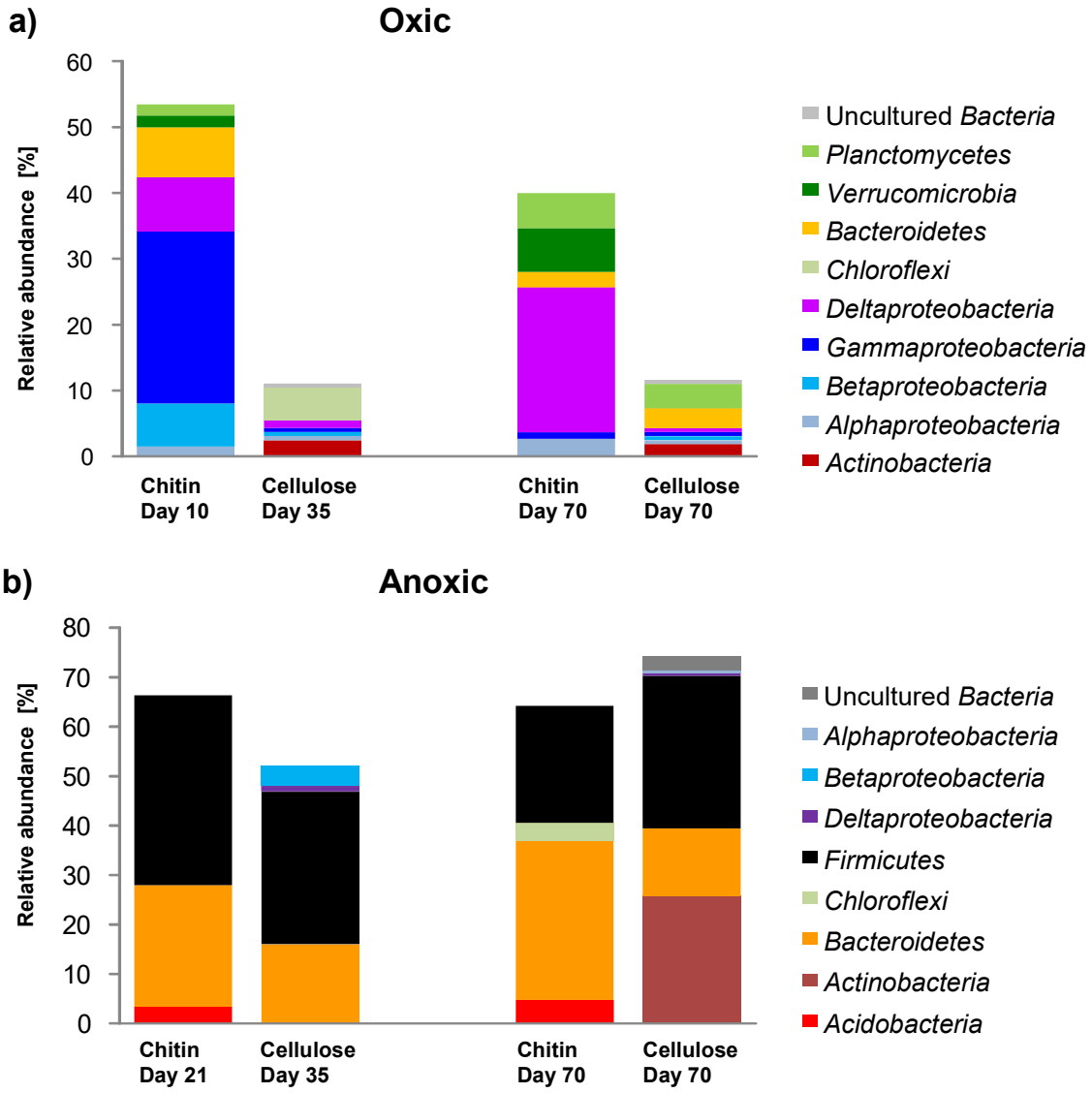

Figure 34. Relative abundances of active taxa that assimilated carbon from [^{13}C]-chitin or [^{13}C]-cellulose in the same agricultural soil. Note that data were obtained by different methods. Chitin data are R_{CS} scores obtained by amplicon pyrosequencing (2.7.4.) and are already depicted in Figs. 25, 26. Data for cellulose are relative abundances of labeled phylotypes obtained from 16S rRNA cDNA gene libraries from heavy fractions of [^{13}C]-incubations (cellulose data from Schellenberger *et al.*, 2010).

3.3.1. Comparison of taxa labeled by [^{13}C]-chitin and [^{13}C]-cellulose under oxic conditions.

The relative abundances of phyla labeled by [^{13}C]-chitin and [^{13}C]-cellulose derived carbon were compared, 10 and 35 days after the start of the incubation respectively (Fig. 34). Apparent differences were that *Planctomycetes*, *Verrucomicrobia,* and *Bacteroidetes* were exclusively labeled by [^{13}C]-chitin whereas *Actinobacteria*, *Chloroflexi,* and uncultured *Bacteria* were only labeled by [^{13}C]-cellulose. *Alpha*-, *Beta*-, *Gamma*-, and *Deltaproteobacteria* were labeled by both substrates but relative abundances of the labeled taxa differed considerably (Fig. 34). At day 70, however, also *Bacteroidetes* and *Planctomycetes* were labeled in the cellulose treatment with 3.1% and 3.7% relative abundance, respectively. Phylogenetic analysis revealed that most OTUs labeled by both substrates affiliated with the same families but were not identical on genus or species level (Fig. 34). The only exception was labeled *Betaproteobacteria,* since in this specific case, the same genus was labeled (Fig. 34).

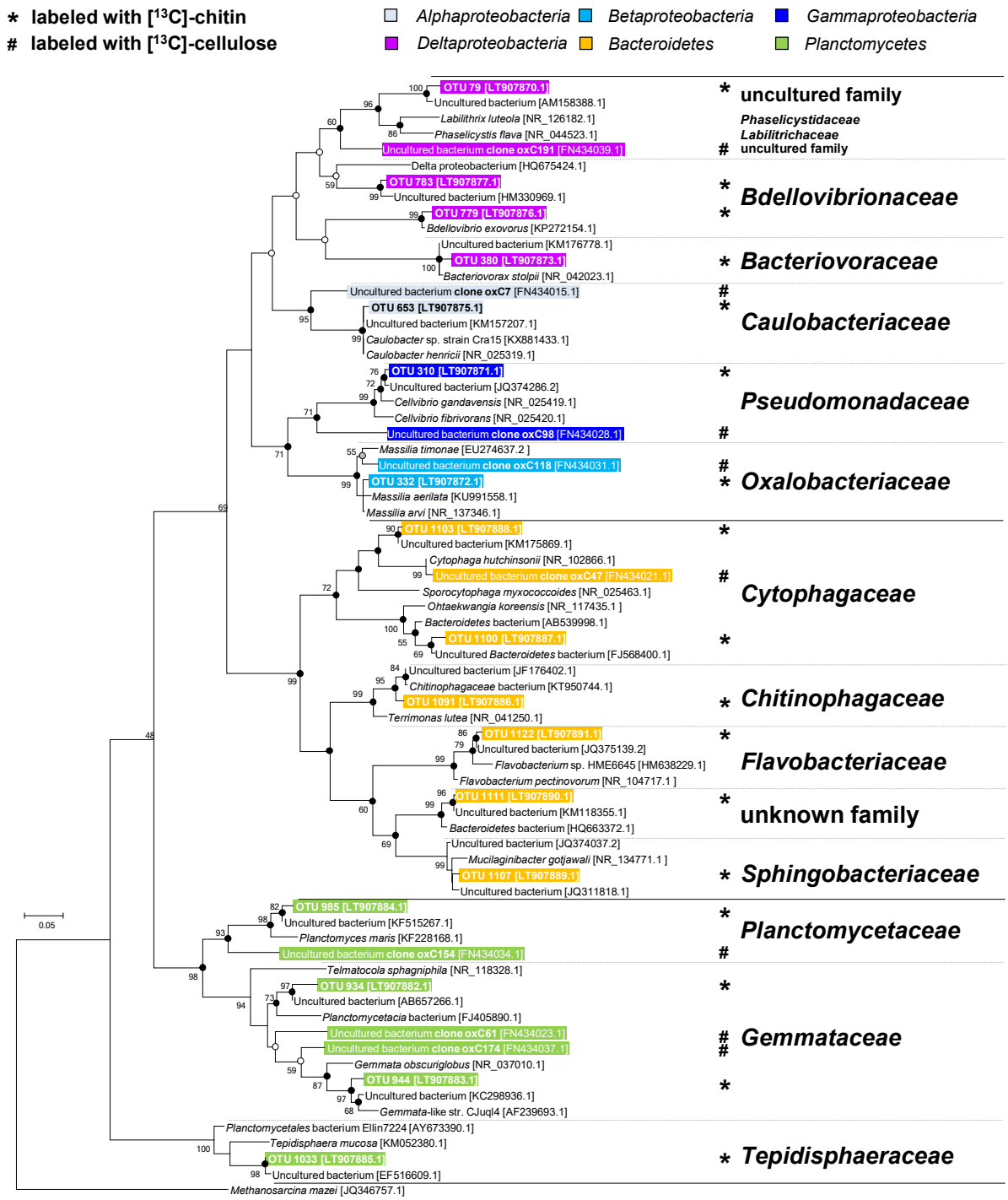

Figure 35. Phylogenetic tree of 16S rRNA cDNA sequences (bold) from taxa labeled by assimilation of [^{13}C]-chitin derived carbon (star; this study) and by assimilation of [^{13}C]-cellulose derived carbon (hashtag; Schellenberger *et al.*, 2010) in soil slurries under oxic conditions from the same agricultural soil. The consensus tree was calculated with the maximum likelihood method and 1,000 bootstraps. Dots at nodes indicate confirmation of topology by neighbor-joining (white circles) and maximum parsimony (grey circles) algorithms. Black circles indicate confirmation by both algorithms. Accession numbers are given in brackets. Scale bar, 5% sequence divergence. *Methanosarcina mazei* [JQ346757.1] was used as the out group.

3.3.2. Comparison of taxa labeled by [^{13}C]-chitin and [^{13}C]-cellulose under anoxic conditions.

In contrast to oxic conditions, relative abundances of taxa labeled by both substrates were in a comparable range and showed high similarity on sequence level (Fig. 34, 36). Apparent differences were that *Acidobacteria* were exclusively labeled by [^{13}C]-chitin-derived carbon whereas *Beta-* and *Deltaproteobacteria* were only labeled by [^{13}C]-cellulose-derived carbon.

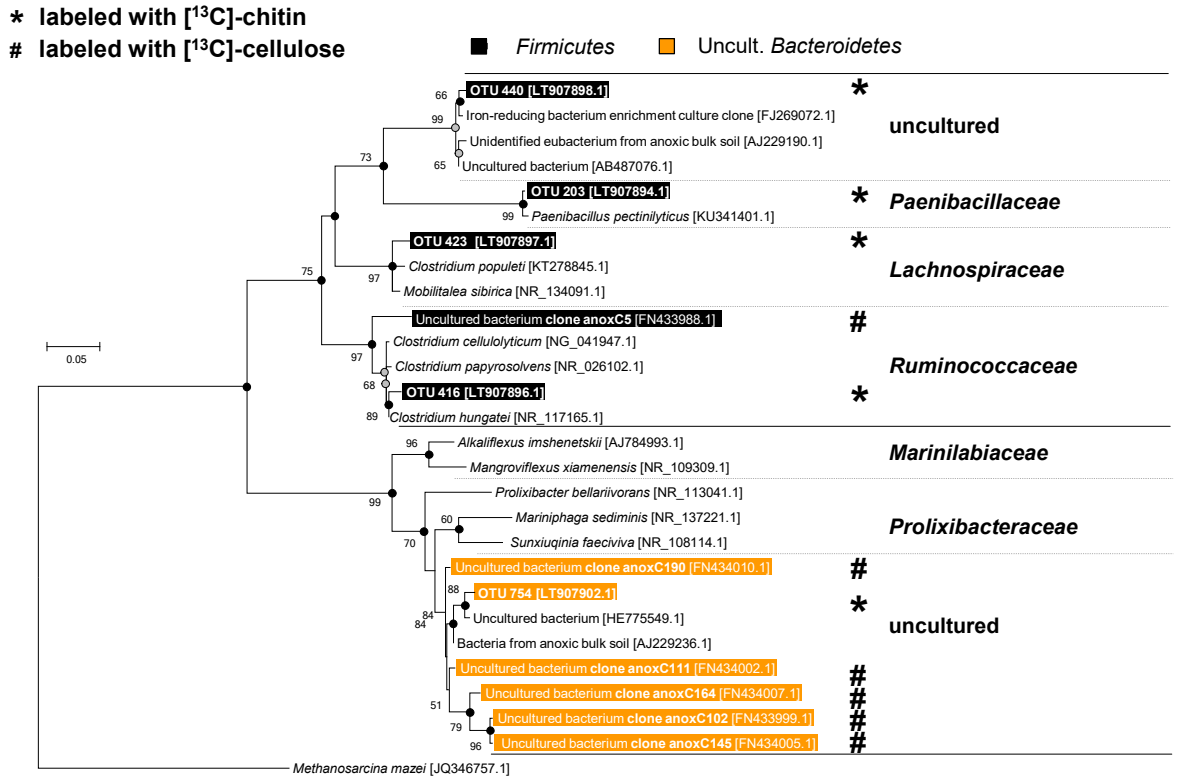

Figure 36. Phylogenetic tree of 16S rRNA cDNA sequences (bold) from taxa labeled by assimilation of [^{13}C]-chitin derived carbon (star; this study) and by assimilation of [^{13}C]-cellulose derived carbon (hashtag; Schellenberger *et al.*, 2010) in soil slurries under anoxic conditions from the same agricultural soil. The consensus tree was calculated with the maximum likelihood method and based on 1,000 bootstrapped datasets. Dots at nodes indicate confirmation of topology by neighbor-joining (white circles) and maximum parsimony (grey circles) algorithms. Black circles indicate confirmation by both algorithms. Accession numbers are given in brackets. Scale bar, 5% sequence divergence. *Methanosarcina mazei* [JQ346757.1] was used as the out group.

4. Discussion

4.1. Route of chitin degradation in an aerated agricultural soil

4.1.1. Degradation of chitin and chitosan under oxic and anoxic conditions

Under oxic conditions, chitin was degraded and stimulated microbial activity without apparent delay (Fig. 11; 3.1.1.). Carbon dioxide was the sole detected carbonaceous product. The mineralization of chitin to carbon dioxide under oxic conditions is in line with the few existing studies analyzing the degradation of chitin in aerated soil under *in situ* conditions (Anderson & Domsch 1973; Howard & Howard 1993). The increasing nitrate concentrations under oxic conditions were likely caused by nitrification of the observed release of ammonium from the amine group of the amino sugars monomers GlcNAc and GlcN (Erguder *et al*., 2009; Kowalchuk & Stephen 2001; Schulten & Schnitzer 1997). Nitrogen from chitin was not fully utilized and 17% were recovered as ammonium and nitrate in the oxic treatments (Fig. 11; 3.1.1.). Likely, nitrogen was not limiting in the investigated agricultural soil as the initial nitrate concentrations were high (Fig. 11; 3.1.1.).

Anaerobic degradation of chitin was slower compared to the aerobic degradation. Only after three weeks of incubation microbial activity was stimulated (Fig. 13; 3.1.2.). The overall lower degradation rate of amino sugars under anoxic conditions (Fig. 14, 15; 3.1.3., 3.1.4.) is in line with this finding and might partially explain the lower rate of chitin degradation under anoxic conditions. $[GlcNAc]_2$ and GlcNAc (potential products of chitin hydrolysis) were not detected suggesting an efficient consumption leading to low steady state concentrations below the detection limit (i.e., < 30 µM). The hydrolysis products were consumed by the chitinolytic and likely also saccharolytic (‘satellite’) bacteria that were active in the investigated soil. Decreasing nitrate concentrations (Fig. 13; 3.1.2.) and increasing concentrations of ferrous iron (3.1.2.) indicate that nitrate and ferric iron respiring taxa were active, respectively (Kraft *et al*., 2011; Weber *et al*., 2006). As soon as the concentration of nitrate and ferrous iron was too low fermentative chitinolytic and saccharolytic taxa became active or switched to fermentation producing acetate, butyrate, propionate, molecular hydrogen and carbon dioxide (Fig. 13; 3.1.2.). Production of these fermentation products suggests that a mix of fermentation types was active, including mixed, propionic and butyric acid fermentations (Buckel 2005; Gottschalk 1986; Reichardt *et al*., 2014; White 2007; Zidwick *et al*., 2013).

Propionate and butyrate accumulated in the long-term experiment but not in the short-term experiments with $[GlcNAc]_2$, GlcNAc, and GlcN (3.1.2.; 3.1.4.) likely because of the considerable longer incubation time and the higher substrate input. The high substrate input likely favored a decoupling of the sequential reactions during the anaerobic degradation of

chitin. In addition, it is noteworthy that acetate might have been additionally produced by acetogenesis and/or syntrophic fermentation (Drake *et al*., 2009; Wagner *et al*., 1996). However, the stoichiometry of the products and the high molecular hydrogen concentrations indicated that it was unlikely that syntrophic interactions were prevailing (Wagner *et al*., 1996). The detected products and microbial processes during the aerobic and anaerobic degradation of chitin largely resemble the ones detected during aerobic and anaerobic degradation of cellulose in the same agricultural soil (Schellenberger *et al*., 2010).

The results from chitosan-supplemented soil slurries indicated that chitosan was, at least under oxic conditions, degradable in the investigated agricultural soil (3.1.1.). However, the long delay indicated that the microbiome in the sampled soil was not prone to utilize this substrate.

4.1.2. *ChiA* phylotypes responding to chitin

The investigated agricultural soil harbored a broad diversity of potentially chitinolytic microorganisms as measured by the detection of *chiA* phylotypes (Fig. 16, 17; 3.1.5.). However, few of the detected *chiA* phylotypes responded to the supplementation of chitin under experimental conditions (Fig. 17; 3.1.5.). Affiliated taxa responding to chitin were *Betaproteobacteria* (OTU 2; TRFs 114bp and 264bp), *Gammaproteobacteria* (OTU 19; TRF 188bp), *Planctomycetes* (OTU 1, 34; TRF 54bp), and a novel *chiA* phylotype (OTU 3; TRF 188bp) (Fig. 17, 19; 3.1.5., 3.1.6.). TRFs 114bp (*Betaproteobacteria*) and 54bp (*Planctomycetes*) likely represented aerobic microorganisms as they were detected in oxic treatments, whereas TRF 188bp (novel *chiA* phylotype with unknown affiliation) likely represented obligate anaerobic (or potentially, facultative aerobic) microorganisms. TRF 264bp was detected under both oxygen conditions. Thus, it likely was a facultative aerobic chitinolytic microorganism. OTU 3 showed 5-44% amino acid dissimilarity to the most similar sequences, which were two environmental sequences from a previous study on Antarctic lake sediments (clones L5-24, L11-50; Xiao *et al*., 2005). In the aforementioned study, the closest sequence relatives from isolates were endochitinases from *Bacillus* species (53% dissimilarity; Xiao *et al*., 2005). *Bacillus cereus* and *Bacillus thuringiensis* are facultative aerobes and can ferment carbohydrates in the absence of exogenous electron acceptors (Logan & De Vos 2009). Thus, there is no conflict between its detection in this and the aforementioned study, since the sediments investigated by Xiao and coauthors were most likely anoxic (no information on that was stated). Furthermore, the data presented in this doctoral thesis suggest that OTU 3 likely represented previously unknown anaerobic chitinolytic *Bacteria*. The *chiA* OTU 1 was stimulated under oxic conditions and affiliated with *Singulisphaera acidiphila*. To date, *Planctomycetes* are not known to be chitinolytic (Ivanova & Dedysh 2012). *Planctomycetes* (including *Singulisphaera acidiphila*) can utilize the chitin

hydrolysis product GlcNAc as sole carbon and energy source (Fuerst *et al*., 1997; Rabus *et al*., 2002; Schlesner 1994). However, the detection of *chiA* in the genome of *S. acidiphila* suggests that *S. acidiphil*a might hydrolyze chitin (Guo *et al*., 2012; Kulichevskaya *et al*., 2008). In agreement with the assumption that *Planctomycetes* are capable of polysaccharide degradation is the [^{13}C]-labeling of ribosomal RNA of *Planctomycetes* in [^{13}C]-cellulose-supplemented oxic soil slurries of the same agricultural soil (Schellenberger *et al*., 2010).

ChiA phylotypes affiliating with *Beta-* and *Gammaproteobacteria* were abundant (Fig. 17, 19; 3.1.5., 3.1.6.) and responded positively to chitin supplementation under oxic and anoxic conditions (Fig. 17; 3.1.5.). In agreement with this finding, *Beta- and Gammaproteobacteria* were also rapidly stimulated by the supplementation of chitin to agricultural soil in a previous field experiment (Kielak *et al*., 2013). In another field study, the supplementation of chitin led to increased abundances of *Actinobacteria* and *Oxalobacteraceae* (*Betaproteobacteria*) (Cretoiu *et al*., 2013). It seems that the experimental conditions, i.e. soil slurries vs. field conditions, affect which taxa are stimulated by chitin supplementation. In addition, the agricultural field from which samples were obtained for this project differed compared to the field from aforementioned studies in grown plant species, soil type, crop rotation and soil treatment, which are important factors shaping the structure and function of root and soil microbiomes (Berg & Smalla 2009; Bulgarelli *et al*., 2013; Lareen *et al*., 2016; Philippot *et al*., 2013). The responding *Betaproteobacteria*-like *chiA* phylotypes (Fig. 17; 3.1.5.) had high similarities (66% to 94%) with ChiA sequences of two species of *Oxalobacteraceae*, i.e. *Janthinobacterium lividum* PAMC 25724 (ZP 10443966.1) and *Janthinobacterium* sp. HH01 Jab 2c (ZP 21465866.1) (Fig. 19; 3.1.6.). Considering the results of Kielak *et al*. (2013) the findings here indicate a crucial role of *Oxalobacteraceae* in the degradation of chitin in agricultural soil.

4.1.3. *ChiA* phylotypes responding to chitosan supplementation

Various *chiA* TRFs positively responded to chitosan supplementation under oxic conditions (3.1.5.), although chitosan was apparently not degraded under oxic and anoxic conditions in the course of the incubation (3.1.1., 4.1.1.). Therefore, it is unlikely that stimulation of the TRFs was caused by degradation of chitosan and utilization of the emerging hydrolysis products. An explanation for the stimulation of the TRFs might be that chitosan promoted growth of *chiA* harboring *Bacteria* by an unknown mechanism and that these *Bacteria* utilized substrates other than chitosan and outcompeted those that were active in the absence of chitosan. However, alternative explanations based on the physiochemical properties of chitosan are conceivable. First, chitosan is well known for its antimicrobial properties (Goy *et al*., 2009; Kong *et al*., 2010; Pillai *et al*., 2009; Raafat *et al*., 2008; Raafat & Sahl 2009;

Rabea *et al*., 2003). Antimicrobial activity might have affected the microbial structure resulting in the altered *chiA* TRF pattern oxic conditions (Fig. 17; 3.1.5.). Thereby, the antimicrobial activity of chitosan likely relies on more than one mechanism (Raafat *et al*., 2008; Raafat & Sahl 2009) due to complex chemical interactions that are possible. However, microbial respiration as measured by the release of carbon dioxide apparently was unaffected by chitosan supplementation (Fig. 11; 3.1.1.). The second alternative explanation is based on the well-known capacity of cationic chitosan to form complexes with anionic DNA (Amaduzzi *et al*., 2014; Il'ina & Varlamov 2005; Jayakumar *et al*., 2010a,b). During the extraction of nucleic acids from the soil slurry samples, cationic chitosan to some extent might have formed complexes with DNA, i.e. after cell disruption by beat beating, so chitosan and DNA theoretically can reside in the same matrix. The formation of chitosan conjugates together with genomic DNA artificially might have shifted the microbial community structure. The ratio of extracted DNA from samples without to samples with supplemented chitin was 0.5 ± 0.2 while the ratio from samples without to samples with supplemented chitosan was 6.6 ± 5.3. Thus, chitosan apparently had a negative effect on the DNA extraction yield indicating that formation of chitosan-DNA conjugates during extraction of nucleic acids indeed might have been an issue. Further experiments are required to resolve this issue.

4.1.4. *ChiA* phylotypes not responding to chitin supplementation

48% of the detected *chiA* phylotypes that did not respond to chitin supplementation were distantly related (≤ 60% protein sequence similarity) to known *chiA* phylotypes of cultivated chitinolytic bacteria. Therefore, the phylogeny of the taxa harboring the detected *chiA* phylotypes remains elusive. 52% of the not-responding *chiA* phylotypes affiliated with *Actinobacteria*, *Bacteroidetes*, *Gammaproteobacteria*, *Firmicutes*, *Acidobacteria*, *Chloroflexi*, and eukaryotes.

Bacteroidetes, *Firmicutes*, and *Actinobacteria* are known to harbor chitinolytic members, whereby *Actinobacteria* are often regarded as the most important chitin degraders in aerated soils (Gooday 1990a,b; Krsek & Wellington 2001; Metcalfe *et al*., 2002; Williamson *et al*., 2000). The lack of response of *chiA* TRFs of other well-known chitinolytic soil bacteria such as *Actinobacteria* is intriguing. In general, the applied experimental conditions, i.e. soils slurries (liquid) that were permanently shaken, might have affect those taxa. However, the lack of response of *Actinobacteria* on the *chiA* level might be reflection of a 'cheater' acquisition strategy as suggested in a study by Beier & Bertilsson (2011). Therein, *Actinobacteria* rather rely on the uptake of chitin hydrolysis products without expressing their own chitin degradation machinery (Beier & Bertilsson 2011). This 'cheater' acquisition strategy can also be referred to as a saccharolytic lifestyle of 'satellite' microbes (Fig. 5; 1.3.)

and it needs to be evaluated if the lack of response was due to this strategy. Speaking against this, *Actinobacteria* were active and actinobacterial *chiA* transcripts detectable, however, *Actinobacteria* were not labeled by [^{13}C]-chitin derived carbon under oxic or anoxic conditions (4.2.). The detection of *Acidobacteria*-like *chiA* phylotypes is interesting, as in contrast to aforementioned phyla, *Acidobacteria* are not well known for chitin degradation. First evidence came with the comparative genome analyses of three acidobacterial strains (Ward *et al*., 2009). With isolation of *Blastocatella fastidiosa*, the first chitinolytic acidobacterial strain has been discovered (Foesel *et al*., 2013). The detected *chiA* phylotypes indicate that *Acidobacteria* are so far overlooked in the degradation of chitin in soils.

4.1.5. Route of chitin degradation

Theoretically, two major degradation pathways for chitin exist. It can be deacetylated to chitosan followed by subsequent degradation or can be hydrolyzed to *N*,*N´*-diacetylchitobiose and oligomers of *N*-acetylglucosamine by aerobic and anaerobic microorganisms (Fig. 3; Beier & Bertilsson 2013; Gooday 1990a,b). Which pathway of chitin hydrolysis is preferred by soil microbial communities is unknown and was studied by oxic and anoxic soil slurries supplemented with chitin and chitosan (3.1.1.; 3.1.2.) as not much is known about chitosan degradation in soils. So far, only two studies have investigated the degradation of chitosan in soils (Sato *et al*., 2010; Sawaguchi *et al*., 2015). Sato and coauthors (2010) reported that degradation of chitin and chitosan flakes was slow. A substantial loss of flakes mass was observed after 50 and 180 days, respectively (Sato *et al*., 2010). In the study by Sawaguchi *et al*., 2015 supplemented chitosan was degraded in silt soil within 38 days. Here, chitin was rapidly degraded, while chitosan degradation was substantially delayed similar to results obtained here (3.1.1.; 3.1.2.). A possible explanation for the faster response to chitin as compared to the observations by Sato *el al*. (2010) might be the higher physical accessibility of the ground chitin used here in the doctoral project.

Chitin was readily degraded under oxic conditions and was, with an apparent delay, also degraded under anoxic conditions (3.1.1.; 3.1.2.). Chitosan was not subject to degradation in the same period of time, neither under oxic conditions nor under anoxic conditions. However, after 156 days the carbon dioxide concentration was threefold higher in chitosan supplemented soil slurries, indicating that chitosan was partially degraded, albeit with a long delay. This finding suggests that microorganisms in the sampled soil were not adapted to this substrate. In addition, this finding implies that the degradation of chitin in the soil tested does not occur via deacetylation to chitosan followed by subsequent degradation as the soil microbiome degrading chitin via this pathway should be adapted to chitosan as a substrate

and therefore be able to degrade it without considerable delay. This finding is not unexpected as chitosan compared to chitin is less abundant in soil. For example, chitosan is only found in *Zygomycetes*, whereas with few exceptions chitin occurs ubiquitously in fungi (Gooday, 1990a; Raafat *et al*., 2008). The delayed product formation in GlcN-supplemented slurries (i.e., a potential product of chitosan hydrolysis) compared to slurries that were supplemented with potential chitin hydrolysis products $[GlcNAc]_2$ and GlcNAc (3.1.3.; 3.1.4.) is an additional endorsement of the assumption that the soil microbiome was prone to utilize chitin as substrate but not chitosan. The relevance of deacetylation and subsequent chitosan hydrolysis for soil microbiomes has not experimentally been addressed in previous studies. The experimental data presented here suggest that chitin degradation without prior deacetylation was the preferential pathway of chitin breakdown.

Interestingly, Sawaguchi and coauthors (Sawaguchi *et al*., 2015) speculate about a link between the degradation of chitosan in a silty soil and the activity and increased abundance of *Actinobacteria*. The abundance of *Actinobacteria* belonging to genera *Streptomyces* and *Kitasatospora* increased within four days after the addition of chitosan in the aforementioned study. Both genera are known to harbor chitosan degraders (Sawaguchi *et al*., 2015). Thus, it cannot be excluded that the substantial delay of beginning of the degradation of chitosan found was caused by the lack of response of *Actinobacteria* (3.1.5., 3.1.6.), which in turn might have been caused by the applied experimental conditions (soil slurries, i.e., liquid phase and permanent shaking).

4.2. Tracking the carbon flow through the soil microbiome from chitin under oxic and anoxic conditions

A time-resolved comparative amplicon pyrosequencing-based SIP experiment (3.2.) using fully labeled [^{13}C]-chitin was conducted in order to analyze microbiome-driven processes during chitin degradation and to link this information with microbial taxa through incorporation of chitin-derived ^{13}C in 16S rRNA.

4.2.1. Aerobic chitin degradation

Under oxic conditions, [^{13}C]-chitin and [^{12}C]-chitin were mineralized to carbon dioxide (3.2.1.1.). The observed product pattern largely resembled the product pattern measured in the chitin/chitosan experiment (3.1.1.). In contrast to the previous measurements a release of ammonium from chitin could not be detected (3.2.1.1.; Wieczorek *et al*., 2014). Because of the apparent consumption of nitrate in the first and second phase of chitin degradation (3.2.1.1.) it is likely that chitin stimulated growth of chitinoclastic members of the soil microbiome which was accompanied by a high nitrogen requirement. In accordance with that, 63% of the chitin-derived carbon was recovered as carbon dioxide and the unrecovered rest likely was used for biomass formation and microbial residues (Gooday 1990b). The mineralization of chitin to carbon dioxide under oxic conditions is in line with previous studies analyzing the degradation of chitin in an aerated soil under *in situ* conditions (Anderson & Domsch 1973; Howard & Howard 1993) and also with the degradation of cellulose in the same agricultural soil (Schellenberger *et al*., 2010). In their study, Fernandez and Koide (Fernandez & Koide 2012) determined chitin concentrations of ectomycorrhizal fungal tissues over the course of their decomposition after burial in a forest soil. In line with the results presented in my doctoral thesis, they observed a rapid decomposition of chitin and concluded that chitin is not as recalcitrant as it is sometimes believed to be (Godbold *et al*., 2006; Langley *et al*., 2006).

4.2.1.1. Initial aerobic chitin degraders

In the first phase of aerobic degradation, *Oxalobacteraceae* (*Betaproteobacteria*) and *Pseudomonadaceae* (*Gammaproteobacteria*) quickly assimilated [^{13}C]-chitin derived carbon to become the dominantly labeled taxa (Fig. 25; 3.2.2.1.). These taxa remained the major labeled taxa also in the second phase of chitin degradation during which the largest part of chitin apparently was degraded and during which the microbial activity peaked (Fig. 25; 3.2.2.1.). In agreement with this finding, two of the identified labeled peptides were affiliated with *Proteobacteria* (Table 23; 3.2.6.) and beta- and gammaproteobacterial *chiA* phylotypes were stimulated by chitin supplementation in the previous experiment (Fig. 16, 19; 3.1.5., 3.1.6.). Furthermore, *Beta*- and *Gammaproteobacteria* also responded positively on *chiA* gene level (Kielak *et al*., 2013) and on 16S rRNA gene level (*Oxalobacteraceae* and *Pseudomonadaceae* respectively; Cretoiu *et al*., 2014) in soil microcosms from an experimental farm located in the Netherlands. Both phyla contain chitinolytic members. The *Gammaproteobacteria* labeled here were represented by a single family-level OTU affiliating with *Pseudomonadaceae*. The next cultivated species of the OTU representative was *Cellvibrio* sp. (98% sequence similarity; Fig. 25; 3.2.2.1.). The genus *Cellvibrio* is well known to comprise versatile biopolymer degraders able to degrade both chitin and cellulose (Humphry *et al*., 2003). In line with this finding, *Cellvibrio* species were predominant in soil after chitin addition as measured by denaturing gradient gel electrophoresis (DGGE) targeting the 16S rRNA gene (Sato *et al*., 2010).

Labeled *Betaproteobacteria* were also represented by one family-level phylotype (*Oxalobacteraceae*), for which the most similar cultivated species was a *Massilia* species (98% sequence identity; Fig. 25; 3.2.2.1.). In addition, an *Oxalobacteraceae*-affiliated *chiA* phylotype (OTU 4) became [^{13}C]-labeled at day 3 under oxic conditions (Fig. 29; 3.2.3.). The genus *Massilia* comprises one cultured chitinolytic strain. However, most *Massilia* species isolated from soil have not been tested for chitinolytic activity, and the few that have been tested do not possess this trait. In addition, the related genera *Collimonas*, *Janthinobacterium*, and *Telluria* are able to degrade chitin (Adrangi *et al*., 2010; Baldani *et al*., 2014; Gleave *et al*., 1995). Chitinolytic lifestyle seems to be a common trait of *Oxalobacteraceae*. Therefore, it is likely that a careful (re)analysis of *Massilia* strains would reveal chitinolytic potentials and that the detected members in this study were truly chitinolytic. In agreement with the findings presented here, the genera *Duganella* and *Massilia* (*Oxalobacteraceae*) responded positively towards chitin amendment in another agricultural soil (Cretoiu *et al*., 2013, 2014). Thus, the results obtained here further underscore an important role of this genus to the aerobic chitin degradation in soils.

Beside *Beta*- and *Gammaproteobacteria*, *Bacteroidetes* were labeled in the first phase of chitin degradation (Fig. 25; 3.2.2.1.). It was the third most intensely labeled bacterial class at this time point (9%; Fig. 25; 3.2.2.1.), however their decrease in the labeling ratio over time (i.e., the percentage of labeled taxa) was not as pronounced as for the *Beta*- and *Gammaproteobacteria* (Fig. 25; 3.2.2.1). Thus, *Bacteroidetes* can also be regarded as initial degraders of chitin in agricultural soils (Fig. 5; 1.3.). [^{13}C]-labeling of *Chitinophagaceae*, *Cytophagaceae*, *Flavobacteriaceae*, *Sphingobacteriaceae* and an uncultured family of Bacteroidetes is consistent with the previously observed increase in the abundance of *Bacteroidetes* after chitin amendment to an agricultural soil (Cretoiu *et al*., 2014). *Chitinophagaceae*, *Flavobacteriaceae*, *Cytophagaceae* and *Sphingobacteriaceae* comprise chitinolytic representatives (McBride 2014; McBride *et al*., 2014; Rosenberg 2014; Yoon *et al*., 2012). Recently, it has been hypothesized that *Bacteroidetes* utilize alternative mechanisms to hydrolyze biopolymers, the so-called 'polysaccharide-utilizing loci', besides glycosidic hydrolases (Berlemont & Martiny 2015; Naas *et al*., 2014). This possibility might be one explanation for why *Bacteroidetes* are known to be efficient polysaccharide degraders and can contribute to biopolymer degradation (Cottrell & Kirchman 2000; Martens *et al*., 2014).

4.2.1.2. Secondary chitin degraders and saccharolytic 'satellite microbes'

After 10 days (Phase II and III), *Planctomycetes* and *Verrucomicrobia* were labeled (Fig. 25; 3.2.2.1.). For both phyla no chitinolytic representatives have been described so far, nor was evidence for a direct involvement found by culture independent methods (Ivanova & Dedysh 2012). *Planctomycetes* are able to utilize the potential chitin hydrolysis GlcNAc (Rabus *et al*., 2002). Thus, they might have an indirect role in the degradation of chitin. However, there is some evidence that the *Planctomycetes* labeled in the current work indeed were chitinolytic. Beside the incorporation of chitin derived ^{13}C in the 16S rRNA, *chiA* transcripts were detected indicating the labeled *Planctomycetes* expressed chitinases (Fig. 29; 3.2.3.). A *chiA* gene was detected in the genome of the planctomycete *S. acidiphila* (Kulichevskaya *et al*., 2008; Guo *et al*., 2012) and genomic studies targeting carbohydrate-active enzymes suggest that *Planctomycetes* as well might be able to degrade polysaccharides like cellulose and chitin (Berlemont & Martiny 2015; Ivanova *et al*., 2017). Although the detection of a chitinase in *Paludisphaera borealis* PX4T indicated chitinolytic abilities of this strain, experimental verification failed to demonstrate growth on chitin (Ivanova *et al*., 2017). However, the predicted potential to degrade polysaccharides was verified with the isolation of *Telmatocola sphagniphila*, i.e., a planctomycete that exhibits weak cellulolytic activity (Kulichevskaya *et al*., 2012). In addition, *Planctomycetes* were labeled by carbon derived from [^{13}C]-cellulose in the same agricultural soil as used in this doctoral project (Schellenberger *et al*., 2010). Taken together, these observations suggest *Planctomycetes* are able to degrade polysaccharides

and that the detected *Planctomycetes* might have been chitinolytic. If so, the labeled *Planctomycetes* could be regarded as secondary degraders slowly replacing the primary degraders (Fig. 37; 4.5.). Succession of secondary after primary degraders has been described on micro-scale in a study using model marine (chitin) particles (Datta *et al*., 2016). A possible explanation for the 'late' detection of labeling for *Planctomycetes* (day 10) might be their low growth rates (Dedysh 2011; Lage & Bondoso 2012).

Likewise for the *Planctomycetes*, genomic studies indicate a potential for polysaccharide degradation in *Verrucomicrobia* (Bai *et al*., 2016; Berlemont & Martiny 2015; Martinez-Garcia *et al*., 2012). But beyond the genome-based findings, only little physiological evidence exists that *Verrucomicrobia* are important polysaccharide degraders as only one potential cellulolytic culture and no chitinolytic *Verrucomicrobia* have been described (Chin *et al*., 1999). The labeling by [^{13}C]-chitin derived carbon provides a clear hint that *Verrucomicrobia* were at least involved in the carbon flux from chitin, although it remains unknown if they can utilize chitin. Cross-feeding via [^{13}C]-carbon dioxide appears to be a conceivable explanation for the labeling of *Planctomycetes* and *Verrucomicrobia* (Dumont & Murrell 2005). However, the gaseous phase in the treatments was periodically exchanged and the soil slurries were incubated in the dark (2.3.1.) minimizing 'cross-labeling' by heterotrophic fixation and almost excluding the possibility of photoautotrophic fixation. For that matter, cross labeling by a substrate other than carbon dioxide seems more likely. Recently, *Planctomycetes* and, to a minor extent, also *Verrucomicrobia* have been shown to be primary degraders of complex heteropolysaccharides in soil (Wang *et al*., 2015). In the aforementioned study, representatives of both phyla were labeled in a SIP-experiment using a [^{13}C]-labeled exopolysaccharide (EPS) produced by the alphaproteobacterial *Beijerinckia indica*. Thus, the activation and labeling of the labeled *Planctomycetes* and *Verrucomicrobia* might be a response to the growth of bacteria labeled by [^{13}C]-derived carbon and capable of EPS production. Therefore, the repertoire of carbohydrate-active enzymes detectable in *Planctomycetes* and *Verrucomicrobia* (Bai *et al*., 2016; Berlemont & Martiny 2015; Martinez-Garcia *et al*., 2012) might as well reflect the capability to degrade exopolysaccharides. The labeled alphaproteobacterial phylotype belongs to *Caulobacteraceae*, which have not been so far described as chitinolytic (Abraham *et al*., 2014). However, *Caulobacteraceae* can grow on chitin hydrolysis products when they are supplied by a chitinolytic partner (Eisenbeis *et al*., 2008). Therefore, detected *Caulobacteraceae* likely functioned as 'satellite microbes', scavenging excess chitin hydrolysis products.

4.2.1.3. Bacterial predators

Deltaproteobacteria was the predominantly labeled bacterial group after 70 days (Fig. 25; 3.2.2.1.). A decreased labeling ratio (Fig. 25; 3.2.2.1.), a low relative isotopic abundance (RIA) value (Table 23; 3.2.6.), and a high carbon recovery in the products (Table 22; 3.2.1.1.) suggest an indirect rather than direct [^{13}C]-carbon uptake from [^{13}C]-chitin. The labeled families *Bdellovibrionaceae* and *Bacteriovoraceae* are known to be bacterial predators but also *Myxococcales* are known to harbor bacteriovorus taxa (Johnke *et al*., 2014; Pérez *et al*., 2016). Thus, the labeled uncultured family within *Myxococcales* likely also is bacteriovorus. Based on previous studies, Gram-negative *Bacteria*, particularly *Pseudomonadaceae* (*Gammaproteobacteria*), can be predated by *Bdellovibrionaceae* and *Bacteriovoraceae* (Sockett 2009). *Bdellovibrio exovorus*, closest cultivated species to OTU 779, (Fig. 25; 3.2.2.1.) has an epibiotic hunting strategy, i.e. it attaches and remains to the outer surface of the cell where it degrades and assimilates the prey molecules (Koval *et al*., 2013; Pasternak *et al*., 2014; Pérez *et al*., 2016). *Bdellovibrio exovorus* was isolated from sewage in enrichment cultures with *Caulobacter crescentus* (Koval *et al*., 2013). Noteworthy, *Caulobacter* species were also labeled by [^{13}C]-chitin derived carbon (Fig. 25; 3.2.2.1.). *B. exovorus* has a very limited prey range preying almost exclusively on *C. crescentus* (Koval *et al*., 2013). After predation, empty stalked cells of *C. crescentus* remain (Koval *et al*., 2013). With the exception of *B. exovorus*, most *Bdellovibrionaceae* and *Bacteriovoraceae* have an endobiotic hunting (direct invasion) strategy, i.e. they penetrate their prey and grow and divide in the peri- or cytoplasm (Pérez *et al*., 2016; Sockett 2009). Several members of *Myxococcales*, i.e. all *Sigmatella*, several *Cystobacteria*, *Myxococcus stipitatus*, *Kofleria flava*, *Jahnia thaxteri* and most *Sorangium* can hydrolyze chitin (Reichenbach 2005). For reasons mentioned above *Myxococcales* likely were labeled by indirect consumption of [^{13}C]-chitin derived carbon and were not actively degrading chitin. Members of *Myxococcales*, e.g., *Myxococcus xanthus*, are also predatory (Berleman *et al*., 2014) suggesting the uncultured family represented by OTU 79 was labeled by predation of bacteria involved in chitin degradation. In agreement with this, *Myxococcales* incorporated [^{13}C]-carbon from [^{13}C]-labeled *Escherichia coli* biomass added to an agricultural soil (Lueders *et al*., 2006). Predatory *Myxococcales* differ in their predatory mechanism (Berleman *et al*., 2014; Pérez *et al*., 2016), i.e. they hunt in groups via the secretion of diffusible antibiotics and lytic compounds that kill and decompose the prey. This cooperative hunting strategy requires a high cell density of predators and two variants are known referred as ‘wolf-pack attack’ (Berleman *et al*., 2014) and ‘frontal attack’ (Pérez *et al*., 2014). Thus, *Deltaproteobacteri*a were likely labeled by preying on [^{13}C]-labeled primary degraders (*Gammaproteobacteria*) and potential ‘satellite microbes’ (*Caulobacteraceae, Alphaproteobacteria*).

4.2.1.4. Micro-eukaryotic predators

Although [^{13}C]-labeling of *Eukaryota* was not detected (i.e., no PCR products were obtained from the cDNA of heavy fractions with taxon-specific primers) *Alveolata* (*Ciliophora*) substantially increased in their relative abundance under oxic conditions (Fig. 32; 3.2.5.). More specifically, the increased relative abundance was caused by two OTUs, affiliating with the families *Kreyellidae* and *Colpodidae*. Members of the class *Colpodea* are soil abundant ciliates predominantly eating bacteria as an energy and carbon source (Clarholm 1981; Drake & Tsuchiya 1976; Ekelund & Rønn 1994; Foissner 1993; Vargas & Hattori 1986) suggesting that these organisms consumed *Bacteria* that were involved in the chitinolytic food web. In agreement with this, among others *Alveolata* (*Ciliophora*) were labeled by [^{13}C]-cellulose derived carbon in the same soil and were the predominant *Eukaryota* in 16S rRNA libraries after 70 days under oxic conditions (Chatzinotas *et al*., 2013). *Colpodea* were also labeled by [^{13}C]-methane in a wetland rice soil (Murase & Frenzel 2007). The authors of that study also showed that soil protozoa were selective grazing on methanotrophs (Murase & Frenzel 2008). Thus, *Alveolata* (*Ciliophora*) likely played a role in the food web, but their [^{13}C]-incorporation was likely not high enough for [^{13}C]-label detection in the present experiment. A secondary label would have been much weaker and may have not been detectable against the background of the much more intensely labeled *Bacteria*.

4.2.2. Anaerobic chitin degradation

The anaerobic degradation of chitin can be separated into three distinct phases on process level. During the first 20 days, carbon dioxide production was only slightly stimulated in the chitin treatments compared with the unsupplemented controls (Fig. 23; 3.2.1.2.), and only small amounts of [^{13}C]-carbon dioxide accumulated (Fig. 21b; 3.2.1.). Nitrate and sulfate likely were respired by soil microorganisms, as their concentrations decreased below detection limit (Fig. 23; 3.2.1.2.). Typical fermentation products did not accumulate significantly, i.e. they were not detectable during this initial phase, and only the production of ferrous iron was slightly stimulated (Fig. 23; 3.2.1.2.). However, hydrolysis of chitin and the fermentation of the hydrolysis products likely were already ongoing. Small amounts of acetate accumulated at day 3 and 7 (240 and 220 µM) and were apparently consumed at day 10 (Fig. 23; 3.2.1.2.). The consumption of acetate is in agreement with the stimulation of ferric iron reduction, as many iron reducing bacteria oxidize typical fermentation products like acetate to conserve energy (Lovley 1991, 1993, 1997; Lovley *et al*., 1993; Weber *et al*., 2006). In a second phase (between days 21 and 42), the iron reduction was still ongoing until the concentration of ferrous iron peaked in chitin-supplemented slurries (Fig. 21b, 23; 3.2.1., 3.2.1.2.) indicating that most of ferric iron was reduced. Once alternative electron acceptors like ferric iron, nitrate and sulfate were consumed and reached a critical threshold, typical

fermentation products like molecular hydrogen, acetate, and propionate accumulated (Fig. 21b, 23; 3.2.1., 3.2.1.2.). The formation of propionate suggested that the chitin hydrolysis products were fermented via methylmalonyl-CoA or acrylyl-CoA pathways (Moat *et al*., 2002; Reichardt *et al*., 2014; Zidwick *et al*., 2013). The products acetate, molecular hydrogen and carbon dioxide can also be formed by mixed acid fermentation (Rogers *et al*., 2013). However, this fermentation pathway is typically associated with the formation of succinate and/or ethanol, i.e., compounds that were not detected. Syntrophic fermentation and acetogenesis might have also been involved in acetate production, but the stoichiometry of the products and the high molecular hydrogen concentrations suggest these metabolic processes were not prevailing (Wagner *et al*., 1996). The production of butyrate was indicative of butyric acid fermentation (Buckel 2005). However, only small amounts were formed after 42 days, suggesting that butyric acid fermentation played only a minor role. In the final phase, iron reduction almost stopped, and fermentation product accumulation slowed down, whereas methane started to accumulate (Fig. 23; 3.2.1.2.). Carbon and electron recoveries were calculated on the assumption that the supplemented chitin was fully degraded, and showed that 57.9% and 54.1% of supplemented carbon and electron moles were recovered in the fermentation products (Table 22; 3.2.1.1.). The collective data suggest that chitin degradation was far advanced under anoxic conditions, however, not yet completed. In addition, anaerobic chitin degradation apparently is slowed compared to aerobic chitin degradation. Polysaccharide monooxygenases (PMOs) facilitate the oxidative cleavage of chitin using atmospheric oxygen (Dimarogona *et al*., 2013; Span & Marletta 2015; Vaaje-Kolstad *et al*., 2010, 2013; Walton & Davies 2016; 1.2.3.4.). PMOs introduce breaks in the chitin fibers creating new chain ends for processive exochitinases and thereby overall boost the degradation of chitin (Dimarogona *et al*., 2013; Span & Marletta 2015; Vaaje-Kolstad *et al*., 2010, 2013; Walton & Davies 2016). Thus, the slowed chitin degradation under anoxic conditions likely is explained by the missing activity of PMOs, as these enzymes require oxygen. Long periods of anoxia can stimulate methanogens that likely survived in anoxic microzones (Angel *et al*., 2012; Küsel & Drake 1994), thus explaining the production of methane although the investigated soil has primarily an oxic nature not favoring methanogenesis. Minor concentrations of ammonium accumulated in these treatments (Fig. 23; 3.2.1.2.), indicating that most of the chitin-derived ammonium was consumed, likely through assimilatory pathways. Hydrolysis products of chitin (i.e., *N*-acetylglucosamine and chitobiose) were not detected in anoxic treatments, suggesting an efficient microbial consumption that resulted in low steady-state concentrations of these hydrolysis products below the detection limit of 30 µM.

4.2.2.1. Initial anaerobic chitin degraders

In the first phase of the anoxic chitin degradation the total labeling ratio was low, at 15.9% (Fig. 26; 3.2.2.2.). This is an additional indication that anaerobic chitin degradation is slowed compared to aerobic chitin degradation (4.2.2.). The genus *Paenibacillus* (*Paenibacillaceae*) is known to be chitinolytic and capable of ferric iron reduction (Grady *et al*., 2016; Lai *et al., 2015*; Lee *et al*., 2004; Li *et al*., 2014; Raza & Shen 2010; Subbanna *et al*., 2016). Thus, the labeled *Paenibacillaceae* likely were involved in the initial anaerobic degradation of chitin and partially might have been responsible for the observed ferric iron reduction. Among the labeled taxa in phase I were *Acidobacteria*, which incorporated the largest fraction of ^{13}C (Fig. 26; 3.2.2.2.). *Acidobacteria* are abundant in soils but little is known about their ecophysiology (Janssen 2006). The recent isolated species *Blastocatella fastidiosa* is chitinolytic (Foesel *et al*., 2013). Genomic evidence supports the view that this physiological trait might be more common in *Acidobacteria* (Ward *et al*., 2009) then previously assumed. Thus, the labeled *Acidobacteria* likely were chitinolytic. Two strains investigated in the study by Ward *et al*. (2009), referred as Ellin345 and Ellin6076 therein, were isolated from an Australian soil (Joseph *et al*., 2003; Davis *et al*., 2005). They have preliminary been given the candidate Latin binomials 'Candidatus *Koribacter versatilis*' (Ellin345) and 'Candidatus *Solibacter usitatus*' (Ellin6076) (Ward *et al*., 2009) and were placed in the subdivisions 1 and 3 of *Acidobacteria* respectively. They were isolated under oxic conditions and described as slow growing aerobic heterotrophs. However, their ability to grow under anaerobic conditions has not been tested. The labeled acidobacterial OTU 410 (Fig. 26; 3.2.2.2.) was closely related with Candidatus *Koribacter versatilis*. In addition, the labeling under anoxic conditions suggest that Candidatus *Koribacter versatilis*-like *Acidobacteria* are facultative aerobic. Furthermore, Ward and coauthors (Ward *et al*. 2009) detected several genes potentially involved in ferric iron reduction and concluded that the investigated *Acidobacteria* use a pathway for ferric iron reduction dissimilar to that of ferric iron reducing *Proteobacteria*. In agreement with the assumption that representatives of subdivision 1 and/or 3 *Acidobacteria* are capable of dissimilatory ferric iron reduction, *Paludibaculum fermentans* was described as a facultative aerobe capable of dissimilatory iron reduction from subdivision 3 of the *Acidobacteria* (Kulichevskaya *et al*., 2014). The aforementioned bacterium is able to ferment glucose and cellobiose or to use these sugars as electron donors for ferric iron reduction (Kulichevskaya *et al*., 2014). Thus, it is tempting to speculate that the labeled *Acidobacteria* were able to reduce ferric iron and/or were able to couple the hydrolysis of chitin to iron respiration.

The labeling and detection of *Anaerolineacae* under anoxic conditions (Fig. 26; 3.2.2.2.) fits well into their known physiology as members of the *Anaerolineacae* ferment sugars (McIlroy *et al*., 2016). Genome studies have revealed that *Chloroflexi* harbor chitinases and

accessory genes (Zimmerman *et al*., 2013; Bai *et al*., 2016). Furthermore, the only known chitinolytic *Chloroflexi* strain described so far belongs to the *Anaerolineaceae* (Nunoura *et al*., 2013). Taken together, there is good evidence the labeled *Chloroflexi* might have been chitinolytic. In contrast to that, labeling of *Verrucomicrobia* is more difficult to explain. The labeled *Verrucomicrobia* were represented by a single family level OTU most similar to *Limisphaera ngatamarikiensis* (87% similarity; NR_134756.1), which is not capable of fermentation or the degradation of chitin (Anders *et al*., 2015). It can aerobically grow on *N*-acetylglucosamine as a carbon source. However, a close relative of *L. ngatamarikiensis*, *Alterococcus agarolyticus*, can ferment sugars (Shieh & Jean 1998). In agreement with this finding, a peptide affiliated with *Verrucomicrobia* was labeled under anoxic conditions (Table 23; 3.2.6.). Nonetheless, beside genomic evidence only little physiological evidence exists that *Verrucomicrobia* are important polysaccharide degraders (4.2.1.2.). Irrespective of that, it can be assumed that labeled *Verrucomicrobia* consumed chitin hydrolysis products that were fermented to conserve energy.

4.2.2.2. Labeling of non-chitinolytic iron reducing bacteria by chitin-derived carbon

The labeled *Geobacteraceae* are not known for chitin degradation or the consumption of chitin hydrolysis products. However, their labeling was consistent with process data (3.2.1.2.; 4.2.2.), as these *Bacteria* are capable of ferric iron dissimilation and utilize typical fermentation products such as acetate (Lovley 1991, 1993, 1997; Lovley *et al*., 1993; Weber *et al*., 2006). *Geobacteraceae* likely consumed the fermentation products, which were formed in low amounts in chitin-supplemented soil slurries in the first phase of chitin degradation and coupled it to the reduction of ferric iron (3.2.1.2.; 4.2.2.).

4.2.2.3. Dominant anaerobic chitin degraders

In phase II of anaerobic chitin degradation, fermentation was clearly stimulated by chitin supplementation as soon as alternative electron acceptors were consumed (Fig. 23; 3.2.1.2.; 4.2.2.) and the labeling ratio increased up to 66.4% (Fig. 26; 3.2.2.2.). In line with the stimulation of fermentative processes is the labeling of typical fermentative bacterial taxa, such as chitinolytic and saccharolytic *Firmicutes* and *Bacteroidetes* (Fig. 26; 3.2.2.2.). The [^{13}C]-incorporation by *Firmicutes*, i.e. *Ruminococcaceae* and *Lachnospiraceae*, agrees with pure culture-based observations, which suggest that members of both families can degrade both chitin and cellulose (Evvyernie *et al*., 2000; Reguera & Leschine 2001). In agreement with this, a *Firmicutes*-like *chiA* transcript (55% protein identity with *Clostridium beijerinckii*) was labeled (Fig. 30; 3.2.3.), emphasizing their significant role in the anaerobic degradation of chitin. *Paenibacillaceae*, which were already labeled in Phase I, increased in their labeling ratio (Fig. 26; 3.2.2.2.). As *Geobacteraceae* were not among the labeled phylotypes in this period, other iron-reducing taxa must have been active. The genus *Paenibacillus* is known to

comprise ferric iron reducing strains (Grady *et al*., 2016; Lai *et al., 2015*; Lee *et al*., 2004; Li *et al*., 2014; Raza & Shen 2010; Subbanna *et al*., 2016). Therefore, it is likely that *Paenibacillaceae* were partly responsible for the anaerobic mineralization of chitin and the observed ferric iron reduction in phase II. *Bacteroidetes* were the second largest group of labeled *Bacteria* at day 21. The OTU representative was affiliated with an uncultured family close to families *Marinilabiaceae* and *Prolixibacteriaceae* (Fig. 26; 3.2.2.2.). For the latter two families the capability to degrade chitin has not been demonstrated. However, the potential to degrade chitin is common among aerobic *Bacteroidetes*. Therefore, the labeled phylotype (OTU 754) represents an uncultured facultative aerobic or obligate anaerobic *Bacteroidetes* that likely was chitinolytic. At the end of the incubation, the total labeling ratio was 64.2%. The uncultured *Bacteroidetes* became the most abundant labeled phylum followed by *Firmicutes*, *Acidobacteria*, and *Chloroflexi* (Fig. 26; 3.2.2.2.). This phase of anaerobic chitin degradation was characterized by a substantial decrease in the ferric iron reduction rate, which can be explained by increasing depletion of ferric iron.

4.2.2.4. Stimulation of methanogenesis by chitin derived carbon

Methanogenesis was stimulated in chitin-supplemented soil slurries (Fig. 23; 3.2.1.2.). In agreement with this, methanogenic *Archaea* were stimulated (Fig. 23, 31; 3.2.1.2., 3.2.4.) that survived long oxic periods in anoxic microzones (Angel *et al*., 2012; Küsel & Drake 1994). No PCR products were obtained from the cDNA of heavy fractions with *Archaea*-specific primers. Nonetheless, in the amplicon libraries obtained with *Bacteria*-specific primers (2.5.8.2.), archaeal 16S rRNA sequences were present in the heavy fractions of [^{13}C]-supplemented soil slurries whereas no sequences were detected in the heavy fractions of [^{12}C]-chitin treatment. The used primer pair (Bakt_341F and Bakt_805R; 2.5.8.) as suggested by Klindworth and coauthors (Klindworth *et al*., 2013) for the use in pyrosequencing is known to also detect some archaeal taxa, including the detected *Methanobacterium* genus (*Methanobacteriaceae*). Although the detected *Methanobacteriaceae* were under the significance threshold for being defined as labeled (2.7.4.) the fact that they were only detectable in the heavy fraction of [^{13}C]-treatments indicates that they incorporated [^{13}C]-chitin derived carbon. *Methanobacteriaceae* are obligate anaerobes that conserve energy by the reduction of carbon dioxide with molecular hydrogen (Oren 2014). However, some *Methanobacterium* genera can use acetate for growth support (Oren 2014). Thus, labeled *Methanobacteriaceae* incorporated carbon from [^{13}C]-carbon dioxide and/or [^{13}C]-acetate.

4.3. Trophic interactions a chitin-degrading soil microbiome

4.3.1. Trophic interactions under oxic conditions

Pseudomonadaceae, *Oxalobacteraceae* and *Bacteroidetes* were initially and primarily degrading chitin under oxic conditions (4.2.1.1.). Potential chitin hydrolysis products, i.e. GlcNAc and $[GlcNAc]_2$ were not detectable, suggesting an efficient consumption by the primarily degraders but also saccharolytic *Caulobacteraceae* (4.2.1.2.). The consumption of excess hydrolysis products by *Caulobacteraceae* resulted in low steady state concentrations below the detection limit. Thus, *Caulobacteraceae* can be referred to as 'satellite microbes' that scavenged excess chitin hydrolysis products and thereby likely pushed the degradation of chitin kinetically forward as suggested as the concept of 'satellite microbes' in cellulose breakdown (Bayer 2006). Hydrolysis products were used as a source of energy, carbon, and/or nitrogen (Geisseler *et al*., 2010; Gooday 1990b; Kellner & Vandenbol 2010; Keyhani & Roseman 1999) by active chitin degraders and 'satellite microbes' as demonstrated by the incorporation of [^{13}C]-carbon into biomass (Fig. 25, 3.2.2.1.). In addition, it is likely that the population of *Bacteria* labeled by the consumption of [^{13}C]-chitin derived carbon was growing and increased in their biomass. Consequently, that set the table for predatory *Bdellovibrionaceae*, *Bacteriovoraceae* and *Myxococcales* that were preying Gram-negative *Proteobacteria*, i.e. *Pseudomonadaceae*, *Oxalobacteraceae* and *Caulobacteraceae* (4.2.1.3.). Not much is known about the predation on *Bacteroidetes* because research of predation *in situ* is very difficult and most predator-prey interaction studies conducted utilized 'typical' prey species (Pérez *et al*., 2016; Sockett 2009). However, due to their Gram-negative cell walls, they also could have been potential prey for endobiotic predators. In any case, group attack hunting strategies, in which lethal antibiotics and lytic compound are secreted, are weakly prey specific (Berleman *et al*., 2014; Pérez *et al*., 2016). In accordance with this, predatory *Myxococcus* isolates can prey on various Gram-positive and Gram-negative *Bacteria*, however the latter are more growth supportive (Morgan *et al*., 2010). The ecological function of the labeled *Planctomycetes* and *Verrucomicrobia* in the chitin degrading food web is more difficult to explain (4.2.1.2.). For *Planctomycetes* good evidence exists that can be interpreted in the way that some of the labeled of OTUs might have been chitinolytic and were actively degrading chitin (4.2.1.2.). Nevertheless, alternative interpretations of the labeling of *Planctomycetes* and *Verrucomicrobia* are conceivable. First of all, labeled taxa might have been saccharolytic, i.e. they were consuming chitin hydrolysis products and like *Caulobacteraceae* functioned as 'satellite microbes' (4.2.1.2.). Thereby, the late occurrence of a labeling can be explained by the slower growth of *Planctomycetes* and *Verrucomicrobia* (Dedysh 2011; Lage & Bondoso 2012). Slow growth rates usually are associated with k-strategists that grow slowly on recalcitrant, complex substances and have an efficient cell metabolism (Fierer *et al*., 2007; Klappenbach *et al*., 2000). However,

Planctomycetes were among labeled phylotypes in [^{13}C]-cellulose but not in [^{13}C]-glucose and [^{13}C]-cellobiose supplemented soil slurries, indicating that they were not competitive in the utilization of cellulose hydrolysis products against *Actinobacteria* (Schellenberger *et al*., 2010).

A different possibility to interpret the data is opened by the labeling of *Planctomycetes* and *Verrucomicrobia* in soil by a [^{13}C]-labeled exopolysaccharide (EPS) produced by *Alphaproteobacteria* (Wang *et al*., 2015). Among the taxa labeled by [^{13}C]-chitin derived carbon, the potential to produce EPSs has been reported for *Caulobacter* (*Alphaproteobacteria*) and *Pseudomonadaceae* (*Gammaproteobacteria*) (Ueda & Saneoka 2015; Ravenscroft *et al*., 1991). Thus, *Planctomycetes* and *Verrucomicrobia* might have assimilated [^{13}C]-chitin derived carbon by the degradation of EPSs produced by primary degraders (e.g. *Pseudomonadaceae*) and/or saccharolytic bacteria (*Caulobacteraceae*). Particularly interesting is the characterization of a novel planctomycetal organelle that is required for (optimized) aerobic growth on L-fucose, L-rhamnose, and the sulfated polysaccharide fucoidan (Erbilgin *et al*., 2014). Notably, the gene cluster encoding this organelle appears to be restricted to the phyla *Planctomycetes* and *Verrucomicrobia* (Erbilgin *et al*., 2014). The sugars L-fucose and L-rhamnose are commonly found in the exopolysaccharides of bacteria and fungi and are known for their thickening, gelling or emulsifying properties (Vanhooren & Vandamme 1999). Furthermore, L-fucose, L-rhamnose, *N*-acetylglucosamine can be found in the liposaccharides of various Gram-negative *Bacteria* (Erridge *et al*., 2002; Flowers 1981). Alginate, i.e. an anionic polysaccharide comprised of 1-4-linked β-D-mannuronic acid (M) and C-5-epimer α-L-guluronic acid (G) can be produced by some *Pseudomonadales* as a component of EPSs (Vu *et al*., 2009) and is a common component of macroalgae cell walls (Boyd & Chakrabarty 1995; Vu *et al*., 2009). In accordance with this, a striking association of *Planctomycetes* with macroalgae can been observed (Lage & Bondoso 2014). Likely, this is due to their potential to degrade heteropolysaccharides and sulfated polysaccharides that are abundant in the algae cell walls (Fuerst & Sagulenko 2011). *Planctomycetes* and *Verrucomicrobia* have a broad repertoire of carbohydrate-active enzymes detectable in their genomes (Bai *et al*., 2016; Berlemont & Martiny 2015; Martinez-Garcia *et al*., 2012). Datta and coauthors (Datta *et al*. 2016) demonstrated that microbial communities on model marine (chitin) particles undergo rapid and reproducible successions. The authors contemplated that chitin metabolizers facilitated growth of successive species by providing them carbon from alternative sources like cell wall polysaccharides, biofilm-associated exopolysaccharides, or small metabolic byproducts (Datta *et al*., 2016). Thus, a potential ecological niche of *Planctomycetes* and *Verrucomicrobia* might be the degradation of complex heteropolysaccharides that can be found in EPSs and cell walls (Kulichevskaya *et al*., 2007; Wang *et al*., 2015).

In this study, direct trophic interactions between chitinolytic primary degraders and predatory bacteria were observed (see above). In consequence of the predation of chitinolytic primary degraders and 'satellite microbes' by predatory *Bacteria,* dead bacterial biomass (i.e. empty and/or fragmented bacterial cell envelopes) should accumulate setting the table for saprotrophic and heterotrophic microorganisms. As an alternative explanation for the labeling, *Planctomycetes* and *Verrucomicrobia* might have assimilated carbon from the degradation of cell wall polysaccharides of the bacterial necromass left by the activity of predatory *Bacteria*. In that case, labeled *Planctomycetes* and *Verrucomicrobia* ecologically functioned as saprotrophs.

Finally, assimilation of carbon from the degradation of heteropolysaccharides of cell walls or EPSs could alternatively explain how *Planctomycetes* were labeled by [^{13}C]-cellulose (Schellenberger *et al*., 2010) and [^{13}C]-chitin (4.2.1.2.) despite little physiological evidence for the degradation of homopolysaccharides by *Planctomycetes* (Dedysh 2011; Ivanova & Dedysh 2012; Kulichevskaya *et al*., 2012).

4.3.2. Trophic interactions under anoxic conditions

Trophic interactions under anoxic conditions differed substantially compared to oxic conditions. Fermentative initial degraders provided fermentation products that likely were consumed by iron reducing *Geobacteraceae* (3.2.1.2.; 4.2.2.2.). Another functional group of *Bacteria* that were indirectly stimulated by chitin degradation were methanogenic *Archaea* that conserve energy by the reduction of carbon dioxide with molecular hydrogen but also could have used acetate for growth support (Oren 2014). Interestingly, no evidence for prey-predator or saprotrophic interactions were observed under anoxic conditions, i.e. typical predatory and/or saprotrophic bacterial and eukaryotic taxa were not labeled (3.2.2.2.; 4.2.2.). To date, most described predatory *Bacteria* have an obligate aerobic metabolism and are preying on Gram-negative *Bacteria* (Pérez *et al*., 2016; Sockett 2009) and only few studies exist that described anaerobic predation by *Bacteria* (Guerrero *et al*., 1986). In the latter study, two bacteriovorus species were described, i.e. *Vampirococcus* and *Daptobacter,* exclusively attacking phototrophic purple sulfur bacteria of the family *Chromatiaceae* (*Gammaproteobacteria*). Therefore, it appears that prerequisites for predation by *Bacteria* are the presence of appropriate Gram-negative prey species and preferably (but not necessarily) oxic conditions. Since prolonged anoxic conditions predominantly favored the activity of obligate anaerobic Gram-positive *Firmicutes* (4.2.2.3.) and phototrophic purple sulfur bacteria were inactive (3.2.2.; 4.2.2.), apparent absence of 'anaerobic' predation by *Bacteria* can be explained by the lack of appropriate prey. In addition to the apparent lack of bacterial predation, also no hints for predation by *Eukaryota* were found (3.2.5.). Same as for predation by *Bacteria*, anaerobic predation by *Eukaryota* is not well investigated, notably little

is known for soils (Ekelund & Rønn 1994). Even though the question of the role of *Eukaryota* in the anaerobic food web of aquatic systems has addressed more attention, only a few studies have directly addressed the *in situ* impact of predation by phagotrophic protozoa (Saccà 2012). Phagotrophic protozoa exist that actively prey on prey populations in anoxic water compartments (Saccà 2012). However, the impact of anaerobic predation is lower than in oxic environments, possibly due to a less-efficient metabolism of the anaerobic protozoa (Fenchel & Finlay 1990).

4.4. Chitin and cellulose degrading *Bacteria*

The sequences of bacterial taxa that were labeled with both substrates were highly similar (Fig. 35, 36; 3.3.1., 3.3.2.), indicating that many bacterial taxa in the investigated agricultural soil are versatile polysaccharide degraders. In the present study, *Oxalobacteraceae* (*Massilia*) and *Pseudomonadaceae* (*Cellvibrio*) were labeled under oxic conditions. The genus *Cellvibrio* is known to be able to degrade both chitin and cellulose (DeBoy *et al*., 2008; Humphry *et al*., 2003; Wynne & Pemberton 1986). In contrast to that, it is known that *Massilia* can be cellulolytic (Hrynkiewicz *et al*., 2010; Ofek *et al*., 2012; Singh *et al*., 2015; Weon *et al*., 2008). However, the ability to degrade chitin is not that well established. So far, only *Massilia timonae* is known to be chitinolytic (Faramarzi *et al*., 2009). Many *Massilia* species isolated from soil were not tested for the ability to degrade chitin, and the few that have been tested were not chitinolytic (Baldani *et al*., 2014). This lack of information goes along with a higher research interest in cellulose compared to chitin. For example, the search term ‘cellulolytic bacteria’ using google scholar yields approximately 51,000 hits while ‘chitinolytic bacteria’ reaches only 13,000 hits. Nonetheless, chitinolytic lifestyle seems to be a common trait of *Oxalobacteraceae* (Adrangi *et al*., 2010; Baldani *et al*., 2014; Gleave *et al*., 1995). Therefore, it is likely that a careful (re)analysis of *Massilia* strains would reveal chitinolytic potentials and this likely holds true for other cellulolytic taxa.

That the labeled taxa are versatile polysaccharide degraders is also nicely illustrated by uncultured *Bacteroidetes* and *Ruminococcaceae* under anoxic conditions, of which the closely related genera were detected when cellulose or chitin were supplemented (3.3.2.). In agreement with this, culture-based studies demonstrated that members *Ruminococcaceae* and *Lachnospiraceae* can degrade both chitin and cellulose (Evvyernie *et al*., 2000; Reguera & Leschine 2001). In addition, degradation of multiple polysaccharides by *Paenibacillaceae* was also likely. *Paenibacillus curdlanolyticus* produces an extracellular enzyme system containing i.a. carboxymethyl cellulase, cellobiohydrolase and chitinase albeit the latter showed low hydrolytic activity (Pason *et al*., 2006). Thus, it is likely that many taxa that are involved in cellulose degradation also contribute to chitin decomposition. Given the structural similarity of chitin and cellulose (Fig. 2), overlapping chitinolytic and cellulolytic potentials in

Bacteria are not surprising. In environments, such as soils, where these polysaccharides co-occur but likely vary in abundance and spatial distribution, the potential to degrade various polysaccharides is an advantageous life strategy.

In the here conducted comparative analysis on cellulose and chitin degrading microorganisms, different methodologies were applied to determine phylotypes (amplicon pyrosequencing vs. terminal restriction fragment length polymorphism). Thus, detected differences in the relative abundance and labeling of taxa have to be regarded with caution. Observable differences between the cellulose and chitin degrading sub-microbiomes can partially be explained by different sampling times after polymer supplementation. As the time difference was 25 days, the low relative abundance of labeled *Beta-* and *Gamma-Proteobacteria* in the cellulose treatment can be explained by a depletion of the label over time as it was observed for chitin in the current study. By comparison, the difference between sampling under anoxic conditions was 14 days and relative abundances of labeled *Bacteroidetes* and *Firmicutes* were in a similar range. On the other hand, general differences, e.g. labeling of *Verrucomicrobia* by exclusively by [^{13}C]-chitin or labeling of *Chloroflexi* by [^{13}C]-cellulose are more difficult to explain. The aforementioned taxa indeed might have been specialized on a given substrate. Yet, different sampling times and methodological divergences hinder a clear conclusion. Although soil samples were obtained from the same agricultural field, the exact spot of sampling likely was not identical. Given that soils are spatially heterogeneous on macro- and micro-scale, i.e. they vary in physicochemical properties, also the activity, function structure of associated microbiomes can differ (Vos *et al*., 2013). However, the determining factor will be that in the time between sampling the agricultural field was subject to soil treatment, e.g. plowing and the use of pesticides, and potential alterations in crops that were cultivated and their rotation. These factors have been shown to shape the structure and function of root and soil microbiomes (Berg & Smalla 2009; Bulgarelli *et al*., 2013; Lareen *et al*., 2016; Philippot *et al*., 2013, Vos *et al*., 2013). Thus, in future this topic should be addressed in an experiment where, for instance, chitin and cellulose degradation is studied in parallel incubations using soil from the same sampling event.

4.5. Recalcitrance of chitin

Terrestrial ecosystems hold the potential to capture and store substantially increased volumes of carbon in soil organic matter and thereby can act as sinks for increasing atmospheric carbon dioxide concentrations counteracting the greenhouse effect (Dungait *et al*., 2012). In order to realize this potential and to predict the role of soils in future climate change not only the amount of stabilized soil organic matter needs to be determined (Dungait *et al*., 2012; von Lützow *et al*., 2006), but also the understanding of turnover dynamics of the

various forms of organic matter must be improved and adapted to existing computer simulation models for the prediction soil carbon dynamics (Dungait *et al*., 2012; von Lützow *et al*., 2006). Although chitin is ubiquitous in nature (it is the second most abundant polysaccharide after cellulose) and has a relatively simple chemistry, there is little empirical data for its specific decomposition dynamics in soils (Dungait *et al*., 2012) and contrasting reports on the degree of its recalcitrance exist. Some authors believe chitin to be recalcitrant (Godbold *et al*., 2006; Langley *et al*., 2006) and von Lützow and coauthors noted in their review of SOM stabilization mechanisms that chitin can accumulate in soil (von Lützow *et al*., 2006). However, Gooday (1990b) concluded that chitin is completely recycled in nature as no apparent accumulation is observable. The results of this thesis clearly show that chitin was readily degradable and likely was not stabilized in the soil organic matter. Thus, the findings reinforce the notion by von Lützow and coauthors (2006) that 'molecular recalcitrance of OM is relative, rather than absolute'. Furthermore, and of special interest, the results demonstrate that chitin is also readily degradable under anoxic conditions, although degradation is slower compared to oxic conditions. Up to date, almost no information on the anaerobic degradation of chitin in arable soils was available (Manucharova *et al*., 2006; Reguera & Leschine 2001). It should be noted that the experimental design likely artificially increased degradability by increasing accessibility of chitin to the soil microbiome. The pore network of the soil was destroyed by the preparation of soil slurries and shaking in an end-over-end shaker. Thus, the soil slurries likely reflected a matrix where chitin was accessible to all microorganisms of the soil microbiome in contrast to limited access of chitin in undisturbed soil. In addition, the used chitin was pure and thus easily accessible, i.e. it was not complexed with other polymeric components as it would occur in insects or fungi (Gooday 1990b). However, it is just this experimental setup that allows reinforcing the perception that recalcitrance of organic matter is a relative and a matter of accessibility to the soil microbiome (Dungait *et al*., 2012; von Lützow *et al*., 2006; Kleber 2010). Thus, the knowledge gained in this study improves the understanding of turnover dynamics of chitin under oxic and anoxic conditions in arable soils and the understanding of stabilization mechanisms of organic matter in soil. Furthermore, this doctoral project gained insight into the complex the food webs that are associated with chitin degradation in arable soils. The findings can help to integrate models of food webs with more general models of carbon turnover, an area of research where little attempts have been made so far (Dungait et al., 2012).

4.6. Methodological limitations

Soil slurry incubations were used to study chitin degradation under oxic and anoxic conditions. This method was chosen as it allows to study microbial processes by the analysis of liquid samples (e.g. by HPLC and colorimetric methods). Together with [^{13}C]-chitin SIP it enabled to link labeled taxa with observed microbial processes. The soil slurries were shaken in an end-over-end shaker to avoid depletion of oxygen and ensure oxic conditions. This reflects a potential bias, as the liquid phase and permanent shaking might have favored or disadvantaged certain taxa, e.g. *Actinobacteria* supposed to be important degraders of chitin and cellulose in soils were not labeled or stimulated (Schellenberger *et al*., 2010; Wieczorek *et al*., 2014, 2019). Furthermore, also the pretreatment of the soil (e.g. sieving) that was necessary for the preparation of the soil reflects a potential bias. However, the comparison here with studies where chitin was added to undisturbed agricultural soil (4.2.2.1.) largely supports the results found in this doctoral thesis.

Functional genes markers, i.e. genes coding for key enzymes metabolic pathways allow the study of functional groups such as methane oxidizers or sulfate reducers (Kolb *et al*. 2003; Meyer & Kuever 2007; Murrell & Radajewski 2000; Muyzer & Stams 2008; Wagner *et al*., 1998). For the study of chitinolytic *Bacteria* in the environment, primer systems targeting exochitinases of subfamily A of GH18 family were developed and have been widely used to study chitinolytic bacteria in various environments (1.5.). In this doctoral project, results of the *chiA* analysis partially reinforced results of 16S RNA SIP approach. However, it became obvious that analysis of *chiA* alone would have failed to detect certain chitinolytic taxa, e.g. *Bacteroidetes* (3.1.5., 3.2.2.1.). For *Bacteroidetes* it was shown that the enzymatic machinery for the degradation of cell-wall polysaccharides is organized in cell-wall associated multiprotein systems, so called ‘polysaccharide utilizing loci’ (PULs) (Martens *et al*., 2009). The chitinases in these systems likely differ in their structure so much that the primer pair used in this project failed to detect them. In addition, the phylogenetic analysis of the obtained *chiA* sequences revealed a high genetic and structural heterogeneity (3.1.6.). That, together with the low amount of good reference *chiA* sequences available in public databases, hindered a high phylogenetic resolution in most cases (3.1.6.). TRFLP is a high-throughput fingerprinting technique, i.e. it allows the simultaneous analysis of microbial community structure and composition of several samples (Liu *et al*. 1997; Marsh 1999, 2005; Nocker *et al*., 2010; Schütte *et al*., 2008; Thies 2007). Therefore, it was chosen to rapidly monitor changes in the abundance and composition of *chiA* phylotypes in response to the supplementation of chitin. However, an inherent problem of this method is that the phylogenetic assignment of the TRFs strongly depends on the quality of the reference database. As mentioned above, compared to other functional gene markers (e.g. *pmoA*), the

amount of *chiA* references sequences in public databases is relatively low, largely due to the small interest of researchers in chitin degradation. That issue likely is going to be minimized or eliminated in future when genome sequencing will be a prerequisite for the publication of validate described species and the quality of annotations will further increase. Read lengths and quality of NGS techniques are steadily increasing while at the same time the costs are decreasing and allow a precise taxonomic identification (de la Fuente *et al*., 2014; Franzosa *et al*., 2015; Mardis 2013; Metzker 2010; Shendure & Ji 2008; Shokralla *et al*., 2012). Thus, NGS amplicon sequencing is the state-of-the-art fingerprinting method for the study of microbial communities in various environments and/or the impact of various factors on them. This was clearly reinforced by results obtained in the present doctoral thesis.

In order to identify known and novel degraders of chitin under *in situ* near conditions a SIP experiment using [^{13}C]-chitin was conducted (3.2.). Consumers of [^{13}C]-chitin derived carbon were enriched in the [^{13}C]-isotope and this 'labeling' could be detected by different methods depending on the marker of interest, i.e. rRNA, mRNA, DNA or protein. Like any other method, stable isotope probing has its limitations that should be considered (Neufeld *et al*., 2007a). During the centrifugation step unlabeled RNA can migrate into 'heavy' fractions whereby in particular RNA with a high GC content is concerned (Lueders *et al*., 2004; Manefield *et al*. 2002a,b; Neufeld *et al*., 2007a; Radajewski *et al*. 2003). An increased RNA content in the 'heavy' fractions of the [^{13}C]-chitin treatment compared to the [^{12}C]-chitin treatment was a good physical indicator for the enrichment of RNA in the [^{13}C]-isotope (Fig. 8; 2.5.6.5.). A solid proof would have been obtained by determining the δ^{13}C value by IRMS as it was done in the initial publication of RNA-SIP (Manefield *et al*., 2002b). However, isotopic enrichment was confirmed indirectly by a comparative amplicon pyrosequencing-based 16S rRNA stable isotope probing (CAP-SIP) approach (Dallinger *et al*., 2014; 2.7.4.; 3.2.2.1., 3.2.2.2.).

In protein-stable isotope probing (protein-SIP) the incorporation of the [^{13}C]-isotope in protein is analyzed. Protein-SIP is much more sensitive than DNA/RNA-SIP, i.e. ~2 at. % compared to 25–30 at. % of [^{13}C]-isotope incorporation is required for successful labeling (Jehmlich *et al*., 2010). The fundamental strength of this technique, however, is that the analysis of proteins enables to link metabolic function to phylogenetic information (Jehmlich *et al*., 2010; Seifert *et al*., 2012). Here, results of the protein-SIP were non-satisfying and did not allow a comparable taxonomic resolution as the RNA SIP approach. In total, 23 labeled peptides were detected (3.2.6.). Unfortunately, useful phylogenetic and functional information could be assigned to only three of the peptides (3.2.6.). Most of the remaining [^{13}C]-labeled peptides were assigned to chaperones with unclear phylogeny. The success of a protein SIP experiment strongly depends on the nature of sample. Environmental samples, like

agricultural soils, contain organic and inorganic contaminations (e.g. iron precipitations) which likely occurred in the investigated soil and can reduce the protein extraction efficiency (Seifert *et al*., 2012). The investigated soil was rich in iron (3.2.1.2.), which could explain the problems in the protein extraction. Beside an optimized protein extraction, another prerequisite for a successful protein-SIP analysis is a low complexity in the investigated system with preferably less than 30 species (Seifert *et al*., 2012). Natural soils are, however, rather complex ecosystems and numbers of up to 10 x 10^9 microorganisms of 6,000 different genomic species per gram soil have been reported (Øvreås 2000; Rosselló-Mora & Amann 2001). In the present study, up to 150 family level OTUs were detected (Fig. S1). Thus, the complexity of the investigated soil likely exceeded the limits of the applied protein-SIP protocol and technology. The efficiency of peptide identification in a protein-SIP experiment can be increased by the use of a high coverage metagenome as reference database (e.g. Delmotte *et al*., 2009). In order to increase the likelihood of identifying [^{13}C]-labeled peptides and to reduce the sequencing effort, the metagenome was created from the 'heavy' fractions of a DNA-SIP (2.5.9.). This strategy obviously could not foil the limits due to system complexity as indicated by the low number of identified peptides, likely because the coverage of the metagenome was insufficient.

4.7. Conclusions and conceptual models

Supplemental chitin was readily degraded in agricultural soil slurries under oxic and anoxic conditions. The lack of response of the soil microbial community to supplementation of chitosan indicated that chitin degradation in aerated soils occurs without prior deacytelation to chitosan supporting *Hypothesis 1* (1.7.). Chitin was degraded differentially under oxic and anoxic conditions.

Under oxic conditions chitin was mineralized to carbon dioxide. In the first ten days of anaerobic chitin degradation, different subsets of the soil microbial community conserved energy from chitin hydrolysis products by nitrate and ferric iron respiration as well by fermentative metabolisms. When concentrations of alternative electron acceptors became limiting, growth supported by fermentative metabolisms became predominant. Few key chitinolytic taxa, i.e. *Pseudomonas* and *Massilia*, were responsible for most of the chitin degradation under oxic conditions. Furthermore, several family taxa of *Bacteroidetes* with known chitinolytic representatives incorporated substantial amounts of [^{13}C]-chitin derived carbon underlining the ecological role of *Bacteroidetes* in the degradation of complex polysaccharides. Excess chitin hydrolysis products were not detectable due to consumption by 'satellite microbes' such as *Caulobacter*. The stimulation of primary consumers and 'satellite microbes' triggered predation by bacteriovorus *Bacteriovoraceae*, *Bdellovibrionaceae* and uncultured *Myxococcales* that likely incorporated [^{13}C]-chitin derived carbon from prey cell content. How *Planctomycetes* and *Verrucomicrobia* obtained their label is difficult to answer and their ecological function in the investigated chitinolytic food web remains enigmatic. Several results of this doctoral thesis and some literature evidence can be interpreted in favor for a direct involvement of *Planctomycetes* in chitin degradation. However, recent findings provided the basis for an alternative, more attractive, explanation. *Planctomycetes* and *Verrucomicrobia* could have obtained their label either by degradation of exopolysaccharides or by the degradation of cell wall polysaccharides. Thus, their ecological function might be saprotrophic degradation of complex heteropolysaccharides of microbial origin.

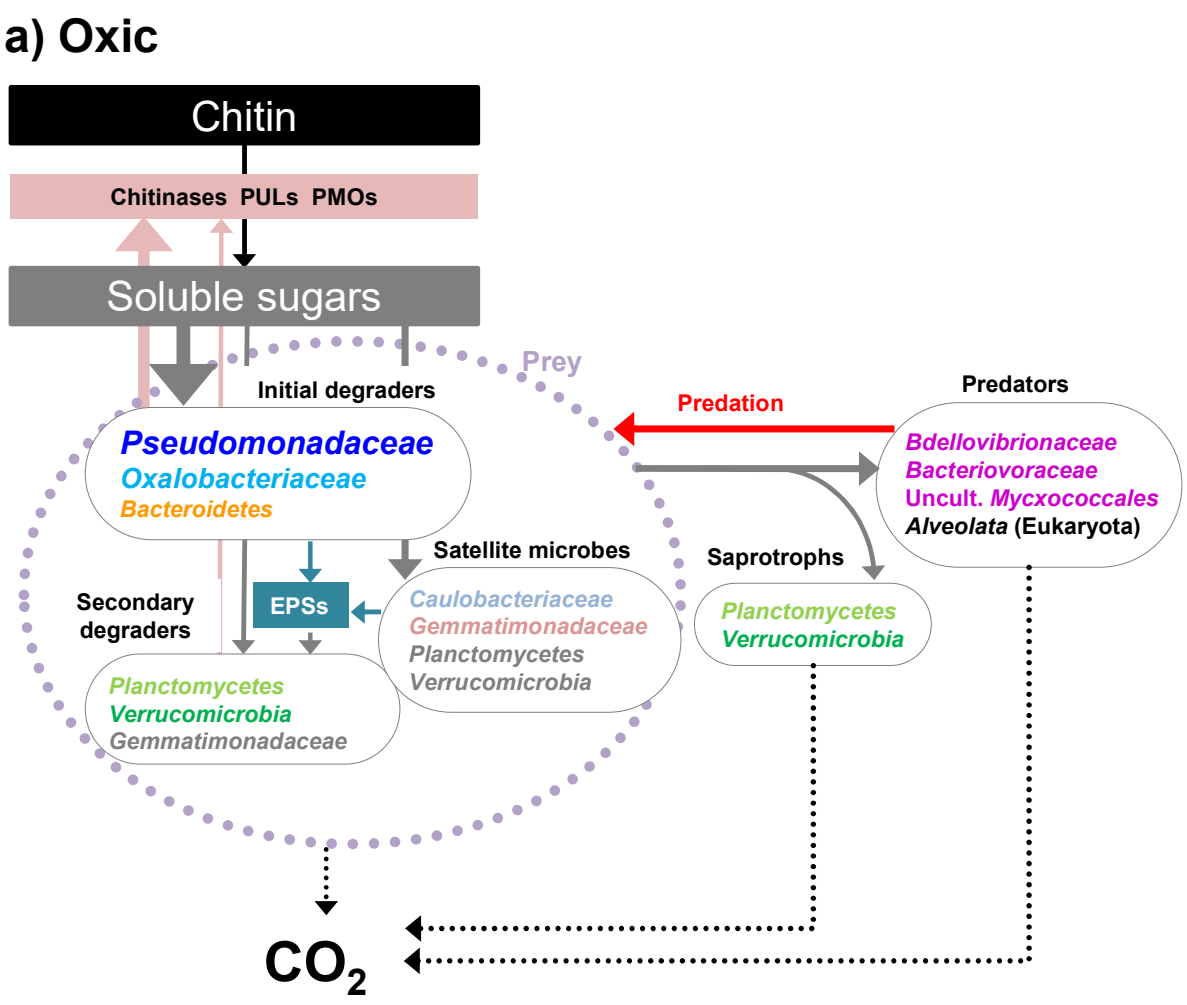

Figure 37. Conceptual model of trophic interactions of the soil microbiome degrading chitin under oxic conditions based on experimental observations and literature. Solid grey lines and arrows indicate the source of carbon and energy. Rose lines and arrows indicate production of enzymes involved in the degradation of homo- and heteropolysaccharides. PMOs, polysaccharide monooxygenases. PULs, polysaccharide utilizing loci. EPSs, exopolysaccharides. Dotted black lines and arrows indicate detectable metabolism products. Grey font indicates weak experimental and/or literature evidence. Colors of taxa, same color code as used in Fig. 25.

Chitin was also readily degradable under anoxic conditions, but degradation was slow compared to oxic conditions. Recently discovered PMOs boost the degradation of polysaccharides such as chitin and cellulose by oxidative cleavage of the bondage between the sugar units. Therefore, slow degradation under anoxic conditions can be explained by inactivity of PMOs as they require oxygen for their enzymatic mechanism. Initial degradation of chitin was characterized by low amounts of degradation products and a low labeling ratio. Thus, in contrast to oxic conditions, chitinolytic *Bacteria* initially responding to chitin under anoxic conditions were of minor importance for the overall degradation. Overall, different members of the soil microbiome were labeled by the assimilation of [^{13}C]-chitin derived carbon under anoxic conditions. In addition, also the mode of trophic interactions differed to oxic conditions.

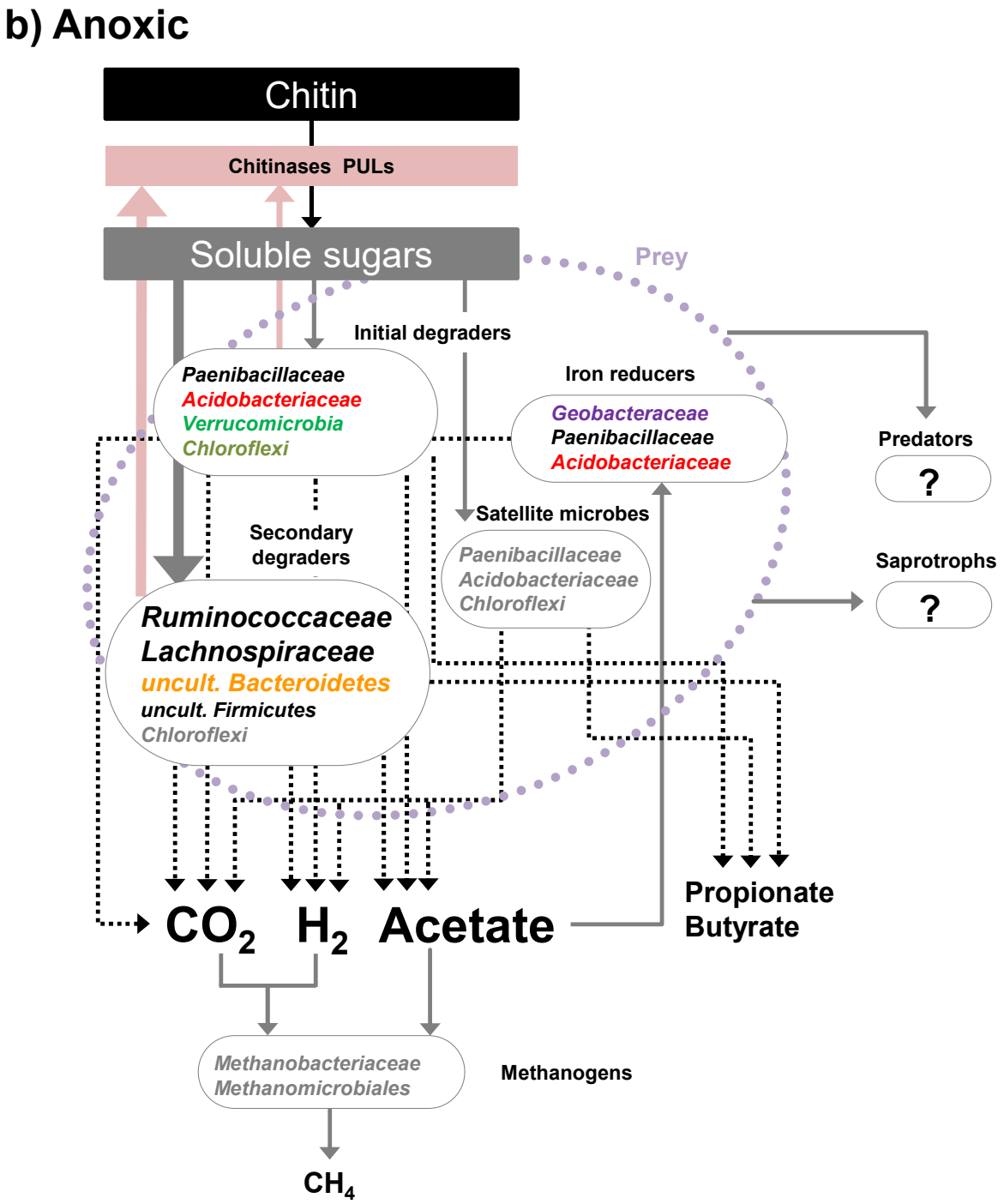

Figure 38. Conceptual model of trophic interactions of the soil microbiome degrading chitin under anoxic conditions based on experimental observations and literature. Solid grey lines and arrows indicate the source of carbon and energy. Rose lines and arrows indicate production of enzymes involved in the degradation of homo- and heteropolysaccharides. PULs, polysaccharide utilizing loci. Dotted black lines and arrows indicate detectable metabolism products. Grey font indicates weak experimental and/or literature evidence. Colors of taxa, same color code as used in Fig. 26.

The accumulation of fermentation products stimulated the activity of iron reducing *Geobacteraceae* and methanogenic *Archaea*. No evidence for prey-predator or saprotrophic interactions was observed in the course of the experiment. Thus, the collective data of the oxic and anoxic experiments with supplemental [^{13}C]-chitin reinforced the *Hypothesis 2* and *3* (1.7.).

The collective data demonstrate that although different taxa were involved in the degradation of chitin, it was readily degradable under oxic and anoxic condition. Thus, the soil microbiome was prone to utilize chitin and functionally redundant, i.e. the highly variable catabolic diversity enabled continued biopolymer degradation despite fluctuations of oxygen concentration. The insights that were gained into the trophic interactions of a chitin-degrading microbiome improve the understanding of turnover dynamics of chitin and the stabilization mechanisms of organic matter in soil, which is important to predict future soil carbon dynamics.

4.8. Future perspectives

Time resolved analysis of 16S rRNA in a [^{13}C]-chitin SIP probing experiment revealed that bacterial taxa and trophic interactions differed during the degradation of chitin under oxic and anoxic conditions. Under oxic conditions clear ecological functions were assigned to labeled taxa for which a good understanding of physiological capabilities and ecological function already existed. *Beta-* and *Gammaproteobacteria* and *Bacteroidetes* likely were responsible for most of the chitin degradation, labeled *Caulobacteraceae* functioned as satellite microbes and *Deltaproteobacteria* were preying on the chitinolytic primary degraders and satellite microbes. The role of labeled *Planctomycetes* and *Verrucomicrobia*, however, is unclear. A potential ecological niche of *Planctomycetes* and *Verrucomicrobia* might be the degradation of complex heteropolysaccharides that can be found in EPSs and cell walls (Datta *et al*., 2016; Wang *et al*., 2015; 4.2.1.2.) and is currently the favored explanation for the labeling. Thus, future studies should focus on the ecological function of these intriguing taxa. A SIP experiment with [^{13}C]-labeled EPSs analogues to the experiment of Wang *et al*. 2015 can be conducted using the same soil as investigated in the present study in order to strengthen this hypothesis. In addition, EPSs or other forms of complex polysaccharides can be potentially used to enrich and finally isolate new planctomycetic and verrucomicrobial species. Alternatively, catabolic abilities of cultivated members can be reinvestigated. The hypothesis that *Planctomycetes* and *Verrucomicrobia* degrade cell wall materials can be studied analogously to experiments conducted in the Kästner lab (Kindler *et al*., 2006, 2009; Miltner *et al*., 2009, 2012) where [^{13}C]-labeled *Escherichia coli* cells or cell components (amino

acids, fatty acids) were supplemented to soil to study the contribution of the cell material to the formation of soil organic matter (SOM). Unfortunately, microbial taxa assimilating [^{13}C]-*E.coli* derived carbon were not identified in the aforementioned studies. However, this leaves the window open for interesting findings in future studies.

Under anoxic conditions, uncultured *Bacteroidetes* incorporated substantial amounts of [^{13}C]-chitin-derived carbon and likely were important (obligate) anaerobic degraders of chitin. Therefore, it would be worthwhile to develop a 'targeted' isolation approach. A starting point could be the use of anoxic enrichment cultures supplemented with chitin. Cells numbers could be monitored by qPCR or FISH (Hirsch *et al*., 2010; Wagner *et al*., 2003; Zwirglmaier 2005) and isolates finally may be obtained by the serial dilution technique combined with appropriate media (Overmann 2013).

Soon after the first DNA/RNA-SIP experiments targeting 16S rRNA were successfully conducted, first considerations and experiments were made to combine DNA-SIP with metagenomics (Friedrich 2006; Radajewski *et al*., 2003; Wellington *et al*., 2003). Yet, metagenomic analysis was restricted by the limitations of available molecular methods, i.e. metagenome libraries were created by cloning of larger DNA fragments into bacterial artificial chromosome (BAC). Consequently, large numbers of clones had to be screened to find a gene of interest and often it was not possible to clearly identify the taxonomy of the detected genes. With the progress of NGS-technologies (de la Fuente *et al*., 2014; Franzosa *et al*., 2015; Mardis 2013; Metzker 2010; Shendure & Ji 2008; Shokralla *et al*., 2012), however, the idea to streamline metagenomic analysis by the use DNA-SIP was revived (Chen & Murrell 2010; Coyotzi *et al*., 2016).

In the present doctoral project, a DNA-SIP derived metagenome was generated in order to increase the likelihood of peptide identification (2.5.9.; Delmotte *et al*., 2009; Jehmlich *et al*., 2010; Seifert *et al*., 2012) while analysis of the metagenome was not in focus. Because of that, DNA extracts of the oxic and anoxic incubations from two different time points were pooled for cesium chloride density gradient centrifugation (2.5.9.). DNA of 'heavy' fractions was amplified by multiple displacement amplification, Illumina-sequenced and assembled into 33.039 contigs (2.5.9.). With a similar approach, however tailored for purpose of metagenome analysis, a near-complete genome of an uncultured *Methylophaga* species was recovered (Grob *et al*., 2015). This was possible, among other things, because of the researchers´ choice to study the metabolically unique methylotrophic *Bacteria*. *Methylophaga* species were predominantly assimilating supplemented [^{13}C]-methanol and, thus, represented 97% of total 16S rRNA gene sequences present in [^{13}C]-DNA. This enrichment of *Methylophaga* DNA facilitated the assembly and finally enabled to retrieve a near-complete genome (Grob *et al*., 2015). In the present doctoral project, [^{13}C]-chitin derived

carbon was assimilated by various taxa. Thus, together with artificial increase of diversity caused by DNA pooling (see above), the diversity of investigated chitin degrading microbiome was high and limited the assembly. Binning, i.e. grouping reads or contigs and assigning them to operational taxonomic units prior assembly, can help to circumvent the limitations of metagenomic analysis of ecosystems with a high diversity (Albertsen *et al*., 2013; Alneberg *et al*., 2014; Sangwan *et al*., 2016). By now, the power of binning has been demonstrated in many studies, in which draft or near-fully assembled genomes where recovered from complex environmental samples, including soil (Delmont *et al*., 2015; Edwards *et al*., 2017; Evans *et al*., 2015; Haroon *et al*., 2016; Speth *et al*., 2016; van Kessel *et al*., 2015). Therefore, DNA-SIP combined with differential abundance binning is in a promising approach to retrieve (near) fully assembled genomes from metagenomes when relatively few microbial community members are labeled (Coyotzi *et al*., 2016). For example, this approach might have been used to potentially assemble the genome(s) of the uncultured *Bacteroidetes* that were labeled under anoxic conditions or of the *Planctomycetes* and *Verrucomicrobia* that were labeled under oxic conditions in this project.

Only potential trophic interactions resulting from prolonged incubation under either oxic or anoxic conditions were investigated. The concentration of oxygen in aerated soils, however, is spatially and temporally dynamic (Or *et al*., 2007). Oxic and anoxic microzones can co-exist in close proximity to each other and oxic-anoxic periods alternate (Küsel & Drake 1995; Or *et al*., 2007; Pett-Ridge & Firestone 2005; Picek *et al*., 2000; Wagner *et al*.,1996). Yet, the important link between aerobic and anaerobic metabolisms was not investigated in this study and should be addressed by future studies. In order to study that, fluctuating availabilities of oxygen could be imposed on chitin-supplemented and unsupplemented agricultural soil slurries by an approach similar to a previous study (Schellenberger *et al*., 2011). Of interest might be the identification of the consumers of chitin-derived fermentation products (e.g. acetate) after reoxygenation of the soil, the carbon flow of chitin derived carbon via (short) altering oxic and anoxic periods, or chitin degradation under microaerophilic (2-10% oxygen) conditions. In addition, predation/fate of taxa that were active under anoxic conditions after reoxygenation might be resolved.

Finally, it is likely that dynamics of chitin degradation and trophic interactions under *in situ* close conditions differ. Thus, future studies should consider the use of naturally occurring forms of chitin (e.g. complexed in the cell walls of fungi or insects) and undisturbed soil to address the following questions: How much chitin derived carbon escapes the turnover in soil microbiomes and in which forms is it stabilized under *in situ* close conditions? What are the effects of rising temperatures and land use management on the soil microbiomes and the turnover dynamics of chitin? These are important questions as global mean temperature is

predicted to increase by 2–7°C in the next 100 years and ‘recalcitrant’ organic matter is believed to be more sensitive to changes of temperature than ‘labile’ organic matter (Dungait *et al*., 2012; Kleber 2010; von Lützow *et al*., 2006, 2008). The world ocean is another important ecosystem where chitin is produced in vast numbers and its degradation occurs in oxic (e.g. oxygenated zones of the water column) and anoxic (e.g. sediments) (Beier & Bertilsson 2013; Datta *et al*., 2016; Gooday 1990a). Global warming and the rise of the atmospheric carbon dioxide concentration have already dramatic effects on this ecosystem, manifested in ocean acidification, deoxygenation and expanding oxygen-minimum zones, and increasing mean water temperatures (Bijma *et al*., 2013; Doney *et al*., 2012; Gruber 2011; Levitus *et al*., 2000; Stramma *et al*., 2008). Crucial challenges remain in the understanding and modelling of the effects of climate change (Bijma *et al*., 2013; Doney *et al*., 2012; Dungait *et al*., 2012; Gruber 2011). How will the microbiomes of terrestrial and aquatic ecosystems adapt to these changes in terms of biopolymer turnover?

5. Summary

Chitin is the second most abundant polysaccharide after cellulose and is subject to rapid microbial turnover in the environment. Microbial degradation of chitin in soil substantially contributes to carbon cycling and release in terrestrial ecosystems. In aerated soil ecosystems, chitin occurs as a structural component in protists, arthropods, and fungi. Thereby, fungi represent the main source of chitin in such soils as fungi have cell walls with up to 25% chitin and account for up to 60-90% of the microbial biomass in aerated soils. Chitin degradation can theoretically occur via two major degradation pathways. It can be deacetylated to chitosan or can be hydrolyzed to *N*,*N´*-diacetylchitobiose and oligomers of *N*-acetylglucosamine by aerobic and anaerobic microorganisms. Which pathway of chitin hydrolysis is preferred by soil microbiomes was unknown prior to this thesis. Therefore, processes, metabolic responses and degradation products associated with chitin and chitosan hydrolysis were assessed. Chitin was immediately broken down by the tested microbiome, but chitosan only with a considerable time delay, which suggests that the microbiome is adjusted to chitin as a substrate, and the degradation of chitin probably likely does not take place via the deacetylation to chitosan. Another objective of this study was to study the trophic interactions and dynamics of members of a chitin-degrading microbiome and the influence of oxygen on the carbon flow from chitin degradation, as these topics are largely uninvestigated in aerated soils. Therefore, a time-resolved 16S rRNA stable isotope probing experiment was conducted to label and identify those members of a soil microbiome that are involved in the aerobic and anaerobic degradation of chitin. [^{13}C]-chitin was largely mineralized within 20 days, and *Cellvibrio*, *Massilia*, and several *Bacteroidetes* families were identified as initial active chitin degraders under oxic conditions. Subsequently, *Planctomycetes* and *Verrucomicrobia* were labeled by assimilating carbon either directly from chitin or from the degradation of cell wall polysaccharides, biofilm-associated exopolysaccharides, and small metabolic byproducts of chitinolytic bacteria. Bacterial predators (e.g., *Bdellovibrio* and *Bacteriovorax*) were labeled and non-labeled micro-eukaryotic predators (*Alveolata*) increased in relative abundance towards the end of the incubation (70 days), indicating that chitin degraders were subject to predation. Under anoxic conditions, trophic interactions differed substantially compared to oxic conditions. Various fermentation types occurred along with iron respiration. While *Acidobacteria* and *Chloroflexi* were initially labeled, *Firmicutes* and uncultured *Bacteroidetes* were predominantly labeled, suggesting that the latter two bacterial groups were mainly responsible for the degradation of chitin, and also provided substrates for iron reducers. The collective data indicated (a) that hitherto unrecognized *Bacteria* were involved in the chitin-degrading food web of an agricultural soil, (b) that trophic interactions of the chitin-degrading microbial food web were

substantially shaped by the oxygen availability, and (c) that predation was restricted to oxic conditions. The functional redundancy of the soil microbiome and the catabolic diversity likely enable continued biopolymer degradation independent of oxygen concentration. Furthermore, chitin was readily and nearly completely degraded, suggesting that chitin is not as recalcitrant as it is sometimes believed to be. Thus, ‘recalcitrance’ of chitin is relative, rather than absolute and a matter of accessibility to the soil microbiome that is collectively adapted to degrade ubiquitous and abundant naturally occurring structural polysaccharides like chitin and cellulose.

6. Zusammenfassung

Chitin ist nach Cellulose das zweithäufigste Polysaccharid und unterliegt einem schnellen mikrobiellen Umsatz in der Umwelt. Der mikrobielle Abbau von Chitin im Boden trägt wesentlich zum Kohlenstoffkreislauf und zur Freisetzung von Kohlenstoff im terrestrischen Ökosystem bei. Chitin kommt in belüfteten Bodenökosystemen als Strukturkomponente in Protisten, Arthropoden und Pilzen vor. Dabei stellen Pilze die Hauptquelle von Chitin in solchen Böden dar, da pilzliche Zellwände bis zu 25% Chitin enthalten und Pilze bis zu 60-90% der mikrobiellen Biomasse in belüfteten Böden ausmachen. Der Abbau von Chitin kann theoretisch über zwei generelle Abbaupfade erfolgen. Es kann zu Chitosan deacetyliert werden oder durch aerobe und anaerobe Mikroorganismen zu *N*,*N*'-Diacetylchitobiose und Oligomeren von *N*-Acetylglucosamin hydrolysiert werden. Welcher Weg des Chitin-Abbaus von Bodenmikrobiomen bevorzugt wird, ist unbekannt. Daher wurden in dieser Arbeit die mit der Hydrolyse von Chitin, Chitosan und deren Hydrolyseprodukten verbunden Prozesse und metabolischen Reaktionen untersucht. Chitin wurde durch das untersuchte Mikrobiom sofort abgebaut, während der Abbau von Chitosan mit erheblicher zeitlicher Verzögerung ablief. Dies bedeutet, dass das Mikrobiom auf Chitin als Substrat eingestellt ist, und dass der Abbau von Chitin wahrscheinlich nicht über die Deacetylierung zu Chitosan erfolgt. Ein weiteres Ziel dieser Arbeit war es, die trophischen Wechselwirkungen und die Dynamik von Mitgliedern eines chitinabbauenden Mikrobioms sowie der Einfluss von Sauerstoff auf den aus dem Chitinabbau resultierenden Kohlenstoffffluss in belüfteten Böden zu untersuchen, da bislang wenig darüber bekannt ist. Daher wurde ein zeitaufgelöstes 16S-rRNA-Stabile Isotopenbeprobung-Experiment durchgeführt, um diejenigen Mitglieder eines Bodenmikrobioms zu markieren und zu identifizieren, die an dem aeroben und anaeroben Abbau von Chitin beteiligt sind. [^{13}C]-Chitin wurde innerhalb von 20 Tagen weitgehend mineralisiert, und *Cellvibrio*, *Massilia* und mehrere *Bacteroidetes*-Familien wurden als initiale aktive chitinolytische Mikroben unter oxischen Bedingungen identifiziert. Anschließend wurden *Planctomyceten* und *Verrucomicrobia* durch die Assimilierung von Kohlenstoff entweder direkt aus Chitin oder aus dem Abbau von Zellwand-Polysacchariden, Biofilm-assoziierten Exopolysacchariden und von chitinolytischen Bakterien produzierten metabolischen Nebenprodukten markiert. Bakterielle Prädatoren (z.B. *Bdellovibrio* und *Bacteriovorax*) wurden markiert und nicht markierte mikro-eukaryotische Prädatoren (*Alveolata*) erhöhten sich gegen Ende der Inkubation (70 Tage) in der relativen Abundanz, was darauf hinweist, dass chitinolytische Mikroben als Nahrungsquelle für Prädatoren dienten. Die trophischen Wechselwirkungen unter anoxischen Bedingungen unterschieden sich, im Vergleich zu den oxischen Bedingungen, erheblich. Verschiedene Fermentationstypen traten zusammen mit der Eisenatmung auf. Während anfänglich

Acidobacteria und *Chloroflexi* geringfügig markiert wurden, wurden später *Firmicutes* und unkultivierte *Bacteroidetes* deutlich markiert, was darauf hindeutet, dass die beiden letztgenannten Bakteriengruppen hauptsächlich für den Abbau von Chitin verantwortlich waren und möglicherweise auch Substrate für die Eisenreduzierer zur Verfügung stellten. Zusammengenommen zeigten die Daten, (a) dass bisher dafür unbekannte Bakterien am Abbau von Chitin und dem damit verbundenen Nahrungsnetz eines Ackerbodens beteiligt waren, (b) dass die trophischen Wechselwirkungen in dem chitinabbauenden mikrobiellen Nahrungsnetz im Wesentlichen durch die Sauerstoffverfügbarkeit bestimmt wurden und (c), dass Prädation nur unter oxischen Bedingungen eine Rolle spielte. Die funktionelle Redundanz des Bodenmikrobioms und die katabole Vielfalt ermöglichen trotzdem einen kontinuierlichen Biopolymerabbau unabhängig von der Sauerstoffkonzentration. Darüber hinaus wurde Chitin schnell und fast vollständig abgebaut, was darauf hindeutet, dass Chitin nicht so schwierig abzubauen ist, wie es manchmal angenommen wird. Daher ist die "schlechte Abbaubarkeit" von Chitin eher relativ als absolut und eine Frage der Zugänglichkeit für das Bodenmikrobiom, das kollektiv angepasst ist, um allgegenwärtige und reichlich vorhandene strukturelle Polysaccharide wie Chitin und Cellulose abzubauen.

7. References

Aaij C, **Borst P (1972)** The gel electrophoresis of DNA. *Biochim Biophys Acta* 269(2):192-200.

Abraham WR, Rohde M, Bennasar A **(2014)** The family *Caulobacteraceae*. In: Rosenberg E, DeLong EF, Lory S, Stackebrandt E, Thompson F (eds). *The Prokaryotes*. Springer: Heidelberg, Germany. pp 179-205.

Achtnich C, Bak F, Conrad R **(1995)** Competition for electron donors among nitrate reducers, ferric iron reducers, sulfate reducers, and methanogens in anoxic paddy soil. *Biol Fertil Soils* 19(1):65-72.

Adrangi S, Faramarzi MA, Shahverdi AR, Sepehrizadeh Z **(2010)** Purification and characterization of two extracellular endochitinases from *Massilia timonae*. *Carbohydr Res* 345(3):402–407.

Adrangi S, **Faramarzi MA (2013)** From bacteria to human: a journey into the world of chitinases. *Biotechnol Adv* 31(8):1786-1795.

Agger JW, Isaksen T, Varnai A, Vidal-Melgosa S, Willats WGT, Ludwig R, Horn SJ, Eijsink VGH, Westereng B **(2014)** Discovery of LPMO activity on hemicelluloses shows the importance of oxidative processes in plant cell wall degradation. *Proc Natl Acad Sci USA* 111(17):6287-6292.

Albertsen M, Hugenholtz P, Skarshewski A, Nielsen KL, Tyson GW, Nielsen PH **(2013)** Genome sequences of rare, uncultured bacteria obtained by differential coverage binning of multiple metagenomes. *Nat Biotechnol* 31(6):533-538.

Allouch J, Helbert W, Henrissat B, Czjzek M **(2004)** Parallel substrate binding sites in a beta-agarase suggest a novel mode of action on double-helical agarose. *Structure* 12(4):623-632.

Alneberg J, Bjarnason BS, de Bruijn I, Schirmer M, Quick J, Ijaz UZ, Lahti L, Loman NJ, Andersson AF, Quince C **(2014)** Binning metagenomic contigs by coverage and composition. *Nat Methods* 11(11):1144-1146.

Altschul SF, Gish W, Miller W, Myers EW, Lipman DJ **(1990)** Basic local alignment search tool. *J Mol Biol* 215(3):403-410.

Amaduzzi F, Bomboi F, Bonincontro A, Bordi F, Casciardi S, Chronopoulou L, Diociaiuti M, Mura F, Palocci C, Sennato S **(2014)** Chitosan-DNA complexes: charge inversion and DNA condensation. *Colloids Surf B Biointerfaces* 114:1-10.

Anders H, Power JF, MacKenzie AD, Lagutin K, Vyssotski M, Hanssen E, Moreau JW, Stott MB **(2015)** *Limisphaera ngatamarikiensis* gen. nov., sp. nov., a thermophilic, pink-pigmented coccus isolated from subaqueous mud of a geothermal hotspring. *Int J Syst Evol Microbiol* 65(4):1114-1121.

Anderson JPE, **Domsch KH (1973)** Quantification of bacterial and fungal contributions to soil respiration. *Arch Mikrobiol* 93(2):113–127.

Angel R, Claus P, Conrad R **(2012)** Methanogenic archaea are globally ubiquitous in aerated soils and become active under wet anoxic conditions. *ISME J* 6(4):847-862.

Arimori T, Kawamoto N, Okazaki N, Nakazawa M, Miyatake K, Shinya S, Fukamizo T, Ueda M, Tamada T **(2013)** Crystal structures of the catalytic domain of a novel glycohydrolase family 23 chitinase from *Ralstonia* sp. A-471 reveals a unique arrangement of the catalytic residues for inverting chitin hydrolysis. *J Biol Chem* 288(26):18696–18706.

Ashry ESHE, **Aly MRE (2007)** Synthesis and biological relevance of *N*-acetylglucosamine-containing oligosaccharides. *Pure Appl Chem* 79(12):2229–2242.

Atomi H, Fukui T, Kanai T, Morikawa M, Imanaka T **(2004)** Description of *Thermococcus kodakaraensis* sp. nov., a well studied hyperthermophilic archaeon previously reported as *Pyrococcus* sp. KOD1. *Archaea* 1(4):263-267.

Bärlocher F (2008) Biostatistik: Praktische Einführung in Konzepte und Methoden. 2. Auflage. Thieme: Stuttgart, Germany.

Bai Y, Eijsink VG, Kielak AM, van Veen JA, de Boer W **(2016)** Genomic comparison of chitinolytic enzyme systems from terrestrial and aquatic bacteria. *Environ Microbiol* 18(1):38-49.

Balch WE, Fox GE, Magrum LJ, Woese CR, Wolfe RS **(1979)** Methanogens: reevaluation of a unique biological group. *Microbiol Rev* 43(2):260-296.

Baldani JI, Rouws L, Cruz LM, Olivares FL, Schmid M, Hartmann A **(2014)** The family *Oxalobacteraceae*. In: Rosenberg E, DeLong EF, Lory S, Stackebrandt E, Thompson F (eds). *The Prokaryotes*. Springer: Heidelberg, Germany. pp 919-974.

Bastias BA, Anderson IC, Rangel-Castro JI, Parkin PI, Prosser JI, Cairney JW **(2009)** Influence of repeated prescribed burning on incorporation of ^{13}C from cellulose by forest soil fungi as determined by RNA stable isotope probing. *Soil Biol Biochem* 41(3):467-472.

Bauer M, Kube M, Teeling H, Richter M, Lombardot T, Allers E, Würdemann CA, Quast C, Kuhl H, Knaust F, Woebken D, Bischof K, Mussmann M, Choudhuri JV, Meyer F, Reinhardt R, Amann RI, Glöckner FO **(2006)** Whole genome analysis of the marine *Bacteroidetes* '*Gramella forsetii*' reveals adaptations to degradation of polymeric organic matter. *Environ Microbiol* 8(12):2201-2213.

Bayer EA, Morag E, Lamed R **(1994)** The cellulosome – a treasure-trove for biotechnology. *Trends Biotechnol* 12(9):379-386.

Bayer EA, Chanzy H, Lamed R, Shoham Y **(1998)** Cellulose, cellulases and cellulosomes. *Curr Opin Struct Biol* 8(5):548-557.

Bayer EA, Belaich JP, Shoham Y, Lamed R **(2004)** The cellulosomes: multienzyme machines for degradation of plant cell wall polysaccharides. *Annu Rev Microbiol* 58:521-554.

Bayer E, Shoham Y, Lamed R **(2006)** Cellulose-decomposing bacteria and their enzyme systems. In: Dworkin M, Falkow S, Rosenberg E, Schleifer K-H, Stackebrandt E (eds). *The Prokaryotes*. Springer: New York, USA. pp 578–617.

Beeson WT, Vu VV, Span EA, Phillips CM, Marletta MA **(2015)** Cellulose degradation by polysaccharide monooxygenases. *Annu Rev Biochem* 84:923-946.

Beier S, Bertilsson S (2011) Uncoupling of chitinase activity and uptake of hydrolysis products in freshwater bacterioplankton. *Limnol Oceanogr* 56(4):1179-1188.

Beier S, Jones CM, Mohit V Hallin S, Bertilsson S **(2011)** Global phylogeography of chitinase genes in aquatic metagenomes. *Appl Environ Microbiol* 77(3):1101-1106.

Beier S, **Bertilsson S (2013)** Bacterial chitin degradation – mechanisms and ecophysiological strategies. *Front Microbiol* 4:149.

Benhamou N, **Asselin A (1989)** Attempted localization of a substrate for chitinases in plant cells reveals abundant *N*-acetyl-*D*-glucosamine residue in secondary walls. *Biol Cell* 67(3):341-350.

Berg G, **Smalla K (2009)** Plant species and soil type cooperatively shape the structure and function of microbial communities in the rhizosphere. *FEMS Microbiol Ecol* 68(1):1-13.

Berleman JE, Allen S, Danielewicz MA, Remis JP, Gorur A, Cunha J, Hadi MZ, Zusman DR, Northen TR, Witkowska HE, Auer M **(2014)** The lethal cargo of *Myxococcus xanthus* outer membrane vesicles. *Front Microbiol* 5:474.

Berlemont R, **Martiny AC (2015)** Genomic potential for polysaccharide deconstruction in bacteria. *Appl Environ Microbiol* 81(4):1513-1519.

Bernard L, Mougel C, Maron PA, Nowak V, Lévêque J, Henault C, Haichar FZ, Berge O, Marol C, Balesdent J, Gibiat F, Lemanceau P, Ranjard L **(2007)** Dynamics and identification of soil microbial populations actively assimilating carbon from ^{13}C-labelled wheat residue as estimated by DNA-and RNA-SIP techniques. *Environ Microbiol* 9(3):752-764.

Berry D, Mahfoudh KB, Wagner M, Loy A **(2011)** Barcoded primers used in multiplex amplicon pyrosequencing bias amplification. *Appl Environ Microbiol* 77(21):7846-7849.

Bhavanandan VP, **Meyer K (1966)** Mucopolysaccharides: *N*-acetylglucosamine-and galactose-6-sulfates from keratosulfate. *Science* 151(3716):1404-1405.

Bijma J, Pörtner HO, Yesson C, Rogers AD **(2013)** Climate change and the oceans – what does the future hold? *Mar Pollut Bull* 74(2):495-505.

Blachnik R (1998) D'Ans Lax Taschenbuch für Chemiker und Physiker. Vol 3. 4th edn. Springer: Berlin, Germany.

Blumenthal HJ, **Roseman S (1957)** Quantitative estimation of chitin in fungi. *J Bacteriol* 74(2):222-224.

Böck A (2000) Fermentation. In: Lederberg J (ed). Encyclopedia of Microbiology. Vol 20. ^{2nd} edn. Academic press: San Diego, USA. pp 343-349.

Book AJ, Yennamalli RM, Takasuka TE, Currie CR, Phillips GN Jr, Fox BG **(2014)** Evolution of substrate specificity in bacterial AA10 lytic polysaccharide monooxygenases. *Biotechnol Biofuels* 7:109.

Bowman SM, **Free SJ (2006)** The structure and synthesis of the fungal cell wall. *Bioessays* 28(8):799-808.

Boyd A, **Chakrabarty AM (1995)** *Pseudomonas aeruginosa* biofilms: role of the alginate exopolysaccharide. *J Ind Microbiol* 15(3):162-168.

Boyer JN (1986) End products of anaerobic chitin degradation by salt marsh bacteria as substrates for dissimilatory sulfate reduction and methanogenesis. *Appl Environ Microbiol* 52(6):1415-1418.

Boyer JN (1994) Aerobic and anaerobic degradation and mineralization of ^{14}C-chitin by water column and sediment inocula of the York River estuary, Virginia. *Appl Environ Microbiol* 60(1):174-179.

Bragg L, Stone G, Imelfort M, Hugenholtz P, Tyson GW **(2012)** Fast, accurate error-correction of amplicon pyrosequences using Acacia. *Nat Methods* 9(5):425-426.

Braun V, **Hantke K (1974)** Biochemistry of bacterial cell envelopes. *Annu Rev Biochem* 43(1):89-121.

Brune A, Frenzel P, Cypionka H **(2000)** Life at the oxic–anoxic interface: microbial activities and adaptations. *FEMS Microbiol Rev* 24(5):691-710.

Brurberg MB, Synstad B, Klemsdal SS, van Aalten DM, Sundheim L, Eijsink VG **(2001)** Chitinases from *Serratia marcescens*. *Recent Res Dev Microbiol* 5:187-204.

Buckel W (2005) Special clostridial enzymes and fermentation pathways. In: Dürre P (ed). Handbook of *Clostridia*. CRC Press: Boca Raton, USA. pp 122-220.

Bulgarelli D, Schlaeppi Spaepen S, Loren Ver, van Themaat E, Schulze-Lefert P **(2013)** Structure and functions of the bacterial microbiota of plants. *Annu Rev Plant Biol* 64:807-838.

Busk PK, **Lange L (2015)** Classification of fungal and bacterial lytic polysaccharide monooxygenases. *BMC genomics* 16(1):368.

Cabeen MT, **Jacobs-Wagner C (2005)**. Bacterial cell shape. *Nat Rev Microbiol* 3(8):601-610.

Chambers MC, Maclean B, Burke R, Amodei D, Ruderman DL, Neumann S, Gatto L, Fischer B, Pratt B, Egertson J, Hoff K, Kessner D, Tasman N, Shulman N, Frewen B, Baker TA, Brusniak MY, Paulse C, Creasy D, Flashner L, Kani K, Moulding C, Seymour SL, Nuwaysir LM, Lefebvre B, Kuhlmann F, Roark J, Rainer P, Detlev S, Hemenway T, Huhmer A, Langridge J, Connolly B, Chadick T, Holly K, Eckels J, Deutsch EW, Moritz RL, Katz JE, Agus DB, MacCoss M, Tabb DL, Mallick P **(2012)** A cross-platform toolkit for mass spectrometry and proteomics. *Nat Biotechnol* 30(10):918-920.

Cantarel BL, Coutinho PM, Rancurel C, Bernard T, Lombard V, Henrissat B **(2009)** The Carbohydrate-Active EnZymes database (CAZy): an expert resource for Glycogenomics. *Nucleic Acids Res* 37(1):D233-D238.

Chater KF, Biró S, Lee KJ, Palmer T, Schrempf H **(2010)** The complex extracellular biology of *Streptomyces*. *FEMS Microbiol Rev* 34(2):171-198.

Chen J-K, Shen C-R, Liu C-L **(2010)** *N*-acetylglucosamine: production and applications. *Mar Drugs* 8(9):2493-2516.

Chen Y, **Murrell JC (2010)** When metagenomics meets stable-isotope probing: progress and perspectives. *Trends Microbiol* 18(4):157-163.

Chin KJ, Hahn D, Hengstmann U, Liesack W, Janssen PH **(1999)** Characterization and identification of numerically abundant culturable bacteria from the anoxic bulk soil of rice paddy microcosms. *Appl Environ Microbiol* 65(11):5042-5049.

Clarholm M (1981) Protozoan grazing of bacteria in soil-impact and importance. *Microb Ecol* 7(4):343-350.

Cohen-Kupiec R, **Chet I (1998)** The molecular biology of chitin digestion. *Curr Opin Biotechnol* 9(3):270–277.

Collins RE, **Rocap G (2007)** REPK: an analytical web server to select restriction endonucleases for terminal restriction fragment length polymorphism analysis. *Nucleic Acids Res* 35:W58-W62.

Cottrell MT, Moore JA, Kirchman DL **(1999)** Chitinases from uncultured marine microorganisms. *Appl Environ Microbiol* 65(6):2553–2557.

Cottrell MT, **Kirchman DL (2000)** Natural assemblages of marine proteobacteria and members of the Cytophaga-Flavobacter cluster consuming low- and high-molecular-weight dissolved organic matter. *Appl Environ Microbiol* 66(4):1692-1697.

Coughlan MP (1985) Cellulose hydrolysis: the potential, the problems and relevant research at Galway. *Biochem Soc Trans* 13(2):405-406.

Coyotzi S, Pratscher J, Murrell JC, Neufeld JD **(2016)** Targeted metagenomics of active microbial populations with stable-isotope probing. *Curr Opin Biotechnol* 41:1-8.

Cretoiu MS, Kielak AM, Al-Soud WA, Sørensen SJ, van Elsas JD **(2012)** Mining of unexplored habitats for novel chitinases—*chiA* as a helper gene proxy in metagenomics. *Appl Microbiol Biotechnol* 94(5):1347-1358.

Cretoiu MS, Korthals GW, Visser JH, van Elsas JD **(2013)** Chitin amendment increases soil suppressiveness toward plant pathogens and modulates the actinobacterial and oxalobacteraceal communities in an experimental agricultural field. *Appl Environ Microbiol* 79(17):5291-5301.

Cretoiu MS, Kielak AM, Schluter A, van Elsas JD **(2014)** Bacterial communities in chitin-amended soil as revealed by 16S rRNA gene based pyrosequencing. *Soil Biol Biochem* 76:5-11.

Dallinger A, **Horn MA (2014)** Agricultural soil and drilosphere as reservoirs of new and unusual assimilators of 2, 4-dichlorophenol carbon. *Environ Microbiol* 16(1):84-100.

Danishefsky I, Steiner H, Bella A Jr, Friedlander A **(1969)** Investigations on the chemistry of heparin. VI. Position of the sulfate ester groups. *J Biol Chem* 244(7):1741-1745.

Das SN, Sarma PVSRN, Neeraja C, Malati N, Podile AR **(2010)** Members of *Gammaproteobacteria* and *Bacilli* represent the culturable diversity of chitinolytic bacteria in chitin-enriched soils. *World J Microbiol Biotechnol* 26(10):1875-1881.

Dassonville F, Renault P, Valles V **(2004)** A model describing the interactions between anaerobic microbiology and geochemistry in a soil amended with glucose and nitrate. *Eur J Soil Sci* 55(1):29-45.

Datta MS, Sliwerska E, Gore J, Polz MF, Cordero OX **(2016)** Microbial interactions lead to rapid micro-scale successions on model marine particles. *Nat Commun* 7:11965.

Davis KE, Joseph SJ, Janssen PH **(2005)** Effects of growth medium, inoculum size, and incubation time on culturability and isolation of soil bacteria. *Appl Environ Microbiol* 71(2):826-834.

DeBoy RT, Mongodin EF, Fouts DE, Tailford LE, Khouri H, Emerson JB, Mohamoud Y, Watkins K, Henrissat B, Gilbert HJ, Nelson KE **(2008)** Insights into plant cell wall degradation from the genome sequence of the soil bacterium *Cellvibrio japonicus*. *J Bacteriol* 190(15):5455-5463.

de la Fuente G, Belanche A, Girwood SE, Pinloche E, Wilkinson T, Newbold CJ **(2014)** Pros and cons of ion-torrent next generation sequencing versus terminal restriction fragment length polymorphism T-RFLP for studying the rumen bacterial community. *PLoS One* 9(7):e101435.

Dedysh SN (2011) Cultivating uncultured bacteria from northern wetlands: knowledge gained and remaining gaps. *Front Microbiol* 2:184.

Degelmann DM, Kolb S, Dumont M, Murrell JC, Drake HL **(2009)** *Enterobacteriaceae* facilitate the anaerobic degradation of glucose by forest soil. *FEMS Microbiol Ecol* 68(3):312-319.

Delmont TO, Eren AM, Maccario L, Prestat E, Esen ÖC, Pelletier E, Le Paslier D, Simonet P, Vogel TM **(2015)** Reconstructing rare soil microbial genomes using *in situ* enrichments and metagenomics. *Front Microbiol* 6:358.

Delmotte N, Knief C, Chaffron S, Innerebner G, Roschitzki B, Schlapbach R, von Mering C, Vorholt JA **(2009)** Community proteogenomics reveals insights into the physiology of phyllosphere bacteria. *Proc Natl Acad Sci USA* 106(38):16428-16433.

Dimarogona M, Topakas E, Christakopoulos P **(2013)** Recalcitrant polysaccharide degradation by novel oxidative biocatalysts. *Appl Microbiol Biotechnol* 97(19):8455-8465.

Doi RH, **Kosugi A (2004)** Cellulosomes: plant-cell-wall-degrading enzyme complexes. *Nat Rev Microbiol* 2(7):541-551.

Doney SC, Ruckelshaus M, Duffy JE, Barry JP, Chan F, English CA, Galindo HM, Grebmeier JM, Hollowed AB, Knowlton N, Polovina J, Rabalais NN, Sydeman WJ, Talley LD **(2012)** Climate change impacts on marine ecosystems. *Ann Rev Mar Sci* 4:11-37.

Dumonceaux ATJ (2005) What are the principal enzymatic mechanisms by which cellulose and lignin are degraded and their carbon returned to the atmosphere? *IUBMB Life* 57(1):45-47

Dumont MG, **Murrell JC (2005)** Stable isotope probing – linking microbial identity to function. *Nat Rev Microbiol* 3(6):499-504.

Dungait JA, Hopkins DW, Gregory AS, Whitmore AP **(2012)** Soil organic matter turnover is governed by accessibility not recalcitrance. *Glob Change Biol* 18(6):1781-1796.

Drake HL, Horn MA, Wüst PK **(2009)** Intermediary ecosystem metabolism as a main driver of methanogenesis in acidic wetland soil. *Environ Microbiol Rep* 1(5):307-318.

Drake JF, **Tsuchiya HM (1976)** Predation of *Escherichia coli* by *Colpoda steinii*. *Appl Environ Microbiol* 31(6):870-874.

Eckelmann W (2005) Bodenkundliche Kartieranleitung. Bundesanstalt für Geowissenschaften und Rohstoffe in Zusammenarbeit mit den Staatlichen Geologischen Diensten der Bundesrepublik Deutschland. Schweizerbart Science Publishers: Stuttgart, Germany.

Edgar RC, Haas BJ, Clemente JC, Quince C, Knight R **(2011)** UCHIME improves sensitivity and speed of chimera detection. *Bioinformatics* 27(16):2194-2200.

Edwards CR, Onstott TC, Miller JM, Wiggins JB, Wang W, Lee CK, Cary SC, Pointing SB, Lau MCY **(2017)** Draft genome sequence of uncultured upland soil cluster *Gammaproteobacteria* gives molecular insights into high-affinity methanotrophy. *Genome Announc* 5(17):e00047-17.

Egert M, **Friedrich MW (2003)** Formation of pseudo-terminal restriction fragments, a PCR-related bias affecting terminal restriction fragment length polymorphism analysis of microbial community structure. *Appl Environ Microbiol* 69(5):2555-2562.

Eichorst SA, **Kuske CR (2012)** Identification of cellulose-responsive bacterial and fungal communities in geographically and edaphically different soils by using stable isotope probing. *Appl Environ Microbiol* 78(7):2316-2327.

Eisenbeis S, Lohmiller S, Valdebenito M, Leicht S, Braun V **(2008)** NagA-dependent uptake of *N*-acetyl-glucosamine and *N*-acetyl-chitin oligosaccharides across the outer membrane of *Caulobacter crescentus*. *J Bacteriol* 190(15):5230-5238.

Ekelund F, **Rønn R (1994)** Notes on protozoa in agricultural soil with emphasis on heterotrophic flagellates and naked amoebae and their ecology. *FEMS Microbiol Rev* 15(4):321-353.

Erbilgin O, McDonald KL, Kerfeld CA **(2014)** Characterization of a planctomycetal organelle: a novel bacterial microcompartment for the aerobic degradation of plant saccharides. *Appl Environ Microbiol* 80(7):2193-2205.

Erguder TH, Boon N, Wittebolle L, Marzorati M, Verstraete W **(2009)** Environmental factors shaping the ecological niches of ammonia-oxidizing archaea. *FEMS Microbiol Rev* 33(5):855-869.

Erridge C, Bennett-Guerrero E, Poxton IR **(2002)** Structure and function of lipopolysaccharides. *Microbes Infect* 4(8):837-851.

Evans PN, Parks DH, Chadwick GL, Robbins SJ, Orphan VJ, Golding SD, Tyson GW **(2015)** Methane metabolism in the archaeal phylum *Bathyarchaeota* revealed by genome-centric metagenomics. *Science* 350(6259):434-438.

Evvyernie D, Yamazaki S, Morimoto K, Karita S, Kimura T, Sakka K, Ohmiya K **(2000)** Identification and characterization of *Clostridium paraputrificum* M-21, a chitinolytic, mesophilic and hydrogen-producing bacterium. *J Biosci Bioeng* 89(6):596-601.

Falkowski P, Scholes RJ, Boyle E, Canadell J, Canfield D, Elser J, Gruber N, Hibbard K, Högberg P, Linder S, Mackenzie FT, Moore B 3rd, Pedersen T, Rosenthal Y, Seitzinger S, Smetacek V, Steffen W **(2000)** The global carbon cycle: a test of our knowledge of earth as a system. *Science* 290(5490):291-296.

Faramarzi MA, Fazeli M, Yazdi MT, Adrangi S, Al-Ahmadi KJ, Tasharrofi N, Mohseni FA **(2009)** Optimization of cultural conditions for production of chitinase by a soil isolate of *Massilia timonae*. *Biotechnology* 8(1):93-99.

Fenchel T, **Finlay BJ (1990)** Anaerobic free-living protozoa: growth efficiencies and the structure of anaerobic communities. *FEMS Microbiol Lett* 74(4):269-275.

Fenner G (1931) Das Genauigkeitsmaß von Summen, Produkten und Quotienten der Beobachtungsreihe. *Naturwissenschaften* 19(14):310-310.

Fernandez CW, **Koide RT (2012)** The role of chitin in the decomposition of ectomycorrhizal fungal litter. *Ecology* 93(1):24-28.

Fernandez CW, Langley JA, Chapman S, McCormack ML, Koide RT **(2016)** The decomposition of ectomycorrhizal fungal necromass. *Soil Biol Biochem* 93:38-49.

Fierer N, Bradford MA, Jackson RB **(2007)** Toward an ecological classification of soil bacteria. *Ecology* 88(6):1354–1364.

Fiala G, **Stetter KO (1986)** *Pyrococcus furiosus* sp. nov. represents a novel genus of marine heterotrophic archaebacteria growing optimally at 100°C. *Arch Microbiol* 145(1):56-61.

Floudas D, Binder M, Riley R, Barry K, Blanchette RA, Henrissat B, Martínez AT, Otillar R, Spatafora JW, Yadav JS, Aerts A, Benoit I, Boyd A, Carlson A, Copeland A, Coutinho PM, de Vries RP, Ferreira P, Findley K, Foster B, Gaskell J, Glotzer D, Górecki P, Heitman J, Hesse C, Hori C, Igarashi K, Jurgens JA, Kallen N, Kersten P, Kohler A, Kües U, Kumar TK, Kuo A, LaButti K, Larrondo LF, Lindquist E, Ling A, Lombard V, Lucas S, Lundell T, Martin R, McLaughlin DJ, Morgenstern I, Morin E, Murat C, Nagy LG, Nolan M, Ohm RA, Patyshakuliyeva A, Rokas A, Ruiz-Dueñas FJ, Sabat G, Salamov A, Samejima M, Schmutz J, Slot JC, St John F, Stenlid J, Sun H, Sun S, Syed K, Tsang A, Wiebenga A, Young D, Pisabarro A, Eastwood DC, Martin F, Cullen D, Grigoriev IV, Hibbett DS **(2012)** The Paleozoic origin of enzymatic lignin decomposition reconstructed from 31 fungal genomes. *Science* 336(6089):1715-1719.

Flowers HM (1981) Chemistry and biochemistry of D-and L-fucose. *Adv Carbohydr Chem Biochem* 39:279-345.

Foesel BU, Rohde M, Overmann J **(2013)** *Blastocatella fastidiosa* gen. nov., sp. nov., isolated from semiarid savanna soil–The first described species of *Acidobacteria* subdivision 4. *Syst Appl Microbiol* 36(2):82-89.

Foissner W (1993) *Colpodea* (*Ciliophora*). Gustav Fischer: Stuttgart, Germany.

Fontes CM, **Gilbert HJ (2010**) Cellulosomes: highly efficient nanomachines designed to deconstruct plant cell wall complex carbohydrates. *Annu Rev Biochem* 79:655-681.

Forsberg Z, Vaaje-Kolstad G, Westereng B, Bunæs AC, Stenstrøm Y, MacKenzie A, Sørlie M, Horn SJ, Eijsink VG **(2011)** Cleavage of cellulose by a CBM33 protein. *Protein Sci* 20(9):1479-1483.

Forsberg Z, Mackenzie AK, Sørlie M, Røhr AK, Helland R, Arvai AS, Vaaje-Kolstad G, Eijsink VGH **(2014a)** Structural and functional characterization of a conserved pair of bacterial cellulose-oxidizing lytic polysaccharide monooxygenases. *Proc Natl Acad Sci USA* 111(23):8446–8451.

Forsberg Z, Røhr ÅK, Mekasha S, Andersson KK, Eijsink VGH, Vaaje-Kolstad G, Sørlie M **(2014b)** Comparative study of two chitin-active and two cellulose-active AA10-type lytic polysaccharide monooxygenases. *Biochemistry* 53(10):1647-1656.

Franzosa EA, Hsu T, Sirota-Madi A, Shafquat A, Abu-Ali G, Morgan XC, Huttenhower C **(2015)** Sequencing and beyond: integrating molecular 'omics' for microbial community profiling. *Nat Rev Microbiol* 13(6):360-372.

Friedrich MW (2006) Stable-isotope probing of DNA: insights into the function of uncultivated microorganisms from isotopically labeled metagenomes. *Curr Opin Biotechnol* 17(1):59-66.

Fuka MM, Engel M, Gattinger A, Bausenwein U, Sommer M, Munch JC, Schloter M **(2008)** Factors influencing variability of proteolytic genes and activities in arable soils. *Soil Biol Biochem* 40(7):1646-1653.

Fuerst JA, Gwilliam HG, Lindsay M, Lichanska A, Belcher C, Vickers JE, Hugenholtz P **(1997)** Isolation and molecular identification of planctomycete bacteria from postlarvae of the giant tiger prawn, *Penaeus monodon*. *Appl Environ Microbiol* 63(1):254-262.

Fuerst JA, **Sagulenko E (2011)** Beyond the bacterium: planctomycetes challenge our concepts of microbial structure and function. *Nat Rev Microbiol* 9(6):403-413.

Fujita K, Shimomura K, Yamamoto K, Yamashita T, Suzuki K **(2006)** A chitinase structurally related to the glycoside hydrolase family 48 is indispensable for the hormonally induced diapause termination in a beetle. *Biochem Biophys Res Commun* 345(1):502-507.

Gao J, Bauer MW, Shockley KR, Pysz MA, Kelly RM **(2003)** Growth of hyperthermophilic archaeon *Pyrococcus furiosus* on chitin involves two family 18 chitinases. *Appl Environ Microbiol* 69(6):3119-3128.

Garcia R, **Müller R (2014)** The family *Haliangiaceae*. In: Rosenberg E, DeLong EF, Lory S, Stackebrandt E, Thompson F (eds). *The Prokaryotes*. Springer: Heidelberg, Germany. pp 919-974.

Geer LY, Markey SP, Kowalak JA, Wagner L, Xu M, Maynard DM, Yang X, Shi W, Bryant SH **(2004)** Open Mass Spectrometry Search Algorithm. *J Proteome Res* 3(5):958-964.

Geisseler D, Horwath WR, Joergensen RG, Ludwig B **(2010)** Pathways of nitrogen utilization by soil microorganisms – a review. *Soil Biol Biochem* 42(12):2058-2067.

Gleave AP, Taylor RK, Morris BA, Greenwood DR **(1995)** Cloning and sequencing of a gene encoding the 69-kDa extracellular chitinase of *Janthinobacterium lividum*. *FEMS Microbiol Lett* 131(3):279-288.

Godbold DL, Hoosbeek MR, Lukac M, Cotrufo MF, Janssens IA, Ceulemans R, Polle A, Velthorst EJ, Scarascia-Mugnozza G, De Angelis P, Miglietta F, Peressotti A **(2006)** Mycorrhizal hyphal turnover as a dominant process for carbon input into soil organic matter. *Plant Soil* 281(1-2):15-24.

Good IJ (1953) The population frequencies of species and the estimation of population parameters. *Biometrika* 40(3-4):237-264.

Gooday GW (1990a) The ecology of chitin degradation. *Adv Microb Ecol* 11:387-430.

Gooday GW (1990b) Physiology of microbial degradation of chitin and chitosan. *Biodegradation* 1:177-190.

Gougoulias C, Clark JM, Shaw LJ **(2014)** The role of soil microbes in the global carbon cycle: tracking the below-ground microbial processing of plant-derived carbon for manipulating carbon dynamics in agricultural systems. *J Sci Food Agric* 94(12):2362-2371.

Gottschalk G (1986) Bacterial Metabolism. 2nd edn. Springer: New York, USA.

Goy RC, Britto DD, Assis OB **(2009)** A review of the antimicrobial activity of chitosan. *Polímeros* 19(3):241-247.

Grady EN, MacDonald J, Liu L, Richman A, Yuan ZC **(2016)** Current knowledge and perspectives of *Paenibacillus*: a review. *Microb Cell Fact* 15(1):203.

Gray TRG, **Baxby P (1968)** Chitin decomposition in soil. The ecology of chitoclastic microorganisms in forest soil. *Tans Br Mycol Soc* 51:293-309.

Gray TRG, **Bell TF (1963)** The decomposition of chitin in an acid soil. In: (Doeksen J, van der Drift J (eds). Soil Organisms. North Hollabd Publishing Co: Amsterdam, Netherlands. pp 222-230.

Green Mr, **Sambrook J (2012)** Molecular cloning. A laboratory manual. 4th edn. Cold Spring Harbor Laboratory Press: New York, USA.

Greenwood DJ (1961) The effect of oxygen concentration on the decomposition of organic materials in soil. *Plant Soil* 14(4):360-376.

Griffiths RI, Whiteley AS, O'Donnell AG, Bailey MJ **(2000)** Rapid method for coextraction of DNA and RNA from natural environments for analysis of ribosomal DNA- and rRNA-based microbial community composition. *Appl Environ Microbiol* 66(12):5488-5491.

Grob C, Taubert M, Howat AM, Burns OJ, Dixon JL, Richnow HH, Jehmlich N, von Bergen M, Chen Y, Murrell JC **(2015)** Combining metagenomics with metaproteomics and stable isotope probing reveals metabolic pathways used by a naturally occurring marine methylotroph. *Environ Microbiol* 17(10):4007-4018.

Gruber N (2011) Warming up, turning sour, losing breath: ocean biogeochemistry under global change. *Philos Trans A Math Phys Eng Sci* 369(1943):1980-1996.

Guerrero R, Pedros-Alio C, Esteve I, Mas J, Chase D, Margulis L **(1986)** Predatory prokaryotes: predation and primary consumption evolved in bacteria. *Proc Natl Acad Sci USA* 83(7):2138-42.

Guo M, Han X, Jin T, Zhou L, Yang J, Li Z, Chen J, Geng B, Zou Y, Wan D, Li D, Dai W, Wang H, Chen Y, Ni P, Fang C, Yang R **(2012)** Genome sequences of three species in the family *Planctomycetaceae*. *J Bacteriol* 194(14):3740-3741.

Haichar FZ, Achouak W, Christen R, Heulin T, Marol C, Marais MF, Mougel C, Ranjard L, Balesdent J, Berge O **(2007)** Identification of cellulolytic bacteria in soil by stable isotope probing. *Environ Microbiol* 9(3):625-634.

Hamberger A, Horn MA, Dumont MG, Murrell JC, Drake HL **(2008)** Anaerobic consumers of monosaccharides in a moderately acidic fen. *Appl Environ Microbiol* 74(10):3112-3120.

Hammer Ø, Harper DAT, Ryan PD **(2001)** PAST: paleontological statistics software package for education and data analysis. *Palaeontol Electron* 4:1-9.

Haroon MF, Thompson LR, Parks DH, Hugenholtz P, Stingl U **(2016)** A catalogue of 136 microbial draft genomes from Red Sea metagenomes. *Sci Data* 3:160050.

Heck KL, Vanbelle G, Simberloff D **(1975)** Explicit calculation of rarefaction diversity measurement and determination of sufficient sample size. *Ecology* 56(6):459-1461.

Hemsworth GR, Henrissat B, Davies GJ, Walton PH **(2014)** Discovery and characterization of a new family of lytic polysaccharide monooxygenases. *Nat Chem Biol* 10(2):122–126.

Hemsworth GR, Déjean G, Davies GJ, Brumer H **(2016)** Learning from microbial strategies for polysaccharide degradation. *Biochem Soc Trans* 44(1):94-108.

Henrissat B, **Bairoch A (1993)** New families in the classification of glycosyl hydrolases based on amino acid sequence similarities. *Biochem J* 293(3):781-788.

Henrissat B (1994) Cellulases and their interaction with cellulose. Cellulose 1(3):169-196.

Herlemann DPR, Labrenz M, Jürgens K, Bertilsson S, Waniek JJ, Andersson AF **(2011)** Transitions in bacterial communities along the 2000km salinity gradient of the Baltic Sea. *ISME J* 5(10):1571–1579.

Hillman K, Gooday GW, Prosser JI **(1989a)** The mineralization of chitin in the sediments of the Ythan Estuary, Aberdeenshire, Scotland. *Estuar Coast Shelf S* 29(6):601–612.

Hillman K, Gooday GW, Prosser JI **(1989b)** A simple model system for small scale *in vitro* study of estuarine sediment ecosystems. *Lett Appl Microbiol* 4(2):41–44.

Hjort K, Bergström M, Adesina MF, Jansson JK, Smalla K, Sjöling S **(2010)** Chitinase genes revealed and compared in bacterial isolates, DNA extracts and a metagenomic library from a phytopathogen-suppressive soil. *FEMS Microbiol Ecol* 71(2):197-207.

Hirsch PR, Mauchline TH, Clark IM **(2010)** Culture-independent molecular techniques for soil microbial ecology. *Soil Biol Biochem* 42(6):878-887.

Hobel CFV, Marteinsson VT, Hauksdóttir S, Fridjónsson ÓH, Skírnisdóttir S, Hreggvidsson GÓ, Kristjánsson JK **(2004)** Use of low nutrient enrichments to access novel amylase genes in silent diversity of thermophiles. *World J Microbiol Biotechnol* 20(8):801-809.

Hobel CFV, Marteinsson VT, Hreggvidsson GO, Kristjánsson JK **(2005)** Investigation of the microbial ecology of intertidal hot springs by using diversity analysis of 16S rRNA and chitinase genes. *Appl Environ Microbiol* 71(5):2771–2776.

Hopwood DA (2007) *Streptomyces* in nature and medicine: the antibiotic makers. Oxford University Press: New York, USA.

Horn SJ, Sørbotten A, Synstad B, Sikorski P, Sørlie M, Vårum KM, Eijsink VG **(2006)** Endo/exo mechanism and processivity of family 18 chitinases produced by *Serratia marcescens*. *FEBS J* 273(3):491-503.

Horn SJ, Vaaje-Kolstad G, Westereng B, Eijsink VG **(2012)** Novel enzymes for the degradation of cellulose. *Biotechnol Biofuels* 5(1):45.

Howard DM, **Howard PJA (1993)** Relationships between CO_2 evolution, moisture content and temperature for a range of soil types. *Soil Biol Biochem* 25(11):1537-1546.

Hrynkiewicz K, Baum C, Leinweber P **(2010)** Density, metabolic activity, and identity of cultivable rhizosphere bacteria on *Salix viminalis* in disturbed arable and landfill soils. *J Plant Nutr Soil Sci* 173(5):747-756.

Huber R, Stöhr J, Hohenhaus S, Rachel R, Burggraf S, Jannasch HW, Stetter KO **(1995)** *Thermococcus chitonophagus* sp. nov., a novel, chitin-degrading, hyperthermophilic archaeum from a deep-sea hydrothermal vent environment. *Arch Microbiol* 164(4):255–264.

Hult EL, Katouno F, Uchiyama T, Watanabe T, Sugiyama J **(2005)** Molecular directionality in crystalline β-chitin: hydrolysis by chitinases A and B from *Serratia marcescens* 2170. *Biochem J* 388(3):851-856.

Humphry DR, Black GW, Cummings SP **(2003)** Reclassification of *'Pseudomonas fluorescens* subsp. *cellulosa*' NCIMB 10462 (Ueda *et al*. 1952) as *Cellvibrio japonicus* sp. nov. and revival of *Cellvibrio vulgaris* sp. nov., nom. rev. and *Cellvibrio fulvus* sp. nov., nom. rev. *Int J Syst Evol Microbiol* 53(2):393-400.

Hunger S, Schmidt O, Hilgarth M, Horn MA, Kolb S, Conrad R, Drake HL **(2011)** Competing formate- and carbon dioxide-utilizing prokaryotes in an anoxic methane-emitting fen soil. *Appl Environ Microbiol* 77(11):3773-3785.

Hurlbert SH (1971) The nonconcept of species diversity: a critique and alternative parameters. *Ecology* 52(4):577-586.

Ikeda S, Ytow N, Ezura H, Minamisawa K, Miyashita K, Fujimura T **(2007)** Analysis of molecular diversity of bacterial chitinase genes in the maize rhizosphere using culture-independent methods. *Microbes Environ* 22(1):71-77.

Il'ina AV, **Varlamov VP (2005)** Chitosan-based polyelectrolyte complexes: a review. *Appl Biochem Microbiol* 41(1):5-11.

Iseli B, Armand S, Boller T, Neuhaus JM, Henrissat B **(1996)** Plant chitinases use two different hydrolytic mechanisms. *FEBS Lett* 382(1-2):186-188.

Ivanova AO, **Dedysh SN (2012)** Abundance, diversity, and depth distribution of planctomycetes in acidic northern wetlands. *Front Microbiol* 3:5.

Ivanova AA, Naumoff DG, Miroshnikov KK, Liesack W, Dedysh SN **(2017)** Comparative genomics of four *Isosphaeraceae Planctomycetes*: A common pool of plasmids and glycoside hydrolase genes shared by *Paludisphaera borealis* PX4^T, *Isosphaera pallida* IS1B^T, *Singulisphaera acidiphila* DSM 18658^T, and strain SH-PL62. *Front Microbiol* 8:412.

Janssen PH (2006) Identifying the dominant soil bacterial taxa in libraries of 16S rRNA and 16S rRNA genes. *Appl Environ Microbiol* 72(3):1719-1728.

Jansson JK, Neufeld JD, Moran MA, Gilbert JA **(2012)** Omics for understanding microbial functional dynamics. *Environ Microbiol* 14(1):1-3.

Jayakumar R, Chennazhi KP, Muzzarelli RAA, Tamura H, Nair SV, Selvamurugan N **(2010a)** Chitosan conjugated DNA nanoparticles in gene therapy. *Carbohydr Polym* 79(1):1-8.

Jayakumar R, Menon D, Manzoor K, Nair SV, Tamura H **(2010b)** Biomedical applications of chitin and chitosan based nanomaterials—A short review. *Carbohydr Polym* 82(2):227-232.

Jehmlich N, Schmidt F, von Bergen M, Richnow HH, Vogt C **(2008)** Protein-based stable isotope probing (Protein-SIP) reveals active species within anoxic mixed cultures. *ISME J* 2(11):1122-1133.

Jehmlich N, Schmidt F, Taubert M, Seifert J, Bastida F, von Bergen M, Richnow HH, Vogt C **(2010)** Protein-based stable isotope probing. *Nat Protoc* 5(12):1957-1966.

Johnke J, Cohen Y, de Leeuw M, Kushmaro A, Jurkevitch E, Chatzinotas A **(2014)** Multiple micro-predators controlling bacterial communities in the environment. *Curr Opin Biotechnol* 27:185-190.

Joseph SJ, Hugenholtz P, Sangwan P, Osborne CA, Janssen PH **(2003)** Laboratory cultivation of widespread and previously uncultured soil bacteria. *Appl Environ Microbiol* 69(12):7210-7215.

Karlsson M, **Stenlid J (2009)** Evolution of family 18 glycoside hydrolases: diversity, domain structures and phylogenetic relationships. *J Mol Microbiol Biotechnol* 16(3-4):208-223.

Kellner H, **Vandenbol M (2010)** Fungi unearthed: transcripts encoding lignocellulolytic and chitinolytic enzymes in forest soil. *PLoS One* 5(6):e10971.

Keyhani NO, **Roseman S (1999)** Physiological aspects of chitin catabolism in marine bacteria. *Biochim Biophys Acta* 1473(1):108-122.

Kielak AM, Cretoiu MS, Semenov AV, Sørensen SJ, van Elsas JD **(2013)** Bacterial chitinolytic communities respond to chitin and pH alteration in soil. *Appl Environ Microbiol* 79(1):263-272.

Kindler R, Miltner A, Richnow HH, Kästner M **(2006)** Fate of gram-negative bacterial biomass in soil – mineralization and contribution to SOM. *Soil Biol Biochem* 38(9):2860-2870.

Kindler R, Miltner A, Thullner M, Richnow HH, Kästner M **(2009)** Fate of bacterial biomass derived fatty acids in soil and their contribution to soil organic matter. *Org Geochem* 40(1):29-37.

Kirk TK, **Farrell RL (1987)** Enzymatic "combustion": the microbial degradation of lignin. *Annu Rev Microbiol* 41(1):465-505.

Kirschbaum MUF (1995) The temperature dependence of soil organic matter decomposition, and the effect of global warming on soil organic C storage. *Soil Biol Biochem* 27(6):753-760.

Klappenbach JA, Dunbar JM, Schmidt TM **(2000)** rRNA operon copy number reflects ecological strategies of bacteria. *Appl Environ Microbiol* 66(4):1328-1333.

Kleber M (2010) What is recalcitrant soil organic matter? *Environ Chem* 7(4):320-332.

Klindworth A, Pruesse E, Schweer T, Peplies J, Quast C, Horn M, Glockner FO **(2013)** Evaluation of general 16S ribosomal RNA gene PCR primers for classical and next-generation sequencing-based diversity studies. *Nucleic Acids Res* 41(1):e1.

Köllner KE, Carstens D, Keller E, Vazquez F, Schubert CJ, Zeyer J, Bürgmann H **(2012)** Bacterial chitin hydrolysis in two lakes with contrasting trophic statuses. *Appl Environ Microbiol* 78(3):695-704.

Kolb S, Knief C, Stubner S, Conrad R **(2003)** Quantitative detection of methanotrophs in soil by novel *pmoA*-targeted real-time PCR assays. *Appl Environ Microbiol* 69(5):2423-2429.

Kong M, Chen XG, Xing K, Park HJ **(2010)** Antimicrobial properties of chitosan and mode of action: a state of the art review. *Int J Food Microbiol* 144(1):51-63.

Koval SF, Hynes SH, Flannagan RS, Pasternak Z, Davidov Y, Jurkevitch E **(2013)** *Bdellovibrio exovorus* sp. nov., a novel predator of *Caulobacter crescentus*. *Int J Syst Evol Microbiol* 63(1):146-151.

Kowalchuk GA, **Stephen JR (2001)** Ammonia-oxidizing bacteria: a model for molecular microbial ecology. *Annu Rev Microbiol* 55(1):485-529.

Kraft B, Strous M, Tegetmeyer HE **(2011)** Microbial nitrate respiration – genes, enzymes and environmental distribution. *J Biotechnol* 155(1):104-117.

Krsek M, **Wellington EM (2000)** Assessment of chitin decomposer diversity within an upland grassland. *Antonie Van Leeuwenhoek* 79(3-4):261-267.

Kruskal WH, **Wallis WA (1952)** Use of ranks in one-criterion variance analysis. J Am Stat Assoc 47(260):583-621.

Kuroshima KI, Sakane T, Takata R, Yokota A (1996) *Bacillus ehimensis* sp. nov. and *Bacillus chitinolyticus* sp. nov., new chitinolytic members of the genus *Bacillus*. *Int J Syst Evol Microbiol* 46(1):76-80.

Küsel K, **Drake HL (1994)** Acetate synthesis in soil from a Bavarian beech forest. *Appl Environ Microbiol* 60(4):1370-1373.

Küsel K, **Drake HL (1995)** Effects of environmental parameters on the formation and turnover of acetate by forest soils. *Appl Environ Microbiol* 61(10):3667-3675.

Kulichevskaya IS, Belova SE, Kevbrin VV, Dedysh SN, Zavarzin GA **(2007)** Analysis of the bacterial community developing in the course of *Sphagnum* moss decomposition. *Microbiology* 76(5):621-629.

Kulichevskaya IS, Ivanova AO, Baulina OI, Bodelier PL, Damsté JS, Dedysh SN **(2008)** *Singulisphaera acidiphila* gen. nov., sp. nov., a non-filamentous, *Isosphaera*-like planctomycete from acidic northern wetlands. *Int J Syst Evol Microbiol* 58(5):1186-1193.

Kulichevskaya IS, Serkebaeva YM, Kim Y, Rijpstra WI, Damsté JS, Liesack W, Dedysh SN **(2012)** *Telmatocola sphagniphila* gen. nov., sp. nov., a novel dendriform planctomycete from northern wetlands. *Front Microbiol* 3:146.

Kulichevskaya IS, Suzina NE, Rijpstra WI, Sinninghe Damsté JS, Dedysh SN **(2014)** *Paludibaculum fermentans* gen. nov., sp. nov., a facultative anaerobe capable of dissimilatory iron reduction from subdivision 3 of the *Acidobacteria*. *Int J Syst Evol Microbiol* 64(8):2857-2864.

Lage OM, **Bondoso J (2012)** Bringing *Planctomycetes* into pure culture. *Front Microbiol* 3:405.

Lage OM, **Bondoso J (2014)** *Planctomycetes* and macroalgae, a striking association. *Front Microbiol* 5:267.

Lai WA, Hameed A, Lin SY, Hung MH, Hsu YH, Liu YC, Shahina M, Shen FT, Young CC **(2015)** *Paenibacillus medicaginis* sp. nov. a chitinolytic endophyte isolated from the root nodule of alfalfa (*Medicago sativa* L.). *Int J Syst Evol Microbiol* 65(11):3853-3860.

Lal R (2008a) Sequestration of atmospheric CO_2 in global carbon pools. *Energ Environ Sci* 1(1)86-100.

Lal R (2008b) Carbon sequestration. *Philos Trans R Soc Lond B Biol Sci* 363(1492):815-830.

Langley JA, Chapman SK, Hungate BA **(2006)** Ectomycorrhizal colonization slows root decomposition: the post-mortem fungal legacy. *Ecol Lett* 9(8):955-959.

Lareen A, Burton F, Schäfer P **(2016)** Plant root-microbe communication in shaping root microbiomes. *Plant Mol Biol* 90(6):575-587.

LeCleir GR, Buchan A, Hollibaugh JT **(2004)** Chitinase gene sequences retrieved from diverse aquatic habitats reveal environment-specific distributions. *Appl Environ Microbiol* 70(12):6977-6983.

LeCleir GR, Buchan A, Maurer J, Moran MA, Hollibaugh JT **(2007)** Comparison of chitinolytic enzymes from an alkaline, hypersaline lake and an estuary. *Environ Microbiol* 9(1):197-205.

Lee JS, Pyun YR, Bae KS **(2004)** Transfer of *Bacillus ehimensis* and *Bacillus chitinolyticus* to the genus *Paenibacillus* with emended descriptions of *Paenibacillus ehimensis* comb. nov. and *Paenibacillus chitinolyticus* comb. nov. *Int J Syst Evol Microbiol* 54(3):929-933.

Lee KC, Dunfield PF, Morgan XC, Crowe MA, Houghton KM, Vyssotski M, Ryan JL, Lagutin K, McDonald IR, Stott MB **(2011)** *Chthonomonas calidirosea* gen. nov., sp. nov., an aerobic, pigmented, thermophilic micro-organism of a novel bacterial class *Chthonomonadetes* classis nov., of the newly described phylum *Armatimonadetes* originally designated candidate division OP10. *Int J Syst Evol Microbiol* 61(10):2482-2490.

Legendre P, **Legendre L (1998)** Numerical Ecology. 2nd edn. Elsevier Science: Amsterdam, Netherlands.

Lengeler JW, Drews G, Schlegel HG **(1999)** Biology of the prokaryotes. Georg Thieme Verlag: Stuttgart, Germany.

Le Quéré C, Andrew RM, Canadell JG, Sitch S, Korsbakken JI, Peters GP, Manning AC, Boden TA, Tans PP, Houghton RA, Keeling RF, Alin S, Andrews OD, Anthoni P, Barbero L, Bopp L, Chevallier F, Chini LP, Ciais P, Currie K, Delire C, Doney SC, Friedlingstein P, Gkritzalis T, Harris I, Hauck J, Haverd V, Hoppema M, Klein Goldewijk K, Jain AK, Kato E, Körtzinger A, Landschützer P, Lefèvre N, Lenton A, Lienert S, Lombardozzi D, Melton JR, Metzl N, Millero F, Monteiro PMS, Munro DR, Nabel JEMS, Nakaoka S-I, O'Brien K, Olsen A, Omar AM, Ono T, Pierrot D, Poulter B, Rödenbeck C, Salisbury J, Schuster U, Schwinger J, Séférian R, Skjelvan I, Stocker BD, Sutton AJ, Takahashi T, Tian H, Tilbrook B, van der Laan-Luijkx IT, van der Werf GR, Viovy N, Walker AP, Wiltshire AJ, Zaehle S **(2016)** Global carbon budget 2016. *Earth Syst Sci Data* 8(2):605-649.

Leschine SB (1995) Cellulose degradation in anaerobic environments. *Annu Rev Microbiol* 49(1):399-426.

Levasseur A, Drula E, Lombard V, Coutinho PM, Henrissat B **(2013)** Expansion of the enzymatic repertoire of the CAZy database to integrate auxiliary redox enzymes. *Biotechnol Biofuels* 6(1):41.

Levitus S, Antonov JI, Boyer TP, Stephens C **(2000)** Warming of the world ocean. *Science* 287(5461):2225-2229.

Lewis K (2000) Programmed death in bacteria. *Microbiol Mol Biol Rev* 64(3):503-514.

Lewis NG, **Yamamoto E (1990)** Lignin: occurrence, biogenesis and biodegradation. *Annu Rev Plant Physiol Plant Mol Biol* 41(1):455-496.

Li J, Lu Q, Liu T, Zhou S, Yang G, Zhao Y **(2014)** *Paenibacillus guangzhouensis* sp. nov., an Fe(III)- and humus-reducing bacterium from a forest soil. *Int J Syst Evol Microbiol* 64(11):3891-3896.

Liu WT, Marsh TL, Cheng H, Forney LJ **(1997)** Characterization of microbial diversity by determining terminal restriction fragment length polymorphisms of genes encoding 16S rRNA. *Appl Environ Microbiol* 63(11):4516-4522.

Logan NA, **De Vos P (2009)** Genus I. *Bacillus*. In: De Vos P, Garrity GM, Jones D, Krieg NR, Ludwig W, Rainey FA, Schleifer K-H, Whitman WB (eds) *Bergey's Manual of Systematic Bacteriology*. 2nd edn. Springer: New York, USA. pp 21-128.

Lo Leggio L, Simmons TJ, Poulsen JC, Frandsen KE, Hemsworth GR, Stringer MA, von Freiesleben P, Tovborg M, Johansen KS, De Maria L, Harris PV, Soong CL, Dupree P, Tryfona T, Lenfant N, Henrissat B, Davies GJ, Walton PH **(2015)** Structure and boosting activity of a starch-degrading lytic polysaccharide monooxygenase. *Nat Commun* 6:5961.

Lottspeich F, **Engels J (2006)** Bioanalytik. Spektrum Akademischer Verlag: Heidelberg, Germany.

Lovley DR (1991) Dissimilatory Fe (III) and Mn (IV) reduction. *Microbiol Rev* 55(2):259-287.

Lovley DR (1993) Dissimilatory metal reduction. *Annu Rev Microbiol* 47(1):263-290.

Lovley DR (1997) Microbial Fe (III) reduction in subsurface environments. *FEMS Microbiol Rev* 20(3-4):305-313.

Lovley DR, Giovannoni SJ, White DC, Champine JE, Phillips EJ, Gorby YA, Goodwin S **(1993)** *Geobacter metallireducens* gen. nov. sp. nov., a microorganism capable of coupling the complete oxidation of organic compounds to the reduction of iron and other metals. *Arch Microbiol* 159(4):336-344.

Lueders T, **Friedrich M (2000)** Archaeal population dynamics during sequential reduction processes in rice field soil. *Appl Environ Microbiol* 66(7):2732-2742.

Lueders T, Manefield M, Friedrich MW **(2004)** Enhanced sensitivity of DNA- and rRNA-based stable isotope probing by fractionation and quantitative analysis of isopycnic centrifugation gradients. *Environ Microbiol* 6(1):73-78.

Lueders T, Kindler R, Miltner A, Friedrich MW, Kaestner M **(2006)** Identification of bacterial micropredators distinctively active in a soil microbial food web. *Appl Environ Microbiol* 72(8):5342-5348.

Lynd LR, Weimer PJ, Van Zyl WH, Pretorius IS **(2002)** Microbial cellulose utilization: fundamentals and biotechnology. *Microbiol Mol Biol Rev* 66(3):506-577.

Madigan MT, **Martinko JM (2006)** Brock-Biology of Microorganisms. 11th Edition. Pearson Prentice Hall: Upper Saddle River, NJ, USA.

Makarios-Laham I, **Lee TC (1995)** Biodegradability of chitin-and chitosan-containing films in soil environment. *J Environ Polym Degr* 3(1):31-36.

Manefield M, Whiteley AS, Ostle N, Ineson P, Bailey MJ **(2002a)**. Technical considerations for RNA-based stable isotope probing: an approach to associating microbial diversity with microbial community function. *Rapid Commun Mass Spectrom* 16(23):2179-2183.

Manefield M, Whiteley AS, Griffiths RI, Bailey MJ **(2002b)** RNA stable isotope probing, a novel means of linking microbial community function to phylogeny. *Appl Environ Microbiol* 68(11):5367-5373.

Manucharova NA, Yaroslavtsev AM, Senchenko DV, Stepanov AL, Zvyagintsev DG **(2006)** Microbial transformation of chitin in soil under anaerobic conditions. *Biol Bull* 33(2):191-194.

Manucharova NA, Vlasenko AN, Men'ko EV, Zviagintsev DG **(2011)** Specificity of the chitinolytic microbial complex of soils incubated at different temperatures. *Microbiology* 80(2):205-215.

Mardis ER (2013) Next-generation sequencing platforms. *Annu Rev Anal Chem* 6:287-303.

Marschner B, Brodowski S, Dreves A, Gleixner G, Gude A, Grootes PM, Hamer U, Heim A, Jandl G, Ji R, Kaiser K, Kalbitz K, Kramer C, Leinweber P, Rethemeyer J, Schäffer A, Schmidt MWI, Schwark L, Wiesenberg GLB **(2008)** How relevant is recalcitrance for the stabilization of organic matter in soils? *J Plant Nutr Soil Sci* 171(1):91-110.

Marsh TL (1999) Terminal restriction fragment length polymorphism (T-RFLP): an emerging method for characterizing diversity among homologous populations of amplification products. *Curr Opin Microbiol* 2(3):323-327.

Marsh TL (2005) Culture-independent microbial community analysis with terminal restriction fragment length polymorphism. *Methods Enzymol* 397:308-329.

Martens EC, Koropatkin NM, Smith TJ, Gordon JI **(2009)** Complex glycan catabolism by the human gut microbiota: the Bacteroidetes Sus-like paradigm. *J Biol Chem* 284(37):24673-24677.

Martens EC, Kelly AG, Tauzin AS, Brumer H **(2014)** The devil lies in the details: How variations in polysaccharide fine-structure impact the physiology and evolution of gut microbes. *J Mol Biol* 426(23):3851-3865.

Martin HH (1966) Biochemistry of bacterial cell walls. *Annu Rev Biochem* 35(1):457-484.

Martínez JP, Falomir MP, Gozalbo D **(2009)** Chitin: A structural biopolysaccharide. eLS. DOI: 10.1002/9780470015902.a0000694.pub3

Martinez-Garcia M, Brazel DM, Swan BK, Arnosti C, Chain PS, Reitenga KG, Xie G, Poulton NJ, Lluesma Gomez M, Masland DE, Thompson B, Bellows WK, Ziervogel K, Lo CC, Ahmed S, Gleasner CD, Detter CJ, Stepanauskas R **(2012)** Capturing single cell genomes of active polysaccharide degraders: an unexpected contribution of *Verrucomicrobia*. *PLoS One* 7(4):e35314.

Mauch F, Mauch-Mani B, Boller T **(1988)** Antifungal hydrolases in pea tissue II. Inhibition of fungal growth by combinations of chitinase and β-1,3-glucanase. *Plant Physiol* 88(3):936-942.

McBride MJ, Braun TF, Brust JL **(2003*)*** *Flavobacterium johnsoniae* GldH is a lipoprotein that is required for gliding motility and chitin utilization. *J Bacteriol* 185(22):6648-6657.

McBride MJ (2014) The family *Flavobacteriaceae*. In: Rosenberg E, DeLong EF, Lory S, Stackebrandt E, Thompson F (eds). *The Prokaryotes*. Springer: Heidelberg, Germany. pp 643-676.

McBride MJ, Liu W, Lu X, Zhu Y, Zhang W **(2014)** The family *Cytophagaceae*. In: Rosenberg E, DeLong EF, Lory S, Stackebrandt E, Thompson F (eds). *The Prokaryotes*. Springer: Heidelberg, Germany. pp 577-593.

McInerney MJ, Struchtemeyer CG, Sieber J, Mouttaki H, Stams AJ, Schink B, Rohlin L, Gunsalus RP **(2008)** Physiology, ecology, phylogeny, and genomics of microorganisms capable of syntrophic metabolism. *Ann NY Acad Sci* 1125:58-72.

McIlroy SJ, Karst SM, Nierychlo M, Dueholm MS, Albertsen M, Kirkegaard RH, Seviour RJ, Nielsen PH **(2016)** Genomic and *in situ* investigations of the novel uncultured Chloroflexi associated with 0092 morphotype filamentous bulking in activated sludge. *ISME J* 10(9):2223-2234.

Mesuere B, Devreese B, Debyser G, Aerts M, Vandamme P, Dawyndt P **(2012)** Unipept: tryptic peptide-based biodiversity analysis of metaproteome samples. *J Proteome Res* 11(12):5773-5780.

Metcalfe AC, Krsek M, Gooday GW, Prosser JI, Wellington EMH **(2002)** Molecular analysis of a bacterial chitinolytic community in an upland pasture. *Appl Environ Microbiol* 68(10):5042-5050.

Metzker ML (2010) Sequencing technologies – the next generation. *Nat Rev Genet* 11(1):31-46.

Meyer B, **Kuever J (2007)** Phylogeny of the alpha and beta subunits of the dissimilatory adenosine-5'-phosphosulfate (APS) reductase from sulfate-reducing prokaryotes – origin and evolution of the dissimilatory sulfate-reduction pathway. *Microbiology* 153(7):2026-2044.

Meyer F, Paarmann D, D'Souza M, Olson R, Glass EM, Kubal M, Paczian T, Rodriguez A, Stevens R, Wilke A, Wilkening J, Edwards RA **(2008)** The metagenomics RAST server – a public resource for the automatic phylogenetic and functional analysis of metagenomes. *BMC Bioinformatics* 9:386.

Miltner A, Kindler R, Knicker H, Richnow HH, Kästner M **(2009)** Fate of microbial biomass-derived amino acids in soil and their contribution to soil organic matter. *Org Geochem* 40(9):978-985.

Miltner A, Bombach P, Schmidt-Brücken B, Kästner M **(2012)** SOM genesis: microbial biomass as a significant source. *Biogeochemistry* 111(1-3):41-55.

Moat AG, Foster JW, Spector MP **(2002)** Fermentation pathways. In: Moat AG, Foster JW, Spector MP (eds). Microbial Physiology. 4th edn. Wiley-Liss: New York, USA. pp 412-433.

Montgomery MT, Welschmeyer NA, Kirchman DL **(1990)** A simple assay for chitin: application to sediment trap samples from the subarctic Pacific. *Mar Ecol Prog Ser* 64(3):301-308.

Murase J, **Frenzel P (2007)** A methane-driven microbial food web in a wetland rice soil. *Environ Microbiol* 9(12):3025-3034.

Murase J, **Frenzel P (2008)** Selective grazing of methanotrophs by protozoa in a rice field soil. *FEMS Microbiol Ecol* 65(3):408-414.

Morgan AD, MacLean RC, Hillesland KL, Velicer GJ **(2010)** Comparative analysis of *Myxococcus* predation on soil bacteria. *Appl Environ Microbiol* 76(20):6920-6927.

Murrell JC, **Radajewski S (2000)** Cultivation-independent techniques for studying methanotroph ecology. *Res Microbiol* 151(10):807-814.

Muyzer G, Brinkhoff T, Nübel U, Santegoeds CM, Schäfer H, Wawer C **(1998)** Denaturing gradient gel electrophoresis (DGGE) in microbial ecology. In: Akkermans ADL, van Elsas JD, de Bruijn FJ (eds) Molecular Microbial Ecology Manual. 3rd edn. Kluwer Academic Publishers: Dordrecht, Netherlands. pp 1–27.

Muyzer G, **Stams AJ (2008)** The ecology and biotechnology of sulphate-reducing bacteria. *Nat Rev Microbiol* 6(6):441-454.

Naas AE, Mackenzie AK, Mravec J, Schückel J, Willats, WGT, Eijsink VGH, Pope PB **(2014)** Do rumen *Bacteroidetes* utilize an alternative mechanism for cellulose degradation? *MBio* 5(4):e01401-14.

Nealson KH, **Saffarini D (1994)** Iron and manganese in anaerobic respiration: environmental significance, physiology, and regulation. *Annu Rev Microbiol* 48(1):311-343.

Nebel ME, Wild S, Holzhauser M, Huettenberger L, Reitzig R, Sperber M, Stoeck T **(2011)** Jaguc – a software package for environmental diversity analyses. *J Bioinform Comput Biol* 9(6):749–773.

Neufeld JD, Dumont MG, Vohra J, Murrell JC **(2007a)** Methodological considerations for the use of stable isotope probing in microbial ecology. *Microb Ecol* 53(3):435-442.

Neufeld JD, Vohra J, Dumont MG, Lueders T, Manefield M, Friedrich MW, Murrell JC **(2007b)** DNA stable-isotope probing. *Nat Protoc* 2(4):860-866.

Nocker A, Burr M, Camper AK **(2010)** Genotypic microbial community profiling: a critical technical review. *Microb Ecol* 54(2):276-289.

Nunoura T, Hirai M, Miyazaki M, Kazama H, Makita H, Hirayama H, Furushima Y, Yamamoto H, Imachi H, Takai K **(2013)** Isolation and characterization of a thermophilic, obligately anaerobic and heterotrophic marine *Chloroflexi* bacterium from a *Chloroflexi*-dominated microbial community associated with a Japanese shallow hydrothermal system, and proposal for *Thermomarinilinea lacunofontalis* gen. nov., sp. nov. *Microbes Environ* 28(2):228-235.

Ofek M, Hadar Y, Minz D **(2012)** Ecology of root colonizing *Massilia* (*Oxalobacteraceae*). *PLoS One* 7(7):e40117.

Okafor N (1966) Ecology of micro-organisms on chitin buried in soil. *J Gen Microbiol* 44(3):311-327.

Okafor N (1967) Decomposition of chitin by micro-organisms isolated from a temperate and a tropical soil. *Nova Hedwigia* 13:209-226.

Or D, Smets BF, Wraith JM, Dechesne A, Friedman SP **(2007)** Physical constraints affecting bacterial habitats and activity in unsaturated porous media – a review. *Adv Water Resour 30*(6):1505-1527.

Oren A (2014) The family *Methanobacteriaceae*. In: Rosenberg E, DeLong EF, Lory S, Stackebrandt E, Thompson F (eds). *The Prokaryotes*. Springer: Heidelberg, Germany. pp 165-193.

Osborn MJ (1969) Structure and biosynthesis of the bacterial cell wall. *Annu Rev Biochem* 38:501-538.

Overmann J (2013) Principles of enrichment, isolation, cultivation, and preservation of prokaryotes. In: Rosenberg E, DeLong EF, Lory S, Stackebrandt E, Thompson F (eds). *The Prokaryotes*. Springer: Heidelberg, Germany. pp 149-207.

Øvreås L (2000) Population and community level approaches for analysing microbial diversity in natural environments. *Ecol Lett* 3(3):236-251.

Pason P, Kyu KL, Ratanakhanokchai K **(2006)** *Paenibacillus curdlanolyticus* strain B-6 xylanolytic-cellulolytic enzyme system that degrades insoluble polysaccharides. *Appl Environ Microbiol* 72(4):2483-2490.

Pasternak Z, Njagi M, Shani Y, Chanyi R, Rotem O, Lurie-Weinberger MN, Koval S, Pietrokovski S, Gophna U, Jurkevitch E **(2014)** In and out: an analysis of epibiotic vs periplasmic bacterial predators. *ISME J* 8(3):625-635.

Pérez J, Jiménez-Zurdo J, Martínez-Abarca F, Millán V, Shimkets LJ, Muñoz-Dorado J **(2014)** Rhizobial galactoglucan determines the predatory pattern of *Myxococcus xanthus* and protects *Sinorhizobium meliloti* from predation. *Environ Microbiol* 16(7):2341-2350.

Pérez J, Moraleda-Muñoz A, Marcos-Torres FJ, Muñoz-Dorado J **(2016)** Bacterial predation: 75 years and counting! *Environ Microbiol* 18(3):766-779.

Peter H, Beier S, Bertilsson S, Lindström ES, Langenheder S, Tranvik LJ **(2011)** Function-specific response to depletion of microbial diversity. *ISME J* 5(2):351-361.

Peters V, **Conrad R (1996)** Sequential reduction processes and initiation of CH_4 production upon flooding of oxic upland soils. *Soil Biol Biochem* 28(3):371-382.

Pett-Ridge J, **Firestone MK (2005)** Redox fluctuation structures microbial communities in a wet tropical soil. *Appl Environ Microbiol* 71(11):6998-7007.

Philippot L, Raaijmakers JM, Lemanceau P, van der Putten WH **(2013)** Going back to the roots: the microbial ecology of the rhizosphere. *Nat Rev Microbiol* 11(11):789-799.

Picek T, Šimek M, Šantrůčková H **(2000)** Microbial responses to fluctuation of soil aeration status and redox conditions. *Biol Fert Soils* 31(3-4):315-322.

Pillai CKS, Paul W, Sharma CP **(2009)** Chitin and chitosan polymers: Chemistry, solubility and fiber formation. *Prog Polym Sci* 34(7):641-678.

Precht M, Kraft R, Bachmaier M **(2005)** Angewandte Statistik 1. 7th edn. Oldenbourg Verlag: Munich, Germany.

Prosser JI (2015) Dispersing misconceptions and identifying opportunities for the use of 'omics' in soil microbial ecology. *Nat Rev Microbiol* 13(7):439-446.

Raafat D, von Bargen K, Haas A, Sahl HG **(2008)** Insights into the mode of action of chitosan as an antibacterial compound. *Appl Environ Microbiol* 74(12):3764-3773.

Raafat D, **Sahl HG (2009)** Chitosan and its antimicrobial potential – a critical literature survey. *Microb Biotechnol* 2(2):186-201.

Rabea EI, Badawy ME, Stevens CV, Smagghe G, Steurbaut W **(2003)** Chitosan as antimicrobial agent: applications and mode of action. *Biomacromolecules* 4(6):1457-1465.

Rabus R, Gade D, Helbig R, Bauer M, Glöckner FO, Kube M, Schlesner H, Reinhardt R, Amann R **(2002)** Analysis of *N*-acetylglucosamine metabolism in the marine bacterium *Pirellula* sp. strain 1 by a proteomic approach. *Proteomics* 2(6):649-655.

Radajewski S, Ineson P, Parekh NR, Murrell JC **(2000)** Stable-isotope probing as a tool in microbial ecology. *Nature* 403(6770):646-649.

Radajewski S, McDonald IR, Murrell JC **(2003)** Stable-isotope probing of nucleic acids: a window to the function of uncultured microorganisms. *Curr Opin Biotechnol* 14(3):296-302.

Ramaiah N, Hill RT, Chun J, Ravel J, Matte MH, Straube WL, Colwell RR **(2000)** Use of a *chiA* probe for detection of chitinase genes in bacteria from the Chesapeake Bay. *FEMS Microbiol Ecol* 34(1):63-71.

Ramette A (2007) Multivariate analyses in microbial ecology. *FEMS Microbiol Ecol* 62(2):142-160.

Rappé MS, **Giovannoni SJ (2003)** The uncultured microbial majority. *Annu Rev Microbiol* 57(1):369-394.

Ravenscroft N, Walker SG, Dutton GG, Smit J **(1991)** Identification, isolation, and structural studies of extracellular polysaccharides produced by *Caulobacter crescentus*. *J Bacteriol* 173(18):5677-5684.

Raza W, **Shen Q (2010)** Growth, Fe^{3+} reductase activity, and siderophore production by *Paenibacillus polymyxa* SQR-21 under differential iron conditions. *Curr Microbiol* 61(5):390-395.

Reguera G, **Leschine SB (2001)** Chitin degradation by cellulolytic anaerobes and facultative aerobes from soils and sediments. *FEMS Microbiol Lett* 204(2):367-374.

Reichardt N, Duncan SH, Young P, Belenguer A, McWilliam Leitch C, Scott KP, Flint HJ, Louis P **(2014)** Phylogenetic distribution of three pathways for propionate production within the human gut microbiota. *ISME J* 8(6):1323-1335.

Reichenbach (2005) Order VIII. *Myxococcales*. In: Brenner DJ, Krieg NR, Staley JT (eds). *Bergey's Manual of Systematic Bacteriology*. 2nd edn. Springer: New York, USA. pp 1059-1072.

Rogers P, Chen JS, Zidwick MJ **(2013)** Organic Acid and solvent production: Acetic, lactic, gluconic, succinic, and polyhydroxyalkanoic acids. In: Rosenberg E, DeLong EF, Lory S, Stackebrandt E, Thompson F (eds). *The Prokaryotes*. Springer: Heidelberg, Germany. pp 3-75.

Rosenberg E (2014) The family *Chitinophagaceae*. In: Rosenberg E, DeLong EF, Lory S, Stackebrandt E, Thompson F (eds). *The Prokaryotes*. Springer: Heidelberg, Germany. pp 493-495.

Rosselló-Mora R, **Amann R (2001)** The species concept for prokaryotes. *FEMS Microbiol Rev* 25(1):39-67.

Royston P (1992) Approximating the Shapiro-Wilk W-Test for non-normality. *Stat Comput* 2(3):117-119.

Saccà A (2012) The role of eukaryotes in the anaerobic food web of stratified lakes. In Altenbach A, Bernhard JM, Seckbach J (eds) *Anoxia: evidence for eukaryote survival and paleontological strategies*. Springer: Dordrecht, Netherlands. pp 403-419.

Sachs L (1999) *Angewandte Statistik*. Springer: Berlin, Germany.

Sachsenberg T, Herbst FA, Taubert M, Kermer R, Jehmlich N, von Bergen M, Seifert J, Kohlbacher O **(2014)** MetaProSIP: automated inference of stable isotope incorporation rates in proteins for functional metaproteomics. *J Proteome Res* 14(2):619-627.

Saito A, Fujii T, Miyashita K **(2003)** Distribution and evolution of chitinase genes in *Streptomyces* species: involvement of gene duplication and domain-deletion. *Antonie Van Leeuwenhoek* 84(1):7-15.

Sambrook J, **Russell D (2001)** Molecular cloning: A laboratory manual. 3rd ed. CSH press: Cold Spring Harbor, USA.

Sanger F, **Coulson AR (1975)** A rapid method for determining sequences in DNA by primed synthesis with DNA polymerase. *J Mol Biol* 94(3):441-448.

Sanger F, Nicklen S, Coulson AR **(1977)** DNA sequencing with chain-terminating inhibitors. *Proc Natl Acad Sci USA* 74(12):5463-5467.

Sangkhobol V, **Skerman VBD (1981)** *Chitinophaga*, a new genus of chitinolytic *Myxobacteria*. *Int J Syst Bacteriol* 31(3):285–293.

Sangwan N, Xia F, Gilbert JA **(2016)** Recovering complete and draft population genomes from metagenome datasets. *Microbiome* 4(1):8.

Sato K, Azama Y, Nogawa M, Taguchi G, Shimosaka M **(2010)** Analysis of a change in bacterial community in different environments with addition of chitin or chitosan. *J Biosci Bioeng* 109(5):472-478.

Salyers AA, Vercellotti JR, West SE, Wilkins TD **(1977)** Fermentation of mucin and plant polysaccharides by strains of *Bacteroides* from the human colon. *Appl Environ Microbiol* 33(2):319-322.

Sawaguchi A, Ono S, Oomura M, Inami K, Kumeta Y, Honda K, Sameshima-Saito R, Sakamoto K, Ando A, Saito A **(2015)** Chitosan degradation and associated changes in bacterial community structures in two contrasting soils. *Soil Sci Plant Nutr* 61(3):471-480.

Schachtschabel P, Blume HP, Brümmer G, Hartge KH, Schwertmann U **(1992)** Lehrbuch der Bodenkunde. 14. Auflage. Ferdinand Enke Verlag, Stuttgart.

Schellenberger S, Kolb S, Drake HL **(2010)** Metabolic responses of novel cellulolytic and saccharolytic agricultural soil bacteria to oxygen. *Environ Microbiol* 12(4):845-861.

Schellenberger S (2011) Impact of oxygen and pesticides on microbial cellulose degradation in aerated agricultural soils: A microscaled analysis of processes and prokaryotic populations. PhD thesis. University of Bayreuth.

Schellenberger S, Drake HL, Kolb S **(2011)** Functionally redundant cellobiose-degrading soil bacteria respond differentially to oxygen. *Appl Environ Microbiol* 77(17):6043-6048.

Scheu S (2002) The soil food web: structure and perspectives. *Eur J of Soil Biol* 38(1):11-20.

Schleifer KH, **Kandler O (1972)** Peptidoglycan types of bacterial cell walls and their taxonomic implications. *Bacteriol Rev* 36(4):407-477.

Schlesinger WH, **Andrews JA (2000)** Soil respiration and the global carbon cycle. *Biogeochemistry* 48(1):7-20.

Schlesner H (1994) The development of media suitable for the microorganisms morphologically resembling *Planctomyces* spp., *Pirellula* spp., and other *Planctomycetales* from various aquatic habitats using dilute media. *Syst Appl Microbiol* 17(1):135-145.

Schloss PD, **Handelsman J (2005)** Introducing DOTUR, a computer program for defining operational taxonomic units and estimating species richness. *Appl Environ Microbiol* 71(3):1501-1506.

Schloss PD, Jenior ML, Koumpouras CC, Westcott SL, Highlander SK **(2016)** Sequencing 16S rRNA gene fragments using the PacBio SMRT DNA sequencing system. *PeerJ* 4:e1869.

Schimel DS (1995) Terrestrial ecosystems and the carbon cycle. *Glob Change Biol* 1(1): 77-91.

Schimel J (2016) Microbial ecology: Linking omics to biogeochemistry. *Nat Microbiol* 1:15028.

Schink B, **Stams A (2013)** Syntrophism among *Prokaryotes*. In: Rosenberg E, DeLong EF, Lory S, Stackebrandt E, Thompson F (eds). *The Prokaryotes*. Springer: Heidelberg, Germany. pp 471–493.

Schmidt MW, Torn MS, Abiven S, Dittmar T, Guggenberger G, Janssens IA, Kleber M, Kögel-Knabner I, Lehmann J, Manning DA, Nannipieri P, Rasse DP, Weiner S, Trumbore SE **(2011)** Persistence of soil organic matter as an ecosystem property. *Nature* 478(7367):49-56.

Schneider T, Schmid E, de Castro JV Jr, Cardinale M, Eberl L, Grube M, Berg G, Riedel K **(2011)** Structure and function of the symbiosis partners of the lung lichen (*Lobaria pulmonaria* L. Hoffm.) analyzed by metaproteomics. *Proteomics* 11(13):2752-2756.

Schrempf H (2007) Biology of *Streptomycetes*. In: Dworkin M, Falkow S, Rosenberg E, Schleifer K-H, Stackebrandt E (eds). *The Prokaryotes*. Springer: New York, USA. pp 21-28.

Schütte UM, Abdo Z, Bent SJ, Shyu C, Williams CJ, Pierson JD, Forney LJ **(2008)** Advances in the use of terminal restriction fragment length polymorphism (T-RFLP) analysis of 16S rRNA genes to characterize microbial communities. *Appl Microbiol Biotechnol* 80(3):365-380.

Schulten HR, **Schnitzer M (1997)** The chemistry of soil organic nitrogen: a review. *Biol Fertil Soils* 26(1):1-15.

Schwarz W (2001) The cellulosome and cellulose degradation by anaerobic bacteria. *Appl Microbiol Biotechnol* 56(5-6):634-649.

Seidl V (2008) Chitinases of filamentous fungi: a large group of diverse proteins with multiple physiological functions. *Fungal Biol Rev* 22(1):36-42.

Seifert J, Taubert M, Jehmlich N, Schmidt F, Völker U, Vogt C, Richnow HH, von Bergen M **(2012)** Protein-based stable isotope probing (protein-SIP) in functional metaproteomics. *Mass Spectrom Rev* 31(6):683-697.

Sharon A, Finkelstein A, Shlezinger N, Hatam I **(2009)** Fungal apoptosis: function, genes and gene function. *FEMS Microbiol Rev* 33(5):833-854.

Shendure J, **Ji H (2008)** Next-generation DNA sequencing. *Nat Biotechnol* 26(10):1135-1145.

Shevchenko A, Tomas H, Havlis J, Olsen JV, Mann M **(2007)** In-gel digestion for mass spectrometric characterization of proteins and proteomes. *Nat Protoc* 1(6):2856-2860.

Shieh WY, **Jean WD (1998)** *Alterococcus agarolyticus*, gen. nov., sp. nov., a halophilic thermophilic bacterium capable of agar degradation. *Can J Microbiol* 44(7):637-645.

Shokralla S, Spall JL, Gibson JF, Hajibabaei M **(2012)** Next-generation sequencing technologies for environmental DNA research. *Mol Ecol* 21(8):1794-1805.

Sikorski P, Sørbotten A, Horn SJ, Eijsink VG, Vårum KM **(2006)** *Serratia marcescens* chitinases with tunnel-shaped substrate-binding grooves show endo activity and different

degrees of processivity during enzymatic hydrolysis of chitosan. *Biochemistry* 45(31):9566-9574.

Silhavy TJ, Kahne D, Walker S **(2010)** The bacterial cell envelope. *Cold Spring Harb Perspect Biol* 2(5):a000414.

Sinclair L, Osman OA, Bertilsson S, Eiler A **(2015)** Microbial community composition and diversity via 16S rRNA gene amplicons: evaluating the illumina platform. *PLoS One* 10(2):e0116955.

Singh H, Du J, Won K, Yang JE, Yin C, Kook M, Yi TH **(2015)** *Massilia arvi* sp. nov., isolated from fallow-land soil previously cultivated with *Brassica oleracea*, and emended description of the genus *Massilia*. *Int J Syst Evol Microbiol* 65(10):3690-3696.

Singh JS, **Gupta SR (1977)** Plant decomposition and soil respiration in terrestrial ecosystems. *Bot Rev* 43(4):449-528.

Sivan A, **Chet I (1989)** Degradation of fungal cell walls by lytic enzymes of *Trichoderma harzianum*. *Microbiology* 135(3):675-682.

Six J, Conant RT, Paul EA, Paustian K **(2002)** Stabilization mechanisms of soil organic matter: implications for C-saturation of soils. *Plant Soil* 241(2):155-176.

Six J, Bossuyt H, Degryze S, Denef K **(2004)** A history of research on the link between (micro)aggregates, soil biota, and soil organic matter dynamics. *Soil Tillage Res* 79(1):7-31.

Skinner CE, **Dravis F (1937)** A quantitative determination of chitin destroying microoganisms in soil. *Ecology* 18(3):391-397.

Sockett RE (2009) Predatory lifestyle of *Bdellovibrio bacteriovorus*. *Annu Rev Microbiol* 63:523-539.

Sollins P, Homann P, Caldwell BA **(1996)** Stabilization and destabilization of soil organic matter: mechanisms and controls. *Geoderma* 74(1-2):65-105.

Someya N, Ikeda S, Morohoshi T, Noguchi Tsujimoto M, Yoshida T, Sawada H, Ikeda T, Tsuchiya K **(2011)** Diversity of culturable chitinolytic bacteria from rhizospheres of agronomic plants in Japan. *Microbes Environ* 26(1):7-14.

Span EA, **Marletta MA (2015)** The framework of polysaccharide monooxygenase structure and chemistry. *Curr Opin Struct Biol* 35:93-99.

Speth DR, Guerrero-Cruz S, Dutilh BE, Jetten MS **(2016)** Genome-based microbial ecology of anammox granules in a full-scale wastewater treatment system. *Nat Commun* 7:11172.

Stockmann U, Adams MA , Crawford JW , Field DJ , Henakaarchchi N , Jenkins M , Minasny B , McBratney AB , de Courcelles VD , Singh K , Wheeler I , Abbott L , Angers DA , Baldock J , Bird M , Brookes PC , Chenu C , Jastrow JD , Lal R , Lehmann J , O'Donnell AG, Parton WJ, Whitehead D , Zimmermann M **(2013)** The knowns, known unknowns and unknowns of sequestration of soil organic carbon. *Agric Ecosyst Environ* 164:80-99.

Stoeck T, Bass D, Nebel M, Christen R, Jones MDM, Breiner H-W, Richards TA **(2010)** Multiple marker parallel tag environmental DNA sequencing reveals a highly complex eukaryotic community in marine anoxic water. *Mol Ecol* 19(1):21-31.

Stramma L, Johnson GC, Sprintall J, Mohrholz V **(2008)** Expanding oxygen-minimum zones in the tropical oceans. *Science* 320(5876):655-658.

Štrojsová M, **Vrba J (2005)** Direct detection of digestive enzymes in planktonic rotifers using enzyme-labelled fluorescence (ELF). *Mar Freshwater Res* 56(2):189-195.

Sturm M, Bertsch A, Gröpl C, Hildebrandt A, Hussong R, Lange E, Pfeifer N, Schulz-Trieglaff O, Zerck A, Reinert K, Kohlbacher O **(2008)** OpenMS – an open-source software framework for mass spectrometry. *BMC Bioinformatics* 9:163.

Subbanna ARNS, Khan MS, Shivashankara H **(2016)** Characterization of antifungal *Paenibacillus illinoisensis* strain UKCH21 and its chitinolytic properties. *Afr J Microbiol Res* 10(34):1380-1387.

Suzuki K, Taiyoji M, Sugawara N, Nikaidou N, Henrissat B, Watanabe T **(1999)** The third chitinase gene (*chiC*) of *Serratia marcescens* 2170 and the relationship of its product to other bacterial chitinases. *Biochem J* 343(3):587-596.

Suzuki K, Sugawara N, Suzuki M, Uchiyama T, Katouno F, Nikaidou N, Watanabe T **(2002)** Chitinases A, B, and C1 of *Serratia marcescens* 2170 produced by recombinant *Escherichia coli*: enzymatic properties and synergism on chitin degradation. *Biosci Biotechnol Biochem* 66(5):1075-1083.

Tamura K, Peterson D, Peterson N, Stecher G, Nei M, Kumar S **(2011)** MEGA5: molecular evolutionary genetics analysis using maximum likelihood, evolutionary distance, and maximum parsimony methods. *Mol Biol Evol* 28(10):2731-2739.

Tamura K, Stecher G, Peterson D, Filipski A, Kumar S **(2013)** MEGA6: Molecular Evolutionary Genetics Analysis version 6.0. *Mol Biol Evol* 30(12):2725-2729.

Tanaka T, Fujiwara S, Nishikori S, Fukui T, Takagi M, Imanaka T **(1999)** A unique chitinase with dual active sites and triple substrate binding sites from the hyperthermophilic archaeon *Pyrococcus kodakaraensis* KOD1. *Appl Environ Microbiol* 65(12):5338-5344.

Tracey MV (1955) Chitinase in some basidiomycetes. *Biochem J* 61(4):579-586.

Taubert M, Vogt C, Wubet T, Kleinsteuber S, Tarkka MT, Harms H, Buscot F, Richnow HH, von Bergen M, Seifert J **(2012)** Protein-SIP enables time-resolved analysis of the carbon flux in a sulfate-reducing, benzene-degrading microbial consortium. *ISME J* 6(12):2291-2301.

Terahara T, Ikeda S, Noritake C, Minamisawa K, Ando K, Tsuneda S, Harayama S **(2009)** Molecular diversity of bacterial chitinases in arable soils and the effects of environmental factors on the chitinolytic bacterial community. *Soil Biol Biochem* 41(3):473-480.

Ter Braak CJ (1986) Canonical correspondence analysis: a new eigenvector technique for multivariate direct gradient analysis. *Ecology* 67(5):1167-1179.

Tiedje JM, Sexstone AJ, Parkin TB, Revsbech NP **(1984)** Anaerobic processes in soil. *Plant Soil* 76(1-3):197-212.

Tiedje JM (1988) Ecology of denitrification and dissimlatory nitrate reduction to ammonium. In: Zehnder AJ, Stumm W (eds). Biology of Anaerobic Microorganisms. Wiley: New York. pp 179–243.

Thauer RK, Jungermann K, Decker K **(1977)** Energy conservation in chemotrophic anaerobic bacteria. *Bacteriol Rev* 41(1):100-180.

Thies JE (2007) Soil microbial community analysis using terminal restriction fragment length polymorphisms. *Soil Sci Soc Am J* 71(2):579-591.

Thevenot M, Dignac MF, Rumpel C **(2010)** Fate of lignins in soils: a review. *Soil Biol Biochem* 42(8):1200-1211.

Totsche KU, Rennert T, Gerzabek MH, Kögel-Knabner I, Smalla K, Spiteller M, Vogel HJ **(2010)** Biogeochemical interfaces in soil: the interdisciplinary challenge for soil science. *J Plant Nutr Soil Sci* 173(1):88-99.

Tsutsuki K, **Kuwatsuka S (1979)** Chemical studies on soil humic acids: VII. pH-Dependent nature of the ultraviolet and visible absorption spectra of humic acids. *Soil Sci Plant Nutr* 25(3):373-384.

Ueda A, **Saneoka H (2015)** Characterization of the ability to form biofilms by plant-associated *Pseudomonas* species. *Curr Microbiol* 70(4):506-513.

Vaaje-Kolstad G, Westereng B, Horn SJ, Liu Z, Zhai H, Sørlie M, Eijsink VGH **(2010)** An oxidative enzyme boosting the enzymatic conversion of recalcitrant polysaccharides. *Science* 330(6001):219-222.

Vaaje-Kolstad G, Horn SJ, Sørlie M, Eijsink VG **(2013)** The chitinolytic machinery of Serratia marcescens – a model system for enzymatic degradation of recalcitrant polysaccharides. *FEBS J* 280(13):3028-3049.

Vargas R, **Hattori T (1986)** Protozoan predation of bacterial cells in soil aggregates. *FEMS Microbiol Ecol* 2(4):233-242.

Van Aalten DMF, Synstad B, Brurberg MB, Hough E, Riise BW, Eijsink VGH, Wierenga RK **(2000)**. Structure of a two-domain chitotriosidase from *Serratia marcescens* at 1.9-Å resolution. *Proc Natl Acad Sci USA* 97(11):5842-5847.

Van Elsas JD, **Boersma FGH (2011)** A review of molecular methods to study the microbiota of soil and the mycosphere. *Eur J Soil Biol* 47(2):77-87.

Vanhooren PT, **Vandamme EJ (1999)** L-Fucose: occurrence, physiological role, chemical, enzymatic and microbial synthesis. *J Chem Technol Biotechnol* 74(6):479-497.

van Kessel MA, Speth DR, Albertsen M, Nielsen PH, Op den Camp HJ, Kartal B, Jetten MS, Lücker S **(2015)** Complete nitrification by a single microorganism. *Nature* 528(7583):555-559.

van Scheltinga ACT, Kalk KH, Beintema JJ, Dijkstra BW **(1994)** Crystal structures of hevamine, a plant defence protein with chitinase and lysozyme activity, and its complex with an inhibitor. *Structure* 2(12):1181-1189.

Veldkamp H (1955) A study of the aerobic decomposition of chitin by microorganisms. Mededelingen van de Landbouwhogeschool te Wageningen/Nederland 55(3):127-174.

Vilchez-Vargas R, Junca H, Pieper DH **(2010)** Metabolic networks, microbial ecology and 'omics' technologies: towards understanding *in situ* biodegradation processes. *Environ Microbiol* 12(12):3089-3104.

von Bergen M, Jehmlich N, Taubert M, Vogt C, Bastida F, Herbst FA, Schmidt F, Richnow HH, Seifert J **(2013)** Insights from quantitative metaproteomics and protein-stable isotope probing into microbial ecology. *ISME J* 7(10):1877-1885.

von Lützow M, Kögel-Knabner I, Ekschmitt K, Matzner E, Guggenberger G, Marschner B, Flessa H **(2006)** Stabilization of organic matter in temperate soils: mechanisms and their relevance under different soil conditions – a review. *Eur J Soil Sci* 57(4):426-445.

von Lützow M, Kögel-Knabner I, Ludwig B, Matzner E, Flessa H, Ekschmitt K, Guggenberger G, Marschner B, Kalbitz, K **(2008)** Stabilization mechanisms of organic matter in four temperate soils: development and application of a conceptual model. *J Plant Nutr Soil Sci* 171(1):111-124.

von Lützow M, **Kögel-Knabner I (2009)** Temperature sensitivity of soil organic matter decomposition—what do we know? *Biol Fertil Soils* 46(1):1-15.

Vos M, Wolf AB, Jennings SJ, Kowalchuk GA **(2013)** Micro-scale determinants of bacterial diversity in soil. *FEMS Microbiol Rev* 37(6):936-954.

Vrba J, Filandr P, Nedoma J, Simek K **(1996)** Different sources of extracellular β-*N*-acetylhexosaminidases-like activitiesin freshwaters. In: Muzzarelli RAA (ed). *Chitin Enzymology*. Atec Edizioni: Senigallia, Italy. pp 293-301.

Vu B, Chen M, Crawford RJ, Ivanova EP **(2009)** Bacterial extracellular polysaccharides involved in biofilm formation. *Molecules* 14(7):2535-2554.

Vu VV, Beeson WT, Span EA, Farquhar ER, Marletta MA **(2014)** A family of starch-active polysaccharide monooxygenases. *Proc Natl Acad Sci USA* 111(38):13822-13827.

Wagner C, Grießhammer A, Drake HL **(1996)** Acetogenic capacities and the anaerobic turnover of carbon in a Kansas prairie soil. *Appl Environ Microbiol* 62(2):494-500.

Wagner M, Roger AJ, Flax JL, Brusseau GA, Stahl DA **(1998)** Phylogeny of dissimilatory sulfite reductases supports an early origin of sulfate respiration. *J Bacteriol* 180(11):2975-2982.

Wagner M, Horn M, Daims H **(2003)** Fluorescence in situ hybridisation for the identification and characterisation of prokaryotes. *Curr Opin Microbiol* 6(3):302-309.

Walton PH, **Davies GJ (2016**) On the catalytic mechanisms of lytic polysaccharide monooxygenases. *Curr Opin Chem Biol* 31:195-207.

Wang Y, **Qian PY (2009)** Conservative fragments in bacterial 16S rRNA genes and primer design for 16S ribosomal DNA amplicons in metagenomic studies. *PLoS ONE* 4(10):e7401.

Wang X, Sharp CE, Jones GM, Grasby SE, Brady AL, Dunfield PF **(2015)** Stable-isotope probing identifies uncultured *Planctomycetes* as primary degraders of a complex heteropolysaccharide in soil. *Appl Environ Microbiol* 81(14):4607-4615.

Ward NL, Challacombe JF, Janssen PH, Henrissat B, Coutinho PM, Wu M, Xie G, Haft DH, Sait M, Badger J, Barabote RD, Bradley B, Brettin TS, Brinkac LM, Bruce D, Creasy T, Daugherty SC, Davidsen TM, DeBoy RT, Detter JC, Dodson RJ, Durkin AS, Ganapathy A, Gwinn-Giglio M, Han CS, Khouri H, Kiss H, Kothari SP, Madupu R, Nelson KE, Nelson WC, Paulsen I, Penn K, Ren Q, Rosovitz MJ, Selengut JD, Shrivastava S, Sullivan SA, Tapia R, Thompson LS, Watkins KL, Yang Q, Yu C, Zafar N, Zhou L, Kuske CR **(2009)** Three genomes from the phylum *Acidobacteria* provide insight into the lifestyles of these microorganisms in soils. *Appl Environ Microbiol* 75(7):2046-2056.

Wardle DA (1992) A comparative assessment of factors which influence microbial biomass carbon and nitrogen levels in soil. *Biol Rev* 67(3):321-358.

Weber KA, Achenbach LA, Coates JD **(2006)** Microorganisms pumping iron: anaerobic microbial iron oxidation and reduction. *Nat Rev Microbiol* 4(10):752-764.

Wellington EM, Berry A, Krsek M **(2003)** Resolving functional diversity in relation to microbial community structure in soil: exploiting genomics and stable isotope probing. *Curr Opin Microbiol* 6(3):295-301.

Weon HY, Kim BY, Son JA, Jang HB, Hong SK, Go SJ, Kwon SW **(2008)** *Massilia aerilata* sp. nov., isolated from an air sample. *Int J Syst Evol Microbiol* 58(6):1422-1425.

Westgard JO, Barry BL, Hunt MR, Groth T **(1981)** A multi-rule Shewhart chart for quality control in clinical chemistry. *Clin Chem* 27(3):493-501.

Westermann P (1993) Wetland and swamp microbiology. In: Ford TE (ed). *Aquatic microbiology: an ecological approach*. Blackwell Publishers: Oxford, England. pp 215-238.

White D (2007) The physiology and biochemistry of Prokaryotes. 3rd edn. Oxford University Press: New York, USA.

Whiteley AS, Thomson B, Lueders T, Manefield M **(2007)** RNA stable isotope probing. *Nat Protoc* 2(4):838-844.

Wieczorek AS, Hetz SA, Kolb S **(2014)** Microbial responses to chitin and chitosan in oxic and anoxic agricultural soil slurries. *Biogeosciences* 11(12):3339-3352.

Wieczorek AS, Schmidt O, Chatzinotas A, von Bergen M, Gorissen A, Kolb S **(2019)** Ecological functions of agricultural soil bacteria and microeukaryotes in chitin degradation: A case study. *Front Microbiol* 10:1293.

Winderl C, Penning H, von Netzer F, Meckenstock RU, Lueders T **(2010)** DNA-SIP identifies sulfate-reducing *Clostridia* as important toluene degraders in tar-oil-contaminated aquifer sediment. *ISME J* 4(10):1314-1325.

Williamson N, Brian P, Wellington EMH **(2000)** Molecular detection of bacterial and streptomycete chitinases in the environment. *Antonie Van Leeuwenhoek* 78(3-4):315-321.

Wu T, **Zivanovic S (2008)** Determination of the degree of acetylation (DA) of chitin and chitosan by an improved first derivative UV method. *Carbohydr Polym* 73(2):248-253.

Wüst PK, Horn MA, Drake HL **(2009)** Trophic links between fermenters and methanogens in a moderately acidic fen soil. *Environ Microbiol* 11(6):1395-1409.

Wynne EC, **Pemberton JM (1986)** Cloning of a gene cluster from *Cellvibrio mixtus* which codes for cellulase, chitinase, amylase, and pectinase. *Appl Environ Microbiol* 52(6):1362-1367.

Xie G, Bruce DC, Challacombe JF, Chertkov O, Detter JC, Gilna P, Han CS, Lucas S, Misra M, Myers GL, Richardson P, Tapia R, Thayer N, Thompson LS, Brettin TS, Henrissat B, Wilson DB, McBride MJ **(2007)** Genome sequence of the cellulolytic gliding bacterium *Cytophaga hutchinsonii*. *Appl Environ Microbiol* 73(11):3536-3546.

Xiao X, Yin X, Lin J, Sun L, You Z, Wang P, Wang F **(2005)** Chitinase genes in lake sediments of Ardley Island, Antarctica. *Appl Environ Microbiol* 71(12):7904-7909.

Yang HC, Im WT, An DS, Park WS, Kim IS, Lee ST **(2005)** *Silvimonas terrae* gen. nov., sp. nov., a novel chitin-degrading facultative anaerobe belonging to the '*Betaproteobacteria*'. *Int J Syst Evol Microbiol* 55(6):2329-2332.

Yaroslavtsev AM, Manucharova NA, Stepanov AL, Zvyagintsev DG, Sudnitsyn II **(2009)** Microbial destruction of chitin in soils under different moisture conditions. *Eurasian Soil Sci* 42(7):797-806.

Yarza P, Ludwig W, Euzéby J, Amann R, Schleifer KH, Glöckner FO, Rosselló-Móra R **(2010)** Update of the All-species living tree project based on 16S and 23S rRNA sequence analyses. *Syst Appl Microbiol* 33(6):291-299.

Yasir M, Aslam Z, Kim SW, Lee SW, Jeon CO, Chung YR **(2009)** Bacterial community composition and chitinase gene diversity of vermicompost with antifungal activity. *Bioresour Technol* 100(19):4396-4403.

Yoon JH, Kang SJ, Park S, Oh TK **(2012)** *Mucilaginibacter litoreus* sp. nov., isolated from marine sand. *Int J Syst Evol Microbiol* 62(12):2822-2827.

Yoshida N, Yagi K, Sato D, Watanabe N, Kuroishi T, Nishimoto K, Yanagida A, Katsuragi T, Kanagawa T, Kurane R, Tani Y **(2005)** Bacterial communities in petroleum oil in stockpiles. *J Biosci Bioeng* 99(2):143-149.

Zar JH (1996) *Biostatistical analysis*. 3rd edn. Practice Hall: New Jersey, USA.

Zargar V, Asghari M, Dashti A **(2015)** A review on chitin and chitosan polymers: structure, chemistry, solubility, derivatives, and applications. *Chem Bio Eng Rev* 2(3):204-226.

Zehnder AJB, **Stumm W (1988)** Geochemistry and biogeochemistry of anaerobic habitats. In: Zehnder AJB (ed) *Biology of anaerobic microorganisms*. Wiley: New York, USA. pp 1-38.

Zidwick MJ, Chen JS, Rogers P **(2013)** Organic acid and solvent production: Propionic and butyric acids and ethanol. In: Rosenberg E, DeLong EF, Lory S, Stackebrandt E, Thompson F (eds). *The Prokaryotes*. Springer: Heidelberg, Germany. pp 135-167.

Zimmerman AE, Martiny AC, Allison SD **(2013)** Microdiversity of extracellular enzyme genes among sequenced prokaryotic genomes. *ISME J* 7(6):1187-1199.

Zwirglmaier K (2005) Fluorescence in situ hybridisation (FISH) – the next generation. *FEMS Microbiol Lett* 246(2):151-158.

Zybailov B, Mosley AL, Sardiu ME, Coleman MK, Florens L, Washburn MP **(2006)** Statistical analysis of membrane proteome expression changes in *Saccharomyces cerevisiae*. *J Proteome Res* 5(9):2339-2347.

Zverlov VV, Fuchs KP, Schwarz WH **(2002)** Chi18A, the endochitinase in the cellulosome of the thermophilic, cellulolytic bacterium *Clostridium thermocellum*. *Appl Environ Microbiol* 68(6):3176-3179.

8. Acknowledgments

I want to thank everyone who contributed to this work directly or indirectly by scientific or financial support.

I want to deeply thank PD Dr. Steffen Kolb for making it possible for me to work on this interesting project, for helpful and inspiring discussions and an open door every time I needed help. I also want to thank Prof. Harold L. Drake for the scientific and financial support, helpful remarks and constructive criticism.

The work was financially supported by the Deutsche Forschungsgemeinschaft (Ko2912/3-2) and the University of Bayreuth.

Special thanks go to Dr. Oliver Schmidt for the good discussions we had, scientific help, continuous constructive[a] criticism on my work and for being a role model in scientific and analytic thinking[b], and also being an easy-going colleague. Just as much I want to thank Prof. Dr. Marcus Horn for inspiring discussions covering all fields of microbiology and being a walking library. I want to thank Dr. Sindy Hunger for her helpful comments in lab seminars.

I want to thank all my current and former colleagues and also guest researchers at the Department of Ecological Microbiology for the good times and the relaxed atmosphere.

I want to thank: Dr. Antonis Chatzinotas, Dr. Antonie Gorissen, Dr. Huub J.M. Op den Camp, Vanessa Lünsmann, Dr. Nico Jehmlich, Henrike Höke, Prof. Dr. Martin von Bergen, PD Dr. Lorenz Adrian and Sara Ferdi for the GC-MS data, proteome analysis and contributions on the 2017 manuscript. I further want to thank Prof. Dr. Michael Schloter for providing soil samples. Dr. Berthold Fartmann at LGC for cloning. Dr. Andrea Thürmer for pyrosequencing. Steffi Hetz for contributions to TRFLP analysis and to the 2014 manuscript. Florian Just for contributions to DNA extractions.

And of course I apologize to anyone whom I forgot to thank.

My greatest thanks go to my parents[c], my brother[d] and my friends[e]. Your scientific support was not worth mentioning. However, to the best of my knowledge, it was the best support I can imagine.

[a] and discouraging
[b] although it might did not help to improve this work
[c] for all the support, keeping my spirits high and the delicious input of carbon[f] and energy
[d] for being a genuine and genius humor motive force
[e] **Peter DJ**, Daniel 'Bikosaurus' S, **Aniela**, Simon Z, Ju, Christian and Lena H, B[g], Fabi[h], Fabi[i], **Sonja**, Dimi, Katharina E, Thomas and Kristin B., Naomi, Pace, U, Mareen M, Timo, Uda, Daan, Vicky, Viktor, Steffen 'Schimi', Rike, Milto, Alina, Matthias, Friedericke 'Högi' H, Luisa, Oss, Anja M, Ramona H, all my former colleagues in Nijmegen
[f] and of course also all the other macro and microelements
[g] Boran K
[h] from Bayreuth
[i] from Münster

9. Publications

To date, the results of this work have yielded two publications in peer-reviewed journals. In addition, the work has been presented at numerous national and international conferences.

9.1. Publications and manuscripts resulting from this work

Wieczorek AS, Hetz SA, Kolb S **(2014)** Microbial responses to chitin and chitosan in oxic and anoxic agricultural soil slurries. *Biogeosciences* 11(12):3339-3352. IF=3.851

Wieczorek AS, Schmidt O, Chatzinotas A, von Bergen M, Gorissen A, Kolb S **(2019)** Ecological functions of agricultural soil bacteria and microeukaryotes in chitin degradation: A case study. *Front Microbiol* 10:1293.

9.2. Publications not related to this work

Wieczorek AS, Drake HL, Kolb S **(2011)** Organic acids and ethanol inhibit the oxidation of methane by mire methanotrophs. *FEMS Microbiol Ecol* 77(1):28-39.

Khadem AF, Pol A, **Wieczorek A**, Mohammadi SS, Francoijs KJ, Stunnenberg HG, Jetten MS, Op den Camp HJM **(2011)** Autotrophic methanotrophy in *Verrucomicrobia*: *Methylacidiphilum fumariolicum* SolV uses the Calvin-Benson-Bassham Cycle for carbon dioxide fixation. *J Bacteriol* 193(17):4438-4446.

Khadem AF, **Wieczorek AS**, Pol A, Vuilleumier S, Harhangi HR, Dunfield PF, Kalyuzhnaya MG, Murrell JC, Francoijs KJ, Stunnenberg HG, Stein LY, DiSpirito AA, Semrau JD, Lajus A, Médigue C, Klotz MG, Jetten MS, Op den Camp HJM **(2012)** Draft genome sequence of the volcano-inhabiting thermoacidophilic methanotroph *Methylacidiphilum fumariolicum* strain SolV. *J Bacteriol* 194(14):3729-3730.

Khadem AF, Pol A, **Wieczorek AS**, Jetten MS, Op den Camp HJM **(2012)** Metabolic regulation of "Ca*. Methylacidiphilum fumariolicum*" SolV cells grown under different nitrogen and oxygen limitations. *Front Microbiol* 3:266.

9.3. Presentations based on this work

Wieczorek A, Hetz S, Drake HL, Kolb S **(2012)** Effect of oxygen availability on microbial chitin degraders in an agricultural soil. Presented at Annual Conference of the Association for General and Applied Microbiology – VAAM, Tübingen, 18.3.2012 – 21.3.2012.

Wieczorek A, Hetz S, Just F, Drake HL, Kolb S **(2013)** Formation of *N*-acetyl sugars by chitinases is the primary step of chitin hydrolysis by microorganisms in an agricultural soil. Presented at Annual Conference of the Association for General and Applied Microbiology – VAAM, Bremen, 10.3.2013 – 13.3.2013

Wieczorek AS, Hetz SA, Drake HL, Kolb S **(2014)** Metabolic responses of chitinolytic and saccharolytic *Bacteria* to oxygen. Presented at the International Symposium of the German Priority Programme SPP 1315 Biogeochemical Interfaces in Soil on: Biogeochemical Interfaces in Soil – Towards a Comprehensive and Mechanistic Understanding of Soil Functions, Leipzig, 5.10.2014 – 8.10.2014.

Wieczorek AS, Jehmlich N, von Bergen M, Chatzinotas A, Gorissen A, Op den Camp HJM, Kolb S **(2015)** Chitin degradation by a complex microbial community in soil. Oral presentation at Annual Conference of the Association for General and Applied Microbiology – VAAM, Marburg, 1.3.2015 – 4.3.2015.

Wieczorek AS, Jehmlich N, von Bergen M, Höke H, Chatzinotas A, Gorissen A, Drake HL, Op den Camp HJM, Kolb S **(2015)** Chitin degradation by a soil microbiome. Presented at the Applied and Environmental Microbiology Gordon Research Conference, South Hadley, 12.7.2015 – 17.7.2015.

9.4. Presentations not related to this work

Gittel A, **Wieczorek A**, Sørensen K, Skovhus T, Ingvorsen K, Schramm A **(2008)** Effect of nitrate addition on prokaryotic diversity and the activity of sulfate-reducing prokaryotes in high-temperature oil production systems. Presented at Reservoir Microbiology Forum, London, 25.11.2008 – 26.11.2008.

Gittel A, **Wieczorek A**, Sørensen K, Skovhus T, Ingvorsen K, Schramm A (2008) Effect of nitrate addition on the diversity and activity of sulfate-reducing prokaryotes in high-temperature oil production systems. Presented at 12th International Symposium on Microbial Ecology (ISME-12), Cairns, 17.8.2008 – 22.8.2008.

Wieczorek A, Drake HL, Kolb S **(2010)** Fatty acids and ethanol affect methanotroph activity in an acidic fen capable of utilizing atmospheric methane. Presented at 13th International Symposium on Microbial Ecology (ISME-13), Seattle, 22.8.2010 – 27.8.2010.

Khadem AF, Pol A, Harhangi HR, **Wieczorek A**, Jetten MSM, Op den Camp HJM **(2010)** Methanotrophy below ph 1 by a new Verrucomicrobia species. Presented at 13th International Symposium on Microbial Ecology (ISME-13), Seattle, 22.8.2010 – 27.8.2010.

10. Supplemental information

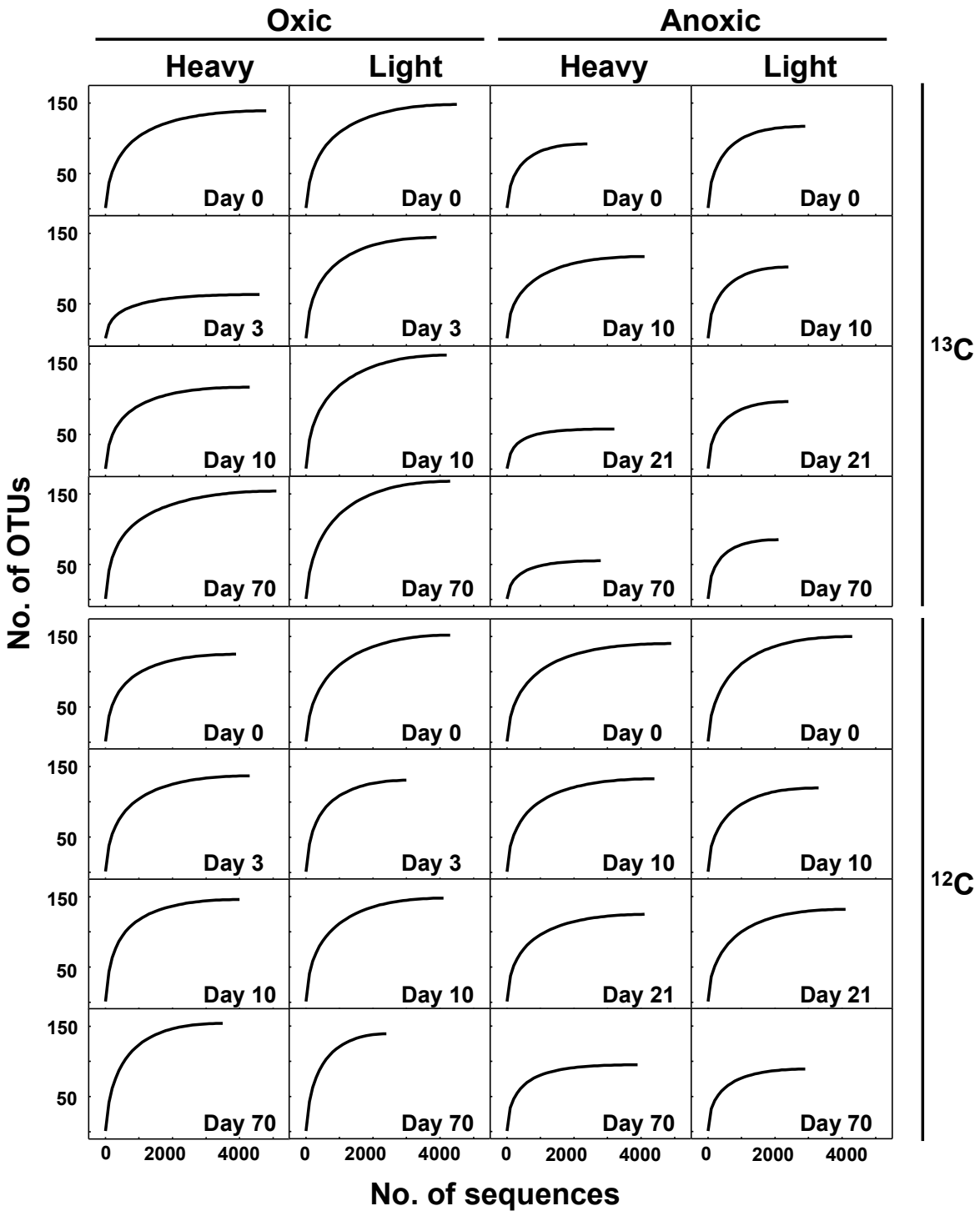

Figure S1. Rarefaction analysis of bacterial 16S rRNA sequences. OTUs were called based on a similarity cutoff of 87.5%. The program 'aRarefact' was used to calculate the curves according to the Hurlbert rarefaction (Hurlbert 1971).

Table S1. Relative abundances and calculated R_{CS} scores of labeled OTUs under oxic conditions. R_{CS} sores were calculated using the values for the relative abundance of a given OTU in the heavy (H) and light (L) fractions of [^{13}C]-chitin and [^{12}C]-chitin incubations. See materials and methods (2.7.4.) for details on the calculation.

			[^{13}C]-chitin								[^{12}C]-chitin								R_{CS} score		
			Day 0		Day 3		Day 10		Day 70		Day 0		Day 3		Day 10		Day 70		Day 3	Day 10	Day 70
Phylum/Class		Family	H	L	H	L	H	L	H	L	H	L	H	L	H	L	H	L			
Bacteroidetes		*Flammeovirgaceae* 1100	0.0	0.2	1.2	0.0	1.8	0.2	0.1	0.0	0.0	0.1	0.1	0.1	0.3	0.2	0.0	0.0	1.2 ± 0.0	1.6 ± 0.1	
		1103	0.1	0.0	1.1	0.3	1.1	0.3	0.7	0.1	0.2	0.2	0.3	0.6	0.5	0.2	0.1	0.4	0.9 ± 0.1	0.8 ± 0.1	0.6 ± 0.1
		Flavobacteriaceae 1122	0.1	0.2	1.4	0.3	2.7	1.3	0.7	0.0	0.1	0.2	0.7	0.7	1.7	1.1	0.2	0.0	1.1 ± 0.3	1.7 ± 0.8	0.6 ± 0.1
		Sphingobacteriaceae 1107	0.1	0.1	2.8	0.0	2.2	0.9	0.3	0.0	0.0	0.2	0.6	0.5	1.1	1.7	0.1	0.1	2.5 ± 0.3	1.5 ± 0.5	
		Chitinophagaceae 1091	0.2	0.9	4.0	0.9	2.2	1.5	1.4	0.4	0.1	0.9	0.9	2.0	0.0	3.1	0.5	0.5	3.3 ± 0.4	1.3 ± 0.7	1.1 ± 0.2
		unclassified 1111	0.1	0.1	0.1	0.5	1.0	0.4	0.3	0.5	0.0	0.1	1.0	0.9	0.3	0.6	0.0	0.5		0.7 ± 0.1	
Gemmatimonadetes		*Gemmatimonadaceae* 400	0.4	0.4	1.2	0.1	0.0	0.0	0.7	0.0	0.6	0.2	0.5	0.3	0.2	0.1	0.1	0.0	0.9 ± 0.2		
Planctomycetes		*Gemmataceae* 934	1.4	0.9	0.5	1.3	0.1	1.4	3.7	1.9	1.9	0.8	1.0	0.5	1.5	1.0	2.8	1.4			1.7 ± 0.7
		944	0.4	0.5	0.3	0.3	0.4	0.1	1.4	0.2	0.2	0.5	0.2	0.4	0.9	0.1	0.7	1.1			1.0 ± 0.3
		Tepidisphaeraceae 985	0.1	0.1	0.1	0.1	0.3	0.1	1.1	0.1	0.0	0.3	0.3	0.2	0.2	0.3	0.5	0.1			0.9 ± 0.2
		Phycisphaerae 1033	1.4	2.1	1.4	1.7	3.4	2.7	3.0	0.6	1.4	1.6	1.1	2.1	1.2	3.0	1.5	1.9		1.7 ± 0.8	1.8 ± 0.5
Proteobacteria	α	*Caulobacteraceae* 653	0.7	0.7	3.2	0.0	2.3	0.6	3.3	0.5	0.9	0.5	0.4	0.9	1.2	1.3	0.7	0.9	2.9 ± 0.3	1.5 ± 0.3	2.6 ± 0.1
	β	*Oxalobacteraceae* 332	2.3	2.7	21.9	2.5	11.0	4.9	2.9	7.3	1.7	1.6	6.5	7.4	6.0	6.6	5.6	6.7	18.2 ± 2.4	6.6 ± 1.9	
	γ	*Pseudomonadaceae* 310	0.0	0.0	45.7	0.1	29.9	4.7	1.1	0.0	0.0	0.0	9.9	8.7	6.8	6.6	0.3	0.0	42.3 ± 5.6	26.1 ± 3.5	1.0 ± 0.1
	δ	*Bacteriovoracaceae* 380	0.0	0.0	0.1	0.0	1.9	0.1	3.9	0.1	0.0	0.0	0.2	0.0	0.8	0.3	0.1	0.2		1.6 ± 0.5	3.8 ± 0.0
		Bdellovibrionaceae 779	0.0	0.0	0.0	0.0	1.6	1.0	0.5	0.0	0.0	0.0	0.0	0.0	0.6	0.2	0.0	0.0		1.1 ± 0.5	
		783	0.1	0.1	0.0	0.1	1.6	0.5	5.0	0.4	0.0	0.0	0.0	0.1	0.4	0.9	0.1	0.4		1.3 ± 0.2	4.8 ± 0.1
		unclassified 79	0.0	0.0	0.0	0.0	5.1	0.6	13.7	0.3	0.0	0.0	0.0	0.0	1.7	1.0	0.6	1.2		4.3 ± 0.9	13.4 ± 0.3
Verrucomicrobia		unclassified 868	0.7	0.8	0.8	2.0	1.5	1.0	2.5	0.6	0.4	0.7	1.0	0.8	0.9	0.7	0.2	0.4			2.0 ± 0.3
		unclassified 878	0.0	0.1	0.0	0.0	0.3	0.1	4.8	0.1	0.0	0.0	0.0	0.0	0.2	0.1	0.2	0.3			4.6 ± 0.1
		Opitutaceae 914	0.0	0.1	0.2	0.0	1.1	0.6	0.6	0.1	0.0	0.1	0.0	0.3	0.2	0.8	0.0	0.0		0.8 ± 0.3	
		Verrucomicrobiaceae 875	0.0	0.0	0.0	0.0	1.2	0.2	0.2	0.0	0.0	0.0	0.0	0.0	0.6	0.6	0.1	0.1		1.0 ± 0.3	

Table S2. Relative abundances and calculated R_{CS} scores abundances of labeled OTUs under anoxic conditions. R_{CS} sores were calculated using the values for the relative abundance of a given OTU in the heavy (H) and light (L) fractions of [^{13}C]-chitin and [^{12}C]-chitin incubations. See materials and methods (2.7.4.) for details on the calculation.

			[^{13}C]-Chitin								[^{12}C]-Chitin								R_{CS} score		
			Day 0		Day 10		Day 21		Day 70		Day 0		Day 10		Day 21		Day 70		Day 10	Day 21	Day 70
Phylum	Family	OTU	H	L	H	L	H	L	H	L	H	L	H	L	H	L	H	L			
Acidobacteria	*Acidobacteriaceae*	410	0.4	0.8	6.9	0.5	4.7	0.8	5.4	0.6	0.6	0.8	1.7	1.8	2.8	2.3	0.9	1.2	6.0 ± 0.7	3.4 ± 1.3	4.8 ± 0.3
Bacteroidetes	unclassified	754	0.0	0.0	0.9	0.0	27.3	0.1	35.7	2.7	0.0	0.0	0.0	0.1	8.0	13.7	7.6	16.4		24.6 ± 4.6	32.2 ± 3.8
Chloroflexi	*Anaerolineaceae*	547	0.1	0.8	0.6	0.5	1.4	0.4	2.3	0.6	0.0	0.1	0.1	0.1	0.6	0.4	0.1	0.4			2.0 ± 0.3
	Anaerolineaceae	548	0.6	0.3	2.5	1.2	1.0	0.1	0.0	0.0	0.6	0.3	0.4	0.8	0.4	0.3	0.0	0.1	1.8 ± 0.4		
	unclassified	530	2.6	2.4	3.8	3.3	1.9	2.9	4.2	1.9	3.1	2.9	3.1	3.4	3.7	3.3	3.1	3.1			1.6 ± 0.6
Firmicutes	*Paenibacillaceae*	203	0.9	1.0	5.2	1.9	12.9	1.7	15.1	1.7	2.2	1.3	1.6	1.4	1.3	1.7	2.0	1.8	3.7 ± 0.5	11.6 ± 0.4	13.5 ± 0.6
	uncultured	440	0.0	0.0	0.0	0.0	0.2	0.0	2.7	0.0	0.0	0.0	0.0	0.0	0.0	0.0	0.6	0.3			2.4 ± 0.3
	Lachnospiraceae	423	0.0	0.2	0.0	0.0	11.8	0.4	6.3	0.1	0.0	0.1	0.0	0.1	0.1	0.4	0.5	0.6		11.6 ± 0.2	6.1 ± 0.3
	Ruminococcaceae	416	0.0	0.2	0.3	0.0	15.6	0.7	2.2	0.3	0.1	0.0	0.4	0.1	0.4	0.4	1.6	1.0		15.2 ± 0.3	1.5 ± 0.8
Proteobacteria	*Geobacteraceae*	120	0.2	0.3	3.7	1.0	1.3	1.0	0.2	0.7	0.4	0.3	0.9	0.8	1.4	1.0	0.5	0.9	3.0 ± 0.4		
Verrucomicrobia	unclassified	2	1.0	1.2	2.1	0.6	1.1	0.9	0.6	0.5	1.0	0.6	0.5	1.2	1.1	1.3	0.5	0.6	1.4 ± 0.3		

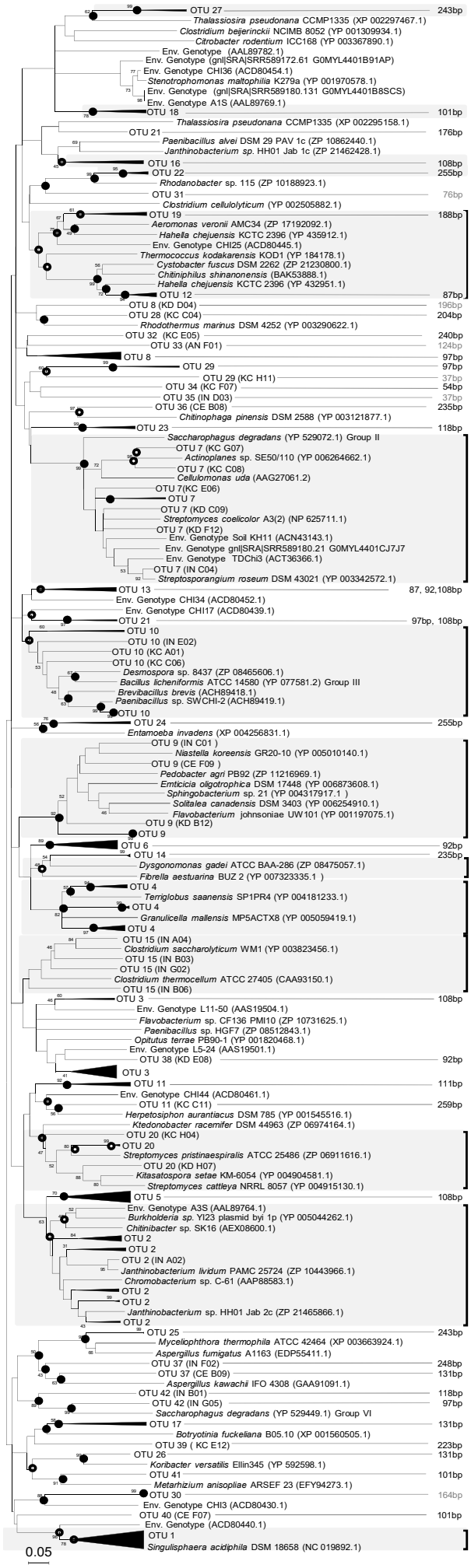

Proteobacteria / OTU 19 [TRFs 87, 188bp]

Actinobacteria / OTU 7 [TRFs 42, 111bp]

Firmicutes / OTU 10 [TRF 108bp]

Bacteroidetes / OTU 9 [TRFs 97, 108bp]

Bacteroidetes / OTU 14 [TRF 235bp]

Acidobacteria / OTU 4 [TRFs 92, 235, 259bp]

Firmicutes / OTU 15 [TRF 108bp]

OTU 3 [TRFs 105,176, 188, 248, 268bp]

Actinobacteria / OTU 20 [TRFs 108, 111bp]

Betaproteobacteria / OTU 2

[TRFs 108, 111, 114, 240, 264, 268bp]

Planctomycetes / OTU 1 [TRFs 54, 63, 81, 92, 211bp]

Figure S2. Neighbor joining tree of *chiA* OTUs and reference sequences. The tree is the ungrouped version of the tree presented as Fig. 19. Gene libraries were prepared from pooled samples. The total number of sequences was 285 (206 revealed in the current study, 78 references from public databases). Accession numbers or names of sequences of the current study are given in parentheses. TRFs corresponding to OTUs that were identified by in silico digestion with AluI are given in square brackets. The tree was calculated applying the Neighbor Joining algorithm implemented in MEGA 5 with translated amino acid sequences. Partial deletion with a site coverage cutoff of 80% was chosen for the gaps and missing data treatment. Percentage values at nodes are bootstrap values of 1,000 replicates. Open circles and grey filled circles at nodes indicate that these nodes were confirmed by MEGA-implemented Maximum Likelihood and Maximum Parsimony algorithms, respectively, using the same dataset. Black circles indicate confirmation by both algorithms. Scale bar, 5% sequence divergence.

11. (Eidesstattliche) Versicherungen und Erklärungen

(§ 5 Nr. 4 PromO)

Hiermit erkläre ich, dass keine Tatsachen vorliegen, die mich nach den gesetzlichen Bestimmungen über die Führung akademischer Grade zur Führung eines Doktorgrades unwürdig erscheinen lassen.

(§ 8 S. 2 Nr. 5 PromO)

Hiermit erkläre ich mich damit einverstanden, dass die elektronische Fassung meiner Dissertation unter Wahrung meiner Urheberrechte und des Datenschutzes einer gesonderten Überprüfung hinsichtlich der eigenständigen Anfertigung der Dissertation unterzogen werden kann.

(§ 8 S. 2 Nr. 7 PromO)

Hiermit erkläre ich eidesstattlich, dass ich die Dissertation selbständig verfasst und keine anderen als die von mir angegebenen Quellen und Hilfsmittel benutzt habe.

(§ 8 S. 2 Nr. 8 PromO)

Ich habe die Dissertation nicht bereits zur Erlangung eines akademischen Grades anderweitig eingereicht und habe auch nicht bereits diese oder eine gleichartige Doktorprüfung endgültig nicht bestanden.

(§ 8 S. 2 Nr. 9 PromO)

Hiermit erkläre ich, dass ich keine Hilfe von gewerblichen Promotionsberatern bzw. -vermittlern in Anspruch genommen habe und auch künftig nicht nehmen werde.

Ort, Datum, Unterschrift